INTERNATIONAL SCHOOL FOR ADVANCED STUDIES

A study of excitotoxicity as pathological process responsible for spinal cord injury: insight from an in vitro rat spinal cord model with a focus on neuroprotection

Thesis submitted for the degree of "Doctor Philosophiae"

Academic year 2011-2012

Candidate   **Supervisor**

Sara Ebrahimi Nasrabady   **Prof. Andrea Nistri**

Scuola Internazionale Superiore di Studi Avanzati (SISSA/ISAS)

Via Bonomea 265, 34136, Trieste, Italy

تقدیم به بانوی پر مهری که انسان بودنم آموخت

به مامانی عزیزم که روح آموزگارش جاودانه است

«در این خاک، در این خاک، در این مزرعه پاک

به جز مهر، به جز عشق، دگر بذر نکاریم»

To the loving lady who taught me how to be a human,

To my beloved grandmother who owned an everlasting teaching soul

"On this soil, on this holy field of the world,

Do not grow anything but passion and love"

LIST OF CONTENTS

Declaration

Mazzone GL, Margaryan G, Kuzhandaivel A, Nasrabady SE, Mladinic M, Nistri A (2010) Kainate-induced delayed onset of excitotoxicity with functional loss unrelated to the extent of neuronal damage in the in vitro spinal cord. Neuroscience 168:451-462.

Nasrabady SE, Kuzhandaivel A, Mladinic M, Nistri A (2011) Effects of 6(5H)-phenanthridinone, an inhibitor of poly(ADP-ribose)polymerase-1 activity (PARP-1), on locomotor networks of the rat isolated spinal cord. Cellular and molecular neurobiology 31:503-508.

Nasrabady SE, Kuzhandaivel A, Nistri A (2011) Studies of locomotor network neuroprotection by the selective poly(ADP-ribose) polymerase-1 inhibitor PJ-34 against excitotoxic injury to the rat spinal cord in vitro. The European journal of neuroscience 33:2216-2227.

Nasrabady SE, Kuzhandaivel A, Akrami A, Bianchetti E, Milanese M, Bonanno G, Nistri A (2012) Unusual increase in lumbar network excitability of the rat spinal cord evoked by the PARP-1 inhibitor PJ-34 through inhibition of glutamate uptake. Neuropharmacology 63:415-426.

Declaration

The candidate has performed electrophysiological experiments including isolating spinal cord preparations, recording, data acquiring and data analysis. In addition, the candidate has performed some limited work in order to prepare the slices for immunohistological experiments.

The immunohistological experiments are performed by Dr. Kuzhandaivel, Dr. Mazzone, Dr. Samano and Miss Bianchetti.

Data analysis using MATLAB program is performed by Dr. Akrami (using the data acquired by the candidate).

Experiments using purified synaptosome are performed by Dr. Milanese.

The data which are reported in the present thesis have been published in following articles and in all cases the candidate has contributed to the interpretation, discussion of the data and writing the manuscript:

1. Samano C, Nasrabady SE, Nistri A (2012) A study of the potential neuroprotective effect of riluzole on locomotor networks of the neonatal rat spinal cord in vitro damaged by excitotoxicity. Neuroscience 222:356-365.

2. Nasrabady SE, Kuzhandaivel A, Akrami A, Bianchetti E, Milanese M, Bonanno G, Nistri A (2012) Unusual increase in lumbar network excitability of the rat spinal cord evoked by the PARP-1 inhibitor PJ-34 through inhibition of glutamate uptake. Neuropharmacology 63:415-426.

3. Nasrabady SE, Kuzhandaivel A, Nistri A (2011) Studies of locomotor network neuroprotection by the selective poly(ADP-ribose) polymerase-1 inhibitor PJ-34 against excitotoxic injury to the rat spinal cord in vitro. The European journal of neuroscience 33:2216-2227.

4. Nasrabady SE, Kuzhandaivel A, Mladinic M, Nistri A (2011) Effects of 6(5H)-phenanthridinone, an inhibitor of poly(ADP-ribose)polymerase-1 activity (PARP-1), on locomotor networks of the rat isolated spinal cord. Cellular and molecular neurobiology 31:503-508.

5. Mazzone GL, Margaryan G, Kuzhandaivel A, Nasrabady SE, Mladinic M, Nistri A (2010) Kainate-induced delayed onset of excitotoxicity with functional loss unrelated to the extent of neuronal damage in the in vitro spinal cord. Neuroscience 168:451-462.

Abstract

Excitotoxicity is considered to be a major contributor to pathophysiological mechanisms responsible for spinal cord damage after acute injury. Hyperactivation of poly(ADP-ribose) polymerase (PARP) is the chief effector of neuronal death which leads to cell energy depletion and DNA damage with the manifestation of non-apoptotic cell death termed parthanatos. Glutamate mediated excitotoxicity is also one important component of post-traumatic degeneration following spinal cord injury (SCI).

Kainate (1 h), a potent non-degradable analog of glutamate, was used to induce excitotoxic injury in our in vitro model. The neonatal rat isolated spinal cord preparation allowed investigating changes in locomotor network activity after application of this excitotoxic agent with or without potential neuroprotective drugs. Synaptic transmission, cumulative depolarization, fictive locomotion and disinhibited bursting were studied in order to observe the functional properties of locomotor network and related to network hictology.

Our results showed that the locomotor network was very sensitive to excitotoxic damage and excitotoxicity grew gradually leaving a time window in which neuroprotection might be attempted to preserve the circuits which are still capable of expressing basic rhythmogenesis. Our result confirmed that PARP-1 overactivity is closely related to neuronal loss after kainate induced excitotoxicity. Application of PJ-34 (60 µM; PARP-1 selective inhibitor)

blocked PARP-1 activation and preserved dorsal, central and ventral grey matter with maintained reflex activity. Fictive locomotion was restored in more than half of the preparations when the excitotoxic stimulus was moderate. Histological damage by 50 µM kainate (moderate injury) was widely prevented by PJ-34. At the same time, this drug strongly increased spontaneous network discharges which occured synchronously on ventral roots and persisted for 24 h even after PJ-34 washout. Neurochemical experiments showed that PJ-34 induced up to 33% inhibition of synaptosomal glutamate uptake with no effect on GABA uptake. However, chemically or electrically induced fictive locomotion was present 24 h after PJ-34 application and neurons and glia remain unchanged. The other PARP-1 inhibitor, PHE, failed to recover locomotor network function, while basic network rhythmicity persisted and appeared to be a moderate histological neuroprotector. Riluzole, by inhibiting glutamate release and neuronal excitability, could prevent neuronal loss 24 h later, but this drug per se (applied for 24 h) exerted strong and persistant neurodepressant effects on network synaptic transmission from which recovery was very slow and partial. Although, the number of pyknotic cells in the grey matter was decreased by riluzole application after kainate washout, no fictive locomotion was observed. Three hours application of riluzole was not sufficient enough to contrast the deleterious effect of kainate on locomotor activity.

In conclusion, the divergence between histological and functional outcome in case of PARP-1 inhibition, proposes a narrow borderline between loss of fictive locomotion and neuronal preservation and suggests that protecting the motoneurons is not enough to ensure the persistence of fictive locomotion. It is also discovered that PJ-34 plays the role of a partial blocker of glutamate uptake. Despite the increased network discharges induced by PJ-34, there was no neurotoxic consequence due to this drug. In general, in order to protect the damaged spinal locomotor network, the neuroprotective strategy should be directed toward identified biomedical targets which play the most important role in cell death mechanism. On the other hand, neuroprotection should be applied at the early stages after the insult. Survival of premotoneurons in the grey matter is as important as motoneuron protection in order to achieve the goal of locomotor function preservation.

Introduction

1. Spinal Cord Injury

1.1. Definition and statistics

Spinal cord injury (SCI) is an insult to the spinal cord resulting in functional and structural changes, which can be temporary or permanent. SCI affects the normal sensory, motor or autonomic function of the spinal cord. Patients with spinal cord injury usually have permanent and often devastating neurologic deficits and disability. According to the National Institutes of Health (NIH), among neurological disorders, the cost to society for SCI is exceeded by the cost for mental retardation (Westgren and Levi, 1998). Acute spinal cord injury begins with a sudden, traumatic blow to the spine that fractures or dislocates vertebrae. The damage begins at the moment of injury when displaced bone fragments, disc material, or ligaments bruise or tear into spinal cord tissue.

Published reports show that the incidence of SCI in the United States varies from 25 to 59 new cases per million population per year with an average of 40 per million (Acton et al., 1993, Price et al., 1994, Thurman et al., 1994, Johnson et al., 1997, Surkin et al., 1998).

According to National Spinal Cord Injury Statistical Center (NSCISC) report, published in 2011, the most common age of injury is 19 and a quarter of all injuries occurs between 17 and 22 (24.9 %). Mean age of SCI patients is 34.2 (±16.6) years and children with 14 years old or younger consist 1.95% of SCI patients. Most of the population affected by SCI are male (80.6%) and the automobile accident is at the top of the list of SCI causes (33.5%) while falls (21.2 %) and gunshot wounds (15.7%) are at the next levels in the United States. A trend toward increased incidence in the elderly was also observed, likely due to falls and non-traumatic injury (van den Berg et al., 2010).

Spinal cord injuries may produce one or more of the following signs and symptoms: loss of movement (paralysis), loss of sensation, including the ability to feel heat, cold and touch, loss of bowel or bladder control, hyper reflexia or spasms, changes in sexual function, pain or an intense stinging sensation caused by damage to the nerve fibers and breathing difficulties. Paralysis may be referred to as: 1) Tetraplegia or quadriplegia; this means that arms, hands, trunk, legs and pelvic organs are all affected by spinal cord injury. 2) Paraplegia; it affects all or part of the trunk, legs and pelvic organs.

1.2. History of SCI

Spinal cord injury and its treatment date back to ancient times. The first evidence of this problem dates to 3000 to 2500 years B.C. when Imhotep, Egyptian physician, in Edwin Smith papyrus described the injuries of the cervical spinal cord and stated that the best treatment for the injured vertebrae is rest and support. Egyptians did not make surgical interventions for spinal cord injury but they performed surgical decompression following skull fractures. Centuries later in ancient Greece, Hippocrates (460-370 B.C.) created a method called succession on a ladder, as well as other methods of traction, for the treatment of SCI. He described paraplegia with bowel and bladder dysfunction, pressure ulcers, gibbosity at different levels and paralysis accompanied by cold abscess. He wrote the book "anatomy of the spine" and described the details of the spinal cord, ligaments and muscles. He mentioned that displacement of vertebrae forward is mostly fatal. Later on, in the first century A.D., in Rome Aulus Cornelius Celsus in his treatise "De Medicina" briefly

described the SCI, especially fractures of the spinous processes. He recommended Hippocrates' method of traction and emphasized that, in cases of complete spinal cord lesion, death usually ensued. Galen, another Roman physician (131-201 A.D.) who is considered as a founder of experimental physiology, described injuries to the first and second cervical vertebrae, stating that they are fatal and that respiration stops with injuries occur at the third or fourth vertebrae. 400 years later Greco-Roman Paul of Aegina advised post-reduction spinal splinting for the treatment of dislocations. He is considered the originator of laminectomy for spinal cord decompression and the removal of the offending bony fragments. Persian, Hindu, Arab, and Chinese physicians also developed basic forms of traction to correct spinal deformities. In the seventh century after Arabic and Islamic civilization, many works were translated from Greek, Persian, Latin and Hindu to Arabic. The Persian physician Avicenna (980-1037 A.D.) translated books and made contribution of his own. He wrote about one hundred books during his life. The most comprehensive of them is "Canon of Medicine" in five volumes. For six centuries the Latin translation of this book was the main reference used in European schools. He followed the methods of Paul of Aegina. In nineteenth century antisepsis was adopted, surgical morbidity and mortality decreased. In 1902 Lorenzo Bonomo, Italian surgeon developed the technique of hemilaminectomy. German, American and British experience was increased in the field of SCI after world war. After World War II the work of clinicians and scientists has improved the outlook for SCI victims. Donald Munro, an American surgeon, developed an interest in the care of SCI. Many call him as the true founder of modern SCI care and the "father of paraplegia".

Despite the fact that throughout man's history, SCI has been a catastrophic condition and the prognosis is still very gloomy, all over the world many researchers are working to erase the rule of Imhotep that SCI is "an ailment not to be cured" (Eltorai, 2003).

1.3 . Classification

Clinicians have used a clinical scale to grade the severity of neurological loss. First, before World War II, Stokes Manville score was used and popularized by Frankel in the 1970's. The

original scoring approach divided patients into five categories, i.e. no function (A), sensory only (B), some sensory and motor preservation (C), useful motor function (D), and normal (E).

American Spinal Injury Association (ASIA) impairment scale

A= Complete: No motor or sensory function is preserved in the sacral segments S4-S5.

B= Incomplete: Sensory but not motor function is preserved below the neurological level and includes the sacral segments S4-S5.

C= Incomplete: Motor function is preserved below the neurological level, and more than half of the key muscles below the neurological level have a muscle grade less than 3.

D= Incomplete: Motor function is preserved below the neurological level, and at least half of key muscles below the neurological level have a muscle grade of 3 or more.

E= Normal: Motor and sensory function are normal.

Table 1: ASIA Impairment at Admit, Rehab Admit, and System Discharge

ASIA impairment scale n (%)	Admit	Rhab Admit	System Discharge
Complete (A)	5,662 (46.3)	1,331 (10.9)	5,218 (42.7)
Sensory Incomplete (B)	1,518 (12.4)	410 (3.4)	1,200 (9.8)
Non-functional Motor Incomplete (C)	1,773 (14.5)	596 (4.9)	1,415 (11.6)
Functional Motor Incomplete (D)	2,189 (17.9)	827 (6.8)	3,771 (30.8)
Recovered (E)	0 (0.0)	1 (<0.1)	119 (1.0)
Unknown	1,086 (8.9)	9,063 (74.1)	505 (4.1)
Total	12,228	12,228	12,228

(https://www.nscisc.uab.edu/PublicDocuments/reports/pdf/2011%20NSCISC%20Annual%20Statistical%20Report%20-%20Complete%20Public%20Version.pdf)

National Spinal Cord Injury Statistical Center (NSCISC) last report showed that there was an increase in Functional Motor Incomplete (D), from 17.9% at acute admittance to 30.8% at discharge (Table 1).

1.4. Terminology in spinal cord injury

1.4.1. Spinal Shock

The damage to spinal cord originates from a localized lesion (primary injury) which can be accompanied by spinal shock (Ditunno et al., 2004), and then followed by lesion extension to spared spinal tissues (secondary injury) with significant symptom deterioration (Klussmann and Martin-Villalba, 2005).

From a clinical point of view, Whytt (1750) first explained the term of "spinal shock" as a loss of sensation accompanied by motor paralysis with gradual recovery of reflexes (Sherrington, 1897, Ditunno et al., 2004). Later in 1841, it was called as no reflex in the extremities followed by recovery. Recently, spinal shock is described as compromising four phases starting from the earliest moments after the insult to the spinal cord and continuing for months after that. Phase-1 (areflexia/hyporeflexia) occurs from 0 to 24 h post-injury. Deep tendon reflexes (DTRs) such as AJ (ankle jerk) and the KJ (knee jerk) are initially absent and muscles are flaccid and paralyzed. During this period cutaneous (polysynaptic) reflexes begin to recover. Therefore, the absence of all reflexes is uncommon within hours after injury (Ko et al., 1999). Phase-2 (initial reflex return) lasts for 1-3 days post-injury. Cutaneous reflexes become stronger. DTRs are still absent. Increased neuronal firing in response to neurotransmitters is known to occur after denervation (denervation supersensitivity) and is suggested to be the main cause of initial reflex re-emergence in spinal cord (Burke, 1988, Bach-y-Rita and Illis, 1993, Burke et al., 2001).

Phase-3 extends from approximately 4 days to 1 month. Most DTRs reappear during this period. It is the beginning of hyper-reflexia caused by axon-supported synaptic growth and it will be followed by the last phase (phase-4) which represents the final hyper-reflexia with aberrant plasticity (Ko et al., 1999, Schindler-Ivens and Shields, 2000).

1.4.2. Primary and secondary injury

In SCI primary injury is a compressive-contusive injury initiating a number of pathophysiological processes leading to the prolonged secondary injury phase. Secondary injury is consisted of different phases as the following:

Immediate phase (0-2 hours) begins at the time of the injury and represents the primary phase of injury. The immediate mechanical damage affects neural and other soft tissues, including endothelial cells of the vasculature. Tissue damage in a contusion injury appears to be more predominant in the grey matter of the spinal cord than in the white matter (Fig. 1). Generalized swelling and hemorrhaging appears in the grey matter which make the spinal cord ischemie. Microglial cells are activated almost instantaneously by the upregulation of proinflammatory cytokines (Pineau and Lacroix, 2007, Donnelly and Popovich, 2008). Extracellular glutamate can reach excitotoxic levels within minutes from the injury (Wrathall et al., 1996). Within the first 15 minutes after injury, extracellular concentrations of glutamate and other excitatory amino acids reach cytotoxic concentrations that are six to eightfold higher than normal as a result of cell lysis from mechanical injury and both synaptic and nonsynaptic transport.

Acute phase (2 hours to 2 weeks) is the most likely phase for implementing neuroprotective interventions. The ischemic cellular death, increasing edema and inflammation continue from the immediate phase. The onset of free radical production, ionic dysregulation, glutamate-mediated excitotoxicity and immune-associated neurotoxicity are fully developed.

Intermediate phase (2 weeks to 6 months) is characterized by maturation of the astrocytic scar and by regenerative axonal sprouting (Hill et al., 2001).

Tissue Loss after Spinal Cord Injury

1 Hour Post Injury   60 Days Post Injury
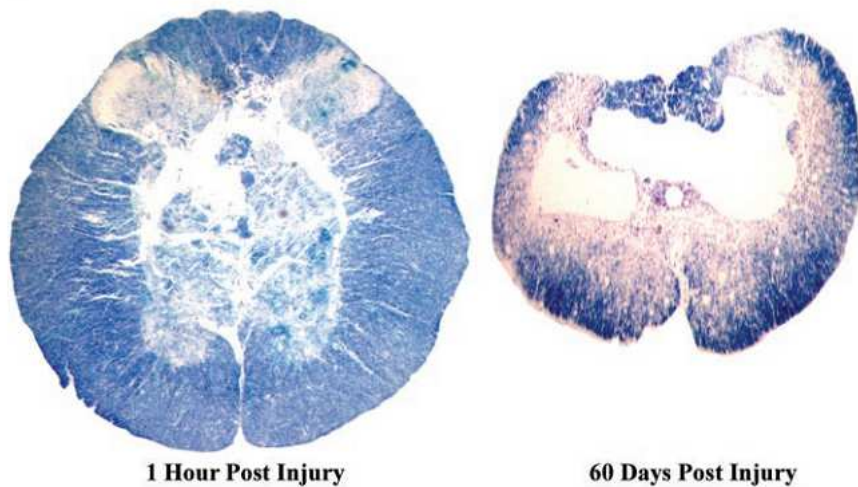
Figure 1: The rodent contusion model of SCI which produces a necrotic core, principally in the central grey matter, that is surrounded by histologically normal-appearing myelinated fibers and portions of grey matter from both dorsal and ventral horns (left). Similar to human SCI pathophysiology, the cell loss continues radially in all directions, so that the lesion expands over time. By 60 days post-SCI, there remains only a thin rim of white matter (right). (Hulsebosch, 2002)

Chronic phase (>6 months) continues throughout the lifetime of the patient. It is characterized by maturation/stabilization of the lesion including continued scar formation and the development of cysts and/or syrinxes. The lesion can produce a cyst cavity and myelomalacia 1-2 years after the injury. The neurological deficits are mostly stabilized, but, in 30% of the patients, SCI can still cause delayed neurological dysfunction (ascending paralysis, brainstem symptoms). Apoptosis continues in both orthograde and retrograde directions including brain regions; a variety of receptors and ion channels are altered in expression levels and activation states, scarring and tethering of the cord occurs in the penetrating injuries (about 25% of all SCI); demyelination results in conduction deficits; cut and nearby uncut axons exhibit regenerative and sprouting responses, but go no farther than 1 mm; neural circuits are altered due to changes in inhibitory and excitatory input; and in many cell types, permanent hyperexcitability develops, which results in chronic pain syndromes

and spasticity in a majority of SCI patients (Fig. 2) (Tator, 1995, Christensen et al., 1996, Tator, 1996, Christensen and Hulsebosch, 1997, Tator, 1998).

Acute phase

1) Direct impact
2) Lacerated axon
3) Contused axons
4) Influx of inflammatory cells

Chronic phase

1) Central cavity
2) Scar tissue
3) Inhibition of axonal regeneration
4) Demyelination
5) Axonal dieback
6) Influx of inflammatory cells
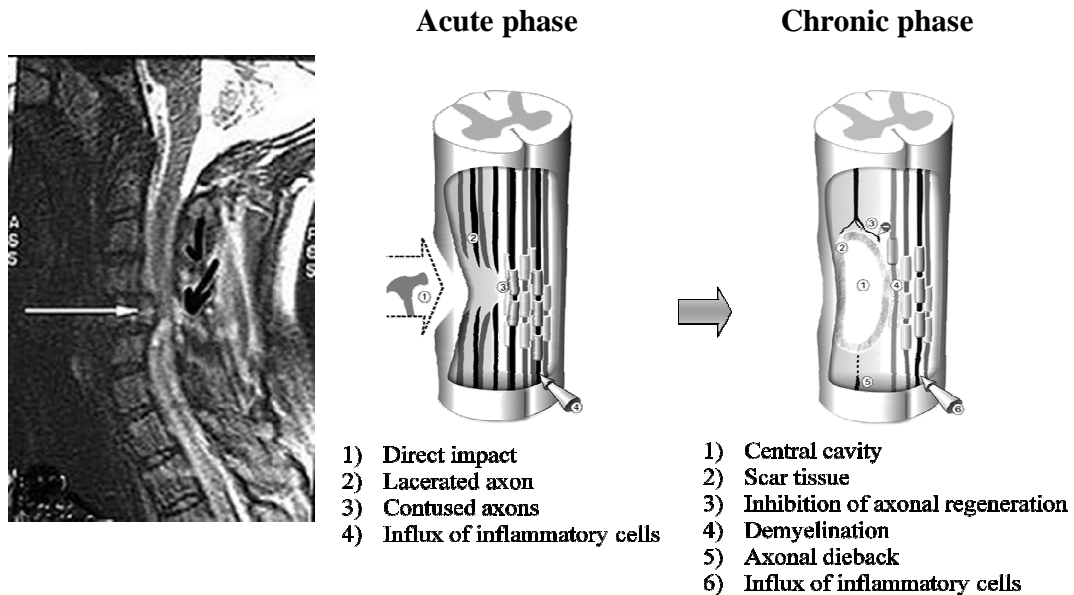
Figure 2: Schematic presentation of acute and chronic phases after traumatic spinal cord injury. (Ronsyn et al., 2008)

Most motor deficits that are following the primary mechanical injury are exacerbated by secondary mechanisms. The damage start to be expanded vertically into the gray matter at first and then it spreads horizontally within the white matter. Since physical primary injury which affects neuronal and endothelial tissue is immediate, it is not suitable for therapeutic intervention. In contrast the secondary phase which is delayed can be the best target for therapeutic intervention.

1.5. Pathophysiolgy of SCI

The secondary degenerative process is initiated by the primary mechanical injury that is proportional to the magnitude of the initial insult (Hall and Springer, 2004). There are several reviews discussing the principal mechasims of post-SCI secondary injury (Hall and Braughler, 1989, Tator and Fehlings, 1991, Faden and Salzman, 1992, Anderson and Hall,

1993, Hall, 1996, Faden, 1997, Hall and Springer, 2004). The most immediate event is mechanically induced depolarization and the consequent opening of voltage-dependent ion channels (i.e., Na^+, K^+, Ca^{2+}). This leads to massive release of a variety of neurotransmitters, including glutamate (Hall and Springer, 2004, Park et al., 2004, Rossignol et al., 2007), which can open glutamate receptor-operated ion channels (e.g., NMDA, AMPA). Probably the most important consequence of these rapidly evolving ionic disturbances is the accumulation of intracellular Ca^{2+} (i.e., Ca^{2+} overload) which initiates several damaging effects. Mitochondrial dysfunction, mitochondrial and cytoplasmic nitric oxide synthase (NOS) activation, phospholipase A_2 activation [leading to increase of arachidonic acid liberation and its consequent prostaglandin $F_{2\alpha}$ (potent vasoconstrictor) as well as thromboxane A_2 (vasoconstrictor/platelet aggregation promoter) and leukotrienes (LTs)] and finally activation of the calcium-activated cysteine protease calpin which attacks several substrates including cytoskeletal proteins. Formation of reactive oxygen species (ROS; including $ONOO^-$), lipid peroxidation, cell energy depletion with the help of all above mechanisms lead to microvascular, axonal and myelin damage which are accompanied by ischemia, polymorphonuclear (PMN) and macrophage influx, inflammatory cell inflammation and final neurological deficit. (Fig. 3)
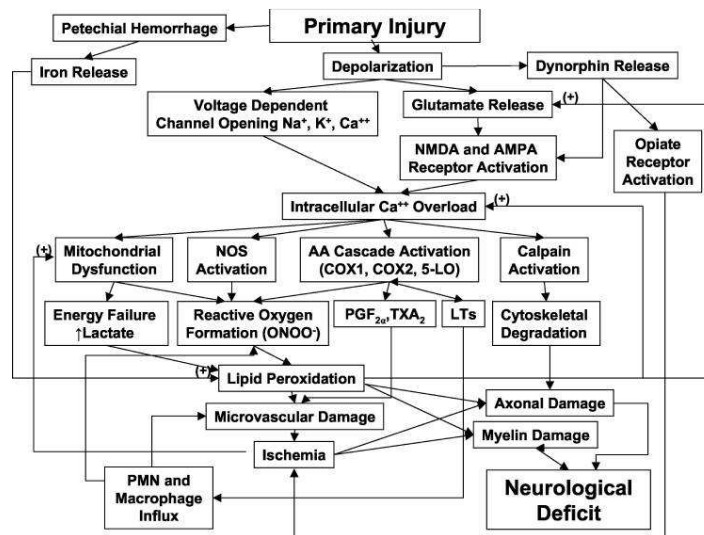
Figure 3: Pathophysiology of secondary injury in SCI. (Hall and Springer, 2004)

There is emerging evidence that glutamate extotoxicity plays a key role not only in neuronal cell death but also in delayed post-traumatic spinal white matter degeneration (Park et al., 2004). Glutamate levels increases transiently to excitotoxic levels within 3 first hours after SCI (Liu et al., 1991, Farooque et al., 1996a, Xu et al., 1998, Liu et al., 1999, McAdoo et al., 1999) (Fig. 4).
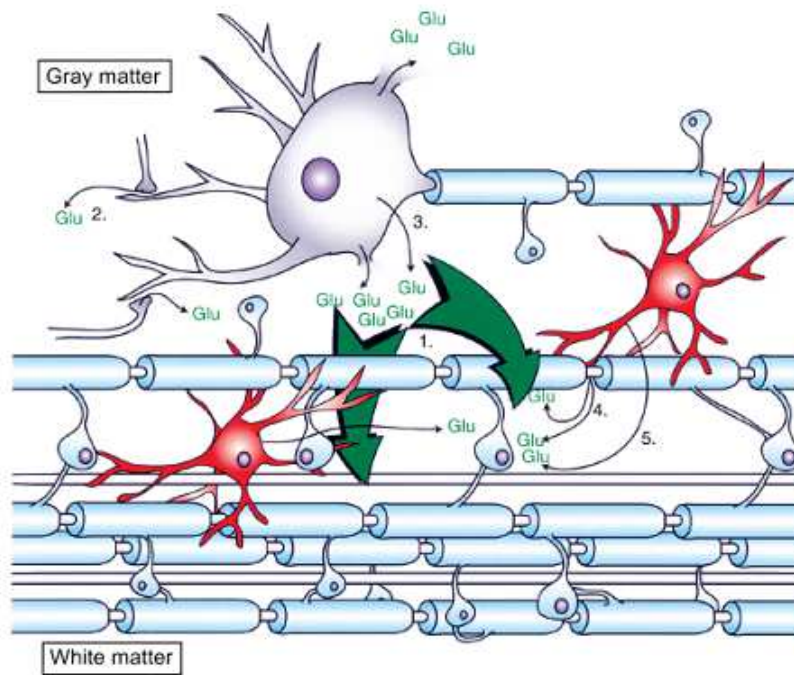
Figure 4: Extracellular glutamate sources. 1) Damaged neurons release glutamate to surrounding tissues. 2) Presynaptic glutamate release in grey matter mediated by group I mGluRs. 3) Upregulation of excitatory amino acid transporter (EAAT 3) may be important in maintaining glutamate homeostasis, but could also increase glutamate levels via reverse operation. 4) Release from axons glutamate reservoirs. 5) Reactive oxygen species may contribute to glial glutamate transport failure. (Modified from Park et al., 2004)

The extensive activation of glutamate receptors (by administration of six fold more than normal concentration of glutamate comparable to its level after trauma; 3.7 mM) was enough to induce neuronal death in an uninjured spinal cord (Liu et al., 1999).
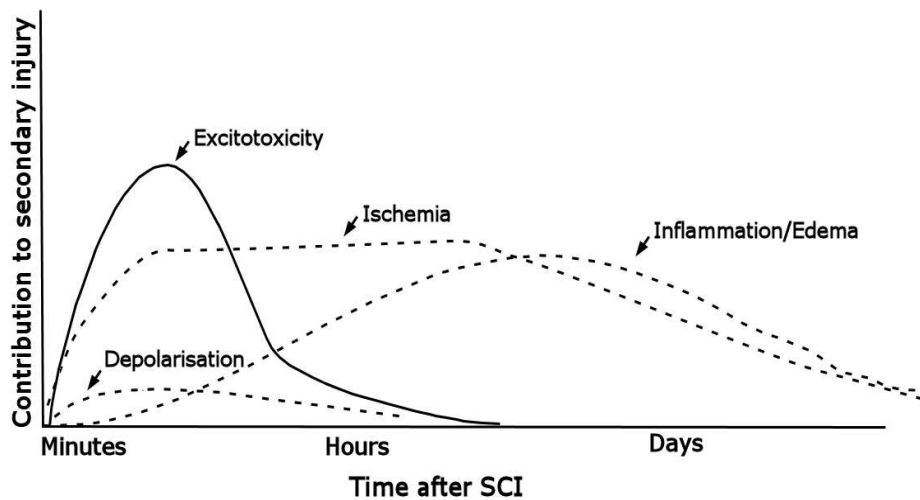
Figure 5: Time course of secondary injury in SCI. Very early after the injury excitotoxic mechanisms can damage neurons and glia. Excitotoxicity triggers the events that can contribute to the secondary injury and finally cell death. (modified from Dirnagl et al., 1999)

1.6. Therapeutic approaches

The present understanding of the many factors involved in the secondary injury process had led to the notion that pharmacological treatments, if applied early, might help the preservation of the necessary anatomic substrate for functional recovery of the spinal cord and interrupt the secondary cascade. At the same time we need to consider other possible options such as non-pharmacological approaches (i.e., surgery) in order to apply cord decompression or using neuronal stem and progenitor cells in order to stimulate or control endogenous neurogenesis and improving remyelination. Physical rehabilitation also plays a very important role in helping recovery of injured locomotor system (Baptiste and Fehlings, 2007).

1.6.1. Lipid peroxidation

Methylprednisolone (MP) therapy was extensively used in the clinical treatment of spinal cord trauma in the mid-1960s to 1970s. Limited experimental evidence showed the possibility of neuroprotective role of glucocorticoids in SCI. Later, in early 1980s, high-dose of MP was used to inhibit post-traumatic lipid peroxidation (LP) (Hall and Braughler, 1981). The first National Acute Spinal Cord Injury Study (NASCIS I) study published in 1984 compared high-dose with a low-dose group. Further studies showed MP not only prevented LP, but in parallel inhibited post-traumatic spinal cord ischemia and hypoperfusion, improved aerobic energy metabolism, reduced intracellular calcium overload, decreased inflammatory markers and improved neurological recovery (Hall and Braughler, 1981, Anderson et al., 1982, Braughler and Hall, 1982, 1983a, b, 1984, Holtz et al., 1990, Hall, 1992, Behrmann et al., 1994, Farooque et al., 1996b, Taoka et al., 2001). However, failure of high-dose MP to improve neurological recovery in rat SCI models have also been reported (Koyanagi and Tator, 1997, Rabchevsky et al., 2002). Beside that, there was a fear of possible side effects of using high-dose of glucocotricoids in human (infection, septic shock, diabetic complications and delayed wound healing).

1.6.2. Ischemia

Dynorphin A, an endogenous opioid, is released following SCI which reduces spinal cord blood flow. Concurrent with the studies on MP, based on the positive effect of endorphin systems antagonism in experimental shock, naloxone was used in acute SCI models (Holaday and Faden, 1981a, b). NASCIS II was designed to examine a higher dose of MP and naloxone given within 24 h of injury. Bracken (1993) showed the improved neurological function below the lesion in patients with incomplete injuries and treated with naloxone within 8 h of injury (Bracken and Holford, 1993).

1.6.3. Reactive oxygen species (ROS), nitric oxide and peroxynitrite

In NASCIS III tirilizad mesylate , a 21-aminosteroid, believed to be an antioxidant without glucocorticoid effect was added to treatment and was compared to the MP treated group. The result demonstrated that tirilizad was not superior to MP (Hall, 1993). The need to replace high-dose of MP resulted in studies on ROS, mostly peroxynitrite which is formed from combination of superoxide and nitric oxide radicals. Prototypical scavengers of peroxynitrite include penicillamine and Tempol, both are neuroprotective in cell culture and in vivo models of acute CNS injury (Hall et al., 1999, Carroll et al., 2000). Using dual inhibitor of LP and neuronal nitric oxide synthase, BN-80933, has been reported to attenuate post-traumatic and post-ischemic degeneration in vivo models (Chabrier et al., 1999). Clinical data are still unavailable.

1.6.4. Inflammation

Regarding the negative effect of inflammation on the injured cord, due to COX2 activation (Fig. 3), COX2 inhibitors were used. They showed neuroprotection and enhanced neurological recovery in animal models of SCI (Resnick et al., 1998, Hoffmann, 2000, Schwab et al., 2000, Hains et al., 2001, Tonai et al., 2002).

1.6.5. Intracellular calcium

High intracellular calcium can activate calpain and other destructive enzymes within the cell that lead to cell death. Excitotoxic glutamate release is also calcium-dependent. Nimodipine is an L-type calcium channel blocker. Its potential benefit in subarachnoid hemorrhage is believed to result from neuroprotective effects rather than a smooth muscle relaxing effect on blood vessels. Since it induces hypotension, when hypotension is avoided, animal studies demonstrated improvement in spinal cord function (Fehlings et al., 1989).

1.6.6. Excitotoxicity

Although glutamate is the main excitatory neurotransmitter in the CNS, its excess following injury leads to excitotoxicity (Liu et al., 1991, Liu et al., 1999, Xu et al., 2004).

Using gacyclidine (GK-11; a new phencyclidine derivative which binds to NMDA receptors with binding parameters similar to non-competitive NMDA receptor antagonists)

has shown some evidence of improvement in histology, function and electrophysiology in rats and it also prevents glutamate-induced neuronal death in primary cortical cultures. French clinical trial observed some improved motor function for just 1 year treatment (Hirbec et al., 2001).

In vitro experiments on neonatal rat spinal cord demonstrate that excitotoxicity is an early and important component to spinal lesion (Margaryan et al., 2010). Other studies have shown that glutamate antagonists have limited usefulness against long term recovery from spinal injury in vivo perhaps for reasons like the clinical predictiveness/relevance of the animal models, the adequacy of pharmacological methodology, and the outcome measures used (Faden and Stoica, 2007). CNQX and APV (1– 4 mg/kg i.p.) showed neuroprotective effect on neonatal rat motoneurons after sciatic nerve transaction (Iwasaki et al., 1995). CNQX and APV co-applied with kainate (glutamate analog) produced partial protection of locomotor networks, as NMDA and 5-HT could still activate fictive locomotion in one-third of preparations (Margaryan et al., 2010). Electrically-induced fictive locomotion was poorly protected and only few oscillatory cycles were sporadically present even if some recovery of cumulative depolarization was detected (Margaryan et al., 2010). It is suggested that the slow pharmacokinetic properties of CNQX and APV require a long time to block glutamate receptors of the rat spinal cord in vitro (Evans et al., 1982, Long et al., 1990).

Riluzole, an agent licensed for ALS treatment, was used to block voltage-sensitive persistent sodium channels (Schwartz and Fehlings, 2001). At the same time, riluzole is a glutamate release inhibitor and it has shown some positive behavioral outcome after experimental brain and spinal cord injury (Wahl et al., 1997, Schwartz and Fehlings, 2001, Lau and Tymianski, 2010).

2. Cell death pathways following SCI

Different cell death pathways which have been classified by the nomenclature of the cell death committee on cell death (NCDD) (Kroemer et al., 2009). Necrosis, apoptosis and parthanatos (which is a newly discovered cell death pathway) are the most important one.

16

Necrosis is a premature type of cell death which is unprogrammed. In primary injury and immediate phase of secondary injury, necrosis appears at the site of the injury. It can be observed mostly in the epicenter of the injury site (Katoh et al., 1996, Crowe et al., 1997, Liu et al., 1997). Cell swelling, mitochondrial dysfunction, energy loss and disruption in cell homeostasis are leading factors and internucleosomal DNA fragmentation is observed in necrosis.

Apoptosis is a programmed cell death pathway. During development, apoptosis helps the living tissues to control the DNA destruction (Nagata, 1997). Chromatin condensation, nuclear fragmentation, round up cells, blebbing and zeosis can be observed in apoptosis. This phenomenon happens after cysteine protease activation (caspase) (Yuan et al., 2003). The caspase dependent apoptotic pathway consists of two main molecular mechanisms: intrinsic (mitochondrial) and extrinsic (death receptor) pathways. Apototic cell death pathway can be involved in the secondary injury, starting at immediate phase (along with necrosis) and continuing to other phases with making damage to white matter, oligodendrocytes and microglia.

Parthanatos is another type of programmed cell death which is mediated by poly (ADP-ribose) (PAR) and was first described by David et al. (2009). Parthanatos shares similarities in morphological and cytological aspects with either apoptosis or necrosis, but it is the result of a special molecular mechanism (David et al., 2009). In fact, after an excitotoxic insult, spinal cord neurons suffer largely through a mechanism involving anucleolytic (without internucleosomal DNA fragmentation) pyknosis mediated by strong activation of poly (ADP-ribose)polymerase-1 (PARP-1) which produces PAR and leads to nuclear translocation of the apoptotic inducing factor (AIF) with DNA damage. This process is the hallmark of parthanatos-type neuronal death (Kuzhandaivel et al., 2010).

3. Poly(ADP-ribose)Polymerase

3.1. Double-edged sword role in cell death

Basal activity of PARP-1 in cells is low but it can be stimulated by damaged DNA, some undamaged DNA structures and nucleosomes (D'Amours et al., 1999, Oei and Shi, 2001, Kun et al., 2002, Kim et al., 2004). On the other hand, PARP-1 is also called the "genomic guardian" because of its role in genomic repair under physiological condition. Several studies using various pharmacological PARP inhibitors have concluded that PARP-1 plays a role in DNA repair (Burkle, 2001, Ziegler and Oei, 2001). It has been shown, for example, that the PARP inhibitor 3-aminobenzamide retarded the rejoining of DNA strand breaks. Therefore, if the damage is mild, this enzyme helps the cell survival process (Masson et al., 1998, Ruscetti et al., 1998), but when there is an extensive DNA damage, PARP-1 plays its role in promoting cell death. It can happen in stroke, trauma and ischemia (Szabo and Dawson, 1998, Mandir et al., 2000, Lorenzo and Susin, 2007). It is also interesting to know that this enzyme plays a role in the pathogenesis of various cardiovascular and inflammatory diseases (Graziani and Szabo, 2005).

The extensive activation of PARP-1 can rapidly lead to cell death through depletion of energy stores because four molecules of ATP are consumed in NAD (the source of ADP-ribose) regeneration (Berger, 1985). At the same time, PAR polymere binds to mitochondrial membranes and changes their membrane potential. Apoptotic inducing factor (AIF) is released due to mitochondrial dysfunction and accelerates the DNA damage and chromatin condensation in nuclei. (Fig. 6)
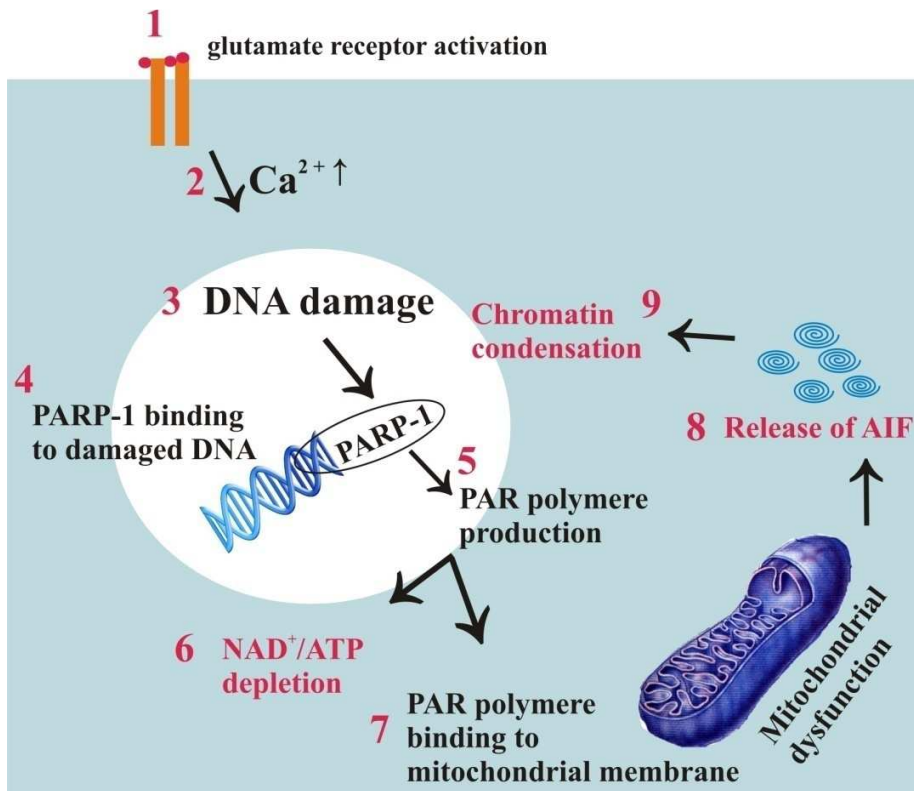
Figure 6: Schematic pathway of Parthanatos induced by excitotoxicity.

3.2. PARP-1 inhibitors and neuroprotection

Involvement of PARP in neuronal damage was initially studied by Zhang group (1994) demostrating the role of PARP in neurotoxicity after nitric oxide (NO) system activation and then it was observed that the inhibition of the enzyme rescued cortical neurons in culture from NO and NMDA-mediated toxicity (Cosi et al., 1994).

Szabo and Dawson (1998) showed that, in the brain after oxidative stress and DNA strand breakage, PARP-1 is activated and then Scott et al. (1999) reported the same effect in spinal cord injury induced by thoracic contusion in rats.

Eliasson et al. (1997) demonstrated protection by PARP^{-/-} phenotype in brain slices exposed to various oxidants. After that Dawson group in Baltimore reported (1999) the role of PARP-1 in excitotoxicity in mice showing that mice lacking PARP-1 are highly resistant to NMDA excitotoxicity.

It was shown by Lo et al. (1998) that inhibition of PARP by 3-aminobenzamide reduces injury after transient focal ischemia in rats and attenuates NMDA-induced glutamate efflux.

Using the in vitro model of neonatal rat isolated spinal cord demonstrated a significantly smaller number of pyknotic cells by pharmacological inhibition of PARP-1 with (6-5(H)-phenanthridinone; PHE) after excitotoxic insult with high dose of kainate (Kuzhandaivel et al., 2010). PHE could also prevent the translocation of AIF which is the main downstream effector of PARP-1 in inducing cell death.

Genovese et al. (2005) indicated that using various inhibitors of PARP-1 in an experimental model of spinal cord trauma (in vivo) reduced inflammation and tissue injury, PAR formation, neutrophil infiltration, apoptosis, DNA binding of NF-kappaB and the motor disturbance after SCI.

Abdelkarim et al. (2001) examined the neuroprotective effect of N-(6-oxo-5,6-dihydrophenanthridin-2-yl)-N,N-dimethylacetamide (PJ34), a novel potent inhibitor of PARP in vitro and in vivo. In the rat model of middle cerebral artery occlusion PJ-34 administration significantly reduced infarct size and the effect of the drug was maintained even if it was given as late as 10 min prior to reperfusion time. PJ-34 significantly protected in a 4 h, but not in a 24 h permanent occlusion model. They suggested that PJ-34 exerts massive neuroprotective agents, with a significant therapeutic window of opportunity (Abdelkarim et al., 2001).

Later, PJ-34 was also tried in another model of stroke (bilateral carotid occlusion-reperfusion) in rats. The positive effects included: suppressing the ischemia-induced microglial activation and astrogliosis, lessened deficits in spatial memory and learning, increased neuronal density in CA1 layer and formation of new neurons in hippocampal CA1 area. In general, it is proposed that treatment with PJ-34 for several days after ischemia enhances long-term neuronal survival and neurogenesis by reducing inflammation (Kauppinen et al., 2009).

4. Central pattern generator (CPG) and locomotor activity in the spinal cord

The ability of movement in animals and humans depends on the locomotor behavior of that specie such as flying, swimming or walking and many of the movements are more or less rhythmic (Buschges et al., 2011). Those fundamental motor acts involve the activation of many muscles and the nervous system is responsible for controlling the movement of those muscles. The nervous system is modular, with discrete network sub-serving various functions such as generating different pattern of motor behavior, being feature detectors in sensory system, critical modules in memory formation or being involved in the expression of the emotions. Because of complexity of the CNS system in mammals, many studies were performed on vertebrate model systems with relatively few neurons such as lamprey and zebrafish (Grillner et al., 1998, Kyriakatos et al., 2011). All classes of vertebrates share many similarities in locomotor behavior and locomotion controlling system (Grillner et al., 1977, Grillner, 1985). Therefore, the same meso-pontine and diencephalic centers initiate locomotor activity in lampreys as in primates, through activation of lower brainstem reticulospinal neurons. They activate localized spinal neuronal networks which generate the timing and pattern of the complex, rhythmic, coordinated muscle activities. This system is called central pattern generator (CPG).

Walking ability requires a rhythm with ipsilateral coordination of flexors and extensor muscles across the same or different joints in a limb as well as left/right coordination. These functions are all integrated in the fully functioning CPG.

Grillner et al. (1998) described the controlling system of locomotion starting with a tonic inhibitory system induced by the basal ganglia which is to be removed once a motor behavior starts. Brainstem locomotor system will be activated and then locomotor activity will be initiated. Increased activity in reticulospinal neurons activates CPG, which makes the locomotor pattern in close interaction with sensory feedback coming from peripheral ascending nerve fibers. If CPG activation increases, the speed of locomotion will also increase. Locomotion can be induced pharmacologically by administration of excitatory amino acid agonists and by sensory input in experimental conditions (Fig. 7).
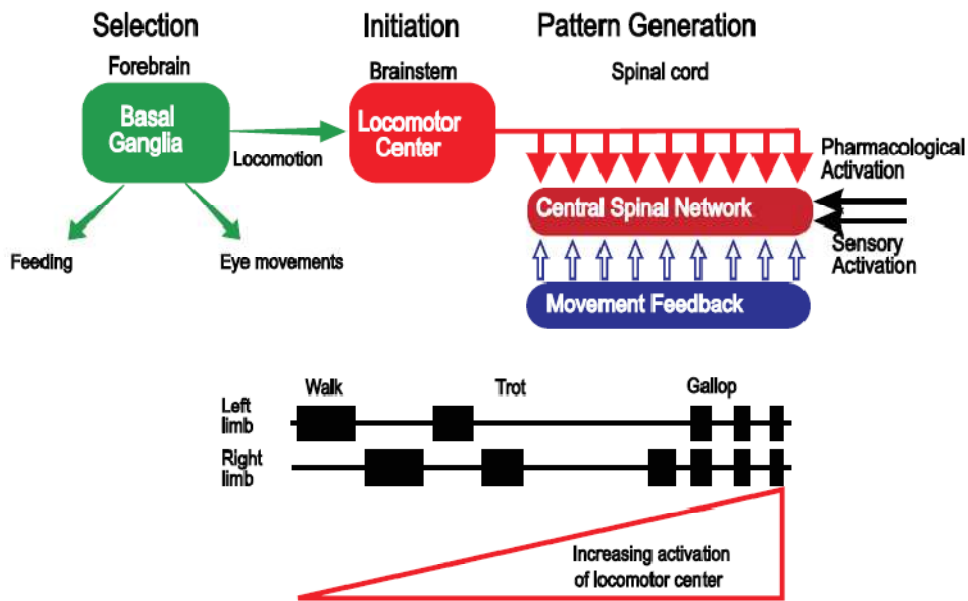
Figure 7: Schematic view of general controlling system of locomotion in vertebtares. (Grillner et al., 1998)

4.1. Localization of CPG

The rostrocaudal extent of rhythmogenic capacity of the hindlimb locomotor CPG was proposed firstly by Grillner and Zangger (1979). Using cat spinal cord transverse sectioning they demonstrated that alternating rhythmic activity could be evoked in ankle flexors and extensors when the caudal lumbar cord (the L6–S1 segments) was isolated from the rest of the cord, suggesting the rhythmogenic capacity in the CPG controlling hindlimb locomotion is distributed throughout the lumbar enlargement (L3–S1 in cats). Similar result was obtained in different laboratories working on isolated spinal cord preparations from newborn rats or mice. They studied spontaneous or drug induced rhythmic activity before and after transverse trans-sectioning at different spinal levels (Kudo and Yamada, 1987, Bracci et al., 1996, Kjaerulff and Kiehn, 1996, Cowley and Schmidt, 1997, Kremer and Lev-Tov, 1997, Bonnot and Morin, 1998, Bonnot et al., 2002a, b, Gabbay et al., 2002, Christie and Whelan, 2005).

L1–L3 in rodents and L3–L5 in cats (rostral lumbar segments) have a greater capacity to generate rhythmic motor output in isolation than caudal segments (L4–L6 and L6–S1, respectively).These studies therefore suggest that the rhythmogenic CPG is distributed along

22

the lumbar cord but the excitability has a rostrocaudal gradient. The reason can be the larger proportion of intraspinal inputs going to rostral segments (Berkowitz, 2004) and/or the differential distribution of receptors or receptive neurons for neuromodulatory substances in the rostral or caudal cord (Christie and Whelan, 2005).

Thus, it has been suggested that spinal interneurons directly involved in producing rhythmic activity are limited to the T13 and L2 (Kiehn, 2006).

Transverse distribution of CPG in spinal cord was studied by activity-labeling studies (Kjaerulff et al., 1994, Cina and Hochman, 2000, Dai et al., 2005) and electrophysiological evidence (Tresch and Kiehn, 1999). It was discovered that rhythmogenic CPG neurons are located in a ventral location (laminae VII, VIII, and X. It has been also confirmed with dorsal horn ablation studies, demonstrating the presence of fictive locomotion (chemically induced by NMDA and 5-HT) by recording from VRs (Taccola and Nistri, 2006).

4.2. Elements of locomotor CPG

4.2.1 Rhythm and pattern generation

The alternation between flexor and extensor motor neuron pools on the same side of the body needs both excitatory and inhibitory networks (Kiehn, 2006). There is a model suggested for the mammalian locomotor CPG which has two layers: 1) a rhythm-generating layer 2) a pattern-generating layer (coordinating flexor-extensor and left-right side activity) (Kriellaars et al., 1994, Burke et al., 2001, Lafreniere-Roula and McCrea, 2005). In this model, the pattern-generating neurons are connected monosynaptically to motor neurons, whereas the neurons in the rhythm generating layer have two or more synapses upstream from motor neurons and project directly to pattern-generating neurons. Pharmacological experiments propose that the rhythmogenic core of the network is composed of excitatory, ipsilaterally projecting interneurons. Ipsilateral excitatory glutamatergic interneurons are also most likely the origin of rhythm generation in the tadpole and lamprey swimming CPGs (Grillner, 2003). These interconnected, excitatory neurons seem to work as burst-generating units that provide rhythmic, excitatory, glutamatergic synaptic drive to motor neurons and other ipsilateral inhibitory and left-right coordinating CPG neurons in each segment. Because

of the presence of the rhythm activity after the block of inhibitory system, it is suggested that excitatory CPG neurons may have some intrinsic pacemaker-like properties (Smith et al., 2000, Pena et al., 2004) or some other set of voltage dependent membrane conductances that support rhythmic firing.

4.2.2 Flexor-extensor coordination

In addition to the rhythm-generating excitatory core, two other elements in the network can be isolated: flexor and extensor coordinating circuits and left-right coordinating circuits. Ipsilaterally inhibitory networks seem to be involved in flexor-extensor coordination since in the presence of inhibition block, flexors and extensors are activated synchronously (Cowley and Schmidt, 1997, Beato and Nistri, 1999). On the other hand, although, ipsilaterally projecting inhibitory interneurons, such as Renshaw cells (RCs) and Ia-INs (glycinergic/GABAergic), may contribute to rhythmic motor neuron inhibition, genetic knockout and silencing experiments indicate that, although these inhibitory cell populations are dispensable for flexor-extensor coordination, they are involved in speed regulation (Kiehn, 2006).

4.2.3 Left-right coordination

The left-right coordinating circuitries have been studied mostly in the mammalian locomotor CPG. Anatomical and electrophysiological research in cats and rodents have shown that these complex circuitries consist of intrasegmental and intersegmental (commissural interneurons) CINs that are both excitatory and inhibitory. A functional analysis of these circuitries suggests that intrasegmental CINs are involved in binding motor synergies along the cord, while intersegmental CINs seem to be directly involved in the coordination of homonymous muscle activity at a segmental level. Therefore, CPG network is proposed to operate with contribution of excitatory neurons responsible for rhythm generation and glycinergic CINs that are directly involved in left-right alternation (Kiehn, 2006).
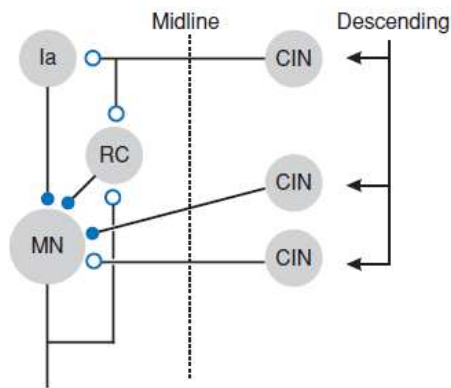
Figure 8: Diagram of intrasegmental commissural interneurons (CINs). Open circles: excitatory synapses; filled circles: inhibitory sypanses; RC: Renshaw cells, Ia: Ia interneurons. (Kiehn, 2006)

5. Neonatal rat isolated spinal cord

As early as 1911, it was recognized, by the experiments of T. Graham Brown, that the basic pattern of stepping can be produced by the spinal cord without the need of descending commands from the cortex (Graham-Brown, 1911, Whelan, 2003). In vivo studies by using treadmill and electromyography (EMG) provide several information about locomotor activity of moving animals or humans. However, generally speaking, in vitro spinal tissue offers several advantages over in vivo experiments. One can benefit from easy manipulation of the external bath medium, application of drugs that do not cross the blood–brain barrier, the use of calcium and voltage-sensitive optical recording techniques and the ability to reversibly manipulate the excitability of networks within discrete segments of the spinal cord (Kudo and Yamada, 1987, Roberts et al., 1998, Bonnot et al., 2002b, Grillner, 2003). Since descending inputs are cut in isolated spinal cord, the spinal CPG is usually activated using bath-applied drugs such as dopamine, NMDA and serotonin (5-HT). Monoamines, such as 5-HT, dopamine and noradrenaline provide a high level of neuronal excitability which is necessary to recruit a sufficient number of neurons to activate the CPG (Kiehn et al., 1999a, Madriaga et al., 2004, Christie and Whelan, 2005, Liu and Jordan, 2005). Another great advantage of the in vitro preparation is its viability. They can stay alive for several hours and even after 24 h, being kept in physiological medium at room temperature, they still can elicit the fictive locomotion pattern with very good survival of neurons and motoneurons (Taccola et al., 2008). Beside the controlled concentration of O_2 and CO_2, there is no movement and mechanical noise due to heart beat or respiration.

25

The pattern of CPG activity can be compared with data from in vivo studies (Fig 9A). If one keeps the preparation consisting of the thoracosacral spinal cord with attached hindlimbs (Whelan et al., 2000), the hindlimbs flexion and extension along with alternating activity of motor nerves can be seen. The locomotor patterns can be recorded reliably by implanting wires into the muscle or by using suction electrodes to record neurograms (ENG) from selected muscle nerves (Whelan et al., 2000) (Fig 9B). Comparing the pattern produced in the ankle extensor and flexors with ventral root recordings, it was found that a signature of locomotor-like activity can be obtained by typically recording from the left and right lumbar 2 (L2) and 5 or 6 (L5/6) ventral roots (Whelan et al., 2000). The preparation can be reduced further (Fig. 9C) by dissecting away all tissue except for the spinal cord and the dorsal and ventral roots (Jiang et al., 1999). Recordings from the L1–3 segments show that bursts occur during the flexor phase, while bursts from L5–6 occur during the extensor phase. Notably, the excellent viability of the isolated in vitro spinal cord preparation has made it a convenient choice for many labs.

Neonatal isolated spinal cord preparations with post-natal age 0-2 demonstrate a good electrical activity for at least 24 h (Taccola et al., 2008) and, moreover, they are less sensitive to anoxia, presumably because of their small size. In general, neonatal isolated spinal cord preparations provide the chance of studying spinal network activity as well as the detailed structure of the network.
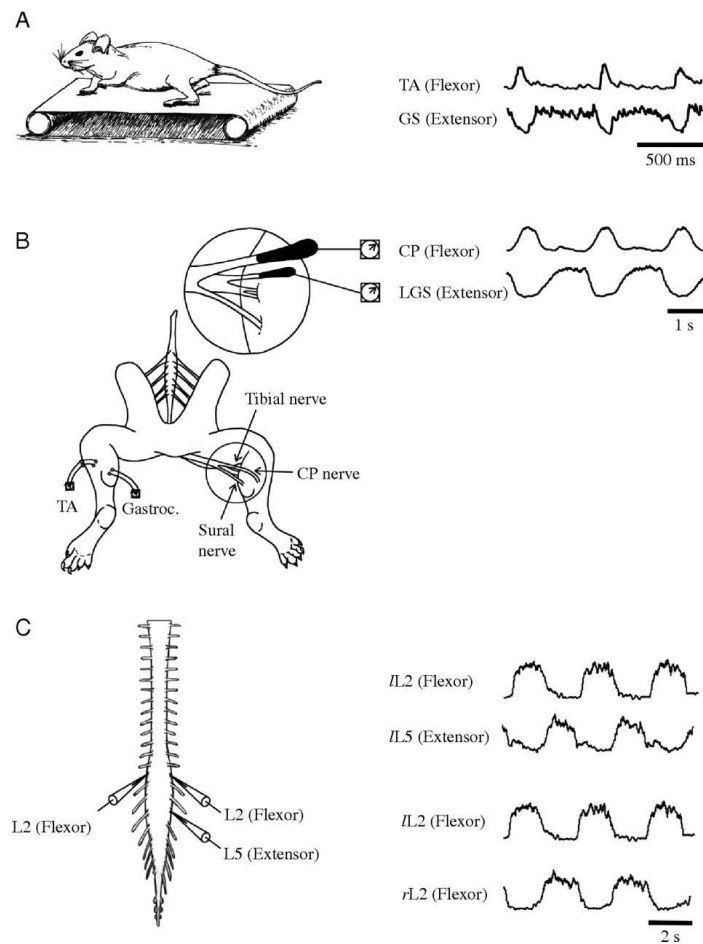
Figure 9: A) Pattern of flexor and extensor muscle activity recorded from a conscious adult mouse walking on treadmill. Adapted from Pearson et al. (Pearson et al., 2005), B) A hindlimbs-attached preparation can be used with electromyographs (EMGs) or electroneurograms (ENGs) to record output from spinal networks (Whelan et al., 2000, Pearson et al., 2003). C) Isolated spinal cord preparation commonly used to record locomotorlike patterns in vitro. Alternation between ipsilateral L2 and L5 ventral root recordings corresponds to flexor–extensor activity, while segmental alternation between the left (l) and right (r) L2 roots reflects left–right alternation (Whelan et al., 2000). CP, Common peroneal nerve; LGS, Lateral gastrocnemius nerve; TA, Tibialis anterior muscle; GS, gastrocnemius muscle. (Gordon and Whelan, 2006)

6. Locomotor network activity in isolated spinal cord

6.1. Reflex response

In the model of isolated neonatal spinal cord by application of electrical stimuli to the dorsal root (afferent fibers), one can observe the electrically evoked reflex response through recording of electrical discharges conveyed by homolateral ventral roots (VR). The minimum stimulus intensity to evoke a VR response homolaterally is considered as equivalent to 1 threshold (Th) value to induce a monosynaptic reflex response (Marchetti et al., 2001). Values of $\geq$ 2xTh stimuli induce polysynaptic responses as reported in our laboratory (Baranauskas and Nistri, 1995, Bracci et al., 1997) (Fig. 10A).

6.2. Fictive locomotion

Grillner et al. (2001) introduced fictive swimming in lamprey spinal cord. The corresponding mechanism in the mammalian spinal cord is called fictive locomotion. Fictive locomotion is the function of locomotor CPG to produce rhythmic oscillations alternating between left (l) and right (r) as well as flexor and extensor motor pools in an isolated spinal cord. Obviously in this case there is no supraspinal control on locomotor activity. Fictive locomotion can be induced chemically or electrically. Chemically induced fictive locomotion (Fig. 10C) appears when the CPG has been excited by application of drugs such as dopamine, NMDA and serotonin (5-HT). As it was mentioned before; serotonin, dopamine and noradrenaline evoke neuronal excitability which is necessary to activate a sufficient number of CPG neurons (Cazalets et al., 1992, Kiehn and Kjaerulff, 1996, Kiehn et al., 1999b, Grillner et al., 2001, Butt et al., 2002, Madriaga et al., 2004, Christie and Whelan, 2005, Liu and Jordan, 2005).

Electrically induced fictive locomotion (Fig. 10B) is also observed by monitoring obtained from electrical recordings of the activity from left (l) and right (r) L2 VRs (mostly flexor motor-pool command to the hindlimbs) and l and r L5 VRs (mostly extensor motor-pool commands to the hindlimbs) by application of DR train of stimuli (Marchetti et al., 2001,

Taccola et al., 2004). It contains the same phase alternation at segmental and intersegmental levels which is the hallmark of chemically induced fictive locomotion (Kiehn et al., 1997). In vivo and human experiments are also in accordance with the usage of electrical stimulation in order to evoke fictive locomotion. Epidural and subdural stimulation of spinal cord (dorsal surface) evoked locomotion in the decerebrate cats and stimulation of the lumbosacral enlargement induced hindlimb stepping (Iwahara et al., 1992). In human with complete SCI epidural stimulation in the level of T11 to L1, elicited locomotor-like EMG activity recorded from five muscle groups of the lower limbs (Dimitrijevic et al., 1998).

6.3. Disinhibited bursting

In vivo experiments on cats demonstrated that in the absence of inhibitory neurons (blocking glycinergic inhibition), which produce alternation between flexors and extensors (Kiehn et al., 1997), the spinal cord evokes paroxysmal activity (Fuortes and Nelson, 1963, Schwindt and Crill, 1981). In cultured spinal neurons, bicuculline, (Heyer et al., 1981) or the mixture of bicuculline and strychnine (Streit, 1993), induces irregular, self-sustained bursting. In the neonatal rat isolated spinal cord when synaptic inhibition is blocked (by strychnine and bicuculline), flexor and extensor motor pools are activated in synchrony (Beato and Nistri, 1999). Therefore, when blocking synaptic inhibition and removing the influence of descending inputs, the basic network function is still preserved, though this is not physiological (Fig. 10D,E).

It is shown that this type of network activity, as well as fictive locomotion, can be elicited and recorded from VRs in the condition of dorsal horn region ablation. However, in general, disinhibited bursting needs a simpler network property since it can be also evoked in a single isolated quadrant of ventral horn of spinal cord (Bracci et al., 1996).
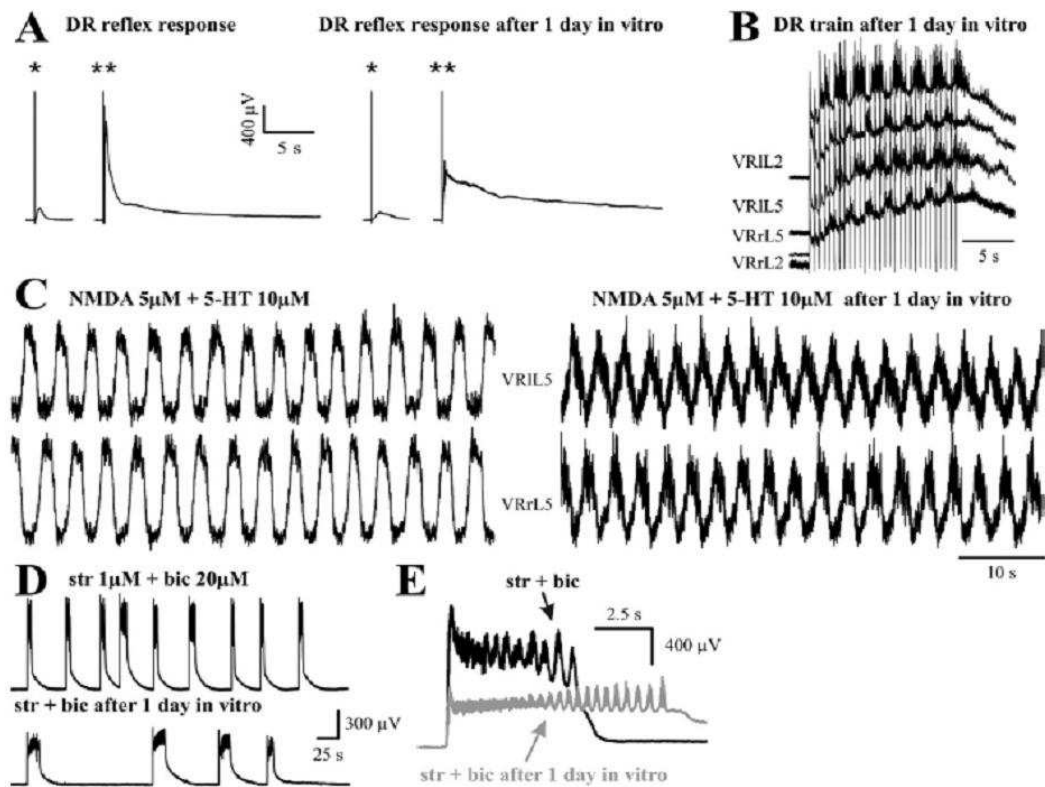
Figure 10: Electrophysiological properties of isolated neonatal rat spinal cord. A) DR reflex response evoked by low and high intensity stimulation in the first day (laft) and after 24 h in vitro (right). B) Fictive locomotion evoked by DR train of stimuli 24 h in vitro. Alternating oscillatory activity amongst four different VRs are observed by 2xTh stimuli intensity. C) Chemically evoked fictive locomotion (NMDA+serotonin) applied shortly after dissection (left) and after 24 in vitro (right) to the same preparation. D) Disinhibited bursting evoked by application of strychnine+ bicuculline on the first day (top) and after 24 h in vitro (bottom). E) Superimposed bursts in the first day (black) and 24 h later (grey). Longer burst duration and smaller amplitude was observed after 24 h. (Modified from Taccola et al., 2008)

Aims of the study

Excitotoxicity is considered to play an important role in the pathophysiological mechanisms of acute spinal cord injury. Pharmacological approaches are suggested to be useful not only to discover some new neuroprotective strategies against excitotoxicity, but also to provide a better understanding of the complex precesses which can contribute to neuronal injury. Electrophysiological recordings performed on the neonatal rat isolated spinal cord provided a good opportunity to test different pharmacological tools. Hyperactivation of Poly(ADP-ribose) polymerase is believed to be the chief effector of excitotoxic cell death. Therefore, in our study, we used different agents in order to protect the spinal cord against excitotoxic damage evoked by the glutamate analog kainate with the aim of understanding:

◆ The potential neuroprotective effect of PARP-1 inhibitors on electrophysiological properties of CPG against kainate evoked excitotoxicity:

   1) 6(5H)-phenanthridinone (PHE)
   2) N-(6-oxo-5,6-dihydrophenanthridin-2-yl)-(N,N-dimethylamino)acetamide.HCl (PJ-34)

◆ The effect of the potent inhibitor of PARP-1 activity, PJ-34, on network excitability.

◆ The potential neuroprotective effect of riluzole on electrophysiological properties of CPG against kainate evoked excitotoxicity.

In collaboration with molecular biology laboratory, we investigated whether fictive locomotion could be retained 24 h after excitotoxic insult and if there was any improvement in the synaptic transmission (reflex responses and cumulative depolarization) and the viability of cells (in grey and white matter) and motoneurons.

Methods, materials and results

Section 1

Mazzone GL, Margaryan G, Kuzhandaivel A, Nasrabady SE, Mladinic M, Nistri A (2010) Kainate-induced delayed onset of excitotoxicity with functional loss unrelated to the extent of neuronal damage in the in vitro spinal cord. Neuroscience 168:451-462.

KAINATE-INDUCED DELAYED ONSET OF EXCITOTOXICITY WITH FUNCTIONAL LOSS UNRELATED TO THE EXTENT OF NEURONAL DAMAGE IN THE *IN VITRO* SPINAL CORD

G. L. MAZZONE,[a1] G. MARGARYAN,[a1,2]
A. KUZHANDAIVEL,[a] S. E. NASRABADY,[a]
M. MLADINIC[a,b] AND A. NISTRI[a,b*]

[a]*Neurobiology Sector, International School for Advanced Studies (SISSA), Via Bonomea 265, 34136 Trieste, Italy*

[b]*Spinal Person Injury Neurorehabilitation Applied Laboratory (SPINAL), Istituto di Medicina Fisica e Riabilitazione, 33100 Udine, Italy*

Abstract—While excitotoxicity is a major contributor to the pathophysiology of acute spinal injury, its time course and the extent of cell damage in relation to locomotor network activity remain unclear. We used two *in vitro* models, that is, the rat isolated spinal cord and spinal organotypic cultures, to explore the basic characteristics of excitotoxicity caused by transient application of the glutamate analogue kainate followed by washout and analysis 24 h later. Electrophysiological records showed that fictive locomotion was slowed down by 10 μM kainate (with no histological loss) and fully abolished by 50 μM, while disinhibited bursting with unchanged periodicity persisted. Kainate concentrations ($\geq$50 μM) larger than those necessary to irreversible suppress fictive locomotion could still elicit dose-dependent motoneuron pool depolarization, and dose-dependent neuronal loss in the grey matter, especially evident in central and dorsal areas. Motoneuron numbers were largely decreased. A similar regional pattern was detected in organotypic slices, as extensive cell loss was dose related and affected motoneurons and premotoneurons: the number of dead neurons (already apparent 1 h after kainate) grew faster with the higher kainate concentration. The histological damage was accompanied by decreased MTT formazan production commensurate with the number of surviving cells. Our data suggest locomotor network function was very sensitive to excitotoxicity, even without observing extensive cell death. Excitotoxicity developed gradually leaving a time window in which neuroprotection might be attempted to preserve circuits still capable of expressing basic rhythmogenesis and reconfigure their function in terms of locomotor output. © 2010 IBRO. Published by Elsevier Ltd. All rights reserved.

Key words: spinal cord injury, kainic acid, kainate, fictive locomotion, motoneuron, organotypic culture.

Acute spinal cord injury (SCI) is a life-threatening condition with loss of motor, sensory, and vegetative functions below the site of injury (McDonald and Sadowsky, 2002; Schwab et al., 2006). SCI consists of a complex process starting with a primary lesion followed by secondary damage amplified and widened by massive release of glutamate, free radical production, and metabolic dysfunction (McDonald and Sadowsky, 2002; Schwab et al., 2006). The extensive release of glutamate causes excitotoxicity (Choi, 1992; Doble, 1999), that is believed to be an important contributor to the overall clinical picture (Hall and Springer, 2004; Park et al., 2004; Rossignol et al., 2007). How to protect neurons from excitotoxicity is still an open question. The results obtained using glutamate antagonists or free radical scavengers remain disappointing, perhaps because of poor understanding of the damage pathophysiology (Hall and Springer, 2004; Adams et al., 2007; Rossignol et al., 2007).

Our previous studies employed the rat isolated spinal cord preparation (Taccola et al., 2008) as an *in vitro* model to investigate the damage of spinal neuronal networks underlying locomotion after excitotoxicity. Using the stable glutamate receptor agonist kainate (a canonical method to induce excitotoxicity; Agrawal and Evans, 1986; Ben Ari and Cossart, 2000; Wang et al., 2005) at a fixed, high concentration, we were able to reliably evoke a reproducible pattern of lesion to spinal networks, and to asses the functional outcome in terms of locomotor network activity (fictive locomotion and disinhibited bursting) in relation with cell damage. Our study end point was the spinal network electrophysiological activity 24 h after a transient (1 h) application of kainate to mimic the reported clinical time course (<3 h) of most spinal cord injuries prior to intensive care treatment, when the impact of the primary insult is expected to be stabilized (Bracken et al., 1990; Pointillart et al., 2000; Hall and Springer, 2004).

Our observations, however, prompted a number of questions which are the subject of the present report. In particular, we wished to explore whether the kainate-evoked damage was dose-dependent and related to the survival of a critical number of cells in strategically important spinal areas. Furthermore, we were interested to find

---

[1] Joint first authors.

[2] Present address: Department of Neuroscience, Karolinska Institute, Stockholm, Sweden.

*Correspondence to: A. Nistri, Neurobiology Sector, SISSA, Via Bonomea 265, 34136 Trieste, Italy. Tel: +39-040-37-56-518; fax: +39-040-37-56-502.

E-mail address: nistri@sissa.it (A. Nistri).

Abbreviations: APV, aminophosphonovalerate; ANOVA, analysis of variance; CNQX, 6-cyano-7-nitroquinoxaline-2,3-dione; CTR, control; CV, coefficient of variation; DAPI, 4′,6-diamidino-2-phenylindole; DIV, days *in vitro*; DME/HIGH, Dulbecco's modified Eagle's medium high glucose; FBS, fetal bovine serum; FCS, fetal calf serum; HCl, hydrochloric acid; KA, kainate; l, left; L, lumbar (followed by root number); MTT, 3(4,5-dimethyltiazolyl-2)-2,5 diphenyl tetrazolium; NeuN, neuronal specific nuclear protein; NIH, National Institutes of Health; NMDA, *N*-methyl-D-aspartate; NSC-34, neuroblastoma-spinal cord subclones 34; PBS, phosphate buffer saline; r, right; r.o.i., region of interest; SCI, spinal cord injury; SD, standard deviation; SMI 32, neurofilament H non-phosphorylated; T, thoracic; VR, ventral root; 5-HT, 5-hydroxy-tryptamine.

out the time course of excitotoxicity to understand the time frame potentially available to pharmacological neuroprotection. Finally, we were concerned to find out the *in vitro* excitotoxicity threshold since this information might be useful to relate it to the excitotoxic process reported for brain regions.

To this end, we used two parallel preparations, namely the *in vitro* spinal cord of the rat and the organotypic spinal slice culture. The first allowed us to collect functional data related to locomotor network activity 24 h after the excitotoxic stimulus, the latter enabled us to perform more detailed time-related observations in terms of cell survival and metabolic activity.

EXPERIMENTAL PROCEDURES

Rat isolated spinal cord preparation

For our experiments, thoracolumbar spinal cord preparations were isolated from neonatal Wistar rats (0–2 days old) in accordance with the National Institutes of Health (NIH) guidelines and the Italian act D.Lgs. 27/1/92 n. 116 (implementing the European Community directives n. 86/609 and 93/88) under urethane anesthesia (0.2 ml i.p. of a 10% w/v solution). All efforts were aimed at reducing the number of animals used for the present project and at minimizing their suffering.

Spinal cords were continuously superfused in a recording chamber with Krebs' solution of the following composition (in mM): NaCl, 113; KCl, 4.5; $MgCl_2 7H_2O$, 1; $CaCl_2$, 2; NaH_2PO_4, 1; $NaHCO_3$, 25; glucose, 11; gassed with 95% O_2 5% CO_2; pH 7.4 at room temperature. All details about laboratory procedures have been previously published (Bracci et al., 1996a,b, 1997; Beato and Nistri, 1999) and the experimental setup has been fully reported (Taccola and Nistri, 2006; Taccola et al., 2008; Margaryan et al., 2009). Drugs were dissolved in Krebs solution and bath-applied at the concentrations indicated in the text.

Electrophysiological recordings

DC-coupled records were obtained from lumbar (L) ventral roots (VRs) with tight-fitting miniature Ag/AgCl suction electrodes (Taccola and Nistri, 2006). Signals were processed with pClamp software (version 9.2; Molecular Devices, Sunnyvale, CA, USA) for subsequent off-line analysis (Taccola and Nistri, 2006). Fictive locomotion was typically induced by continuously bath-applied *N*-methyl-D-aspartate (NMDA) (4 or 5 μM) plus 5-hydroxytryptamine (5-HT; 10 μM; Kiehn and Kjaerulff, 1998; Butt et al., 2002). Signals were recorded from left (l) and right (r) L2 VRs that express mainly flexor motor-pool commands to the hind limbs, and l and r L5 VRs conveying mainly extensor motor-pool commands to the same limbs (Kiehn and Kjaerulff, 1998). The period value for rhythmic discharges was measured as the time between the onset of two cycles of oscillatory activity (calculated after averaging at least 20 cycles), and its regularity indicated by the coefficient of period variation (CV; given by standard deviation [SD] mean^{-1}). Disinhibited bursting (Bracci et al., 1996a,b, 1997) was induced by continuously bath-applied strychnine (1 μM) and bicuculline (10 μM). Full details concerning the definition of bursts and their measurements were in accordance with Bracci et al. (1996a,b).

Kainate-evoked lesion protocol and data analysis

With the aim to find out the excitotoxicity threshold in terms of electrophysiological and histological damage and to assess its dose dependence, we applied kainate for 1 h at different concentrations ranging from 10 μM to 1 mM. Kainate was washed out after 1 h with standard Krebs solution superfused for up to 24 h. In each preparation, only one concentration of kainate was used once. The 1 mM concentration has been empirically found to induce irreversible loss of fictive locomotion (Taccola et al., 2008). The 10 μM concentration was our lowest experimental dose since previous studies have indicated that, on the same preparation, ≤5 μM kainate produced fictive locomotion without toxic effects (Cazalets et al., 1992). Electrophysiological responses, such as fictive locomotion, disinhibited bursting and reflex activity were monitored for up to 24 h. At this end point, spinal cords were fixed and used for histological analysis as detailed below.

Immunohistochemistry

Immunohistochemical labeling was performed using a free-floating method as described previously (Taccola et al., 2008). Briefly, paraformaldehyde-fixed spinal cords were cryoprotected with 30% sucrose and sectioned (30 μm). After incubation in blocking solution (5% normal goat serum, 5% bovine serum albumin, 0.3% Triton-x 100) for 1 h at room temperature, the primary antibody was incubated at 4 °C overnight and visualized using secondary anti-mouse Alexa fluor 488 or 594 antibodies (1:500). Sections were finally stained with 4′,6-diamidino-2-phenylindole (DAPI) for 20 min and analyzed using a Zeiss Axioskop2 microscope and Metavue software (Margaryan et al., 2010). In accordance with our previous reports (Taccola et al., 2008; Margaryan et al., 2009, 2010), the following antibodies were used: mouse anti-NeuN monoclonal antibody (1:50, clone A60; Millipore, Milan, Italy), mouse anti-SMI 32 monoclonal antibody (1:200, clone SMI-32; Covance, Emeryville, CA, USA). Suppl. Fig. 1 shows that, as negative control, omission of the primary antibodies gave minimal signal comparable to the background autofluorescence.

Quantification of dead cells

The identification and quantification of dead or dying cells in the spinal cord after experimental insults were performed as previously reported (Taccola et al., 2008). For each experimental group, three spinal cords were analyzed and for each spinal cord, four to six sections from thoracic T12 to L3 segments were examined because these regions are known to contain the locomotor central pattern generator (Kiehn, 2006). In each section, three areas of the spinal cord were investigated by immunofluorescence: dorsal grey matter (Rexed layers I–IV), central grey matter (Rexed layers V–VIII and X), and ventral grey matter (Rexed layer IX). For each area of the spinal cord, three to seven fields of 280×280 μm size in the grey matter were analyzed by counting NeuN immunopositive elements and quantifying data using eCELLence software (Glance Vision Tech, Trieste, Italy). Motoneurons were counted as large ventral horn cells immunopositive for SMI 32 in laminae VIII and IX.

Preparation of organotypic cultures and protocol to study excitotoxicity

Pregnant Wistar rats, at day 13 of gestation, were used to prepare embryonic organotypic slice cultures of spinal cord in accordance with previously published procedures (Gahwiler et al., 1997; Ballerini and Galante, 1998; Ballerini et al., 1999; Avossa et al., 2003). The fetuses were delivered by Caesarean section from anaesthetized rats (10.5% chloral hydrate, 0.4 ml/100 g i.m.) subsequently killed by an intracardiac injection (2 ml) of chloral hydrate. This procedure is in accordance with the regulations of the Italian Animal Welfare Act and is in accordance with the NIH guidelines. The fetuses were decapitated and their backs, isolated from their limbs and viscera, were cut into 275 μm thick transverse slices from which the spinal cord was punched out and fixed on a glass coverslip with reconstituted chicken plasma coagulated by one drop of thrombin (200 U/ml). Coverslips were inserted into plastic tubes with 1 ml of medium contained 82% Dulbecco's

Modified Eagle's medium, 8% sterile water for tissue culture, 10% fetal bovine serum (FBS; Invitrogen, Italy), osmolarity 300 mOsm, pH 7.35. From each dissection, 30–40 slices were prepared from the thoracic as well as the lumbar segments, and kept in culture for 22 days *in vitro* (DIV) before use. The tubes were kept in a roller drum rotating (120×*g*/h) at 36.5 °C. Dulbecco's Modified Eagle's medium with high glucose (DME/HIGH), penicillin, and streptomycin (purchased from Euroclone, Devon, UK). Fetal calf serum was obtained from Invitrogen, (Carlsbad, CA, USA). Nerve growth factor (NGF) was from Alomone Laboratories (Jerusalem, Israel), chicken plasma from Rockland (Gilbertsville, PA, USA), and thrombin from Merck, (Darmstadt, Germany).

At 22 DIV, organotypic spinal slices were incubated in complete medium using one of the following protocols: (i) control group in standard condition; (ii) kainate group treated with 100 or 1000 μM for 1 h. After treatment, slices were washed thrice and left in complete medium to recover.

Immunofluorescence of organotypic cultures

Slices were fixed in 4% paraformaldehyde for 1 h at room temperature and stored in phosphate buffer saline (PBS) until use. Cultures were processed for immunofluorescence analysis by immersion for 10 min in trypsin solution (0.05% in sterile water) at 37 °C. Slices were then blocked with 3% fetal calf serum (FCS), 3% bovine serum albumin (BSA), 0.3% Triton in PBS (blocking solution) for 1 h at room temperature, followed by overnight incubation at 4 °C in a blocking solution containing the NeuN antibody (at 1:250 dilution). The primary antibody was visualized using corresponding secondary fluorescent antibody (Alexa Fluor 488, at 1:500 dilution, Invitrogen, Carlsbad, CA, USA). To visualize cell nuclei, slices were incubated in 1 μg/ml solution of DAPI for 1 h and mounted using Vectastain mounting medium (Vector Laboratories, Burlingame, CA, USA). DAPI staining results were analyzed using a Zeiss Axioskop2 microscope. NeuN positive cells were analyzed using a Confocal (Leica DMIR2) microscope, equipped with Ar/ArKr (at 488 nm) laser. Motoneurons were visualized with the same SMI 32 antibody (1:1000) employed for tissue histochemistry as previously described (Taccola et al., 2008; Margaryan et al., 2010).

Quantification of dead cells

The identification and quantification of dead or dying cells in the organotypic cultures was performed as previously shown (Taccola et al., 2008), using DAPI nuclear staining and "eCELLence" software. Three different regions of interest (r.o.i.), namely dorsal, central, and ventral, were analyzed in each slice (see scheme in Fig. 3A). The average percent values of nuclei showing condensed chromatin (normalized to the total number of nuclei) were compared between different r.o.i. for control or kainate (KA) treated slices and expressed as mean±SD (using at least three different cell culture series for each experimental group). NeuN positive cells were analyzed using confocal microscopy, whereby a stack of 25–30 images (20× magnification) were counted with "eCELLence" software using the same intensity threshold (ranging from 0 to 1 where 1 refers to the maximum intensity of the image) and cell diameter parameters (in pixels related to the spatial resolution of the identification; http://www.gvt.it/en/ecellence/documentation/index.php) for all experiments. The total number of NeuN positive cells was obtained for each experimental condition as the total number of positive cells in all stacks. Multiple entries of the same object were considered as single entities by the "eCELLence" software algorithm.

MTT mitochondrial toxicity test on organotypic cultures

In accordance with the standard procedure (Mosmann, 1983), a stock solution of 3(4,5-dimethyltiazolyl-2)-2,5 diphenyl tetrazolium (MTT) was dissolved (5 mg/ml) in PBS (pH 7.4) and diluted to final 0.5 mg/ml in DME/HIGH. Cells were incubated with DME/HIGH containing MTT for 2 h at 37 °C; at the end of this incubation period, the medium was discarded and replaced with 1 ml of HCl (with 0.04 M isopropanol) to dissolve cells containing the MTT formazan crystals. These samples were then kept in a roller drum at 36.5 °C overnight. After centrifugation at 10,000×*g* for 5 min, absorbance values (wavelength=570 nm) were obtained with a Bio-Rad microplate reader (model 550, Bio-Rad Laboratories, Inc., Dorset, UK). Results were expressed as percentage of the values obtained from control cultures in complete medium that were considered to be 100% viable. Further checks were run to establish the relation of the signal to the cell metabolic activity: in particular, we checked that by incubating two slices in control condition the MTT signal was doubled. In addition, we wished to find out if there was a clear relation between cell numbers and MTT assay values. To this end, we used the neuroblastoma-spinal cord subclones 34 (NSC-34) cell line, a hybrid cell line produced by fusion of motor neurone-enriched embryonic mouse spinal cord cells with mouse neuroblastoma cells (Cashman et al., 1992; kindly donated by Dr. Silvia Di Angelantonio, University of Rome), that showed a linear relation (r=0.996) between the number of cells (counted with Counting Chamber Thoma, Vetrotecnica, Padova, Italy) and the MTT formazan production (Suppl. Fig. 2). This result shows that, under the present experimental conditions, the MTT test was a useful index of cell metabolic activity.

Data analysis

Data were expressed as means±SD; *n* indicates the number of spinal cord preparations for electrophysiology and histochemistry. In organotypic culture experiments (from 22 separate batches), *n*=number of slices unless otherwise stated. Statistical analysis was carried out with SigmaStat (SigmaStat 3.1, Systat Software, Chicago, IL, USA): after using the normality test to distinguish between parametric and non-parametric data, parametric values were analyzed with the Student *t*-test (paired or unpaired) for two groups and one-way analysis of variance (ANOVA) for multiple comparisons (with Tukey–Kramer post hoc test). For non-parametric values, the Mann–Whitney test was used for two groups. The accepted level of significance was always $P < 0.05$.

Drugs

Kainate was purchased from Ascent Scientific (Weston-supermare, UK), NMDA was purchased from Tocris (Bristol, UK), while 5-HT and strychnine hydrochloride were purchased from Sigma (Milan, Italy). Bicuculline methiodide was obtained from Fluka (Milan, Italy). Other reagents and chemicals were purchased from Sigma.

RESULTS

Electrophysiological effects of different concentrations of kainate on the isolated spinal cord

The concentration range of kainate used for such experiments varied 100 fold from 10 to 1000 μM to examine the issue of dose-related excitotoxicity since previous studies have shown that concentrations of kainate below 10 μM were well tolerated in terms of locomotor cycle activity by the neonatal rat spinal cord (Cazalets et al., 1992). In all our experiments, fictive locomotion was first tested with standard applications of NMDA (4 μM) and 5HT (10 μM) in control conditions, thereafter the kainate solution was applied for 60 min, and washed out for further 24 h when electrophysiological tests were repeated prior to histological analysis.
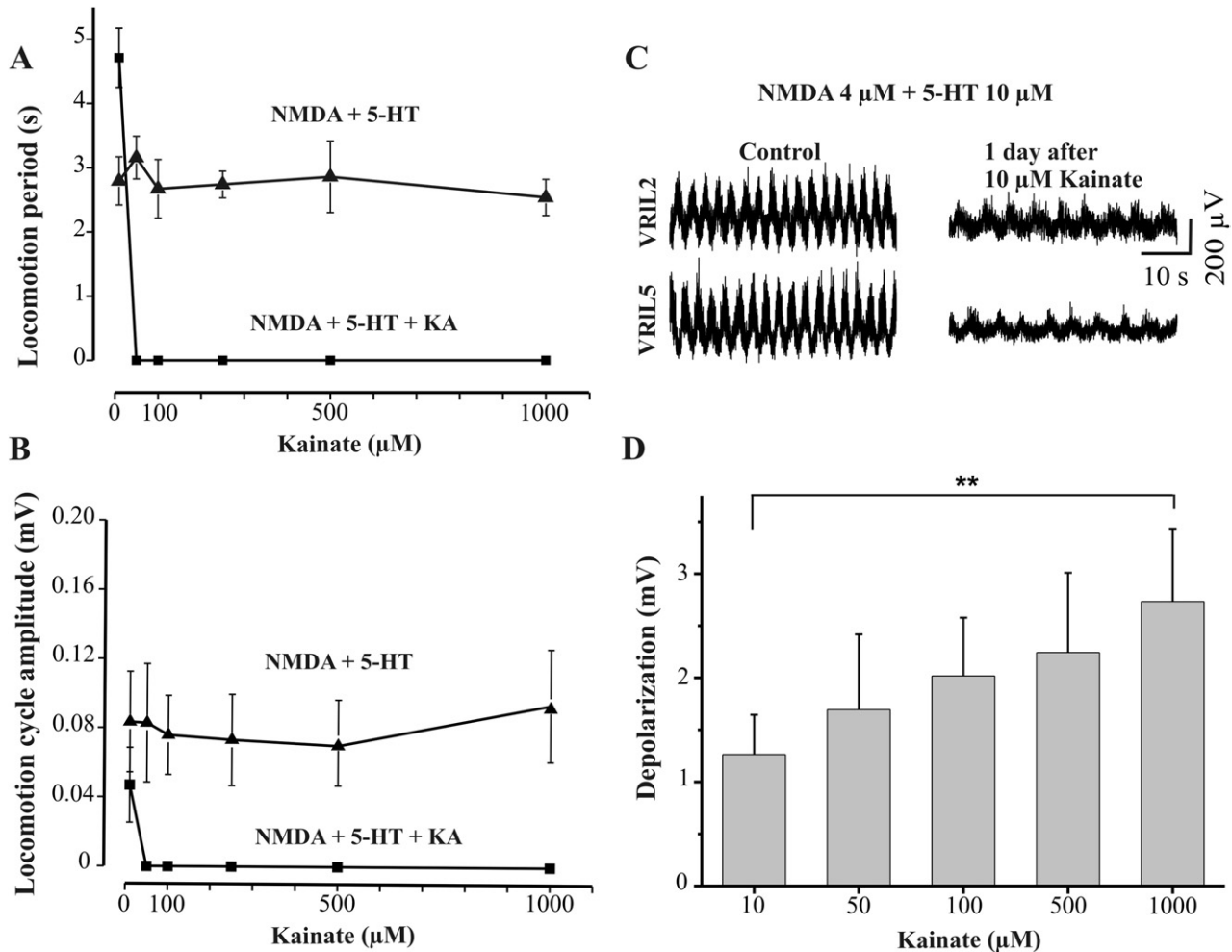
Fig. 1. Dose-dependent functional effects of kainate on the isolated spinal cord. (A, B) Plot of fictive locomotion periodicity or cycle amplitude versus kainate concentrations in sham preparations (filled triangles) or kainate-treated preparations (filled squares). Note that fictive locomotion was detectable only after 10 μM kainate (KA). $P<0.001$; $n=5$. (C) example of fictive locomotor patterns recorded from IL2 and IL5 VRs in the presence of NMDA and 5-HT. On the same preparation, these patterns were recorded 24 h following 1 h application of 10 μM kainate. Note reduction in cycle periodicity and amplitude. (D) histograms plotting the amplitude of VR depolarization evoked by different kainate concentrations. $n=4-6$. ** $P=0.01$.

Fig. 1A, B show that the alternating oscillations (recorded from IL 2 and IL5VRs) typical of fictive locomotion recorded in control solution had slower periodicity (4.97± 0.45 vs. 2.56±0.25 s control; $P\leq0.001$) and smaller amplitude (0.02±0.004 vs. 0.04±0.01 mV control; $P\leq0.001$) 24 h after 1 h application of kainate (10 μM) as exemplified in Fig. 1C. The data plotted in Fig. 1A, B indicate that, following 10 μM kainate application, cycle period, and amplitude were significantly ($P=0.027$; $n=5$) different from those of control sham preparations.

Concentrations of kainate equal to (or above) 50 μM produced consistent disappearance of fictive locomotion (Fig. 1A, B) with no recovery. Despite the irreversible, full suppression of this pattern, we could still observe a dose-dependent VR depolarization by kainate as shown by the histograms of Fig. 1D. Thus, loss of fictive locomotion was observed even in the presence of kainate-mediated VR depolarizations that were only half of the depolarization produced by 1 mM kainate (known to induce extensive

neurotoxic damage to the spinal cord; Taccola et al., 2008).

The functional activity of the spinal networks following application of 10 μM kainate was evaluated in four preparations by monitoring disinhibited bursting that had slower, irregular periodicity (89±33 s with CV=0.57± 0.23), longer burst duration (12.8±3.3 s), and lower burst amplitude (0.81±0.32 mV) than the one normally observed in control (Taccola et al., 2008; Margaryan et al., 2010). Nevertheless, comparing such data after 10 μM kainate with those recorded 24 h after the application of a very large (1 mM) dose of kainate showed that the only significant ($P<0.001$) difference was in the burst amplitude (0.22±0.10 mV; $n=13$) since period (67±26 s with CV= 0.36±0.16) and burst duration (10.5±4.2 s) were unchanged.

We also examined the characteristics of disinhibited bursting 24 h after 100 μM kainate, that showed 95.9± 14.5 s periodicity (CV=0.45±0.27), 0.39±0.16 mV ampli-

tude, and 13.5±1.9 s duration. Again, only the burst amplitude was significantly larger ($P<0.05$) than the value found after 1 mM kainate. These data demonstrate that the pattern of disinhibited bursting was relatively constant despite pretreatment with distinct doses of kainate, whose delayed consequences were observed as smaller amplitude of bursts and loss of rhythm regularity as indicated by the large CV value.

The electrophysiological records, thus, suggested that there was a critical threshold for kainate-mediated excitotoxicity in terms of suppression of fictive locomotion despite preservation of intrinsic rhythmicity and motoneuron pool depolarization. Using the same preparations employed for electrophysiology, we therefore analyzed their histological picture.

Histological characterization of kainate-evoked spinal damage

Since our previous experiments have demonstrated that kainate (1 mM) primarily damages the gray matter with minimal destruction of the white matter (Taccola et al., 2008), we focused on the ventral and dorsal horns which were analyzed as formerly reported. First, we examined large (>25 μm somatic diameter) ventral horn cells which were immunopositive for SMI 32 and, thus, identified as motoneurons (Taccola et al., 2008). Fig. 2A shows an example of the ventral horn laminae VIII–IX with motoneurons from sham or kainate-treated preparations. The excitotoxic action of kainate was manifested by a much lower number of motoneurons as quantified in Fig. 2B in which motoneuron numbers drastically fell 24 h after 50 or 100 μM kainate in analogy with the effects previously observed after 1 mM kainate (Taccola et al., 2008). Conversely, global neuron numbers (examined with NeuN immunoreactivity; see Fig. 2C) were less severely decreased by kainate in the ventral horn as indicated by the histograms summarizing data for the three r.o.i. under investigation (Fig. 2D). The largest fall in neuronal number affected the gray matter of the dorsal horn region, where the majority of kainate receptors are expressed in the neonatal spinal cord (Tölle et al., 1993). From these results, it is apparent that 10 μM kainate preserved nearly typical numbers of motoneurons and propriospinal neurons together with impaired locomotor network activity, implying dysfunction rather than cell loss.

Excitotoxicity of kainate on spinal organotypic cultures

We first mimicked the experimental protocol employed for the isolated spinal cord preparations in order to investigate how this model was sensitive to kainate excitotoxicity. Thus, organotypic spinal slices were treated with kainate for 1 h, rinsed and examined at three time points to check for early and delayed toxicity. In accordance with previous quantitative studies of organotypic spinal cultures at the same stage of development (Sibilla et al., 2009), we examined the topographic distribution of cells with condensed chromatin in three r.o.i. (indicated by the dotted lines), namely dorsal, central, and ventral as exemplified in Fig. 3A.

The lower panels of Fig. 3A (larger magnification) show cells with condensed chromatin nucleus in the central area incubated in control medium (top) or 24 h after 1000 μM kainate (bottom), indicating substantial cell damage. Fig. 3B, C quantifies this phenomenon observed following 100 or 1000 μM kainate application. Inspection of these histograms indicates that, in all three r.o.i. examined, there was a time-related rise in the percentage of nuclei with condensed chromatin which reached the largest value at 24 h. Fig. 4A shows, for the central region, that the cell damage (in terms of condensed chromatin appearance plotted versus time elapsed after the end of kainate application) grew by 75 cells/4 h following 100 μM kainate, while it increased by 132 cells/4 h after 1000 μM kainate. On the other hand, application of NMDA (4 μM) and 5-HT (10 μM) for 1 h followed by 24 wash did not induce any increment in the number of condensed chromatin cells (Fig. 4A). These results, thus, indicate a delayed onset of excitotoxicity with spinal cell loss dependent on kainate concentration.

We next wished to assess whether the surviving cells displayed metabolic activity significantly impaired 24 h after kainate application. Fig. 4B shows that the MTT formazan formation (filled bars; taken as a non-invasive index of metabolic activity of the network) was 79±15% ($n=8$) and 67±12% ($n=18$) after 100 and 1000 μM kainate, respectively. This observation suggested metabolic dysfunction that closely corresponded to the parallel emergence of dead cells (Fig. 4C; expressed as % of the global DAPI positive cell number) rising from 3±1% (control) to 27±8% and 38±4% after 100 and 1000 μM kainate, respectively.

These observations led us to examine the cell populations involved in such a damage. Fig. 5A exemplifies neuronal damage (taken as fewer immunoreactive NeuN positive cells in the central region of the organotypic slice) induced by kainate 24 h after its application and washout. The extent and time course of neuronal loss are plotted in Fig. 5B, C for 100 or 1000 μM kainate. Pooling data from the three r.o.i. showed that the average control value of 235±92 neurons ($n=8$) fell to 97±42 ($n=5$) or 102±61 ($n=7$) following 100 or 1000 μM kainate, respectively. We could then compare the NeuN positive cell disappearance during the first 4 h after washing out kainate. The 100 μM concentration led to a loss of 17 neurons/4 h, a value which was approximately half of the one (27/4 h) found after 1000 μM kainate. The neuronal loss was, therefore, comparable to the appearance of condensed chromatin nuclei (Fig. 4A), confirming that the damage was primarily affecting neurons rather than glia.

Fig. 6A shows that a similar cell loss was observed when we examined the number of motoneurons 24 h after 100 or 1000 μM kainate. In fact, in the ventral r.o.i., the number of motoneurons fell from 11±3 ($n=12$) to 7±3 ($n=13$) and 7±2 ($n=6$), a result in accordance with the observation on the isolated spinal cord treated with kainate (Fig. 2B).
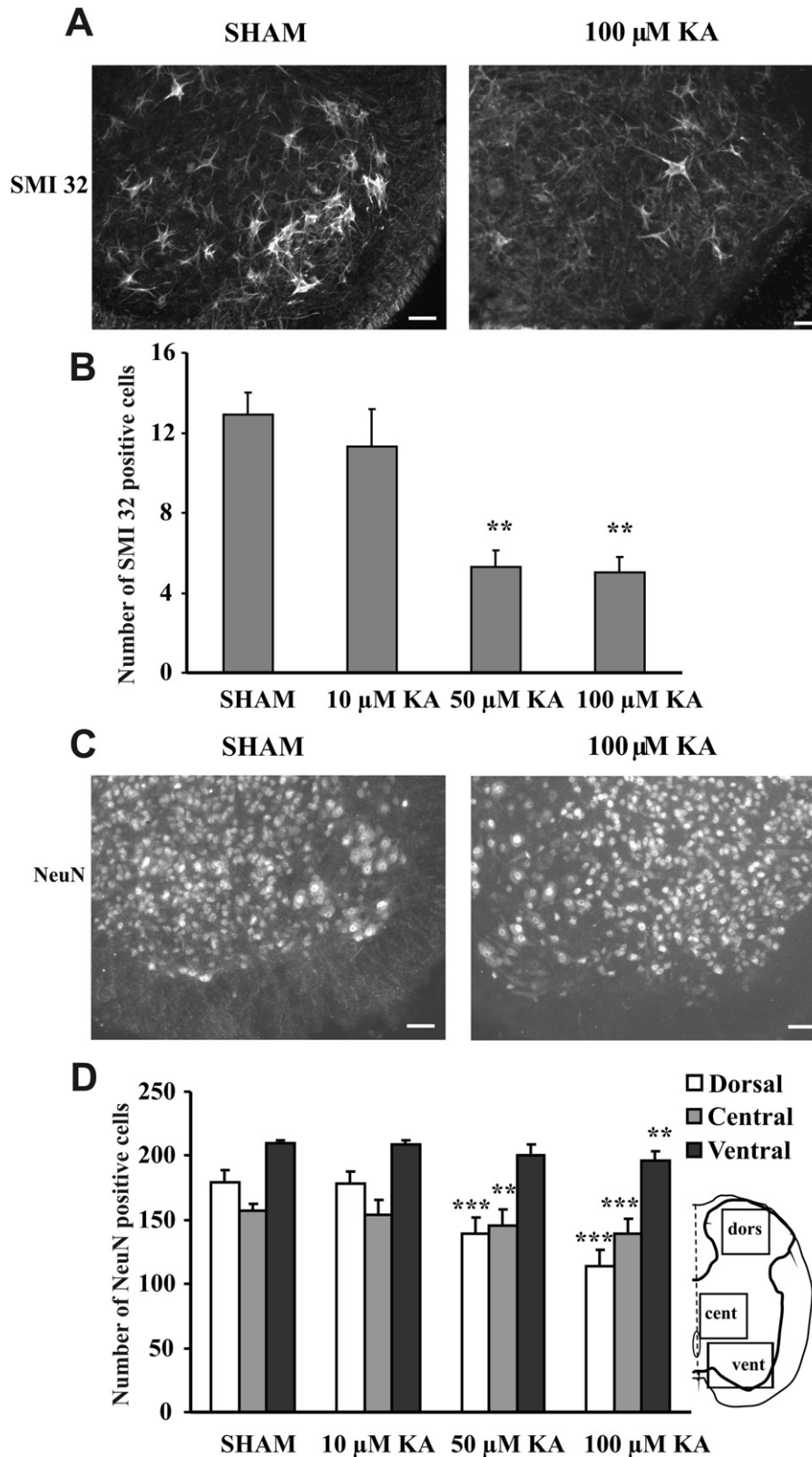
Fig. 2. Quantification of concentration-dependent effect of kainate on motoneurons and neurons of the isolated spinal cord. (A) Representative images showing SMI 32 positive neurons in the laminae VIII and IX of sham (left) or 100 μM kainate-treated (right) spinal cords. (B) Histograms showing number of SMI 32 positive neurons counted in 30 μm sections of sham or kainate (10–100 μM) treated spinal cords. (C) NeuN immunoreactivity in the ventral region of sham or 100 μM kainate-treated spinal cords. (D) Histograms showing number of NeuN positive neurons, counted in a 230×230 μm area of the dorsal (open bar) or central gray matter (gray bar), and in an 500×500 μm (filled bar) area of the ventral gray matter. Data in (B) and (D) were collected from the same spinal cord preparations (n=3–5). Inset shows schematic diagram indicating r.o.i. used for NeuN counting. Bar=50 μm. For (B, D), *** P<0.001, ** P<0.01.

Fig. 3. Quantification of cell loss in rat organotypic slices cultures after application of kainate. (A) Top panel shows a low power view of one organotypic slice in which the three r.o.i. used for cell counting are outlined with a dotted line. Middle and lower panels show higher magnification view of the cent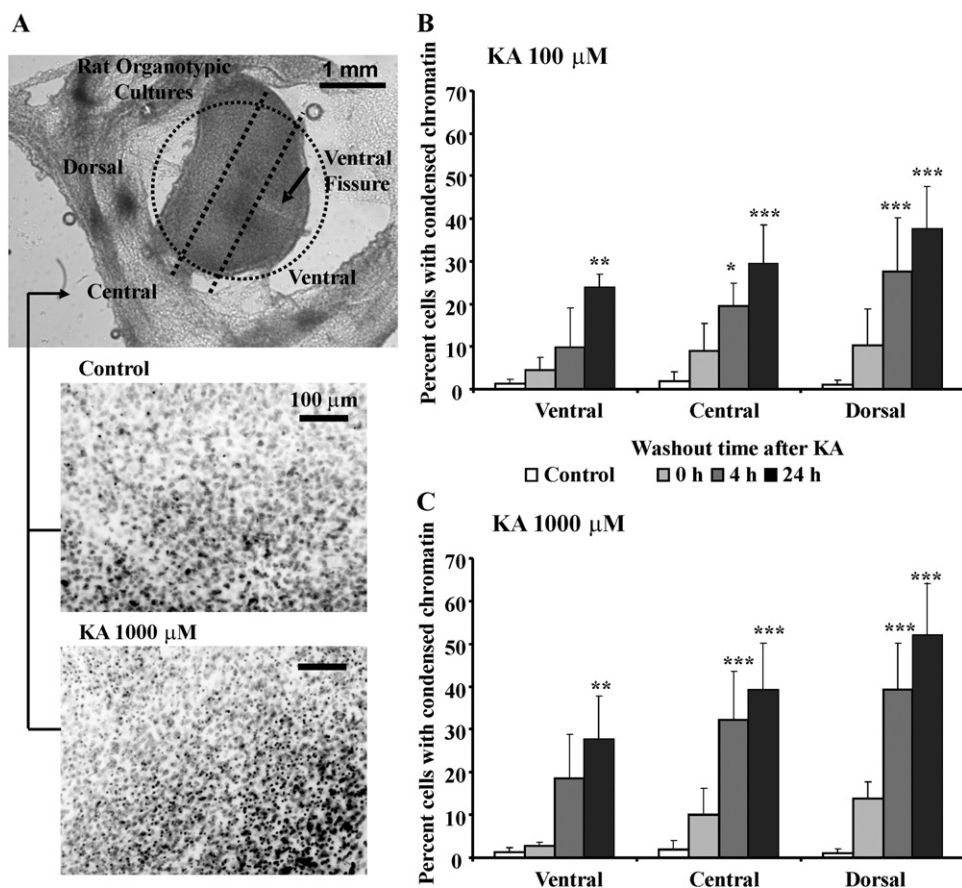ral area in control or 24 h after kainate (1000 μM; 1 h) application which produced increased occurrence of cells with condensed chromatin nucleus (stained with DAPI). (B, C) Histograms showing, for the three r.o.i., the number of cells with condensed chromatin (expressed as percent of total cells in the same region) counted at 4 or 24 h after 1 h application of kainate (100 in B or 1000 μM in C). The average data are from three experiments: in each one of them six slices were used (running in duplicate for control or the two kainate concentrations used). * $P<0.05$, ** $P<0.01$, *** $P<0.001$ vs. controls (untreated cultures).

DISCUSSION

The principal finding of this study is that even a relatively short excitotoxic stimulus (below the maximal tissue effect) induced a clear impairment in spinal locomotor network function without histological damage. A small increment in the concentration of the excitotoxic agent irreversibly abolished locomotor patterns despite preservation of substantial numbers of network neurons. This observation implies a strongly non-linear relation between the network ability to express the locomotor program and the number of viable neurons.

Excitotoxicity mediated by kainate

Our previous studies have shown how a large concentration of kainate irreversibly suppresses locomotor output in the rat spinal cord *in vitro* (Taccola et al., 2008). The goal of that investigation was to induce maximum histological damage and to find out the functional consequences in electrophysiological terms. Despite the 1 mM kainate concentration used, it was surprising to see that at least half of the network neurons survived and that disinhibited bursting

was still present (Taccola et al., 2008). We then argued that, if a very strong excitotoxic stimulus had left residual cells and function in spinal networks (that we could not, however, neuroprotect satisfactorily; Margaryan et al., 2010), perhaps weaker excitotoxic insults could spare a larger fraction of the networks and be more susceptible to neuroprotection. These considerations, thus, led us to carry out the present study in which, by using two different preparations, we wished to find out the extent, the time course and the functional consequences of excitotoxicity of graded intensity. Our focus was on neurons since glia was rather resistant to kainate damage even when applied at 1 mM concentration (Taccola et al., 2008).

Although the *in vitro* spinal cord model suffers of limitations because of tissue immaturity and absence of vascular supply, it has been proven useful to investigate the basic mechanisms of rhythmogenesis, including the locomotor program, and the minimal network membership required to generate it (Nistri et al., 2010). These data are possibly relevant to future studies of tissue repair and regrowth, and may also be interesting to understand the pathophysiology of paediatric spinal cord injury, a rather
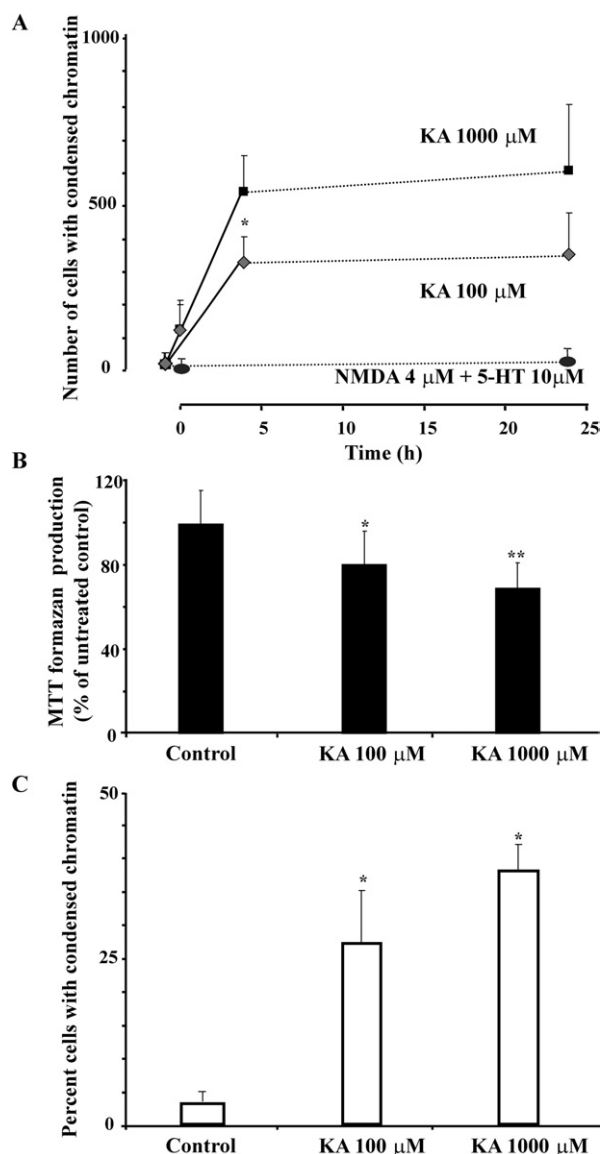
Fig. 4. Cell loss and metabolic dysfunction of organotypic slices after kainate. (A) Plot of cells, in the central region, showing condensed chromatin nucleus at various times after washout (0 h) of 100 μM (grey diamonds) or 1000 μM (filled squares) kainate. Data points prior to 0 time refer to values collected from untreated sister cultures and indicate the baseline control occurrence of condensed chromatin nuclei (21 ± 23; six slices run in duplicate). Note the steeper emergence of damaged cells following the larger concentration of kainate. At 4 h, the values for 100 or 1000 μM kainate plots were significantly different ($P=0.0005$; data are from pooling values for the three r.o.i. analyzed in Fig. 3B, C). Application of NMDA and 5-HT for 1 h followed by 24 wash does not increase the number of cells with condensed chromatin ($n=2$ slices at 0 time and $n=4$ slices at 24 h). Controls were untreated cultures. (B) Histograms showing the MTT formazan production (index of metabolic activity) 24 h after 100 or 1000 μM kainate application (1 h). Results are expressed as mean percent values of five independent experiments ($n=19$ slices for control; $n=7$ slices for 100 μM kainate; $n=18$ slices for 1000 μM kainate) where controls were taken as 100%. * $P<0.05$, ** $P<0.01$ vs. control. (C) Histograms showing the dose-related increment in cells with condensed chromatin 24 h after 100 or 1000 μM kainate (* $P<0.05$; data are from pooling values for the three r.o.i. analyzed in Fig. 3B, C). As the percent of damaged cells grows, there is a similar fall in % production of MTT formazan.

common type of trauma (Vitale et al., 2006; Achildi et al., 2007). Previous studies have shown that motoneurons in mixed embryonic mouse spinal cultures (Carriedo et al., 1996) or adult rat acute slices (Pizzi et al., 2000) are readily damaged by kainate concentrations in the 10–300 μM range. Both reports indicate motoneuronal loss higher than the ones reported in the present study. These investigations, however, lack functional measurements of network (or motoneuron) activity and of the time course of kainate damage. Furthermore, adult slice preparations have limited viability in vitro as suggested by the widespread apoptosis detected even in the absence of kainate application (Pizzi et al., 2000). To circumvent these problems, the current study thought it useful to employ isolated or organotypic spinal cord preparations that retained their function, connectivity, and long-term viability.

We started with a kainate concentration above 5 μM (that was previously shown to generate fictive locomotor patterns without toxic consequence; Cazalets et al., 1992), and, at 10 μM kainate, we already observed significant retardation in fictive locomotion periodicity: irreversible loss ensued with 50 μM (or higher doses). Previous studies have demonstrated that the neonatal rat brain is more vulnerable than the adult one to kainate-evoked lesions and seizures (Cherubini et al., 1983; Kesslak et al., 1995). Thus, the excitotoxic consequences of kainate administration to the neonatal spinal cord might have been enhanced by tissue immaturity. Nevertheless, former experiments with rat hippocampal slices (Robinson and Deadwyler, 1981) have shown that the kainate concentrations that induce reversible neuronal depolarization (1 μM) and irreversible damage (10 μM) are comparable to the ones used on the neonatal spinal cord (Cazalets et al., 1992; and our present data).

Functional consequences of kainate evoked damage

In the rat spinal cord, the distribution of kainate receptor subunits is primarily found in the most superficial laminae of the dorsal horn and at the level of motoneurons (Tölle et al., 1993). Since AMPA and NMDA receptor subunits are also abundantly expressed in the dorsal and ventral horns (Tölle et al., 1993), it is likely that even the lowest concentration (10 μM) of kainate evoked effects largely contributed by release of endogenous glutamate acting on multiple receptor subclasses and on downstream non-glutamatergic neurons (Ben Ari and Cossart, 2000). It is noteworthy that the amplitude of VR depolarization (reflecting the response of motoneuron pools) was related to the kainate concentration, indicating that the effects measured in terms of neuronal depolarization were far from being maximal, yet fully efficient in evoking loss of locomotor function.

In contrast with the loss of fictive locomotion, disinhibited bursting was maintained with little difference in its periodicity between 10 and 1000 μM kainate. While this pattern is likely to reflect basic rhythmogenesis (Ballerini et al., 1999; Darbon et al., 2002), it was interesting to observe that its periodicity was relatively insensitive to neuronal loss. This result implies that the basic network character-
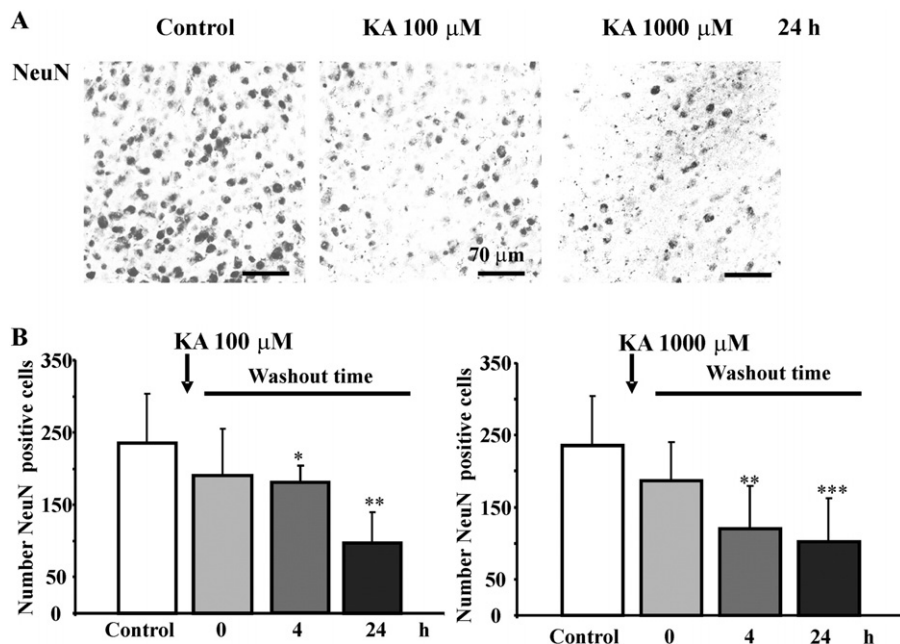
Fig. 5. Extent and time course of neuronal loss evoked by kainate in organotypic cultures. (A) Examples of neuronal staining with NeuN antibody in the central region 24 h after the application of kainate (100 or 1000 μM) for 1 h. (B) Histograms showing the percent of NeuN positive cells counted at 4 and 24 h after the application of kainate (100 or 1000 μM) for 1 h (indicated by arrows). The column bars represent the pooled data from all r.o.i. in four experiments in which the number of slices was four to eight. * $P<0.05$, ** $P<0.01$, *** $P<0.001$ vs. controls that were untreated cultures analyzed 24 h later *in vitro* (23 DIV).

istics necessary to drive the rhythm were spared and expressed by a comparatively small number of surviving neurons, even though the global number of neurons was progressively reduced as indicated by the gradual diminution of cycle amplitude. These observations accord with experimental and theoretical studies of cortical networks in which neuronal loss may produce synaptic scaling and reconfiguration to preserve activity levels when the size of the network shrinks (Wilson et al., 2007).

Histological pattern of spinal cell damage

With 10 μM kainate there was no detectable neuronal loss despite the functional impairment of fictive locomotion. We surmise that some cells were damaged only functionally, and/or a very small number of neurons (below our method resolution) critical for rhythm generation had been destroyed. With 50 or 100 μM kainate, the global neuronal damage became apparent and grew in a dose-dependent fashion. It is, however, noteworthy that the loss of motoneurons was already observed after 50 μM kainate concentration and did not intensify with larger doses. Several data concur to suggest a special sensitivity of motoneurons to excitotoxicity. In fact, motoneurons were also highly sensitive to this insult in organotypic slice cultures, and primary cultures of motoneurons are readily destroyed by kainate (Comoletti et al., 2001). Future studies will be necessary to understand the mechanism of motoneuron death evoked by kainate and whether there are motoneuron subtypes more resistant than others, because we never detected complete disappearance of such cells. In the few cases of effective neuroprotection by 6-cyano-7-

nitroquinoxaline-2,3-dione (CNQX) and aminophosphono-valerate (APV) against kainate, the histological outcome was better preservation of motoneurons (Margaryan et al., 2010). Our present finding, thus, accords with previous reports demonstrating differential vulnerability to the excitotoxic stimulus of distinct cell types in the rat hippocampus (Akaike et al., 2001; Holopainen et al., 2004; Reid et al., 2008). It is noteworthy that the excitotoxic damage to motoneurons provides a model of loss of locomotor patterns clearly different from the one observed after application of toxic radicals in hypoxic/aglycemic conditions that largely spare motoneurons and primarily target interneurons and white matter (Margaryan et al., 2009).

Timecourse of kainate excitotoxicity

The realization of the severe excitotoxic damage to motoneurons led us to examine the issue of the extent and time course of excitotoxicity affecting other neurons as well. This is not a trivial point because the interneuronal network could retain rhythmogenesis after excitotoxic stimulus and might therefore be a step to try to rebuild or repair the network especially if their elements can reconfigure their function (Barriere et al., 2008). To this end, we used organotypic cultures of the rat spinal which are very useful models to investigate physiological and pathological properties of spinal networks (Sibilla and Ballerini, 2009). In accordance with the isolated spinal cord data, we observed kainate-mediated widespread neuronal damage with a maximum loss concerning the dorsal horn. In the three r.o.i., the extent of such a damage was related to the kainate concentration. Even if it is necessary to take into
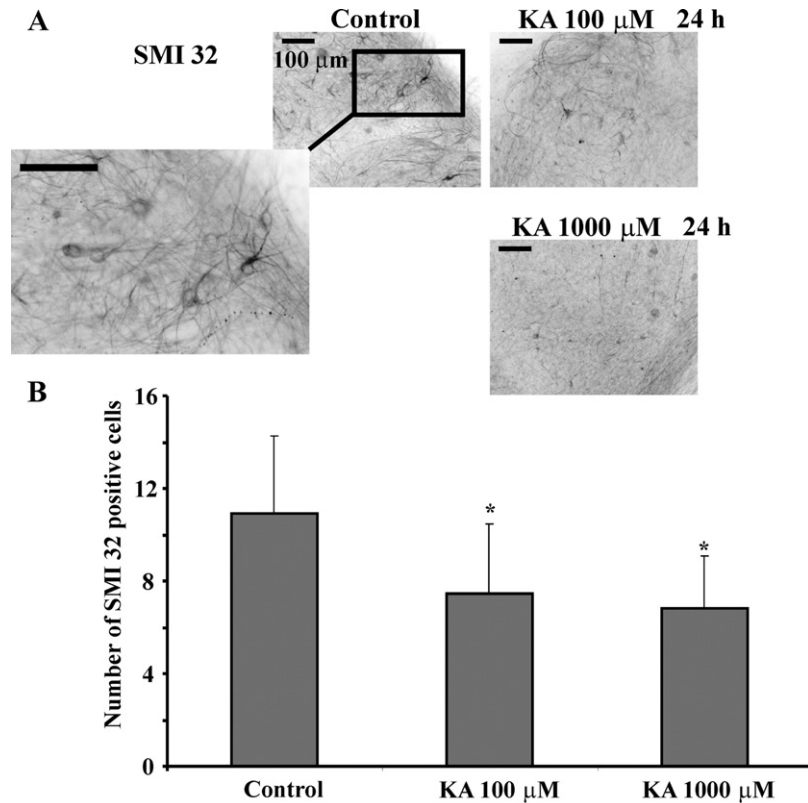
Fig. 6. Kainate induced damage of motoneurons in organotypic slice cultures. (A) Examples of motoneuron staining with SMI 32 antibody 24 h after the application of kainate (100 or 1000 μM) for 1 h. The inset shows higher magnification view of the ventral region with large SMI 32 cells identified as motoneurons. All calibration bars=100 μm. (B) Histograms showing the number of SMI 32 positive cells 24 h after application of kainate (100 or 1000 μM for 1 h). The data represent the numbers from three experiments with 6–12 slices each, * $P < 0.05$ vs. control (untreated cultures).

account the fact that organotypic cultures are made up, on average, by three layers of cells only (Ballerini et al., 1999), lacking the complexity of the intact tissue, we could estimate the consequences of kainate application over a span of 4 h: the global cell loss ranged between 75 and 132 elements, while neuronal deficit was between 17 and 27. Future studies are needed to examine the phenotype of surviving neurons and their functional role (excitatory or inhibitory), plus the precise identification of non-neuronal cells.

Notwithstanding these issues, the present values indicate that excitotoxicity affecting spinal neurons other than motoneurons showed a delayed development related to the strength of the excitotoxic stimulus: this time course should perhaps leave open a time window during which neuroprotection might be attempted.

Kainate effects on cell viability markers

One issue was whether the organotypic culture cells surviving after kainate were metabolically impaired. To assess this condition, we applied to these cultures a viability test that relies on cell metabolic activity and membrane integrity (Nocker and Camper, 2009). In particular, we employed the MTT assay which is based on the mitochondrial transformation of this substance (Wang et al., 2005) and provides an inexpensive and expeditious means to assess

viability of organotypic cultures (Connelly et al., 2000). After checking that MTT assay values were linearly related to the number of cells under test (Suppl. Fig. 2), we could observe a tight inverse relation between MTT mitochondrial metabolism and the number of chromatin condensed cells. Our data are, thus, best explained by assuming that, while excitotoxicity killed cells, the survivors remained metabolically competent, adding therefore impetus to any attempt to obtain neuroprotection even at a late phase.

CONCLUSION

On the understanding that excitotoxicity is a major early component of acute spinal cord injury (Hall and Springer, 2004; Park et al., 2004; Rossignol et al., 2007), the present results provide novel information concerning the sensitivity of *in vitro* spinal networks to an excitotoxic stimulus, the time course of this damage and the main cell types affected. While motoneurons were readily destroyed by excitotoxicity, the fact that some of them did survive together with the extent of premotoneuron survival in relation to the intensity of excitotoxicity can provide a first estimate of the lesion scale that neuroprotection or neurorepair (Schwab et al., 2006) should face to arrest or limit the functional consequences of an acute spinal injury.

REFERENCES

Achildi O, Betz RR, Grewal H (2007) Lapbelt injuries and the seatbelt syndrome in pediatric spinal cord injury. J Spinal Cord Med 30(Suppl 1):S21–S24.

Adams M, Carlstedt T, Cavanagh J, Lemon RN, McKernan R, Priestley JV, Raisman G, Verhaagen J (2007) International spinal research trust research strategy. Part III: a discussion document. Spinal Cord 45:2–14.

Agrawal SG, Evans RH (1986) The primary afferent depolarizing action of kainate in the rat. Br J Pharmacol 87:345–355.

Akaike K, Tanaka S, Tojo H, Fukumoto S, Imamura S, Takigawa M (2001) Kainic acid-induced dorsal and ventral hippocampal seizures in rats. Brain Res 900:65–71.

Avossa D, Rosato-Siri MD, Mazzarol F, Ballerini L (2003) Spinal circuits formation: a study of developmentally regulated markers in organotypic cultures of embryonic mouse spinal cord. Neuroscience 122:391–405.

Ballerini L, Galante M (1998) Network bursting by organotypic spinal slice cultures in the presence of bicuculline and/or strychnine is developmentally regulated. Eur J Neurosci 10:2871–2879.

Ballerini L, Galante M, Grandolfo M, Nistri A (1999) Generation of rhythmic patterns of activity by ventral interneurones in rat organotypic spinal slice culture. J Physiol 517:459–475.

Barriere G, Leblond H, Provencher J, Rossignol S (2008) Prominent role of the spinal central pattern generator in the recovery of locomotion after partial spinal cord injuries. J Neurosci 28:3976–3987.

Beato M, Nistri A (1999) Interaction between disinhibited bursting and fictive locomotor patterns in the rat isolated spinal cord. J Neurophysiol 82:2029–2038.

Ben Ari Y, Cossart R (2000) Kainate, a double agent that generates seizures: two decades of progress. Trends Neurosci 23:580–587.

Bracci E, Ballerini L, Nistri A (1996a) Localization of rhythmogenic networks responsible for spontaneous bursts induced by strychnine and bicuculline in the rat isolated spinal cord. J Neurosci 16:7063–7076.

Bracci E, Ballerini L, Nistri A (1996b) Spontaneous rhythmic bursts induced by pharmacological block of inhibition in lumbar motoneurons of the neonatal rat spinal cord. J Neurophysiol 75:640–647.

Bracci E, Beato M, Nistri A (1997) Afferent inputs modulate the activity of a rhythmic burst generator in the rat disinhibited spinal cord in vitro. J Neurophysiol 77:3157–3167.

Bracken MB, Shepard MJ, Collins WF, Holford TR, Young W, Baskin DS, Eisenberg HM, Flamm E, Leo-Summers L, Maroon J (1990) A randomized, controlled trial of methylprednisolone or naloxone in the treatment of acute spinal-cord injury: results of the second national acute spinal Cord injury study. N Engl J Med 322:1405–1411.

Butt SJ, Harris-Warrick RM, Kiehn O (2002) Firing properties of identified interneuron populations in the mammalian hindlimb central pattern generator. J Neurosci 22:9961–9971.

Carriedo SG, Yin HZ, Weiss JH (1996) Motor neurons are selectively vulnerable to AMPA/kainate receptor-mediated injury in vitro. J Neurosci 16:4069–4079.

Cashman NR, Durham HD, Blusztajn JK, Oda K, Tabira T, Shaw IT, Dahrouge S, Antel JP (1992) Neuroblastoma × spinal cord (NSC) hybrid cell lines resemble developing motor neurons. Dev Dyn 194:209–221.

Cazalets JR, Sqalli-Houssaini Y, Clarac F (1992) Activation of the central pattern generators for locomotion by serotonin and excitatory amino acids in neonatal rat. J Physiol 455:187–204.

Cherubini E, De Feo MR, Mecarelli O, Ricci GF (1983) Behavioral and electrographic patterns induced by systemic administration of kainic acid in developing rats. Brain Res 285:69–77.

Choi DW (1992) Excitotoxic cell death. J Neurobiol 23:1261–1276.

Comoletti D, Muzio V, Capobianco A, Ravizza T, Mennini T (2001) Nitric oxide produced by non-motoneuron cells enhances rat embryonic motoneuron sensitivity to excitotoxins: comparison in mixed neuron/glia or purified cultures. J Neurol Sci 192:61–69.

Connelly CA, Chen LC, Colquhoun SD (2000) Metabolic activity of cultured rat brainstem, hippocampal and spinal cord slices. J Neurosci Methods 99:1–7.

Darbon P, Scicluna L, Tscherter A, Streit J (2002) Mechanisms controlling bursting activity induced by disinhibition in spinal cord networks. Eur J Neurosci 15:671–683.

Doble A (1999) The role of excitotoxicity in neurodegenerative disease: implications for therapy. Pharmacol Ther 81:163–221.

Gahwiler BH, Capogna M, Debanne D, McKinney RA, Thompson SM (1997) Organotypic slice cultures: a technique has come of age. Trends Neurosci 20:471–477.

Hall ED, Springer JE (2004) Neuroprotection and acute spinal cord injury: a reappraisal. NeuroRx 1:80–100.

Holopainen IE, Jarvela J, Lopez-Picon FR, Pelliniemi LJ, Kukko-Lukjanov TK (2004) Mechanisms of kainate-induced region-specific neuronal death in immature organotypic hippocampal slice cultures. Neurochem Int 45:1–10.

Kesslak JP, Yuan D, Neeper S, Cotman CW (1995) Vulnerability of the hippocampus to kainate excitotoxicity in the aged, mature and young adult rat. Neurosci Lett 188:117–120.

Kiehn O, Kjaerulff O (1998) Distribution of central pattern generators for rhythmic motor outputs in the spinal cord of limbed vertebrates. Ann N Y Acad Sci 860:110–129.

Kiehn O (2006) Locomotor circuits in the mammalian spinal cord. Annu Rev Neurosci 29:279–306.

Margaryan G, Mattioli C, Mladinic M, Nistri A (2010) Neuroprotection of locomotor networks after experimental injury to the neonatal rat spinal cord in vitro. Neuroscience 165:996–1010.

Margaryan G, Mladinic M, Mattioli C, Nistri A (2009) Extracellular magnesium enhances the damage to locomotor networks produced by metabolic perturbation mimicking spinal injury in the neonatal rat spinal cord in vitro. Neuroscience 163:669–682.

McDonald JW, Sadowsky C (2002) Spinal-cord injury. Lancet 359:417–425.

Mosmann T (1983) Rapid colorimetric assay for cellular growth and survival: application to proliferation and cytotoxicity assays. J Immunol Methods 65:55–63.

Nistri A, Taccola G, Mladinic M, Margaryan G, Kuzhandaivel A (2010) Deconstructing locomotor networks with experimental injury to define their membership. Ann N Y Acad Sci, in press.

Nocker A, Camper AK (2009) Novel approaches toward preferential detection of viable cells using nucleic acid amplification techniques. FEMS Microbiol Lett 291:137–142.

Park E, Velumian AA, Fehlings MG (2004) The role of excitotoxicity in secondary mechanisms of spinal cord injury: a review with an emphasis on the implications for white matter degeneration. J Neurotrauma 21:754–774.

Pizzi M, Benarese M, Boroni F, Goffi F, Valerio A, Spano PF (2000) Neuroprotection by metabotropic glutamate receptor agonists on kainate-induced degeneration of motor neurons in spinal cord slices from adult rat. Neuropharmacology 39:903–910.

Pointillart V, Petitjean ME, Wiart L, Vital JM, Lassie P, Thicoipe M, Dabadie P (2000) Pharmacological therapy of spinal cord injury during the acute phase. Spinal Cord 38:71–76.

Reid CA, Adams BE, Myers D, O'Brien TJ, Williams DA (2008) Sub region-specific modulation of synchronous neuronal burst firing

after a kainic acid insult in organotypic hippocampal cultures. BMC Neurosci 9:59.

Robinson JH, Deadwyler SA (1981) Kainic acid produces depolarization of CA3 pyramidal cells in the vitro hippocampal slice. Brain Res 221:117–127.

Rossignol S, Schwab M, Schwartz M, Fehlings MG (2007) Spinal cord injury: time to move? J Neurosci 27:11782–11792.

Schwab JM, Brechtel K, Mueller CA, Failli V, Kaps HP, Tuli SK, Schluesener HJ (2006) Experimental strategies to promote spinal cord regeneration—an integrative perspective. Prog Neurobiol 78:91–116.

Sibilla S, Ballerini L (2009) GABAergic and glycinergic interneuron expression during spinal cord development: dynamic interplay between inhibition and excitation in the control of ventral network outputs. Prog Neurobiol 89:46–60.

Sibilla S, Fabbro A, Grandolfo M, D'Andrea P, Nistri A, Ballerini L (2009) The patterns of spontaneous Ca^{2+} signals generated by ventral spinal neurons in vitro show time-dependent refinement. Eur J Neurosci 29:1543–1559.

Taccola G, Margaryan G, Mladinic M, Nistri A (2008) Kainate and metabolic perturbation mimicking spinal injury differentially contribute to early damage of locomotor networks in the in vitro neonatal rat spinal cord. Neuroscience 155:538–555.

Taccola G, Nistri A (2006) Fictive locomotor patterns generated by tetraethylammonium application to the neonatal rat spinal cord in vitro. Neuroscience 137:659–670.

Tölle TR, Berthele A, Zieglgansberger W, Seeburg PH, Wisden W (1993) The differential expression of 16 NMDA and non-NMDA receptor subunits in the rat spinal cord and in periaqueductal gray. J Neurosci 13:5009–5028.

Vitale MG, Goss JM, Matsumoto H, Roye DP Jr (2006) Epidemiology of pediatric spinal cord injury in the United States: years 1997 and 2000. J Pediatr Orthop 26:745–749.

Wang Q, Yu S, Simonyi A, Sun GY, Sun AY (2005) Kainic acid-mediated excitotoxicity as a model for neurodegeneration. Mol Neurobiol 31:3–16.

Wilson NR, Ty MT, Ingber DE, Sur M, Liu G (2007) Synaptic reorganization in scaled networks of controlled size. J Neurosci 27:13581–13589.

APPENDIX

Supplementary data

Methods, materials and results

Section 2

Nasrabady SE, Kuzhandaivel A, Mladinic M, Nistri A (2011) Effects of 6(5H)-phenanthridinone, an inhibitor of poly(ADP-ribose)polymerase-1 activity (PARP-1), on locomotor networks of the rat isolated spinal cord. Cellular and molecular neurobiology 31:503-508.

SHORT COMMUNICATION

Effects of 6(5H)-phenanthridinone, an Inhibitor of Poly(ADP-ribose)Polymerase-1 Activity (PARP-1), on Locomotor Networks of the Rat Isolated Spinal Cord

Sara Ebrahimi Nasrabady · Anujaianthi Kuzhandaivel ·
Miranda Mladinic · Andrea Nistri

Abstract Excitotoxicity is considered to be a major pathophysiological mechanism responsible for extensive neuronal death after acute spinal injury. The chief effector of such a neuronal death is thought to be the hyperactivation of intracellular PARP-1 that leads to cell energy depletion and DNA damage with the manifestation of non-apoptotic cell death termed parthanatos. An in vitro lesion model using the neonatal rat spinal cord has recently shown PARP-1 overactivity to be closely related to neuronal losses after an excitotoxic challenge by kainate: in this system the PARP-1 inhibitor 6(5H)-phenanthridinone (PHE) appeared to be a moderate histological neuroprotector. This article investigated whether PHE could actually preserve the function of locomotor networks in vitro from excitotoxicity. Bath-applied PHE (after a 60 min kainate application) failed to recover locomotor network function 24 h later. When the PHE administration was advanced by 30 min (during the administration of kainate), locomotor function could still not be recovered, while basic network rhythmicity persisted. Histochemical analysis showed that, even if the number of surviving neurons was improved with this protocol, it had failed to reach the threshold of minimal network membership necessary for expressing locomotor patterns. These results suggest that PARP-1 hyperactivity was a rapid onset mechanism of neuronal loss after an excitotoxic challenge and that more selective and faster-acting PARP-1 inhibitors are warranted to explore their potential neuroprotective role.

Sara Ebrahimi Nasrabady, and Anujaianthi Kuzhandaivel are joint first authors.

S. E. Nasrabady · A. Kuzhandaivel · M. Mladinic · A. Nistri (✉)
Neurobiology Sector, International School for Advanced Studies (SISSA), Via Bonomea 265, 34136 Trieste, Italy
e-mail: nistri@sissa.it

M. Mladinic · A. Nistri
Spinal Person Injury Neurorehabilitation Applied Laboratory (SPINAL), Istituto di Medicina Fisica e Riabilitazione, Udine, Italy

Introduction

During the process of neuronal excitotoxicity, hyperactivation of the intracellular enzyme poly(ADP-ribose)polymerase-1 (PARP-1) is thought to be a major step to trigger a non-apoptotic form of cell death termed parthanatos (Narasimhan et al. 2003; Wang et al. 2009; Kuzhandaivel et al. 2010).

Parthanatos is believed to be an essential mechanism to produce neuronal loss following brain ischemia/anoxia during which extensive release of glutamate is regarded as a primary cause for irreversible damage (Eliasson et al. 1997; Koh et al. 2004). A similar process has also been suggested to occur in the spinal cord after an acute lesion (Scott et al. 1999; Genovese et al. 2005; Kuzhandaivel et al. 2010). Our in vitro model using the rat-isolated spinal cord subjected to a transient excitotoxic stimulus by the glutamate receptor agonist kainate has demonstrated substantial neuronal losses attributable to parthanatos (with preservation of glia) that was attenuated by the PARP-1 inhibitor 6(5H)-phenanthridinone (PHE; Kuzhandaivel et al. 2010). Nonetheless, this observation needs validation with electrophysiological recording to prove whether locomotor network activity in vitro is preserved as well.

This article aims at investigating if fictive locomotion (Butt et al. 2002; Taccola and Nistri 2006), an alternating pattern of lumbar ventral root (VR) discharges rhythmically produced by either electrical stimulation or neurochemicals like NMDA and 5-hydroxytryptamine (5-HT), can be detected 24 h after kainate-evoked excitotoxicity and application of PHE, and how it might be related to neuronal survival.

Materials and Methods

Full details of the experimental methods have recently been published (Taccola et al. 2008; Margaryan et al. 2010). In brief, we used neonatal (age: 0–2 days) rat spinal cords with the following protocols: sham preparations were maintained in vitro for up to 24 h in standard Krebs solution (Taccola et al. 2008); injured preparations were treated with a maximally effective dose (1 mM) of the glutamate agonist kainate (60 min) followed by wash and maintenance in Krebs solution for 24 h. PHE (60 μM; Sigma, Milan, Italy)-treated preparations received this drug either at the time of kainate washout or after the first 30 min of kainate application. In all cases, PHE application continued for 24 h and was washed out immediately before electrophysiological recording. L2 and L5 pairs of lumbar ventral roots were continuously recorded to monitor reflex activity induced by stimulating either the left or the right lumbar five dorsal root (DR). We first assessed the minimal stimulus intensity to evoke a VR threshold response homolaterally (on average this was 2.0 ± 0.95 V). In accordance with previous studies (Marchetti et al. 2001), we considered this as equivalent to 1 threshold (Th) value to induce a monosynaptic reflex. Thereafter, values of Th < 2 stimuli were used to evoke monosynaptic responses, while larger Th values were used for polysynaptic responses as previously reported in detail (Baranauskas and Nistri 1995; Bracci et al. 1997). In control conditions, the peak amplitude of monosynaptic responses was 0.24 ± 0.06 mV ($n = 7$) which corresponded to 33% of the peak amplitude of the polysynaptic responses (0.73 ± 0.3 mV; $n = 7$). With pCLAMP 9 software (Molecular Devices, Sunnyvale, CA, USA), the reflex area was measured by simple summation of data points within the search region comprising the foot of the response to its decay corresponding to 20% of the peak (Baranauskas and Nistri 1995; Bracci et al. 1997; Marchetti et al. 2001). In the present experiments, the duration of polysynaptic responses was usually 20 s. Single pulses were used to elicit synaptic responses, while pulse trains were employed for inducing repeated cycles of electrical oscillation alternating homolaterally between L2 and L5 segments or from left to right in the same segment. These patterns, therefore, had all the typical properties of

fictive locomotion (Butt et al. 2002). Fictive locomotion was also evoked by bath-applied NMDA (4–5 μM, Tocris, Bristol, UK), and 5-HT (10 μM; Sigma, Milan, Italy) (Butt et al. 2002). Disinhibited bursting was induced by application of bicuculline (20 μM, Fluka, Milan, Italy) plus strychnine (1 μM, Sigma, Milan, Italy) (Bracci et al. 1996). The amplitude of such bursts was measured at their plateau phase, after high-frequency discharges subsided (Bracci et al. 2006). At the end of each experiment, spinal cords were histologically fixed and sectioned to investigate the immunostaining of neurons with the selective marker NeuN (Millipore, Milan, Italy) in the three regions of interest. Motoneurons immunolabeled with the marker SMI 32 (Covance, Emeryville, CA) were counted in the ventral horn gray matter. Data were expressed as mean ± standard deviation. The statistics of data were performed by analysis of variance (ANOVA), and Tukey test with SigmaStat 3.1 (Systat Software, Chicago, USA). The accepted level for statistical significance was $P < 0.05$ where $n =$ number of spinal cords.

Results

In view of the partial protection exerted by PHE against neuronal losses evoked by kainate (Kuzhandaivel et al. 2010), we first investigated whether this treatment could produce significant improvements in electrophysiological responses. After 60-min kainate application followed by washout, and subsequent administration of PHE (24 h), the average peak amplitude of polysynaptic reflexes (induced by DR stimuli >2 Th value for eliciting monosynaptic responses) was 0.11 ± 0.04 mV ($n = 4$), a result not different from 0.16 ± 0.1 mV ($n = 6$) observed after kainate alone. Increasing the stimulus intensity fails to reinstate the initial amplitude of these reflexes (Taccola et al. 2008). Sham reflex amplitude was 0.73 ± 0.30 ($n = 7$). Previous studies have shown that kainate (1 mM) induced irreversible loss of fictive locomotion tested with trains of electrical pulses applied to a lumbar DR (Taccola et al. 2008): this result was confirmed in this study with kainate alone or kainate followed by PHE. It was, however, possible to detect disinhibited bursting, that after kainate alone, had 58 ± 25 s period (CV = 0.21 ± 0.17), a value not significantly different from the one when PHE was later applied (34 ± 16 s; CV = 0.28 ± 0.18; $n = 4$). The same findings applied also to the average burst amplitude (measured at plateau; not shown). These observations suggested that with this administration protocol, PHE was ineffective to protect spinal networks from kainate excitotoxicity manifested as loss of fictive locomotion and reflex impairment.

Our previous study has shown that 60-min application of kainate was sufficient to produce significant PARP-1 hyperactivity (Kuzhandaivel et al. 2010). Thus, we reasoned that any protective action of PHE should perhaps be tested by applying this drug before a significant onset of PARP-1 activation, but with a certain delay from the start of kainate application to enable the development of excitotoxicity. To this end, the experimental protocol was based on application of PHE 30 min after the start of kainate (always 60 min application) and kept throughout for the next 24 h. Figures 1, 2 summarize these data. Figure 1a shows examples of lack of effectiveness even of this protocol on monosynaptic reflex amplitude (see inset to Fig. 1a) or area; similar data were obtained for polysynaptic responses in the same preparation (Fig. 1a). Average results are quantified in the histograms of Fig. 1b, c.

Recovery of fictive locomotion was never found, regardless of whether trains of electrical pulses (Fig. 1d; $n = 4$) or bath-application of NMDA plus 5-HT were
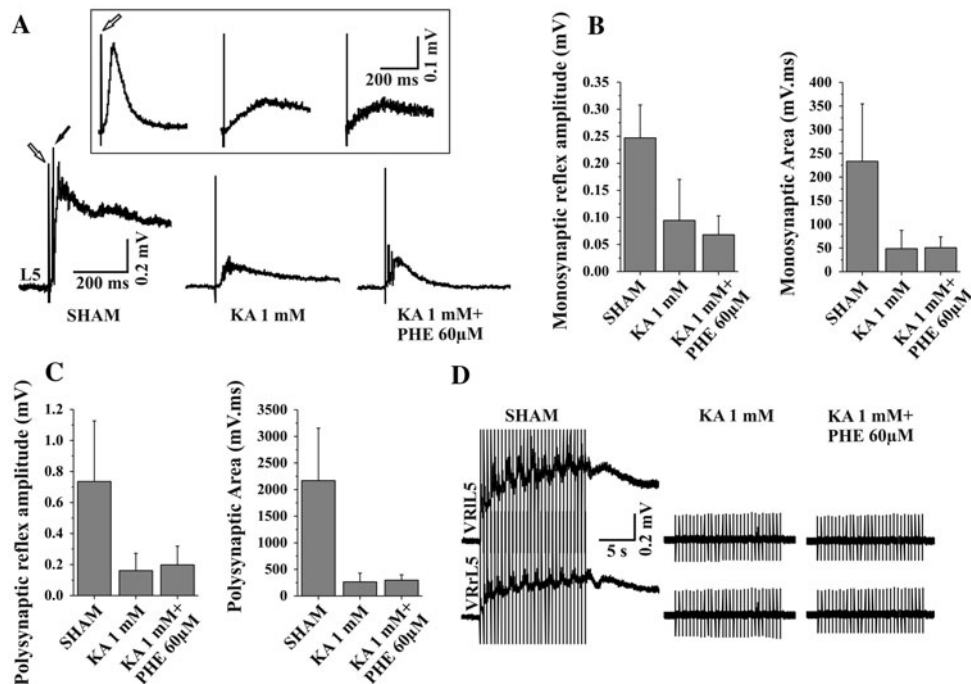
tested (Fig. 2c; $n = 4$). As shown in Fig. 2a, b, the period and amplitude of disinhibited bursts after kainate and PHE were similar to those obtained with kainate alone.

The different application protocol of PHE (namely, during kainate administration) with respect to our previous article (Kuzhandaivel et al. 2010) required the analysis of the histological damage in relation to the electrophysiological effects. Fig. 3a shows examples of neuronal losses evoked by kainate in the dorsal horn of the isolated spinal cord (this example refers to L5). After applying PHE (60 μM) following kainate (bottom panel of Fig. 3a), neuronal losses in the kainate's most-sensitive region (namely, the dorsal horn; cf. Mazzone et al. 2010) appeared to be decreased as quantified in the histograms of Fig. 3b depicting the number of neurons (as NeuN-positive elements) detected in the three main spinal regions of pooled L3–L5 segments. For each region investigated, the effect of PHE against kainate toxicity was significant with percent values of surviving neurons of approximately 75% with

Fig. 1 Effect of PHE (60 μM) application (30 min after start of injury) on electrophysiological responses recorded after 24 h from in vitro spinal cord preparations exposed to excitotoxic injury by kainate (1 mM). **a** Examples of mono (1× Th; see *inset*) and polysynaptic VRlL5 responses evoked by single electrical stimuli (2× Th intensity for polysynaptic response) applied to the homolateral DRlL5 in sham (*left*), kainate (*middle*) or PHE treated condition (30 min after kainate application; *right*). The *open arrows* indicate the artifact while the filled *arrow* indicates the peak amplitude of the polysynaptic reflex measured from baseline. **b** *Histograms* show reflex amplitude and area of monosynaptic responses in sham, kainate, and kainate + PHE ($n = 7$, 6, and 4 respectively). No improvement was found after 24 h PHE application. Statistical analysis using ANOVA shows the significant difference between sham and two other groups (peak

amplitude: $P = 0.003$ for kainate and $P = 0.002$ for kainate + PHE; area: $P = 0.01$ for kainate and $P = 0.02$ for kainate + PHE). **c** Lack of recovery of peak response amplitude and area of polysynaptic responses after application of PHE in comparison with kainate alone ($n = 7$, 6, and 4 for sham, kainate, and kainate + PHE, respectively). Significant decreases in peak amplitude and area of polysynaptic response in comparison with sham remained unchanged (peak amplitude: $P = 0.005$ for kainate and $P = 0.01$ for kainate + PHE; area: $P = 0.009$ for kainate and $P = 0.03$ for kainate + PHE). **d** Example of VR alternating cycles of a sham preparation in response to a train of DR stimuli (30 stimuli, 2× threshold intensity, 2 Hz frequency); this pattern disappears in both groups treated with kainate, and kainate + PHE (30 min after application of kainate). All data refer to the electrophysiological activity after 24 h. KA, kainate

A   Strychnine 1 μM+Bicuculline 20 μM

SHAM

KA 1 mM

KA 1 mM+
PHE 60μM

B

C   NMDA 4 μM + 5-HT 10 μM

SHAM   KA 1 mM   KA 1 mM+
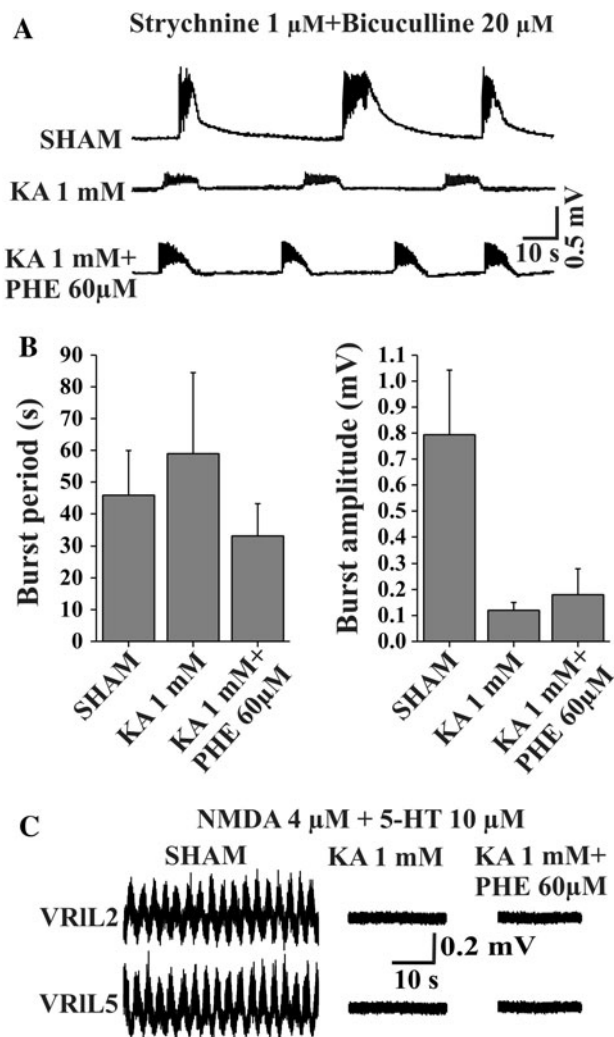   PHE 60μM

VRlL2

VRlL5

Fig. 2 Effect of PHE (60 μM) on chemically induced locomotor patterns 24 h after excitotoxic injury evoked by kainate (1 mM). **a** Examples of disinhibited bursting induced by strychnine and bicuculline in sham, kainate or kainate + PHE treated condition (started 30 min after kainate application). **b** *Histograms* show similar burst period for all the three conditions, while amplitude values for kainate, and kainate + PHE are significantly different from sham ($P = 0.005$, and 0.002, respectively; $n = 7$, 6, and 4 for sham, kainate, and kainate + PHE, respectively). Amplitude values are similar for kainate, and kainate + PHE groups. All data were analyzed with ANOVA. **c** Example of fictive locomotion induced by NMDA plus 5-HT in sham preparation: this pattern is not preserved following kainate or kainate + PHE. VRs are identified by their segmental numbering (lumbar L2 and L5 on the *left*, l, side of the spinal cord). Alternation between L2 flexor motor pools and L5 extensor motor pools is an index of fictive locomotion. All data refer to the electrophysiological activity after 24 h. KA, kainate

respect to corresponding sham values. Fig. 3c, d shows that kainate evoked, on average, strong loss of motoneurons (SMI 32 positive large cells in the ventral horn; Taccola et al. 2008) 24 h later, and that this effect could not be significantly counteracted by PHE.

Discussion

The principal finding of this article is that the PARP-1 inhibitor, PHE, could not contrast the excitotoxic damage evoked by kainate in functional terms, despite significant protection against neuronal losses, and the previous demonstration of the tight correlation between excitotoxicity and PARP-1 activity.

This observation raises several interesting issues related to the basic pathophysiology of spinal cord excitotoxicity. First, the damage to synaptic transmission induced by kainate was multifactorial because of the widespread chemical injury involving dorsal, central and ventral neurons, including motoneurons. This functional lesion was not significantly prevented by PHE since mono- and polysynaptic reflexes were strongly depressed after kainate administration, regardless of the PHE application protocol. This observation probably explains why even DR pulse trains were unable to activate fictive locomotion because afferent stimuli could not be efficiently integrated into spinal networks. Second, the persistence of disinhibited rhythmicity despite kainate being followed (or not) by PHE indicated that, in accordance with histochemical data, there was a residual circuitry still able to express a basic form of spontaneous network pattern. Improving the number of these survivors with PHE treatment had no significant consequence on disinhibited bursting presumably because this type of rhythmicity was a scale-free phenomenon generated by a relatively small subset of interneurons (Bracci et al. 1996; Taccola and Nistri 2006). The larger number of surviving neurons was, however, unable to generate locomotor patterns (which, in control conditions, are directly triggered by NMDA and 5-HT acting on intrinsic locomotor networks; Butt et al. 2002) presumably because it overall remained below the threshold (~ 155 neurons/central and ventral region) that constitutes the minimal membership required to produce fictive locomotion (Nistri et al. 2010).

The poor functional outcome of the PHE effect was likely to be due to the early hyperactivation of PARP-1 which presumably started even before 30 min time-point coincident with the PHE application. Furthermore, PHE is a relatively non-selective blocker of this enzymatic activity (Banasik et al. 1992; Li et al. 2001), and impairs the activity of lymphocytes (Chiarugi 2002). It is unclear whether these effects may also occur in the in vitro spinal cord, and what contribution, if any, they might have brought to the overall functional outcome. Hence, future studies with more selective inhibitors of PARP-1 are warranted to explore the early neuroprotective value of blocking this enzymatic activity.
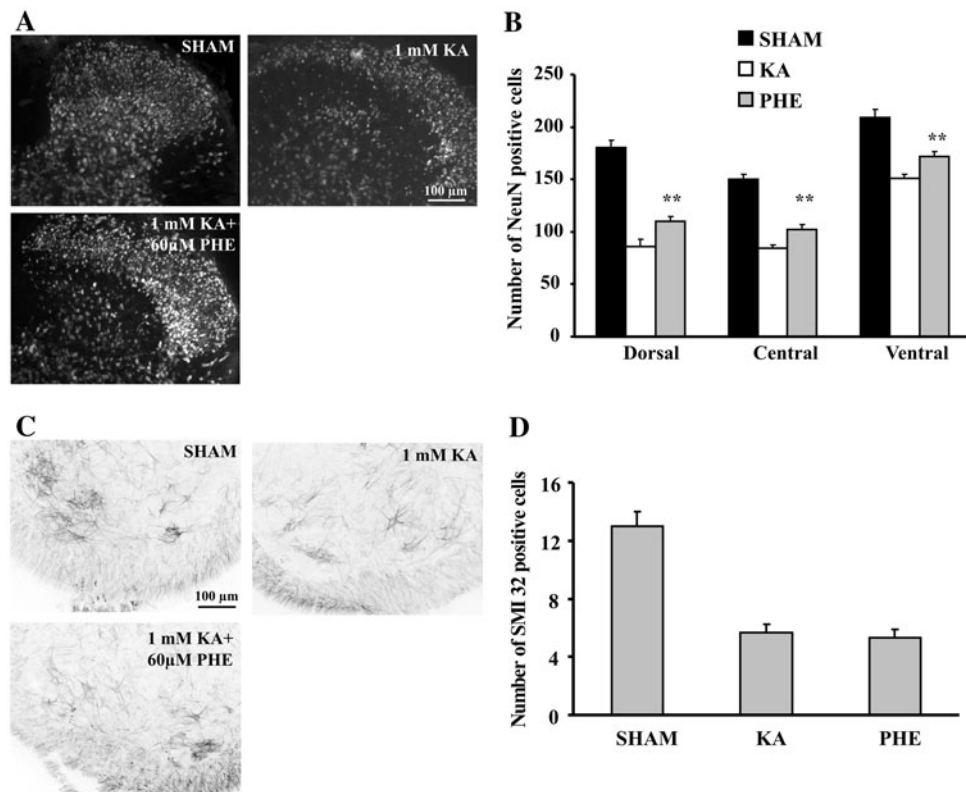
Fig. 3 Quantification of effect of kainate and PHE on neurons and motoneurons of the isolated spinal cord. **a** Examples of NeuN immunoreactivity in the L5 dorsal region of 1 mM kainate or 1 mM kainate + 60 μM PHE treated spinal cords. PHE was always applied 30 min after the start of kainate administration. **b** *Histograms* showing number of NeuN positive neurons in sham (*filled bar*)-, kainate (*open bar*)-, or kainate plus PHE (*gray bar*)-treated spinal cord for pooled L3–L5 segments ($n = 4$–7 spinal cords).

c Representative images showing SMI 32 positive neurons (motoneurons) in L5 laminae VIII and IX of 1 mM kainate- or 1 mM kainate + 60 μM PHE-treated spinal cords. **d** *Histograms* showing number of SMI 32 positive neurons counted in 30-μm sections of 1 mM kainate- or 1 mM kainate + 60 μM PHE-treated spinal cords; $n = 4$–7 spinal cords. For **b** $*P < 0.05$, $**P < 0.01$ when compared with data from kainate alone. All data were analyzed with ANOVA

References

Banasik M, Komura H, Shimoyama M, Ueda K (1992) Specific inhibitors of poly(ADP-ribose) synthetase and mono(ADP-ribosyl)transferase. J Biol Chem 267:1569–1575

Baranauskas G, Nistri A (1995) Membrane potential oscillations of neonatal rat spinal motoneurons evoked by electrical stimulation of dorsal root fibres. Eur J Neurosci 7:2403–2408

Bracci E, Ballerini L, Nistri A (1996) Localization of rhythmogenic networks responsible for spontaneous bursts induced by strychnine and bicuculline in the rat isolated spinal cord. J Neurosci 16:7063–7076

Bracci E, Beato M, Nistri A (1997) Afferent inputs modulate the activity of a rhythmic burst generator in the rat disinhibited spinal cord in vitro. J Neurophysiol 77:3157–3167

Butt SJ, Lebret JM, Kiehn O (2002) Organization of left-right coordination in the mammalian locomotor network. Brain Res Brain Res Rev 40:107–117

Chiarugi A (2002) Inhibitors of poly(ADP-ribose) polymerase-1 suppress transcriptional activation in lymphocytes and ameliorate autoimmune encephalomyelitis in rats. Br J Pharmacol 137:761–770

Eliasson MJ, Sampei K, Mandir AS, Hurn PD, Traystman RJ, Bao J, Pieper A, Wang ZQ, Dawson TM, Snyder SH, Dawson VL (1997) Poly(ADP-ribose) polymerase gene disruption renders mice resistant to cerebral ischemia. Nat Med 3:1089–1095

Genovese T, Mazzon E, Muia C, Patel NS, Threadgill MD, Bramanti P, De Sarro A, Thiemermann C, Cuzzocrea S (2005) Inhibitors of poly(ADP-ribose) polymerase modulate signal transduction pathways and secondary damage in experimental spinal cord trauma. J Pharmacol Exp Ther 312:449–457

Koh SH, Park Y, Song CW, Kim JG, Kim K, Kim J, Kim MH, Lee SR, Kim DW, Yu HJ, Chang DI, Hwang SJ, Kim SH (2004) The effect of PARP inhibitor on ischaemic cell death, its related inflammation and survival signals. Eur J Neurosci 20:1461–1472

Kuzhandaivel A, Nistri A, Mladinic M (2010) Kainate-mediated excitotoxicity induces neuronal death in the rat spinal cord in vitro via a PARP-1 dependent cell death pathway (Parthanatos). Cell Mol Neurobiol 30:1001–1012

Li JH, Serdyuk L, Ferraris DV, Xiao G, Tays KL, Kletzly PW, Li W, Lautar S, Zhang J, Kalish VJ (2001) Synthesis of substituted 5[H]phenanthridin-6-ones as potent poly(ADP-ribose)polymerase-1 (PARP1) inhibitors. Bioorg Med Chem Lett 11:1687–1690

Marchetti C, Beato M, Nistri A (2001) Alternating rhythmic activity induced by dorsal root stimulation in the neonatal rat spinal cord in vitro. J Physiol 530:105–112

Margaryan G, Mattioli C, Mladinic M, Nistri A (2010) Neuroprotection of locomotor networks after experimental injury to the neonatal rat spinal cord in vitro. Neuroscience 165:996–1010

Mazzone GL, Margaryan G, Kuzhandaivel A, Nasrabady SE, Mladinic M, Nistri A (2010) Kainate-induced delayed onset of excitotoxicity with functional loss unrelated to the extent of neuronal damage in the in vitro spinal cord. Neuroscience 168:451–462

Narasimhan P, Fujimura M, Noshita N, Chan PH (2003) Role of superoxide in poly(ADP-ribose) polymerase upregulation after transient cerebral ischemia. Brain Res Mol Brain Res 113:28–36

Nistri A, Taccola G, Mladinic M, Margaryan G, Kuzhandaivel A (2010) Deconstructing locomotor networks with experimental injury to define their membership. Ann N Y Acad Sci 1198:242–251

Scott GS, Jakeman LB, Stokes BT, Szabo C (1999) Peroxynitrite production and activation of poly (adenosine diphosphate-ribose) synthetase in spinal cord injury. Ann Neurol 45:120–124

Taccola G, Nistri A (2006) Oscillatory circuits underlying locomotor networks in the rat spinal cord. Crit Rev Neurobiol 18:25–36

Taccola G, Margaryan G, Mladinic M, Nistri A (2008) Kainate and metabolic perturbation mimicking spinal injury differentially contribute to early damage of locomotor networks in the in vitro neonatal rat spinal cord. Neuroscience 155:538–555

Wang Y, Dawson VL, Dawson TM (2009) Poly(ADP-ribose) signals to mitochondrial AIF: a key event in parthanatos. Exp Neurol 218:193–202

Methods, materials and results

Section 3

Nasrabady SE, Kuzhandaivel A, Nistri A (2011) Studies of locomotor network neuroprotection by the selective poly(ADP-ribose) polymerase-1 inhibitor PJ-34 against excitotoxic injury to the rat spinal cord in vitro. The European journal of neuroscience 33:2216-2227.

NEUROSYSTEMS

Studies of locomotor network neuroprotection by the selective poly(ADP-ribose) polymerase-1 inhibitor PJ-34 against excitotoxic injury to the rat spinal cord *in vitro*

Sara E. Nasrabady,[1,*] Anujaianthi Kuzhandaivel[1,*] and Andrea Nistri[1,2]

[1]Neurobiology Sector, International School for Advanced Studies (SISSA), Via Bonomea 265, 34136 Trieste, Italy
[2]Spinal Person Injury Neurorehabilitation Applied Laboratory, Istituto di Medicina Fisica e Riabilitazione, Udine, Italy

Abstract

Delayed neuronal destruction after acute spinal injury is attributed to excitotoxicity mediated by hyperactivation of poly(ADP-ribose) polymerase-1 (PARP-1) that induces 'parthanatos', namely a non-apoptotic cell death mechanism. With an *in vitro* model of excitotoxicity, we have previously observed parthanatos of rat spinal cord locomotor networks to be decreased by a broad spectrum PARP-1 inhibitor. The present study investigated whether the selective PARP-1 inhibitor N-(6-oxo-5,6-dihydrophenanthridin-2-yl)-(N,N-dimethylamino)acetamide.HCl (PJ-34) not only protected networks from kainate-evoked excitotoxicity, but also prevented loss of locomotor patterns recorded as fictive locomotion from lumbar (L) ventral roots (VRs) 24 h later. PJ-34 (60 μM) blocked PARP-1 activation and preserved dorsal, central and ventral gray matter with maintained reflex activity even after a large dose of kainate. Fictive locomotion could not, however, be restored by either electrical stimulation or bath-applied neurochemicals (N-methyl-D-aspartate plus 5-hydroxytryptamine). A low kainate concentration induced less histological damage that was widely prevented by PJ-34. Nonetheless, fictive locomotion was observed in just over 50% of preparations whose histological profile did not differ (except for the dorsal horn) from those lacking such a rhythm. Our data show that inhibition of PARP-1 could amply preserve spinal network histology after excitotoxicity, with return of locomotor patterns only when the excitotoxic stimulus was moderate. These results demonstrated divergence between histological and functional outcome, implying a narrow borderline between loss of fictive locomotion and neuronal preservation. Our data suggest that either damage of a few unidentified neurons or functional network inhibition was critical for ensuring locomotor cycles.

Introduction

Acute spinal cord injury remains one important cause of long-term morbidity and mortality (McDonald & Sadowsky, 2002; Fehlings & Perrin, 2006) with an incidence rate of 22 people/million/year, in particular young adults (Hall & Springer, 2004; Rossignol et al., 2007). This problem also largely affects children as it includes 1–2% of pediatric fractures and is the reason for the highest mortality of all orthopedic injuries in infants (Leonard et al., 2007). Despite intense clinical efforts, the outcome remains poor as only about 5% of patients with severe spinal cord injury will walk again (Dobkin & Havton, 2004).

Following the primary injury, the secondary biochemical cascades (developing over minutes, hours and days) responsible for motor deficits are thought to be triggered by excitotoxicity due to massive release of glutamate (Hall & Springer, 2004; Park et al., 2004; Rossignol et al., 2007). Although excitotoxicity has been traditionally associated with apoptosis and necrosis (Choi, 1992; Liu et al., 1997; Yuan et al., 2003; Baptiste & Fehlings, 2006), a recently discovered

cell death pathway named parthanatos, which involves the hyperactivity of poly(ADP-ribose) polymerase-1 (PARP-1), is believed to be as important to spinal cord injury (Scott et al., 1999; Genovese et al., 2005; Wu et al., 2009; Kuzhandaivel et al., 2010) as to brain ischemia (Eliasson et al., 1997; Koh et al., 2004). A glutamate-mediated increase in PARP-1 activity generates poly(ADP-ribose) (PAR) that disrupts mitochondrial membrane potential, and stimulates translocation of apoptosis-inducing factor (AIF) to the cell nucleus leading to extensive DNA damage that together with energy depletion will produce parthanatos (Narasimhan et al., 2003; Wang et al., 2009a).

Our *in vitro* model of spinal cord injury caused by excitotoxicity has recently shown neurons rather than glial cells to be highly affected by parthanatos (Kuzhandaivel et al., 2010). In that study, application of a relatively non-selective PARP-1 inhibitor immediately after washout of kainate decreased PARP-1-mediated cell death and reduced AIF translocation to the nucleus (Kuzhandaivel et al., 2010). However, a poor outcome in terms of locomotor network activity has been subsequently reported (Nasrabady et al., 2011).

In the present study we investigated the potential neuroprotective role of a highly selective inhibitor of PARP-1, namely N-(6-oxo-5,6-dihydrophenanthridin-2-yl)-(N,N-dimethylamino)acetamide.HCl (PJ-34) (Abdelkarim et al., 2001; Kauppinen et al., 2009), on

Correspondence: Andrea Nistri, [1]Neurobiology Sector, as above.
E-mail: nistri@sissa.it

*S.E.N. and A.K. contributed equally to this work.

locomotor network activity of neonatal rat isolated spinal cord together with histochemical characterization of the spinal damage after excitotoxic injury.

Methods and materials

Spinal cord preparation

The experiments were performed on neonatal Wistar rats with a postnatal age of 0–2 days in accordance with the guidelines of the National Institutes of Health and the Italian act D.Lgs. 27/1/92 no. 116 (implementing the European Community directives no. 86/609 and 93/88). Spinal cords were carefully dissected out under urethane anesthesia (0.2 mL i.p. of a 10% w/v solution). Neonatal rat spinal cords were superfused (7.5 mL/min) with Krebs solution containing (in mM): 113 NaCl, 4.5 KCl, 1 $MgCl_2 7H_2O$, 2 $CaCl_2$, 1 NaH_2PO_4, 25 $NaHCO_3$ and 11 glucose, gassed with 95% O_2/5% CO_2, pH 7.4 at room temperature (22°C) (fully described previously by Beato & Nistri, 1999; Taccola & Nistri, 2006a; Margaryan et al., 2009).

Electrophysiological recording

The experiments were based on DC-coupled recordings from L VRs using tight-fitting suction electrodes (Taccola & Nistri, 2006a). Signals were recorded from left (l) and right (r) L2 VRs producing mainly flexor motor signals to the hindlimb muscles, and from L5 VRs, which convey mainly extensor motor commands to the same limb (Kiehn & Kjaerulff, 1998; Kiehn, 2006; Taccola & Nistri, 2006b). Using pClamp software (version 9.2; Molecular Devices, Sunnyvale, CA, USA), signals were captured, digitized and analyzed.

In order to stimulate the spinal cord through afferent fibers, single electrical stimuli were applied to the ipsilateral homosegmental dorsal root (DR) every 60 s. Normally, one train of DR stimuli (0.1 ms duration, 30 pulse trains at 2 Hz) was used to induce cumulative depolarization with superimposed alternating oscillatory activity typical of fictive locomotion. The stimulation strength was 2× threshold, where threshold was taken as the minimum intensity to elicit a detectable response in the homolateral VR (Taccola et al., 2004). The peak amplitude and area of the responses were calculated by averaging at least five events. Fictive locomotion was also chemically induced by application of N-methyl-D-aspartate (NMDA) (4 μM) (Tocris Bioscience, Bristol, UK) plus 5-hydroxytryptamine (5-HT) (10 μM, Sigma, Milan, Italy) (Cazalets et al., 1992; Kiehn & Kjaerulff, 1996; Butt et al., 2002). The period (time interval between the onsets of two cycles) and its coefficient of variation were measured from at least 20 continuous cycles. The criterion to diagnose the presence of fictive locomotion was continuous generation of at least 20 cycles alternating between homosegmental and left–right four L VRs. Disinhibited bursting (Bracci et al., 1996, 1997) was elicited by application of strychnine (1 μM) (Sigma) and bicuculline (20 μM) (Fluka, Milan, Italy) and the burst parameters (recorded from the same VRs) were calculated in accordance with Bracci et al. (1996).

Protocols of lesion and neuroprotection

The protocol for excitotoxic spinal lesion in vitro relies on the application of the strong excitotoxic agent kainate (Ascent Scientific, Weston-super-mare, UK) for 1 h in standard Krebs solution (Taccola et al., 2008). Kainate was applied at 1 mM, 0.1 mM or 50 μM concentration to induce either an extensive or a threshold (50 μM) lesion that always abolished locomotor network function for at least 24 h as detailed by Mazzone et al. (2010).

With each toxic dose, we tried neuroprotection by applying the selective inhibitor of PARP-1, PJ-34 (Sigma). Two protocols were employed. In a first series of experiments, we applied 10–60 μM PJ-34 immediately at the washout of kainate and explored its effects on PARP-1 activity measured with enzyme-linked immunosorbent assay (ELISA), or on the number of pyknotic cells, or on the translocation of AIF (see below). In a second series of experiments that comprised electrophysiological and immunohistochemical tests, PJ-34 (60 μM) was applied halfway (30 min) through kainate application. This time schedule was chosen because of the previous report that hyperactivation of PARP-1 was already detected at the time of washout of kainate (Kuzhandaivel et al., 2010). In all cases, PJ-34 application was extended for the subsequent 24 h after which PJ-34 was washed out and electrophysiological responses retested in standard Krebs solution. Previous experiments indicated that micromolar concentrations of PJ-34 were necessary to neuroprotect organotypic spinal cultures from kainate toxicity (Mazzone & Nistri, 2011).

For functional studies, systematic testing of the electrophysiological responses in terms of reflex or fictive locomotor activity was performed on the first day of each experiment to obtain control data prior to any treatment. Untreated sham spinal cords kept for 24 h in Krebs solution (Taccola et al., 2008) or treated with PJ-34 alone (for 24 h) were used for comparison with kainate with or without PJ-34 preparations tested 24 h later. All preparations were fixed after the end of the experiment as previously described (Taccola et al., 2008).

Immunohistochemistry

Our previous experiments have validated the use of the antibodies employed for the present investigation. In particular, the mouse monoclonal anti-neuronal specific nuclear protein (NeuN; Millipore, Milan, Italy) (Taccola et al., 2008; Margaryan et al., 2010) and the mouse monoclonal anti-neurofilament H non-phosphorylated (SMI 32) (Covance, Emeryville, CA, USA) (Taccola et al., 2008; Margaryan et al., 2010) antibodies were used for immunohistochemical labeling with the free-floating method as described previously (Taccola et al., 2008). Briefly, paraformaldehye-fixed spinal cords were cryoprotected with 30% sucrose and sectioned (30 μm). After incubation in blocking solution (5% normal goat serum, 5% bovine serum albumin, 0.3% Triton-X 100) for 1 h at room temperature, the primary antibody (NeuN, 1 : 50 or SMI 32, 1 : 200 dilution) was incubated at 4 °C overnight. The primary antibodies were visualized using secondary anti-mouse Alexa fluor 488 or 594 antibodies (1 : 500). Sections were finally stained with 4′,6-diamidino-2-phenylindole (DAPI) for 20 min and analyzed using a Zeiss Axioskop2 microscope and Metavue software.

Quantification of dead cells

Pyknotic nuclei DAPI staining or NeuN-positive cells were counted in four regions (ventral, central, dorsal gray matter and ventrolateral white matter) of the spinal cord using 'eCELLence' (Glance Vision Tech., Trieste, Italy) software (Taccola et al., 2008; Margaryan et al., 2009). Pyknosis was readily observed as a change in nuclear morphology resulting from chromatin condensation (either nucleolytic or anucleolytic) (Burgoyne, 1999). For each histological cross-section of the spinal cord, four different regions were investigated: dorsal gray matter (Rexed laminae I–IV), central gray matter (Rexed laminae V–VII and X), ventral gray matter (Rexed laminae VIII–IX) and ventrolateral white matter. For each region, three to seven fields of 280 × 280 μm (gray matter) or 100 × 280 μm (white matter) area

were analyzed. For each experimental group, 4–11 spinal cords were analyzed and, for each spinal cord, 4–6 different sections from T12 to L3 segments were examined.

Quantification of poly(ADP-ribose) (PAR)

Previous studies have indicated that excitotoxicity largely activates PARP-1 in the rat brain tissue (Endres *et al.*, 1997; Chiarugi, 2005; Moroni, 2008) as well as in the rat spinal cord (Genovese *et al.*, 2005; Kuzhandaivel *et al.*, 2010). Nonetheless, in the present report we investigated whether, under the current experimental conditions, namely kainate (50 μM or 1 mM)-mediated excitotoxicity, there was direct evidence for PARP-1 activation by measuring its product PAR, and whether PJ-34 (60 μM) was an effective inhibitor of this process when added immediately after the washout of kainate (applied for 1 h). For this purpose, PARP-1 activity was determined by measuring the PAR levels in the tissue lysates of spinal cords treated with different concentrations of kainate and/or PJ-34, or in sham conditions. PAR levels were always quantified 4 h after the application of kainate and/or PJ-34 because our former study has shown that, at this time, the maximum activity of PARP-1 evoked by kainate is detected with western immunoblotting (Kuzhandaivel *et al.*, 2010). After preparing tissue lysates from the spinal cords, their PAR levels were measured using the PARP *in vivo* Pharmacodynamic Assay II (http://www.trevigen.com/protocols/pdf/4520-096-K.pdf) following the manufacturer's protocol (Trevigen, Bologna, Italy). This assay is based on the ELISA immunoreactivity resulting in chemiluminescence signals recorded with the Glo®max multi-detection system (Promega, Milan, Italy). Whenever tests were performed for the action of PJ-34, this substance was also added to cell lysis buffer to avoid inhibitor dilution as per the manufacturer's instructions. All samples were run in triplicate. After background subtraction (blank samples), the net PAR levels were quantified using a standard linear plot ($r = 0.98$) based on the immunoreactivity induced by known concentrations (20–1000 pg/mL) of PAR. Data were expressed as pg/mL per 100 μg of protein (estimated as indicated below).

Nuclear and mitochondrial protein extraction

The nuclear extraction was prepared in accordance with published reports (Cox & Emili, 2006; Kuzhandaivel *et al.*, 2010). Thus, isolated spinal cords were washed with ice-cold 250-STMDPS buffer (50 mM Tris-HCl, pH 7.4, 250 mM sucrose, 5 mM MgCl$_2$, 1 mM dithiothreitol (DTT), 1 mM phenylmethylsulfonyl fluoride (PMSF), 25 μg/mL spermine and 25 μg/mL spermidine) and then submerged in the same. After 15 strokes in a Dounce homogenizer, the extract was centrifuged at 800 ***g*** for 15 min. The pellet (Pellet I) was used to prepare the nuclear fraction. The supernatant was again centrifuged at 6000 ***g*** for 15 min to remove mitochondria (Pellet II). To prepare the nuclear fraction, Pellet I was homogenized with a single stroke in a Dounce homogenizer in 2 M-STMDPS buffer (50 mM Tris-HCl, pH 7.4, 2 M sucrose, 5 mM MgCl$_2$, 1 mM DTT, 1 mM PMSF, 25 μg/mL spermine and 25 μg/mL spermidine) and fractionated at 80 000 ***g*** for 35 min. The resulting pellet was resuspended in nuclear extract buffer (20 mM HEPES, pH 7.9, 1.5 mM MgCl$_2$, 0.5 M NaCl, 0.2 mM EDTA and 20% glycerol) and used as the nuclear fraction (Pellet I). Pellet II was resuspended in hypotonic lysis buffer (10 mM HEPES, pH 7.9, 1 mM DTT, plus the protease inhibitor cocktail; Sigma) and incubated on ice for 30 min. The suspension was sonicated at a high setting (50–10 s burst with 30 s pause) to lyse mitochondria. Protein concentrations were determined for the nuclear fraction and the mitochondrial

lysate using the standard bicinchoninic acid assay following the manufacturer's protocol (Sigma). For each individual experiment, three spinal cords were used. The purity of the extracted nuclear fraction was validated by looking for (with western immunoblotting) any mitochondrial contamination indicated by the cytochrome C oxidase IV protein (Abcam, Cambridge, UK) in accordance with the method of Beirowski *et al.* (2009).

Western blotting

The antibodies used for western blot studies and validated in a previous report (Kuzhandaivel *et al.*, 2010) were: rabbit polyclonal anti-AIF (1 : 500) and mouse monoclonal anti-TATA (5′-TATAAA-3′) binding protein (1 : 1000) (Abcam). Equal amounts of protein were separated on a 10–12% sodium dodecyl sulfate–polyacrylamide gel electrophoresis (SDS-PAGE) for 1.5 h at 150 V. The proteins were transferred onto a nitrocellulose membrane (Amersham Biosciences, Milan, Italy) for 2 h at 200 mA. The membrane was blocked in 5% non-fat milk in Tris-buffered saline–Tween (25 mM Tris-Cl, pH 7.5, 150 mM NaCl, 0.1% Tween-20) for 1 h at 25 °C followed by the incubation with the respective primary antibody overnight at 4 °C. The membranes were washed three times for 10 min in Tris-buffered saline–Tween (TBST) and probed with the appropriate horseradish peroxidase-conjugated secondary antibody for 2 h at 25 °C. Immunoreactive bands were calibrated with Colorburst electrophoresis marker (Sigma) to estimate molecular weight. Protein bands were then visualized with enhanced chemiluminescence (Amersham Biosciences). The relative density of the bands was determined using Scion image (Maryland, MD, USA). Results were normalized to TATA binding protein (utilized as loading control).

Data analysis

Statistical analysis was carried out with SigmaStat 3.1 (Systat Software, Chicago, IL, USA). The data are shown as mean ± SD. Parametric and non-parametric data were first distinguished with a normality test and analyzed with the Student's *t*-test or Mann–Whitney test, respectively, in accordance with the software choice. For electrophysiological experiments, the comparison was made between the data obtained on the second day of each experiment and the sham or the group treated with kainate without neuroprotective drug. Full details of the statistical analysis for each test are provided in the figure legends in which *T* and *t* values refer to Mann–Whitney and Student's *t*-test values, respectively. The significance level was always $P < 0.05$ and *n* indicates the number of preparations.

Results

PJ-34 as a pharmacological inhibitor of poly(ADP-ribose) polymerase-1 activity

Initial experiments were performed to find out whether kainate evoked hyperactivation of PARP-1 in the rat spinal cord *in vitro*, whether this effect was related to the concentration of kainate, and whether PJ-34 could inhibit it. Figure 1A summarizes the results of these experiments in which we estimated the activity of PARP-1 by measuring its product PAR 4 h after the washout of either a high (1 mM) or low (50 μM) concentration of kainate (1 h application). Sham preparations showed a PAR level larger than that observed in the presence of PJ-34, indicating constitutive PARP-1 activity under the present experimental conditions (4 h *in vitro*). Nonetheless, kainate (1 mM) elicited a large increment in PAR levels that were approximately three times higher

than in sham preparations. This effect was fully suppressed by delayed application of PJ-34 (60 μM; applied at kainate washout) (Mazzone & Nistri, 2011). A lower concentration of kainate (50 μM) evoked a smaller level of PAR that was again inhibited by PJ-34 (Fig. 1A). These data confirm that kainate-evoked excitotoxicity was associated with robust hyperactivation of PARP-1 and that this effect was blocked by PJ-34.

In order to compare the neuroprotective action of PJ-34 with that produced by the non-selective PARP-1 inhibitor 6-5(H)-phenathridinone (Kuzhandaivel et al., 2010; Nasrabady et al., 2011), we applied various concentrations of PJ-34 on the washout of kainate and assessed the number of pyknotic nuclei in the four areas of the spinal cord as detailed earlier. Figure 1B shows that the best histological protection (low percentage of pyknosis) was observed with 60 μM PJ-34 in all three gray matter regions examined (the white matter was comparatively spared by excitotoxicity) (Taccola et al., 2008). For this reason the present study used PJ-34 at a concentration of 60 μM for subsequent experiments. We sought additional evidence that this PJ-34 concentration could block the consequences of PARP-1 hyperactivity evoked by 1 mM or 50 μM kainate by measuring the translocation of the PARP-1 effector, namely the AIF, which is translocated from

stressed mitochondria to the cell nucleus (Li et al., 2010). TATA binding protein (TBP) was used as a marker for nuclear loading control, whereas cytochrome C oxidase IV (COX IV) was used to check the purity of the nuclear fraction and as a mitochondrial loading control. Figure 1C and D demonstrates that kainate (1 mM) strongly enhanced the translocation of AIF (normalized for loading with the nuclear marker TBP), a process significantly reduced by 60 μM PJ-34. A smaller dose of kainate (50 μM) produced less AIF translocation that was almost suppressed by 60 μM PJ-34. The absence of COX IV in the nuclear fraction confirmed lack of cross-contamination by mitochondrial fractions (Fig. 1C). The molecular weight of AIF (62 kDa; Fig. 1C) indicated that it was translocated to the nucleus in its full-length form in accordance with a previous report (Wang et al., 2009b).

These data suggested that 60 μM was, in principle, a suitable test dose of PJ-34 to explore its potential functional and histological neuroprotection against excitotoxicity. To maximize the chances of neuroprotection, we decided to apply PJ-34 after 30 min application of kainate (always applied for 60 min) and to continue the PJ-34 application throughout the following 24 h in oxygenated Krebs solution. In fact, previous observations have shown that significantly
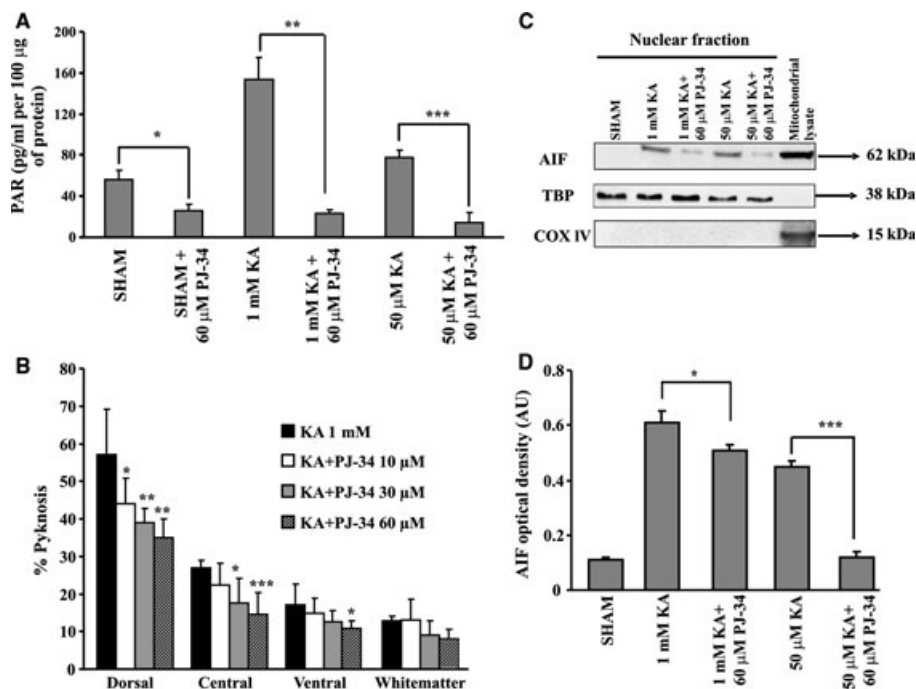

FIG. 1. Effect of PJ-34 on PARP-1 activity, AIF translocation and cell pyknosis induced by kainate (KA). (A) Net PAR levels produced by PARP-1 activity of tissue lysates from sham or KA (50 μM or 1 mM) treated spinal cords, with or without subsequent application of 60 μM PJ-34 (for each group $n = 4$). Data are significantly different between PJ-34 treated and untreated preparations (*$t_4 = 5.385$ and $P = 0.006$; **$t_4 = 12.061$ and $P \leq 0.001$; ***$t_4 = 9.420$ and $P \leq 0.001$). (B) Percent of pyknosis occurrence (as percentage of total count of cell nuclei) detected in different spinal cord regions at 24 h after KA treatment alone (1 mM) or followed by treatment with the PARP-1 inhibitor PJ-34 (three different concentrations; 10–60 μM). PJ-34 significantly reduces (*$P < 0.05$, **$P < 0.01$, ***$P < 0.001$) the number of pyknotic cells in a dose-dependent manner in all four spinal cord regions. Comparison of data for 1 mM KA vs. 10 μM PJ-34 gave $t_8 = -2.344$ and $P = 0.047$ for the dorsal region, $T = 101$ and $P = 0.185$ for the central region, $t_8 = -0.247$ and $P = 0.811$ for the ventral region, and $t_8 = -1.734$ and $P = 0.121$ for white matter. Comparison of data for 1 mM KA vs. 30 μM PJ-34 gave $t_8 = 4.413$ and $P = 0.005$ for the dorsal region, $T = 26$ and $P = 0.029$ for the central region, $t_8 = 1.853$ and $P = 0.101$ for the ventral region, and $t_8 = 0.261$ and $P = 0.261$ for the white matter region. Comparison of data for 1 mM KA vs. 60 μM PJ-34 gave $t_4 = -6.957$ and $P = 0.002$ for the dorsal region, $t_4 = -8.041$ and $P = 0.001$ for the central region, $t_8 = -2.916$ and $P = 0.043$ for the ventral region, and $t_8 = 0.108$ and $P = 0.917$ for the white matter region. (C) Example of AIF immunoblotting of spinal cord samples (nuclear fraction) obtained from sham, KA-treated preparations (50 μM or 1 mM) and preparations that, after KA application, were treated with PJ-34 (60 μM). The AIF specific reactivity (62 kDa band) in the nuclear fraction of KA-treated spinal cords is reduced after PJ-34 application. Nuclear loading was assessed with TATA binding protein (TBP). The purity of the nuclear fraction was assessed with cytochrome C oxidase IV (COX IV), which was absent from the nuclear fraction lanes and present in the mitochondrial lysate (last lane). (D) Expression (by western immunoblotting) of AIF in the nuclear fraction of KA-treated spinal cords, with or without subsequent application of 60 μM PJ-34 (for each sample $n = 4$ experiments, in each of which three spinal cords were pooled). Data (expressed in arbitrary units) are significantly different between PJ-34-treated and untreated preparations (*$t_4 = 4.35$ and $P = 0.012$; *** $t_4 = 30.94$ and $P = 0.001$) during the first 24 h after KA.

high PARP-1 expression already emerges at the time of kainate washout (Kuzhandaivel *et al.*, 2010), raising the possibility that any attempts to pharmacologically block it should not be attempted too late.

PJ-34 can protect locomotor network patterns against a moderate but not a high dose of kainate

With the protocol of PJ-34 application staggered by 30 min after the start of kainate application, we checked whether significant protection of synaptic transmission, cumulative depolarization, fictive locomotion and disinhibited bursting was present. Figure 2A and B shows that the very dramatic reduction in polysynaptic responses recorded from L VRs at 24 h after 1 mM kainate was partly counteracted by PJ-34 in terms of amplitude and area. Much less successful was the protection by PJ-34 of cumulative depolarization induced by trains of electrical pulses applied to an adjacent DR and recorded from a single VR of two different preparations as shown in Fig. 2C and D. Full suppression of this phenomenon by 1 mM kainate was recorded 24 h later (Fig. 2C and D). When kainate application was followed by PJ-34, only a very modest depolarization was observed 24 h later (Fig. 2C and D). In all of these preparations, there was complete absence of alternating oscillations amongst left and right L2 and L5 VRs, typical of fictive locomotion.

Despite the lost ability of spinal networks to integrate afferent inputs to produce cumulative depolarization and express fictive locomotion, we could observe significant ($P = 0.035$, $t_8 = 2.54$) recovery in the amplitude of disinhibited bursts (elicited by co-applied strychnine and bicuculline) that expresses the elementary rhythmicity of these circuits. No significant change in the periodicity of rhythmic bursting was observed after kainate alone or kainate plus

PJ-34 (Fig. 3A and B). In order to see whether the surviving network could still be activated by afferent inputs, the same preparations were entrained by 0.05 Hz DR stimulation (Bracci *et al.*, 1997; Taccola *et al.*, 2008). Figure 3C shows an example of how each DR stimulus in a pulse train reliably evoked a burst at 24 h after kainate (middle row) or kainate plus PJ-34 (bottom row). Average data indicate that the burst amplitude increased in the group treated with PJ-34 ($n = 4$) in comparison with the group treated with kainate alone ($n = 4$) ($P = 0.029$, $t_6 = 10$), whereas the burst duration was similar in these two groups (Fig. 3D).

We next investigated whether a weaker excitotoxic stimulus (50 μM kainate; 60 min) could produce less spinal network damage and be more efficaciously counteracted by PJ-34. Previous studies have indicated that 50 μM kainate is the threshold concentration for inducing full suppression of locomotor network activity (Mazzone *et al.*, 2010). In accordance with our previous study (Mazzone *et al.*, 2010), we measured the VR depolarization (indicative of motoneuron pool average responses) induced by two concentrations of kainate. We found 1.42 ± 0.63 mV depolarization by 50 μM kainate and 2.81 ± 0.6 mV by 1 mM kainate ($n = 8$ in both groups), confirming the dose-dependent change in VR polarization elicited by this agent. Our previous study on single motoneurons showed strong membrane potential depolarization from −76 to −30 mV by 1 mM kainate (Taccola *et al.*, 2008). In keeping with such large changes in motoneuron properties, we have also observed a large suppression of polysynaptic transmission (Taccola *et al.*, 2008).

Figure 4A and B shows that applying PJ-34 at 30 min after starting 50 μM kainate could result (24 h later) in substantial protection of VR reflex activity from kainate damage. The response amplitude and area were both significantly enhanced by PJ-34 when compared with those from kainate-treated preparations. Comparison of Fig. 4A and B with

FIG. 2. Effect of PJ-34 (60 μM) application on electrophysiological responses recorded after 24 h from *in vitro* spinal cord preparations exposed to strong excitotoxic injury caused by kainate (KA) (1 mM). (A) Examples of polysynaptic VR responses evoked by electrical stimuli (2× threshold) applied to homolateral DR root and recorded after 24 h in sham (left), KA-treated (middle) or PJ-34-treated (30 min after KA application; right) condition. (B) Despite the dramatic reduction in polysynaptic responses after KA, the reflex peak amplitude and area were significantly increased in the group treated with PJ-34 ($P = 0.047$, $t_8 = 2.34$ and $P = 0.032$, $t_8 = 2.58$, respectively; see asterisks for statistical comparison) ($n = 7$, 6 and 4 for sham, KA and KA + PJ-34 respectively). (C) Examples of VR alternating cycles elicited by a train of DR stimuli (30 stimuli, 2× threshold intensity, 2 Hz) in control (before KA application) and their full suppression after 24 h after KA alone or KA + PJ-34. (D) A modest increment of cumulative depolarization and area was observed after 24 h of PJ-34 application, whereas they were completely abolished in the KA group.
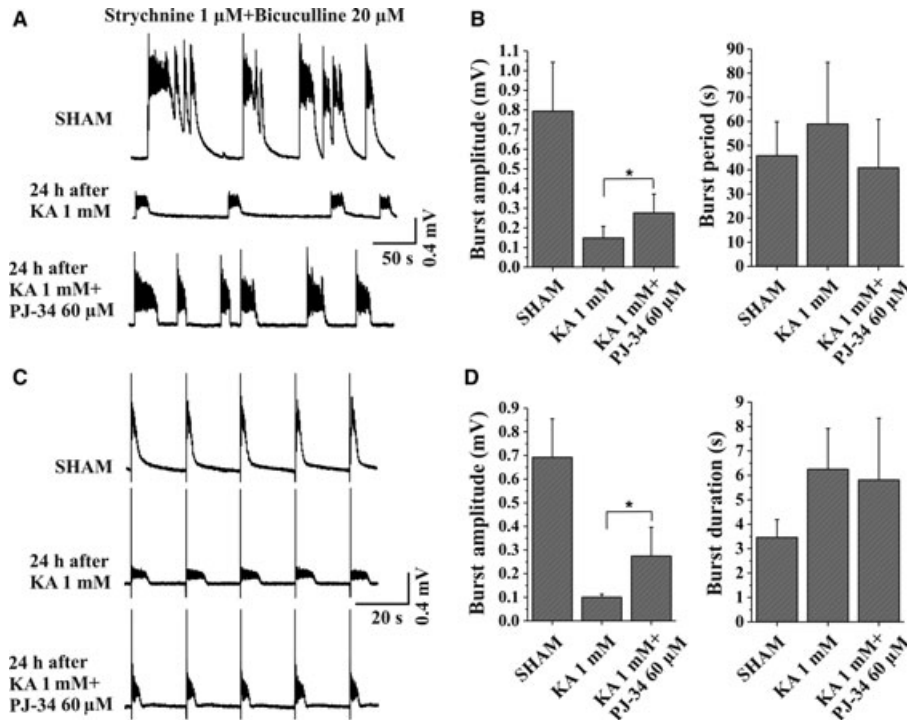
FIG. 3. Effect of PJ-34 after strong excitotoxic injury by kainate (KA) (1 mM) on intrinsic rhythmicity of the spinal cord. (A) Examples of disinhibited bursts (elicited by strychnine plus bicuculline) in sham, after KA alone (1 mM) or KA + PJ-34 (30 min after KA application). (B) Higher burst amplitude (left; $P = 0.035$, $t_8 = 2.54$) with similar periodicity (right) in the group treated with PJ-34 in comparison with the KA group [$n = 7$, 6 and 4 for sham, KA (1 mM) and KA + PJ-34, respectively]. Asterisks indicate the statistically significant difference. (C) Network bursting is always entrained (1 : 1) by a DR train of 20 stimuli (0.05 Hz, 0.1 ms, 1–4 V) in sham, KA or KA + PJ-34 condition. (D) Burst amplitude induced by DR stimuli in the group treated with PJ-34 is higher than in the group treated with KA (1 mM) alone ($P = 0.029$, $t_6 = 10$; $n = 4$ for both groups), whereas burst duration does not change with PJ-34 application.

Fig. 2A and B indicates, however, that the electrophysiological deficit evoked by 50 μM kainate was smaller than that produced by 1 mM kainate.

In fact, unlike the effect of 1 mM kainate, 50 μM kainate did not eliminate cumulative depolarization, which remained at about 20% of sham, even though no oscillations could be detected at 24 h (Fig. 4C and D). The size of the cumulative depolarization was not, however, improved by PJ-34 (applied 30 min after kainate) 24 h later (Fig. 4C and D). In the PJ-34-treated preparations, sparse superimposed alternating oscillations emerged (3 ± 1; $n = 3$; see for instance Fig. 4C, bottom right), but they were comparatively fewer ($P < 0.001$) than those observed in sham or control preparations (5 ± 1; $n = 6$; see example in Fig. 4C, left). Thus, the locomotor-like patterns produced by sensory afferent stimulation were very sensitive to excitotoxic damage even by a small dose of kainate, and could not be fully restored by PJ-34.

We therefore studied whether the locomotor central pattern generator (CPG) could be activated in a different fashion and its operation protected by PJ-34. To examine this issue, we first used the standard combined application of NMDA and 5-HT to generate fictive locomotion in control solution, and then we washed out these agents and applied kainate (or kainate + PJ-34). Figure 5A and B (left panels) shows, on the first day of the experiment, control alternating oscillations recorded from pairs of L2 and L5 VRs prior to applying kainate. Figure 5A (right panels) shows that, at 24 h after 50 μM kainate (60 min), fictive locomotion could not be elicited by NMDA plus 5-HT as only irregular firing emerged from the four L roots (inset shows spike activity with time expansion). This observation was repeated on a total of 11 preparations (four of which displayed < 10 cycles of oscillations from one or two VRs only, thus

unable to meet the criterion for fictive locomotion) and accords with our previous report (Mazzone et al., 2010). Figure 5B (right panels) shows that, when 50 μM kainate was followed 30 min later by PJ-34 application, fictive locomotion could be observed with alternating patterns on all four VRs 24 h later. The inset to Fig. 5B (right) depicts an example of the oscillatory pattern recorded from VRlL2. This neuroprotective action towards chemically-evoked fictive locomotion was observed 24 h later in 6/11 spinal cords. In such preparations the fictive locomotion average period was 6.6 ± 1.6 s (CV = 0.15 ± 0.03), a value significantly ($P = 0.018$, $t_{13} = 2.712$) slower than the 4.6 ± 1.2 s (CV= 0.10 ± 0.04; $n = 9$) value obtained from sham preparations kept in Krebs solution for 24 h. In the remaining five spinal cords, no fictive locomotion was observed even after increasing the concentration of NMDA to 6 μM. A separate batch of tests investigated the effect of an intermediate concentration of kainate (100 μM) followed 30 min later by PJ-34. As reported previously (Mazzone et al., 2010), 100 μM kainate per se fully abolished fictive locomotion elicited by DR train pulses or NMDA plus 5-HT ($n = 6$). When 100 μM kainate was associated (30 min later) with PJ-34, again there was no recovery of fictive locomotion tested 24 h later ($n = 4$).

Neurotoxicity produced by kainate and its block by PJ-34

A hallmark of excitotoxic damage to the in vitro spinal cord is the appearance of condensed chromatin (pyknosis) as previously reported (Taccola et al., 2008; Margaryan et al., 2009; Kuzhandaivel et al., 2010). In the present study we measured the occurrence of pyknosis in four spinal regions after applying various concentrations of kainate
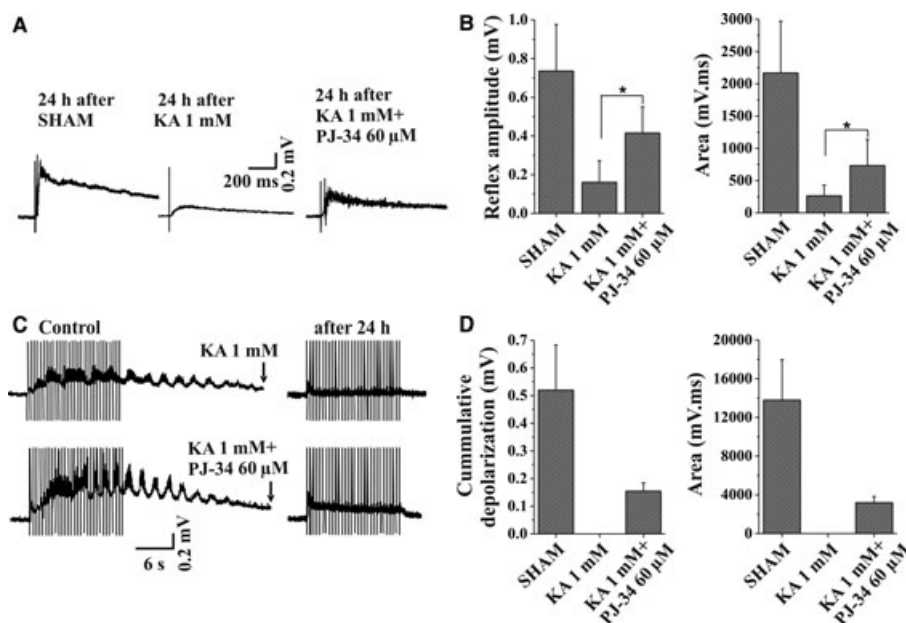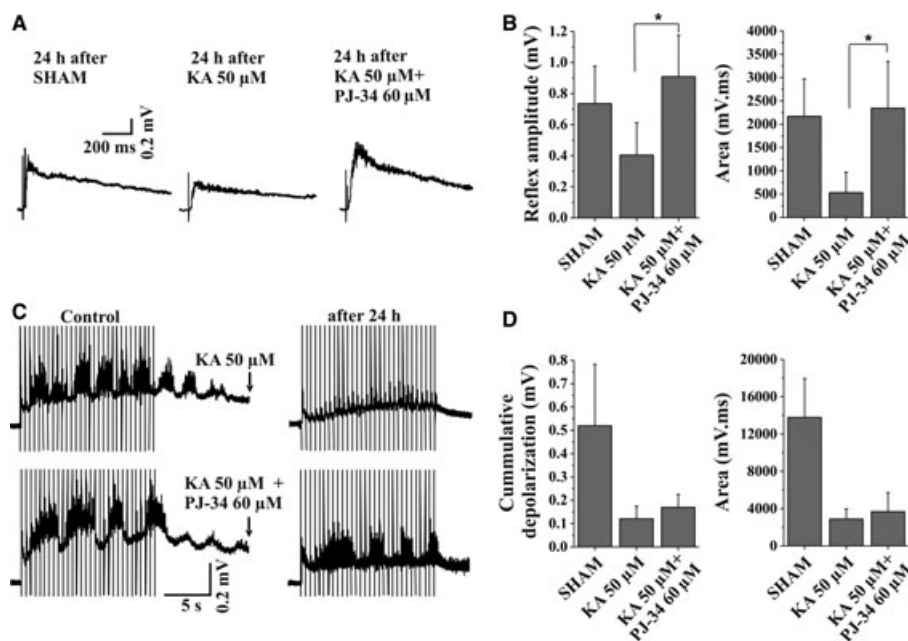
FIG. 4. Effect of PJ-34 (60 μM) application on electrophysiological responses recorded after 24 h from *in vitro* spinal cord preparations exposed to moderate excitotoxic injury by kainate (KA) (50 μM). (A) Examples of polysynaptic VR responses evoked by electrical stimuli (2× threshold) applied to the homolateral DR root and recorded after 24 h in sham (left), KA- (middle) or PJ-34-treated (30 min after KA application; right) condition. (B) Significant increase of peak amplitude ($P = 0.031$, $t_9 = 2.55$) and area ($P = 0.044$, $t_9 = 2.33$) of responses to electrical stimuli ($n = 7$, 5 and 6 for sham, KA and KA + PJ-34, respectively). Asterisks indicate statistically significant difference. (C) Examples of VR alternating cycles to a train of DR stimuli (30 stimuli, 2× threshold intensity, 2 Hz) in control (before KA application) and after 24 h. Fictive locomotion superimposed on cumulative depolarization completely disappeared in the KA group after 24 h, whereas it was partially preserved in half of the preparations treated with PJ-34. The average number of oscillations detected after KA + PJ-34 was 3 ± 1 ($n = 3$ spinal cords) vs. 5 ± 1 in control ($n = 6$; $P < 0.001$, $T = 126.5$). (D) Cumulative depolarization and area induced by train of stimuli were similar in KA and KA + PJ-34 and they were smaller than sham ($n = 7$, 5 and 6 for sham, KA and KA + PJ-34, respectively).

with or without subsequent application of PJ-34 (Fig. 6). As indicated in Fig. 6A and B, pyknosis was strongly present in the dorsal horn area (which contains the largest density of kainate receptors) (Tolle *et al.*, 1993) and was related to the kainate concentration. In keeping with our previous reports (Taccola *et al.*, 2008; Margaryan *et al.*, 2009; Kuzhandaivel *et al.*, 2010), pyknosis was less frequent in the central and ventral gray matter regions as well as in the ventrolateral white matter. Figure 6C and D shows that, by comparison with preparations treated with kainate alone (Fig. 6B), PJ-34 applied after 1 mM or 100 μM kainate produced a clear reduction in the number of pyknotic nuclei for the gray matter regions examined, in particular the dorsal and central regions (statistical details are given in the legend to Fig. 6). It is, however, important to note that, as reported above, no such preparation generated fictive locomotion.

For our analysis, we split the preparations treated with 50 μM kainate followed by PJ-34 into two groups, namely those without fictive locomotion ($n = 5$) and those that retained this pattern after NMDA and 5-HT ($n = 6$). Figure 6D shows that in the first group there was significantly more pyknosis in the dorsal and central regions. Note that PJ-34 alone did not induce pyknosis (Fig. 6D).

Because of the complex cytoarchitecture of the spinal cord, we further investigated the distribution of neurons affected by kainate and potentially protected by PJ-34. Neurons were stained with NeuN antibody (a neuronal nucleus marker) and were counted in the three gray matter regions indicated in Fig. 7B and exemplified for the dorsal horn in Fig. 7A. In accordance with the pyknosis data (expressed as percentage change of DAPI-positive elements in Fig. 6B and D), the lowest absolute number of neurons was observed in the dorsal region after 1 mM kainate (Fig. 7B). These values grew as the concentration of kainate was smaller so that, for example, the neuronal counts in the

ventral horn after 50 μM kainate were close to those of sham preparations as previously reported (Mazzone *et al.*, 2010). Figure 7C shows that, for a preparation retaining fictive locomotion after applying 50 μM kainate followed by PJ-34, the neuronal population of the dorsal horn was better preserved. Indeed, PJ-34 exerted a degree of neuronal protection against various kainate concentrations (Fig. 7D) when compared with the values reported in Fig. 7B; in the case of preparations generating fictive locomotion after 50 μM kainate and PJ-34, the main difference was the larger number of dorsal horn neurons. Figure 7D shows that PJ-34 alone had no effect on neuronal counts. The legend to Fig. 7 contains statistical details of this analysis.

Motoneurons are a relatively small number of neurons in the ventral horn, yet they possess high vulnerability to excitotoxicity *in vitro* (Mazzone *et al.*, 2010; Taccola *et al.*, 2010). Thus, we counted motoneurons after kainate alone or followed by PJ-34. Motoneurons were identified as large (> 20 μm soma) cells in the ventral horn immunopositive to SMI 32, which labels a non-phosphorylated form of motoneuronal cytoplasmic neurofilament (Mazzone *et al.*, 2010; Taccola *et al.*, 2010). We checked whether loss of motoneurons induced by kainate and estimated on the basis of absence of SMI 32 positivity was indeed a sign of cell death and not merely the biochemical disappearance of this protein label. Figure 8A shows examples of double staining of ventral horn cells with the nuclear dye DAPI to evaluate pyknosis (see arrows, left panel) and SMI 32 (middle panel); the overlay panel (right panel) indicates that pyknotic cells were those that lost SMI 32, whereas surviving cells retained this immunoreactivity. A similar observation was obtained when the application of kainate (50 μM) was followed 30 min later by PJ-34 (bottom row of Fig. 8A). These data therefore
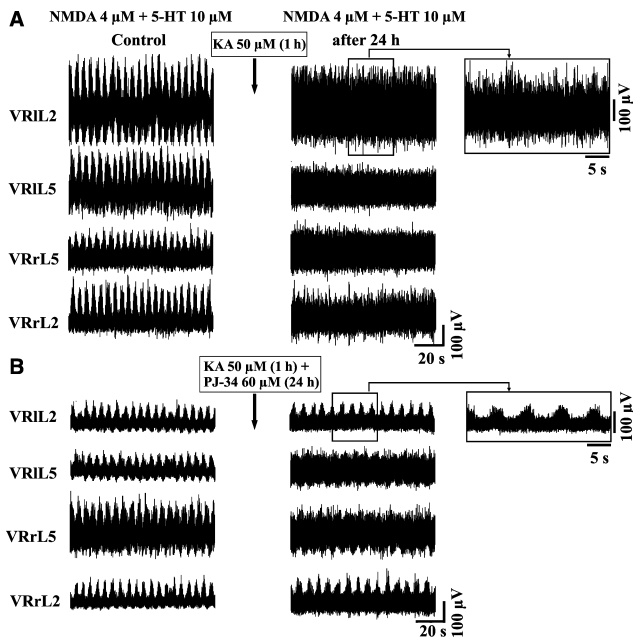
FIG. 5. Effect of PJ-34 (60 μM) application on fictive locomotion induced by co-applied NMDA and 5-HT after 24 h in spinal cord preparations exposed to moderate excitotoxic injury by kainate (KA) (50 μM). (A) Chemically induced alternating oscillations recorded before kainate (KA) application (left panel) are typical of fictive locomotion (alternating cycles of discharges between flexor and extensor motor pools and between right and left sides), and are replaced by irregular firing at 24 h after KA. KA (50 μM, 1 h) was applied after washout of NMDA plus 5-HT with Krebs solution (see gap in the records). At 1 day after KA wash with Krebs solution, NMDA and 5-HT were applied again. Note the lack of fictive locomotion after KA treatment. (B) Example of preparation with fictive locomotion activity at 24 h after KA (50 μM) + PJ-34 (60 μM) application. PJ-34 was applied at 30 min after the application of KA (which was given after washout of NMDA plus 5-HT with Krebs solution) and its application was extended for the subsequent 24 h. The insets indicate the faster time base records taken as shown by boxes.

demonstrated that lack of SMI 32 staining was a reliable index of loss of motoneurons.

Figure 8B shows the extent of motoneuron loss after 50 μM-1 mM kainate with respect to sham or PJ-34 alone data. Nonetheless, PJ-34 systematically protected motoneuron numbers from kainate neurotoxicity (Fig. 8B). Interestingly, the application of PJ-34 after 100 or 50 μM kainate always yielded similar motoneuron numbers, even when we considered the two groups of preparations treated with 50 μM kainate, namely without or with fictive locomotion 24 h later (Fig. 8B). These observations implied that protecting motoneurons was important, but, when histological evidence for excitotoxic damage was quite small (Figs 6 and 7), the functional outcome in terms of fictive locomotion must have depended on the preservation of cell types other than motoneurons.

Discussion

The principal finding of the present *in vitro* study is that pharmacological inhibition of PARP-1 activation could produce significant histological protection of spinal networks, although the functional outcome was limited in terms of locomotor pattern expression. Our data suggest that arresting important effectors of excitotoxicity is feasible, but it needs very early pharmacological intervention on a background of moderate damage. After strong damage evoked by large kainate doses, recovery is never found.

Poly(ADP-ribose) polymerase-1 hyperactivity following excitotoxicity

Application of kainate to the neonatal spinal cord *in vitro* is known to induce extensive damage with loss of locomotor network function (Taccola *et al.*, 2008) analogous to that observed after local injection of the same agent into adult animals or after mechanical injury (Magnuson *et al.*, 1999). The use of neonatal tissue can additionally offer some insights into the basic pathophysiology of acute pediatric spinal injury. Previous observations (Taccola *et al.*, 2008) indicate that most spinal damage produce by kainate is not merely caused by rapid necrosis (or even delayed apoptosis), making it possible to explore neuroprotective strategies applied after the excitotoxic stimulus. PARP-1 is regarded as a major cause of neuronal cell death after spinal injury (Genovese *et al.*, 2005; Wu *et al.*, 2009). It would therefore be desirable to explore the effect of a selective pharmacological PARP-1 inhibitor like PJ-34 (Abdelkarim *et al.*, 2001) and, in particular, to assess the electrophysiological outcome of this treatment. Thus, in the present study, we first demonstrated that kainate induced a large activation of PARP-1 as indicated by the strong tissue production of PAR, and that this phenomenon was blocked by PJ-34. The time point chosen for these measurements (4 h) corresponds to the peak expression of PARP-1 in western immunoblotting (Kuzhandaivel *et al.*, 2010). Furthermore, PARP-1 hyperactivation is known to trigger translocation of AIF to the nucleus (Yu *et al.*, 2006), a process also detected in the present study, and fully suppressed by PJ-34. It is therefore likely that PJ-34 suppressed the principal effect responsible for DNA damage following hyperactivation of PARP-1 (Yu *et al.*, 2002; Culmsee *et al.*, 2005; Wang *et al.*, 2009b). It is noteworthy that, after kainate application, we detected the mature form of AIF translocated to the nucleus in accordance with previous reports of full-length AIF in the nucleus of cortical neurons following PARP-1 activation (Wang *et al.*, 2009b). While PJ-34 is believed to be a selective inhibitor of PARP-1 (Abdelkarim *et al.*, 2001), similar neuroprotective results have recently been observed with another PARP-1 inhibitor, namely 6(5H)-phenanthridinone (Kuzhandaivel *et al.*, 2010; Nasrabady *et al.*, 2011). Hence, our results suggest that, in our model, PARP-1 was strongly activated by kainate and inhibited by PJ-34, prompting us to investigate the functional effects of PJ-34 after kainate toxicity and relate them to the histological scenario.

Excitotoxicity of spinal networks *in vitro*

At 24 h after kainate (50 μM–1 mM) application, locomotor patterns *in vitro* were always lost with the number of surviving neurons consistently below the threshold necessary to express fictive locomotion (Nistri *et al.*, 2010). This observation accords with our previous data showing that varying the concentration of kainate evokes broadly similar final histological damage, although the rate of damage development is dose-dependent (Mazzone *et al.*, 2010). In view of the early onset of PARP-1 hyperactivation (Kuzhandaivel *et al.*, 2010), PJ-34 applied after 30 min of kainate elicited good functional protection of reflex activity, although the outcome was much less favorable for cumulative depolarization that requires non-linear summation of synaptic inputs within the spinal network (Baranauskas & Nistri, 1998). We posit that the damage to dorsal horn interneurons might have severely impaired the integration of DR inputs into spinal networks and impaired electrically-induced fictive locomotion (see also Margaryan *et al.*, 2010). In accordance with this view was the demonstration that DR stimuli could efficiently evoke disinhibited bursts even after kainate or kainate plus PJ-34, indicating that there was no apparent damage to afferent impulse propagation to the spinal cord.
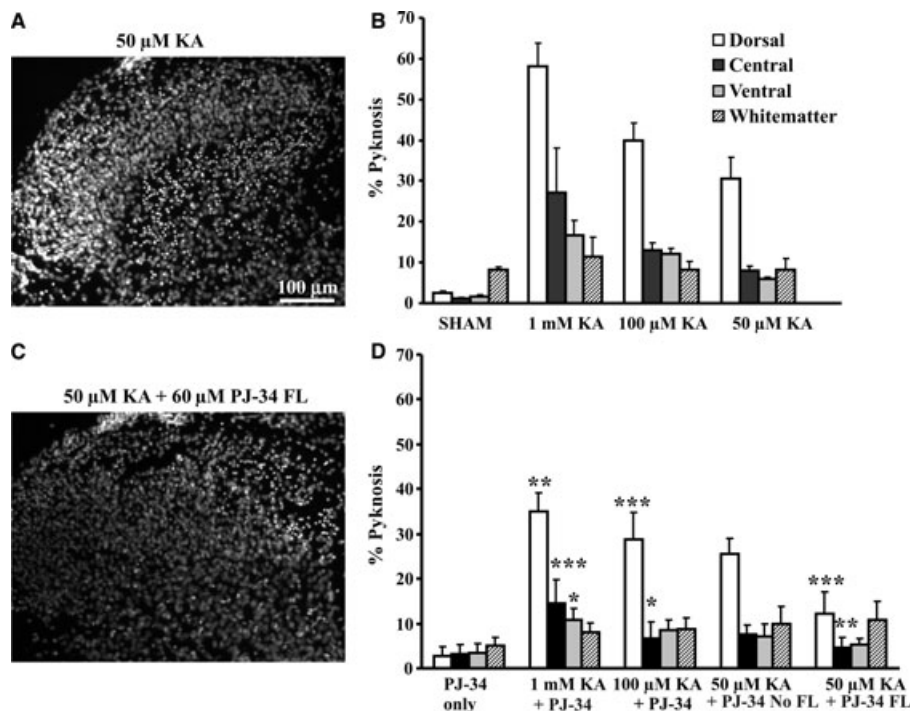
FIG. 6. Concentration-dependent kainate (KA)-evoked cell damage in the spinal cord *in vitro*. (A) Representative images showing DAPI-stained dorsal horn of 50 μM KA-treated spinal cord 24 h later. (B) Percent occurrence of pyknosis detected after washout of KA (1 h application) at different concentrations. Pyknosis is normalized with respect to the total number of DAPI-sensitive cells. For each concentration of KA, $n = 4$ spinal cords. (C) Representative images showing DAPI-stained dorsal horn of 50 μM KA + 60 μM PJ-34-treated spinal cord. (D) Percent occurrence of pyknosis detected after washout of KA (1 h application) at different concentrations followed by 60 μM PJ-34 treatment ($n = 4$–11 spinal cords, *$P < 0.05$, **$P < 0.01$, ***$P < 0.001$). Comparison of data for 100 μM KA vs. 100 μM KA + 60 μM PJ-34 gave $t_6 = 6.353$ and $P < 0.001$ for the dorsal region, $T = 26$ and $P = 0.029$ for the central region, $t_6 = 0.686$ and $P = 0.518$ for the ventral region, and $t_6 = 0.200$, $P = 0.848$ for the white matter region. Comparison of data for 50 μM KA vs. 50 μM KA + 60 μM PJ-34 No FL gave $t_7 = 2.249$ and $P = 0.059$ for the dorsal region, $T = 25$ and $P = 0.286$ for the central region, $t_7 = 0.989$ and $P = 0.356$ for the ventral region, and $t_7 = -1.569$ and $P = 0.161$ for the white matter region. Comparison of data for 50 μM KA vs. 50 μM KA + 60 μM PJ-34 FL gave $t_8 = 6.031$ and $P < 0.001$ for the dorsal region, $T = 34$ and $P = 0.010$ for the central region, $t_8 = 0.433$ and $P = 0.676$ for the ventral region, and $t_8 = -0.749$ and $P = 0.478$ for the white matter region. FL indicates fictive locomotion.

Functional neuroprotection by PJ-34

PJ-34 treatment could not provide any protection of locomotor pattern expression against a high (100 μM–1 mM) concentration of kainate. When the kainate concentration was 50 μM, a majority of preparations were, however, able to reproduce chemically-induced fictive locomotion 1 day later. These findings raised a number of issues. First, they demonstrated that reflex activity is a poor predictor of locomotor network function (Taccola *et al.*, 2008) and that the same conclusion applies to disinhibited bursting as it probably relies on a smaller network size (Bracci *et al.*, 1996). Nonetheless, the observation of spontaneous disinhibited bursting after kainate indicated that basal network excitability spreading through the circuitry and recruiting neurons into synchronous firing (Czarnecki *et al.*, 2008) must have been preserved in an adequate number of interconnected neurons (Magloire & Streit, 2009). Second, chemically-evoked rather than electrically-induced fictive locomotion was more readily expressed, a result compatible, at least in part, with the high density of kainate receptors in the dorsal horn area where large damage could be seen (or prevented by PJ-34) and where polysynaptic inputs are processed for integration into the locomotor networks. Assuming a modular arrangement of the vertebrate locomotor CPG (Stein, 2010), it is proposed that even a limited extent of histological damage could disrupt locomotor patterns but leave disinhibited bursting present.

Third, only a subset of preparations could still manifest NMDA- and 5-HT-elicited fictive locomotion; it is, however, noteworthy that such locomotor patterns were clearly slower than controls, suggesting

that a partial functional deficit had persisted despite a timely PJ-34 application. The other preparations without fictive locomotion retained the preservation of synaptic activity and good excitability as shown by the enhanced firing recorded from VRs after applying NMDA and 5-HT. The differential outcome in terms of locomotor network responses might also have been due to varying degrees of homeostatic upregulation of synaptic inhibition to depress neuronal excitability. A very recent study (Peng *et al.*, 2010) with primary cultures of brain neurons has shown that kainate evokes delayed and persistent facilitation of GABA release. Although we could not observe any obvious difference in terms of disinhibited bursting resulting from GABA receptor block between spinal cords with and without fictive locomotion, the possibility of functional suppression of complex network activity as a contributing factor to suppression of fictive locomotion deserves future study. Nevertheless, it seemed useful first to explore the simplest explanation, namely any relation between neuronal losses and recovery of function, an issue that we investigated by comparing the spinal histological profile with the functional outcome of spinal networks.

Identification of neuronal contributors to fictive locomotion

The global number of ventral horn neurons was significantly diminished by 1 mM kainate and partially protected by PJ-34. When lower kainate concentrations were tested, the number of ventral neurons remained close to sham, despite the application of PJ-34 and
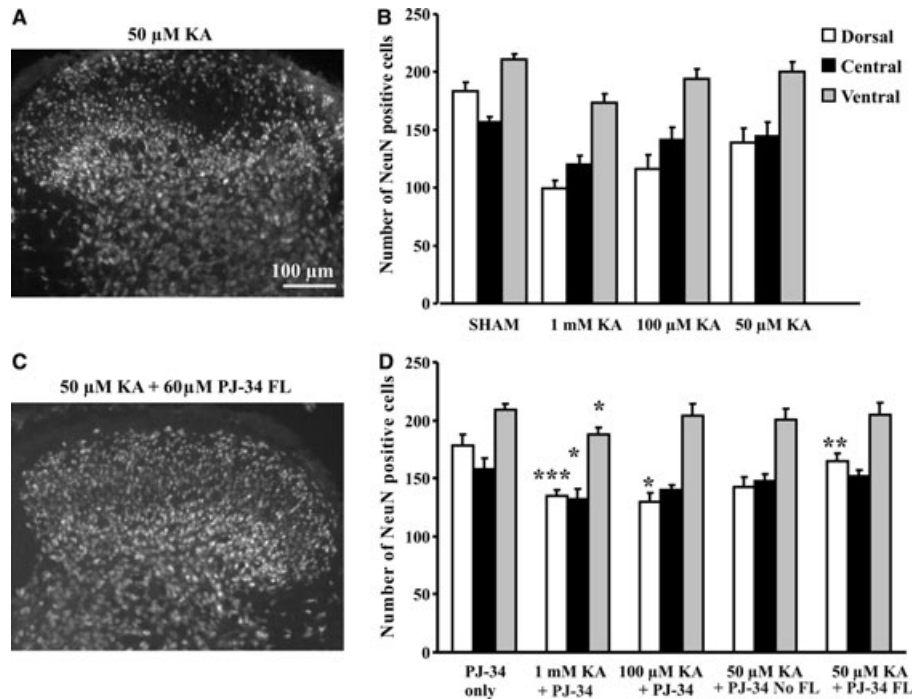
FIG. 7. PJ-34 application increased neuronal survival after kainate (KA)-mediated excitotoxicity. (A) Representative image showing NeuN-stained dorsal horn of 50 μM KA-treated spinal cord. (B) Number of NeuN-positive cells detected after washout of KA (1 h application) at different concentrations. For each concentration of KA, $n = 4$ spinal cords. (C) Representative image showing NeuN-stained dorsal horn of 50 μM KA + 60 μM PJ-34-treated spinal cord. (D) Number of NeuN-positive cells after washout of KA (1 h application) at different concentrations followed by 60 μM PJ-34 treatment ($n = 4$–11 spinal cords, *$P < 0.05$, **$P < 0.01$, ***$P < 0.001$). Comparison of data for 1 mM KA vs. 1 mM KA + 60 μM PJ-34 gave $t_6 = -7.367$ and $P < 0.001$ for the dorsal region, $T = 10$ and $P = 0.029$ for the central region, and $t_6 = -2.793$ and $P = 0.031$ for the ventral region. Comparison of data for 100 μM KA vs. 100 μM KA + 60 μM PJ-34 gave $t_6 = -2.916$ and $P < 0.027$ for the dorsal region, $t_6 = 0.155$ and $P = 0.882$ for the central region, and $t_6 = -1.236$ and $P = 0.263$ for the ventral region. Comparison of data for 50 μM KA vs. 50 μM KA + 60 μM PJ-34 No FL gave $t_7 = 0.378$ and $P = 0.717$ for the dorsal region, $t_6 = 0.589$ and $P = 0.574$ for the central region, and $T = 19.5$ and $P = 0.905$ for the ventral region. Comparison of data for 50 μM KA vs. 50 μM KA + 60 μM PJ-34 FL gave $t_9 = -3.856$ and $P = 0.004$ for the dorsal region, $t_9 = 0.251$ and $P = 0.807$ for the central region, and $t_9 = 1.455$ and $P = 0.180$ for the ventral region. FL indicates fictive locomotion.

the functional outcome. Thus, either our methods could not detect very small changes in the survival of a few neurons strategic for network operation, or the functional outcome was decided by cells outside this region. In the ventral horn, although the number of motoneurons was strongly decreased by kainate (regardless of its concentration), it remained at control level after PJ-34 plus 50–100 μM kainate. Thus, protecting motoneurons was obviously an achievable target, yet reaching this goal was simply not enough to ensure persistence of fictive locomotion.

The fall in the number of central gray neurons (where most locomotor CPG neurons are proposed to be located) (Kiehn, 2006) was presumably an important factor for the locomotor function outcome (Taccola et al., 2008). Following 50 μM kainate plus PJ-34, whenever locomotor patterns could be detected, their periodicity was significantly slow, suggesting a far from perfect operation of these
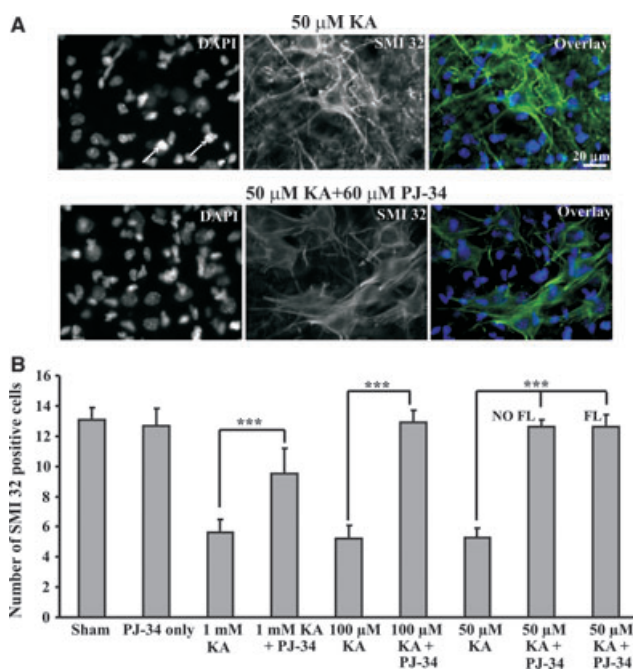
FIG. 8. PJ-34 application protected motoneurons after excitotoxic insult. (A) Left panels show examples of cell nuclei stained with DAPI in the ventral region of the 50 μM kainate- (KA) (top) or 50 μM KA + 60 μM PJ-34- (bottom) treated spinal cords. The arrows mark pyknotic nuclei. Middle panels show examples of motoneurons stained with SMI 32 in the ventral region of the 50 μM KA- (top) or 50 μM KA + 60 μM PJ-34- (bottom) treated spinal cords. Right panels show overlay of DAPI and SMI 32 staining in the same ventral region. Note the loss of SMI 32 staining coincident with pyknosis. (B) Number of SMI 32-positive cells in the ventral horn region after washout of KA (1 h application) at different concentrations followed by 60 μM PJ-34 treatment ($n = 4$–11 spinal cords, ***$P < 0.001$). Comparison of SMI 32 motoneuron data for 1 mM KA vs. 1 mM KA + 60 μM PJ-34 gave $t_9 = -4.982$ and $P < 0.001$, for 100 μM KA vs. 100 μM KA + 60 μM PJ-34 $t_6 = -15$ and $P < 0.001$, for 50 μM KA vs. 50 μM KA + 60 μM PJ-34 No FL $t_7 = -13.2$ and $P = 0.001$, and 50 μM KA vs. 50 μM KA + 60 μM PJ-34 FL $t_7 = -13.12$ and $P < 0.001$. FL indicates fictive locomotion.

networks despite the number of central gray neurons approaching sham values.

Under these conditions, the main histological difference between functionally protected and non-protected preparations by PJ-34 was the number of surviving dorsal horn neurons. Dorsal horn circuits are important to set and refine the excitability of the locomotor CPG (Taccola & Nistri, 2005, 2006a) as *in vitro* surgical ablation of the dorsal horns enables persistence of fictive locomotion, albeit at a slower pace (Taccola & Nistri, 2006b). Thus, we posit that, given the less than optimal number of central gray matter neurons (possibly taking the CPG to the brink of operation), any decrease in dorsal horn neuron numbers might have eventually tilted the balance between loss of function and persistence of function (with slower output). Of course, there is also the alternative explanation that the functional outcome was dependent on the survival of a few unidentified neurons originating and driving these network patterns; future studies, perhaps based on the genetic expression of transcription factors differentially expressed by subsets of spinal interneurons (Goulding, 2009; Kiehn, 2011) will be necessary to test this possibility. Likewise, it would be interesting to explore the consequences of excitotoxicity to the spinal cord from genetically-deficient PARP-1 mice (Hagberg *et al.*, 2004), even though the issue of excitotoxic mechanisms in a different rodent species needs to be fully explored first.

In conclusion, our data validate the former notion that, in the rat spinal cord *in vitro*, parthanatos is the principal cell death mechanism caused by excitotoxicity because impressive histological protection and persistence of reflex activity could be observed after applying a selective pharmacological inhibitor of PARP-1, yet more complex electrophysiological functions like fictive locomotion were less likely to be protected. The identification of the causes of this discrepancy is an important objective for future studies.

Functional implications of *in-vitro* neuroprotection of locomotor networks

Our data suggest that, to preserve a degree of locomotor network function *in vitro*, a neuroprotective strategy should: (i) be directed toward identified biochemical targets implicated in cell death mechanisms; (ii) be applied at an early stage after the primary insult and (iii) achieve combined survival of motoneurons as well as central and dorsal gray neurons. None of these factors *per se* is sufficient to maintain network output despite a number of apparently positive indices like synaptic transmission efficiency or global neuronal counts.

Acknowledgements

Abbreviations

AIF, apoptosis-inducing factor; CPG, central pattern generator; CV, Coefficient of variation; DAPI, 4′,6-diamidino-2-phenylindole; DR, dorsal root; 5-HT, 5-hydroxytryptamine; l, left; L, lumbar; NeuN, neuronal specific nuclear protein; NMDA, *N*-methyl-D-aspartate; PAR, poly(ADP-ribose); PARP-1, poly(ADP-ribose) polymerase-1; PJ-34, N-(6-oxo-5,6-dihydrophenanthridin-2-yl)-(N,N-dimethylamino)acetamide.HCl; r, right; SMI 32, neurofilament H non-phosphorylated; VR, ventral root.

References

Abdelkarim, G.E., Gertz, K., Harms, C., Katchanov, J., Dirnagl, U., Szabo, C. & Endres, M. (2001) Protective effects of PJ-34, a novel, potent inhibitor of poly(ADP-ribose) polymerase (PARP) in in vitro and in vivo models of stroke. *Int. J. Mol. Med.*, **7**, 255–260.

Baptiste, D.C. & Fehlings, M.G. (2006) Pharmacological approaches to repair the injured spinal cord. *J. Neurotrauma*, **23**, 318–334.

Baranauskas, G. & Nistri, A. (1998) Sensitization of pain pathways in the spinal cord: cellular mechanisms. *Prog. Neurobiol.*, **54**, 349–365.

Beato, M. & Nistri, A. (1999) Interaction between disinhibited bursting and fictive locomotor patterns in the rat isolated spinal cord. *J. Neurophysiol.*, **82**, 2029–2038.

Beirowski, B., Babetto, E., Gilley, J., Mazzola, F., Conforti, L., Janeckova, L., Magni, G., Ribchester, R.R. & Coleman, M.P. (2009) Non-Nuclear Wld(S) Determines Its Neuroprotective Efficacy for Axons and Synapses In Vivo. *J. Neurosci.*, **29**, 653–668.

Bracci, E., Ballerini, L. & Nistri, A. (1996) Localization of rhythmogenic networks responsible for spontaneous bursts induced by strychnine and bicuculline in the rat isolated spinal cord. *J. Neurosci.*, **16**, 7063–7076.

Bracci, E., Beato, M. & Nistri, A. (1997) Afferent inputs modulate the activity of a rhythmic burst generator in the rat disinhibited spinal cord in vitro. *J. Neurophysiol.*, **77**, 3157–3167.

Burgoyne, L.A. (1999) Mechanisms of pyknosis: hypercondensation and death. *Exp. Cell Res.*, **248**, 214–222.

Butt, S.J., Lebret, J.M. & Kiehn, O. (2002) Organization of left-right coordination in the mammalian locomotor network. *Brain Res. Brain Res. Rev.*, **40**, 107–117.

Cazalets, J.R., Sqalli-Houssaini, Y. & Clarac, F. (1992) Activation of the central pattern generators for locomotion by serotonin and excitatory amino acids in neonatal rat. *J. Physiol.*, **455**, 187–204.

Chiarugi, A. (2005) Poly(ADP-ribosyl)ation and stroke. *Pharmacol. Res.*, **52**, 15–24.

Choi, D.W. (1992) Excitotoxic cell death. *J. Neurobiol.*, **23**, 1261–1276.

Cox, B. & Emili, A. (2006) Tissue subcellular fractionation and protein extraction for use in mass-spectrometry-based proteomics. *Nat. Protoc.*, **1**, 1872–1878.

Culmsee, C., Zhu, C., Landshamer, S., Becattini, B., Wagner, E., Pellecchia, M., Blomgren, K. & Plesnila, N. (2005) Apoptosis-inducing factor triggered by poly(ADP-ribose) polymerase and Bid mediates neuronal cell death after oxygen-glucose deprivation and focal cerebral ischemia. *J. Neurosci.*, **25**, 10262–10272.

Czarnecki, A., Magloire, V. & Streit, J. (2008) Local oscillations of spiking activity in organotypic spinal cord slice cultures. *Eur. J. Neurosci.*, **27**, 2076–2088.

Dobkin, B.H. & Havton, L.A. (2004) Basic advances and new avenues in therapy of spinal cord injury. *Annu. Rev. Med.*, **55**, 255–282.

Eliasson, M.J., Sampei, K., Mandir, A.S., Hurn, P.D., Traystman, R.J., Bao, J., Pieper, A., Wang, Z.Q., Dawson, T.M., Snyder, S.H. & Dawson, V.L. (1997) Poly(ADP-ribose) polymerase gene disruption renders mice resistant to cerebral ischemia. *Nat. Med.*, **3**, 1089–1095.

Endres, M., Wang, Z.Q., Namura, S., Waeber, C. & Moskowitz, M.A. (1997) Ischemic brain injury is mediated by the activation of poly(ADP-ribose)polymerase. *J. Cereb. Blood Flow Metab.*, **17**, 1143–1151.

Fehlings, M.G. & Perrin, R.G. (2006) The timing of surgical intervention in the treatment of spinal cord injury: a systematic review of recent clinical evidence. *Spine (Phila Pa 1976)*, **31**, S28–S35.

Genovese, T., Mazzon, E., Muia, C., Patel, N.S., Threadgill, M.D., Bramanti, P., De Sarro, A., Thiemermann, C. & Cuzzocrea, S. (2005) Inhibitors of poly(ADP-ribose) polymerase modulate signal transduction pathways and secondary damage in experimental spinal cord trauma. *J. Pharmacol. Exp. Ther.*, **312**, 449–457.

Goulding, M. (2009) Circuits controlling vertebrate locomotion: moving in a new direction. *Nat. Rev. Neurosci.*, **10**, 507–518.

Hagberg, H., Wilson, M.A., Matsushita, H., Zhu, C., Lange, M., Gustavsson, M., Poitras, M.F., Dawson, T.M., Dawson, V.L., Northington, F. & Johnston, M.V. (2004) PARP-1 gene disruption in mice preferentially protects males from perinatal brain injury. *J. Neurochem.*, **90**, 1068–1075.

Hall, E.D. & Springer, J.E. (2004) Neuroprotection and acute spinal cord injury: a reappraisal. *NeuroRx*, **1**, 80–100.

Kauppinen, T.M., Suh, S.W., Berman, A.E., Hamby, A.M. & Swanson, R.A. (2009) Inhibition of poly(ADP-ribose) polymerase suppresses inflammation and promotes recovery after ischemic injury. *J. Cereb. Blood Flow Metab.*, **29**, 820–829.

Kiehn, O. (2001) Locomotor circuits in the mammalian spinal cord. *Annu. Rev. Neurosci.*, **29**, 279–306.

Kiehn, O. (2011) Development and functional organization of spinal locomotor circuits. *Curr. Opin. Neurobiol.*, **21**, 100–109.

Kiehn, O. & Kjaerulff, O. (1996) Spatiotemporal characteristics of 5-HT and dopamine-induced rhythmic hindlimb activity in the in vitro neonatal rat. *J. Neurophysiol.*, **75**, 1472–1482.

Kiehn, O. & Kjaerulff, O. (1998) Distribution of central pattern generators for rhythmic motor outputs in the spinal cord of limbed vertebrates. *Ann. NY Acad. Sci.*, **860**, 110–129.

Koh, S.H., Park, Y., Song, C.W., Kim, J.G., Kim, K., Kim, J., Kim, M.H., Lee, S.R., Kim, D.W., Yu, H.J., Chang, D.I., Hwang, S.J. & Kim, S.H. (2004) The effect of PARP inhibitor on ischaemic cell death, its related inflammation and survival signals. *Eur. J. Neurosci.*, **20**, 1461–1472.

Kuzhandaivel, A., Nistri, A. & Mladinic, M. (2010) Kainate-mediated excitotoxicity induces neuronal death in the rat spinal cord in vitro via a PARP-1 dependent cell death pathway (Parthanatos). *Cell. Mol. Neurobiol.*, **30**, 1001–1012.

Leonard, M., Sproule, J. & McCormack, D. (2007) Paediatric spinal trauma and associated injuries. *Injury*, **38**, 188–193.

Li, X., Klaus, J.A., Zhang, J., Xu, Z., Kibler, K.K., Andrabi, S.A., Rao, K., Yang, Z.J., Dawson, T.M., Dawson, V.L. & Koehler, R.C. (2010) Contributions of poly(ADP-ribose) polymerase-1 and -2 to nuclear translocation of apoptosis-inducing factor and injury from focal cerebral ischemia. *J. Neurochem.*, **113**, 1012–1022.

Liu, X.Z., Xu, X.M., Hu, R., Du, C., Zhang, S.X., McDonald, J.W., Dong, H.X., Wu, Y.J., Fan, G.S., Jacquin, M.F., Hsu, C.Y. & Choi, D.W. (1997) Neuronal and glial apoptosis after traumatic spinal cord injury. *J. Neurosci.*, **17**, 5395–5406.

Magloire, V. & Streit, J. (2009) Intrinsic activity and positive feedback in motor circuits in organotypic spinal cord slice cultures. *Eur. J. Neurosci.*, **30**, 1487–1497.

Magnuson, D.S., Trinder, T.C., Zhang, Y.P., Burke, D., Morassutti, D.J. & Shields, C.B. (1999) Comparing deficits following excitotoxic and contusion injuries in the thoracic and lumbar spinal cord of the adult rat. *Exp. Neurol.*, **156**, 191–204.

Margaryan, G., Mladinic, M., Mattioli, C. & Nistri, A. (2009) Extracellular magnesium enhances the damage to locomotor networks produced by metabolic perturbation mimicking spinal injury in the neonatal rat spinal cord in vitro. *Neuroscience*, **163**, 669–682.

Margaryan, G., Mattioli, C., Mladinic, M. & Nistri, A. (2010) Neuroprotection of locomotor networks after experimental injury to the neonatal rat spinal cord in vitro. *Neuroscience*, **165**, 996–1010.

Mazzone, G.L. & Nistri, A. (2011) Effect of the PARP-1 Inhibitor PJ 34 on Excitotoxic Damage Evoked by Kainate on Rat Spinal Cord Organotypic Slices. *Cell. Mol. Neurobiol.*, **31**, 469–478.

Mazzone, G.L., Margaryan, G., Kuzhandaivel, A., Nasrabady, S.E., Mladinic, M. & Nistri, A. (2010) Kainate-induced delayed onset of excitotoxicity with functional loss unrelated to the extent of neuronal damage in the in vitro spinal cord. *Neuroscience*, **168**, 451–462.

McDonald, J.W. & Sadowsky, C. (2002) Spinal-cord injury. *Lancet*, **359**, 417–425.

Moroni, F. (2008) Poly(ADP-ribose)polymerase 1 (PARP-1) and postischemic brain damage. *Curr. Opin. Pharmacol.*, **8**, 96–103.

Narasimhan, P., Fujimura, M., Noshita, N. & Chan, P.H. (2003) Role of superoxide in poly(ADP-ribose) polymerase upregulation after transient cerebral ischemia. *Brain Res. Mol. Brain Res.*, **113**, 28–36.

Nasrabady, S.E., Kuzhandaivel, A., Mladinic, M. & Nistri, A. (2011) Effects of 6(5H)-phenanthridinone, an Inhibitor of Poly(ADP-ribose)Polymerase-1 Activity (PARP-1), on Locomotor Networks of the Rat Isolated Spinal Cord. *Cell. Mol. Neurobiol.*, **31**, 503–508.

Nistri, A., Taccola, G., Mladinic, M., Margaryan, G. & Kuzhandaivel, A. (2010) Deconstructing locomotor networks with experimental injury to define their membership. *Ann. NY Acad. Sci.*, **1198**, 242–251.

Park, E., Velumian, A.A. & Fehlings, M.G. (2004) The role of excitotoxicity in secondary mechanisms of spinal cord injury: a review with an emphasis on the implications for white matter degeneration. *J. Neurotrauma*, **21**, 754–774.

Peng, Y.R., Zeng, S.Y., Song, H.L., Li, M.Y., Yamada, M.K. & Yu, X. (2010) Postsynaptic spiking homeostatically induces cell-autonomous regulation of inhibitory inputs via retrograde signaling. *J. Neurosci.*, **30**, 16220–16231.

Rossignol, S., Schwab, M., Schwartz, M. & Fehlings, M.G. (2007) Spinal cord injury: time to move? *J. Neurosci.*, **27**, 11782–11792.

Scott, G.S., Jakeman, L.B., Stokes, B.T. & Szabó, C. (1999) Peroxynitrite production and activation of poly (adenosine diphosphate-ribose) synthetase in spinal cord injury. *Ann. Neurol.*, **45**, 120–124.

Stein, P.S. (2010) Alternation of agonists and antagonists during turtle hindlimb motor rhythms. *Ann. NY Acad. Sci.*, **1198**, 105–118.

Taccola, G. & Nistri, A. (2005) Characteristics of the electrical oscillations evoked by 4-aminopyridine on dorsal root fibers and their relation to fictive locomotor patterns in the rat spinal cord in vitro. *Neuroscience*, **132**, 1187–1197.

Taccola, G. & Nistri, A. (2006a) Fictive locomotor patterns generated by tetraethylammonium application to the neonatal rat spinal cord in vitro. *Neuroscience*, **137**, 659–670.

Taccola, G. & Nistri, A. (2006b) Oscillatory circuits underlying locomotor networks in the rat spinal cord. *Crit. Rev. Neurobiol.*, **18**, 25–36.

Taccola, G., Marchetti, C. & Nistri, A. (2004) Modulation of rhythmic patterns and cumulative depolarization by group I metabotropic glutamate receptors in the neonatal rat spinal cord in vitro. *Eur. J. Neurosci.*, **19**, 533–541.

Taccola, G., Margaryan, G., Mladinic, M. & Nistri, A. (2008) Kainate and metabolic perturbation mimicking spinal injury differentially contribute to early damage of locomotor networks in the in vitro neonatal rat spinal cord. *Neuroscience*, **155**, 538–555.

Taccola, G., Mladinic, M. & Nistri, A. (2010) Dynamics of early locomotor network dysfunction following a focal lesion in an in vitro model of spinal injury. *Eur. J. Neurosci.*, **31**, 60–78.

Tolle, T.R., Berthele, A., Zieglgansberger, W., Seeburg, P.H. & Wisden, W. (1993) The differential expression of 16 NMDA and non-NMDA receptor subunits in the rat spinal cord and in periaqueductal grey. *J. Neurosci.*, **13**, 5009–5028.

Wang, Y., Dawson, V.L. & Dawson, T.M. (2009a) Poly(ADP-ribose) signals to mitochondrial AIF: a key event in parthanatos. *Exp. Neurol.*, **218**, 193–202.

Wang, Y., Kim, N.S., Li, X., Greer, P.A., Koehler, R.C., Dawson, V.L. & Dawson, T.M. (2009b) Calpain activation is not required for AIF translocation in PARP-1-dependent cell death (parthanatos). *J. Neurochem.*, **110**, 687–696.

Wu, K.L., Hsu, C. & Chan, J.Y. (2009) Nitric Oxide and Superoxide Anion Differentially Activate Poly(ADP-ribose) Polymerase-1 and Bax to Induce Nuclear Translocation of Apoptosis-Inducing Factor and Mitochondrial Release of Cytochrome c after Spinal Cord Injury. *J. Neurotrauma*, **26**, 965–977.

Yu, S.W., Wang, H., Poitras, M.F., Coombs, C., Bowers, W.J., Federoff, H.J., Poirier, G.G., Dawson, T.M. & Dawson, V.L. (2002) Mediation of poly(ADP-ribose) polymerase-1-dependent cell death by apoptosis-inducing factor. *Science*, **297**, 259–263.

Yu, S.W., Andrabi, S.A., Wang, H., Kim, N.S., Poirier, G.G., Dawson, T.M. & Dawson, V.L. (2006) Apoptosis-inducing factor mediates poly(ADP-ribose) (PAR) polymer-induced cell death. *Proc. Natl Acad. Sci. USA*, **103**, 18314–18319.

Yuan, J., Lipinski, M. & Degterev, A. (2003) Diversity in the mechanisms of neuronal cell death. *Neuron*, **40**, 401–413.

Methods, materials and results

Section 4

Nasrabady SE, Kuzhandaivel A, Akrami A, Bianchetti E, Milanese M, Bonanno G, Nistri A (2012) Unusual increase in lumbar network excitability of the rat spinal cord evoked by the PARP-1 inhibitor PJ-34 through inhibition of glutamate uptake. Neuropharmacology 63:415-426.

Unusual increase in lumbar network excitability of the rat spinal cord evoked by the PARP-1 inhibitor PJ-34 through inhibition of glutamate uptake

Sara Ebrahimi Nasrabady [a], Anujaianthi Kuzhandaivel [a,1], Athena Akrami [a], Elena Bianchetti [a], Marco Milanese [b], Giambattista Bonanno [b,c], Andrea Nistri [a,d,*]

[a] Neuroscience department, International School for Advanced Studies (SISSA), Trieste, Italy
[b] Unit of Pharmacology and Toxicology, Department of Experimental Medicine, University of Genoa, Genoa, Italy
[c] Center of Excellence for Biomedical Research (CEBR), Genoa, Italy
[d] SPINAL (Spinal Person Injury Neurorehabilitation Applied Laboratory), Istituto di Medicina Fisica e Riabilitazione, Udine, Italy

ARTICLE INFO

ABSTRACT

Overactivity of poly(ADP-ribose) polymerase enzyme 1 (PARP-1) is suggested to be a major contributor to neuronal damage following brain or spinal cord injury, and has led to study the PARP-1 inhibitor 2-(dimethylamino)-N-(5,6-dihydro-6-oxophenanthridin-2yl)acetamide (PJ-34) as a neuroprotective agent. Unexpectedly, electrophysiological recording from the neonatal rat spinal cord in vitro showed that, under control conditions, 1–60 μM PJ-34 per se strongly increased spontaneous network discharges occurring synchronously on ventral roots, persisting for 24 h even after PJ-34 washout. The PARP-1 inhibitor PHE had no similar effect. The action by PJ-34 was reversibly suppressed by glutamate iono-tropic receptor blockers and remained after applying strychnine and bicuculline. Fictive locomotion evoked by neurochemicals or by dorsal root stimulation was present 24 h after PJ-34 application. In accordance with this observation, lumbar neurons and glia were undamaged. Neurochemical experiments showed that PJ-34 produced up to 33% inhibition of synaptosomal glutamate uptake with no effect on GABA uptake. In keeping with this result, the glutamate uptake blocker TBOA (5 μM) induced long-lasting synchronous discharges without suppressing the ability to produce fictive locomotion after 24 h. The novel inhibition of glutamate uptake by PJ-34 suggested that this effect may compound tests for its neuroprotective activity which cannot be merely attributed to PARP-1 block. Furthermore, the current data indicate that the neonatal rat spinal cord could withstand a strong, long-lasting rise in network excitability without compromising locomotor pattern generation or circuit structure in contrast with the damage to brain circuits known to be readily produced by persistent seizures.

1. Introduction

Hyperactivation of poly(ADP-ribose) polymerase enzyme 1 (PARP-1) is an important process contributing to brain damage arising from stroke (Andrabi et al., 2008) and acute spinal injury in vivo (Scott et al., 1999; Genovese et al., 2005; Wu et al., 2009). In vitro models of acute spinal cord injury have confirmed the role of this enzyme in the excitotoxic neuronal death (Kuzhandaivel et al., 2010a; Mazzone and Nistri, 2011), and have led to attempts of pharmacological neuroprotection with PARP-1 inhibitors.

Experimental studies have shown that the PARP-1 inhibitor 2-(dimethylamino)-N-(5,6-dihydro-6-oxophenanthridin-2yl)acet-amide (PJ-34; Abdelkarim et al., 2001; Kauppinen et al., 2009) could provide a degree of neuroprotection against brain and spinal cord ischemia in which excitotoxicity is thought to play a major role (Virág and Szabó, 2002; Casey et al., 2005; Besson, 2009; Kauppinen et al., 2009; Moroni, 2008; Moroni and Chiarugi, 2009). Nonetheless,

delayed application of PJ-34 had limited ability to protect rat spinal neurons in vitro as it could efficiently counteract relatively small excitotoxic damage only (Mazzone and Nistri, 2011; Nasrabady et al., 2011a). In the course of those experiments, it became, however, apparent that PJ-34 per se could persistently facilitate spontaneous synaptic transmission in the spinal cord (Nasrabady et al., 2011a). This serendipitous observation led us to investigate the mechanisms underlying such an unexpected phenomenon. Thus, the present report provides new evidence that PJ-34 enhanced glutamatergic transmission and triggered long-lasting network bursting. Our results indicated that the rat spinal cord in vitro could withstand, for at least 24 h, 1/3rd reduction in glutamate transport processes without apparent structural or functional damage.

2. Methods and materials

2.1. Spinal cord preparations

To perform electrophysiological experiments thoracolumbar spinal cords were carefully dissected from neonatal Wistar rats (0–2 days old) in accordance with the guidelines of the National Institutes of Health and the Italian act D.Lgs. 27/1/92 no. 116 (implementing the European Union directives no. 86/609 and 93/88). Under urethane anesthesia (0.2 ml i.p. of a 10% w/v solution) spinal cords were dissected out and superfused (7.5 ml min^{-1}) in a recording chamber with Krebs solution (in mM): NaCl, 113; KCl, 4.5; MgCl$_2$7H$_2$O, 1; CaCl$_2$, 2; NaH$_2$PO$_4$, 1; NaHCO$_3$, 25; glucose, 11; gassed with 95% O$_2$ 5% CO$_2$; pH 7.4 at room temperature (for full details see Beato and Nistri, 1999; Taccola and Nistri, 2006a; Margaryan et al., 2009). All efforts were aimed at reducing the number of animals and minimizing their suffering.

2.2. Electrophysiological recordings

DC-coupled recordings were performed through lumbar (L) ventral roots (VRs) with tight-fitting miniature Ag/AgCl suction electrodes (Taccola and Nistri, 2006a). Signals were recorded from left (l) and right (r) L2 VRs (producing mainly flexor motor signals to the hind-limb muscles), and from L5 VRs (which convey mainly extensor motor commands to the same limb) (Kiehn and Kjaerulff, 1998; Kiehn, 2006; Taccola and Nistri, 2006b). Signals acquired at 20 kHz were processed with pClamp (version 9.2; Molecular Devices, Sunnyvale, CA, USA) and MATLAB software (version R2010b). Preparations were electrically stimulated with single or train (30 stimuli at 2 Hz) pulses (0.1 ms duration) applied to the ipsilateral homosegmental dorsal root (DR). To evoke cumulative depolarization with superimposed alternating oscillatory activity typical of fictive locomotion, the stimulation strength was ≥2× threshold, whereby threshold was taken as the minimum intensity to elicit a detectable response in the homolateral VR (Taccola et al., 2004; Nasrabady et al., 2011b). On average, threshold was obtained with 1.61 ± 0.58 V stimulus intensity ($n = 6$). VR responses induced by weak stimuli close to threshold were considered to be indicative of monosynaptic reflexes (Fulton and Walton, 1986). The peak amplitude of the responses were calculated by averaging at least 5 events.

Fictive locomotion, defined as rhythmic discharges alternating between homosegmental and left-right lumbar VRs, was induced by co-application of N-methyl-D-aspartate (NMDA; 4 or 5 µM) and 5-hydroxytryptamine (5-HT; 10 µM) (Cazalets et al., 1992; Kiehn and Kjaerulff, 1998; Butt et al., 2002). The period value for rhythmic discharges was measured as the time between the onset of two cycles of oscillatory activity (calculated after averaging at least 20 cycles), and its regularity indicated by the coefficient of period variation (CV). Disinhibited bursting (Bracci et al., 1996a,b, 1997) was induced by continuously bath-applied strychnine (1 µM) and bicuculline (20 µM). Full details concerning the definition of bursts and their measurements were as reported before (Bracci et al., 1996a,b). In order to see the changes in network excitability caused by glutamate uptake block, the non-transportable inhibitor DL-threo-b-benzyloxyaspartate (TBOA; 5 µM; Shigeri et al., 2004) was applied for 1 h in a separate batch of experiments. TBOA has an IC$_{50}$ value of circa 7 µM to selectively block the EAAT2 and 3 glial transporters, while at concentration of 100 µM produces a broad-spectrum inhibition of all glutamate uptake systems (Shigeri et al., 2004).

2.3. Study protocol

First, all preparations were tested for their ability to generate locomotor network activity and reflexes. While untreated sham spinal cords were kept for 24 h in Krebs solution (Taccola et al., 2008), parallel preparations were continuously treated with PJ-34 (1 µM or 60 µM) for up to 24 h when, following washout with Krebs solution, all electrophysiological tests were repeated. The higher concentration of PJ-34 was selected as the one producing full block of PARP-1 activity in the rat spinal cord (Nasrabady et al., 2011a). A batch of experiments was also performed by applying a different PARP-1 inhibitor, namely (6-5(H)-phenanthridinone; PHE), which we have previously investigated for its potential neuroprotection in the rat spinal cord (Kuzhandaivel et al., 2010a).

2.4. Immunohistochemistry

Each preparation was histologically fixed at the end of the electrophysiological experiment as previously described in detail (Taccola et al., 2008). Thus, paraformaldehyde-fixed spinal cords were cryoprotected with 30% sucrose and sectioned (30 µm). The sections were washed in phosphate buffer solution (PBS) and incubated in blocking solution (5% normal goat serum, 5% bovine serum albumin, 0.3% Triton-x 100) for 1 h at room temperature followed by primary antibody (NeuN, 1:50, Millipore, Milan, Italy; SMI 32, 1:200, Convance, Rome, Italy; or S100, 1:100 dilution, Dako, Milan, Italy) incubation at 4 °C overnight. After rinsing with PBS, the sections were incubated with goat antimouse or antirabbit IgG Alexa Fluor 488 or 594 secondary antibodies (1:500; Invitrogen, Milan, Italy) for 1 h at room temperature followed by 20 min of DAPI incubation to label the nuclei. The sections were mounted with Vectashield (Vector Laboratories, Milan, Italy) and analyzed using a Zeiss Axioskop2 microscope and Metavue software.

2.5. Quantification of dead cells

Quantification of dead cells was done as described previously (Margaryan et al., 2009; Kuzhandaivel et al., 2010b). Briefly, pyknotic nuclei (identified with DAPI staining) were counted in the regions of interest (ROIs) comprising ventral, central, dorsal grey matter or ventrolateral white matter. For neuronal or protoplasmic astrocyte counting we used NeuN or S100 immunopositivity, respectively, in ventral, central, or dorsal grey ROIs (Taccola et al., 2008; Margaryan et al., 2009) using "eCELLence" (Glance Vision Tech, Trieste, Italy) software. For each ROI, 3–7 fields of 280 × 280 µm (grey matter) or 100 × 280 µm (white matter) area were analyzed. For each experimental group, 4–11 spinal cords were analyzed and, for each spinal cord, 4–6 different sections from T12 to L3 segments were examined. For estimating motoneuron numbers, SMI32 labelling was performed (Taccola et al., 2008) and Rexed laminae VIII and IX were analyzed.

2.6. PAR ELISA assay

Endogenous PARP-1 activity was determined by measuring PAR levels with an ELISA method as described previously (Nasrabady et al., 2011a). Briefly, tissue lysates were prepared from the spinal cord treated with different concentrations of PJ-34, or from sham preparations. PAR levels were measured using the HT PARP in vivo Pharmacodynamic Assay II kit (http://www.trevigen.com/protocols/pdf/4520-096-K.pdf) following the manufacturer's protocol (Trevigen, Bologna, Italy). PAR levels were always quantified 4 h after application of PJ-34. The present assay is based on the ELISA immunoreactivity resulting in chemiluminescence signals recorded with Glo(R)max multi detection system (Promega, Milan, Italy). All samples were run in triplicate. The net PAR levels were quantified from the known standard concentrations (20–1000 pg/ml) of PAR. Data were expressed as pg/ml per 100 µg of protein.

2.7. Neurochemical measurements of amino acid uptake

Neonatal Wistar rats (0–2 days old) were sacrificed and the spinal cord rapidly removed after exposure of the spinal column. Purified synaptosomes were prepared essentially as previously described (Stigliani et al., 2006). Briefly, the tissue was homogenized in 10 volumes of Tris-buffered sucrose (0.32 M; pH 7.4) using a glass–teflon tissue grinder. The homogenate was centrifuged (5 min, 1000 g) to remove nuclei and debris and the supernatant was gently stratified on a discontinuous Percoll® (GE Healthcare) gradient (2, 6, 10 and 20% v/v in Tris-buffered sucrose) and centrifuged at 33,500 g for 5 min. The layer between 10 and 20% Percoll® (synaptosomal fraction) was collected and washed by centrifugation. All the procedures were performed at 0–4 °C.

Synaptosomes were resuspended in assay buffer (mM: NaCl, 140; KCl, 3; MgSO$_4$ 1.2; NaH$_2$PO$_4$, 1.2; NaHCO$_3$ 5; CaCl$_2$ 1.2; HEPES 10; glucose, 10; pH 7.4). Protein content was measured according to the Bradford method (Bradford, 1976) with bovine serum albumin as standard. Aliquots (0.5 ml) of the synaptosomal suspension were incubated for 5 min at 37 °C; uptake was then started by the addition of [^{3}H]D-aspartate or [^{3}H]GABA to a final concentration of 3 µM and stopped 2 min later by the addition of 5 ml of assay buffer. Samples were immediately filtered under vacuum through cellulose filters and washed twice with 5 ml of assay buffer. PJ-34 (0.1–100 µM), TBOA (0.1–100 µM) or N-(4,4-phenyl-3-butenyl)-nipecotic acid (SKF 89976A; 10 µM; Yunger et al., 1984) was introduced at the beginning of incubation period. Non-specific uptake was determined in presence of 300 µM unlabelled L-glutamate or GABA. Filter radioactivity was evaluated by liquid scintillation counting.

2.8. Data analysis

Statistical analysis was carried out with SigmaStat (SigmaStat 3.1, Systat Software, Chicago, IL, USA) and the data are shown as mean ± SD unless otherwise indicated. Parametric and non-parametric data were first distinguished with a normality test and analyzed with the Student's t-test or Mann–Whitney test, respectively, in accordance with the software choice. Uptake data were analyzed by one-way ANOVA followed by Dunnet's or Newman–Keuls test, as appropriate. For the electrophysiological experiments, comparison was made between the data

obtained on the first day (before and after application of the drug) and on second day of each experiment (comparing sham and the group treated with PJ-34). The significant level was always $P < 0.05$ and n indicates the number of preparations.

For analysis of complex spontaneous events elicited by PJ-34, we applied a bootstrap method (Thomson and Chave, 1991; Kass et al., 2003) whereby temporal windows (1 min size) were randomly chosen from the original records (20 kHz sampling; 5 min long) of pairs of VRs. In each pair, cross correlation values were calculated for two windows of simultaneously recorded traces using MATLAB software. We then repeated this procedure 500 times in order to build a distribution of mean cross correlation values for each condition. Thereafter, data from different conditions were compared using t-test (or its non-parametric equivalent). To analyze the frequency of events from different experimental setting, we used 1 min windows, applied the same boot-strapping method indicated above, and calculated the fast Fourier transform (FFT) values.

2.9. Drugs

[³H]D-aspartate (specific activity = 89.5 Ci/mmol) and [³H]GABA (specific activity = 11.3 Ci/mmol) were obtained from Perkin Elmer (Milan, Italy). NMDA and TBOA were purchased from Tocris (Bristol, UK), while PJ-34, PHE, 5-HT, SKF 89976A, and strychnine hydrochloride were from Sigma (Milan, Italy). Bicuculline methiodide was obtained from Fluka (Milan, Italy).

3. Results

3.1. Onset of spontaneous network activity following PJ-34 application

Fig. 1 shows examples of early changes in electrically-evoked and spontaneous network activity recorded from lumbar VRs after PJ-34 application (60 μM). The amplitude of short-latency synaptic responses induced by low threshold stimuli and usually regarded as indicative of monosynaptic transmission (Fulton and Walton, 1986; Evans, 1989; Kerkut and Bagust, 1995) was increased already after 40 min application (Fig. 1A): on average, this increment was nearly two fold (see Table 1). Furthermore, the average decay time also became significantly longer (from 183 ± 45 ms, $n = 5$, to 298 ± 83 ms, $n = 4$; $P = 0.03$). Fig. 1B shows that the peak of polysynaptic responses generated by stronger DR stimuli ($>2\times$ threshold) was, however, unchanged after PJ-34 application (see Table 1). Conversely, cumulative depolarization with superimposed oscillations induced by DR stimulus trains (Marchetti et al., 2001) was significantly lower 40 min from the start of PJ-34 application (Fig. 1C and Table 1), even if it was accompanied by a similar number of oscillations (Table 1). In addition to these changes in electrically-evoked synaptic responses, it was noteworthy that, in the presence of PJ-34, the baseline trace had become noisier with spontaneous events appearing at irregular interval (see Fig. 1B–D). These complex events appeared with a latency of approximately 15 min from the start of PJ-34 application.

Fig. 2A shows, on the same preparation, examples of the gradual intensification of spontaneous events after application of PJ-34. Although the mammalian spinal cord in vitro normally expresses random spontaneous discharges (Fulton and Walton, 1986; Kerkut and Bagust, 1995), the events observed after PJ-34 were clearly more numerous and larger as shown in the distribution histograms of Fig. 2B. Thus, 15 min later, large discharges emerged (Fig. 2A, middle) and became very intense 24 h later (Fig. 2A, right). Fig. 2C
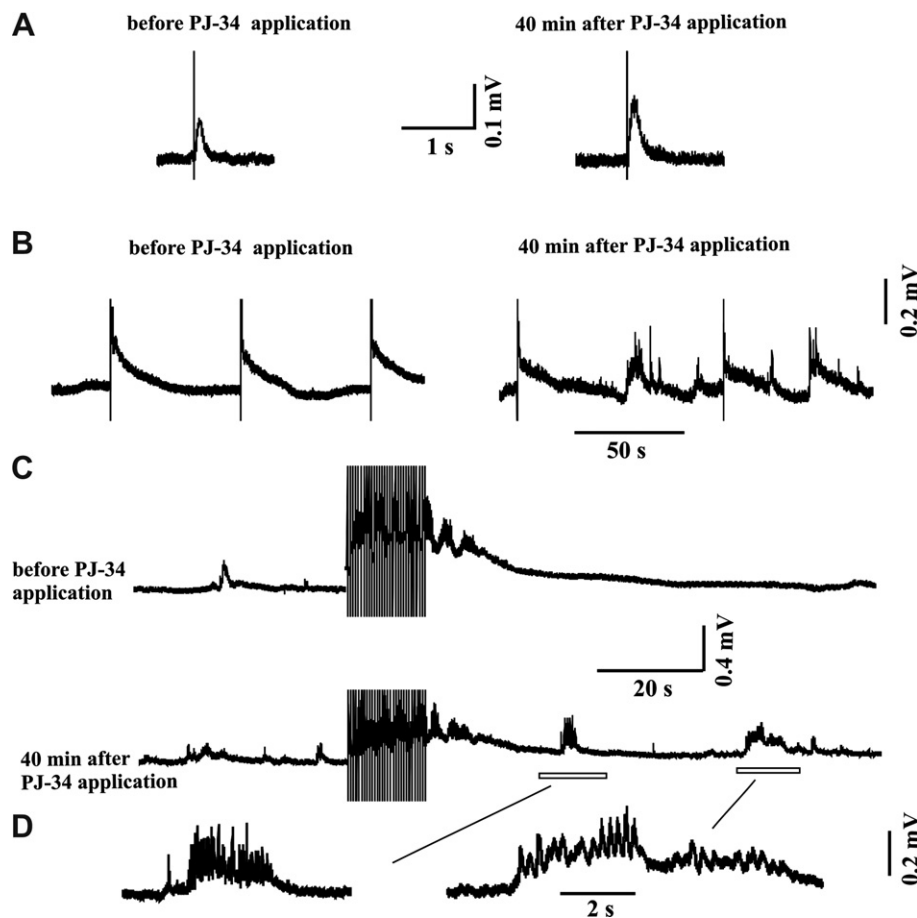
Fig. 1. Electrically-evoked responses recorded from in vitro spinal cord preparations early after PJ-34 (60 μM) application on the first experimental day. (A) Example of average monosynaptic response recorded from L5 homolateral VR in control (left) and after 40 min application of PJ-34. (B) Example of polysynaptic VR responses recorded from the same preparation as in (A). (C) Examples of cumulative depolarization with superimposed oscillatory cycles elicited by train of DR stimuli in control solution and 40 min after the application of PJ-34. (D) Example of spontaneous complex discharges appearing after application of PJ-34 (note faster timebase).

Table 1
Early effects of PJ-34 on VR responses to single (or trains of) DR stimuli.

	Monosynaptic reflex peak amplitude (mV)	Polysynaptic reflex peak amplitude (mV)	Cumulative depolarization amplitude (mV)	Number of oscillations induced by train of stimuli
Control[a]	0.129 ± 0.04 ($n = 5$)	2.59 ± 1.06 ($n = 6$)	0.873 ± 0.228 ($n = 6$)	5.5 ± 1 ($n = 6$)
40 min after application of PJ-34 60 μM	0.277 ± 0.09 ($n = 5$)	2.51 ± 0.87 ($n = 6$)	0.412 ± 0.168 ($n = 6$)	4.5 ± 0.5 ($n = 6$)
P-value	**0.013**	0.889	**0.003**	0.098

[a] Control responses refer to those recorded from the same preparations prior to PJ-34 application. Significant P-values are shown in bold.
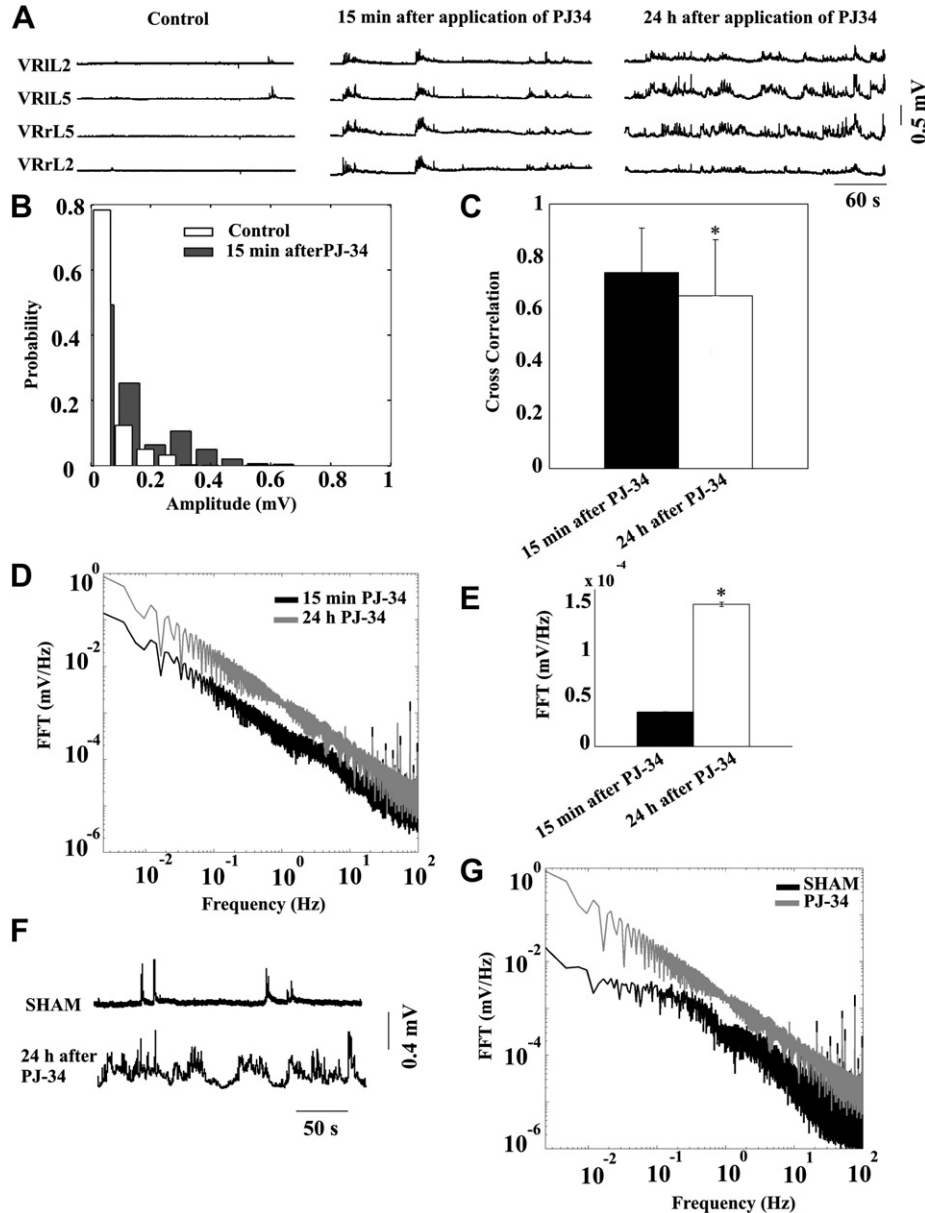
Fig. 2. Persistent effect of PJ-34 on spinal networks. (A) Example of sporadic spontaneous discharges recorded in control solution (before application of PJ-34 60 μM, left) and their gradual intensification after 15 min (middle) and 24 h (right) application of PJ-34. (B) Amplitude probability distribution of depolarizing events in a window of 5 min. Filled bars represent the distribution of the significantly higher average amplitude discharges after PJ-34 application for 15 min ($P < 0.0001$; Mann—Whitney) in comparison with control (open bars); $n = 4$. (C) Histograms demonstrate the significant difference of CCF values between groups treated with PJ-34 for 15 min or 24 h to show discharge synchronicity across segments and across preparations ($^*P < 0.001$; $n = 4$) (D) Plot indicates the mean FFT values of discharges from preparations treated for 15 min or 24 h with PJ-34; $n = 4$. (E) Histograms show increased average FFT values (mean ± s.e.m.) one day after treatment with PJ-34: the frequency power at 15 min PJ-34 application was significantly ($^*P < 0.0001$) smaller than at 24 h ($n = 4$). (F) Example of spontaneous VR discharges recorded on the second day in vitro from a sham (top) or PJ-34 treated (bottom) spinal cord. (G) Plots of mean FFT values show significant ($P < 0.002$) increase after 24 h application of PJ-34.

shows that, on average, events recorded early (filled column) from various VR pairs of different preparations, had a high cross correlation value, indicating their synchronicity across segments and across preparations. Even if 24 h later the cross correlation value was reduced (Fig. 2C, open column), it was still larger than 0.5, suggesting retention of good coupling of electrical discharges between VRs at homo and heterosegmental level.

Fig. 2D plots FFT data from 4 preparations to estimate the prevailing event frequency over a range of 0.1–100 Hz. Thus, for the same spinal cords, the whole frequency power spectrum at 15 min PJ-34 application was significantly ($P < 0.0001$) smaller than 24 h later, indicating the delayed, gradual emergence of slow events (mainly below 10 Hz). This result was accompanied by a significant increase in the average FFT value at 24 h (Fig. 2E) to support a global increment in spontaneous event occurrence.

We also compared, after 24 h in vitro, spontaneous events from sham preparations with those from PJ-34 treated preparations (see example in Fig. 2F). The FFT plot of Fig. 2G demonstrates a significantly ($P < 0.002$) stronger frequency power after PJ-34. In summary, these data suggest that PJ-34 evoked complex and long-lasting synchronous discharges from lumbar VRs, compatible with a substantial rise in network excitability. These delayed effects were, however, absent when spinal cords were treated (for 24 h) with another PARP-1 inhibitor (PHE; 60 µM) that did not induce any detectable change in spontaneous network discharges after 24 h ($n = 5$).

3.2. Relation between PARP-1 inhibition by PJ-34 and network activity

Fig. 3A shows the concentration (1–60 µM)-dependent changes in PARP-1 activity estimated on the amount of measured PAR. In accordance with our previous report (Nasrabady et al., 2011b), after 24 h in vitro, spinal cord samples had a basal PARP-1 activity corresponding to 55.9 ± 7 pg PAR/100 µg protein that fell to 47 ± 6.2 pg PAR/100 µg protein in the presence of 1 µM PJ-34. With 30 µM PJ-34, the PARP-1 activity decreased to 25 ± 8.4 pg PAR/100 µg protein, while with 60 µM PJ-34 it was 26 ± 5.3 pg PAR/100 µg protein, indicating that it had reached a plateau level of inhibition. These values were significantly smaller than those for sham preparations in all three groups ($P = 0.05$ for 1 µM PJ-34, $P = 0.001$ for 30 and 60 µM PJ-34). Fig. 3B shows that even the lowest tested concentration of PJ-34 (1 µM) significantly ($P < 0.001$) increased the FFT values of the spontaneous network discharges after 24 h in comparison with sham preparations, although this effect was less intense than the phenomenon detected after 60 µM PJ-34 (see Fig. 2). As exemplified in Fig. 3C, the onset of the electrophysiological discharges evoked by 1 µM PJ-34 was delayed and fully expressed 24 h later (Fig. 3C) in comparison with the large spontaneous events already detected after 15 min PJ-34 application (see Fig. 2A, middle).

3.3. Effect of PJ-34 on fictive locomotion and disinhibited bursting

We next enquired whether these changes in network excitability evoked by PJ-34 could impact on the ability to generate fictive locomotion. Fig. 4A compares locomotor-like cycles (evoked by co-applied NMDA and 5-HT) recorded, after 24 h, from a sham preparation with those from a PJ-34 treated spinal cord. In fact, fictive locomotion was apparently unperturbed by long-lasting PJ-34 application as indicated by similar cycle period or amplitude values (Fig. 4A, left, right). There was, however, a small, significant increment in the period CV value (Fig. 4A, middle), suggesting a slightly irregular pattern.
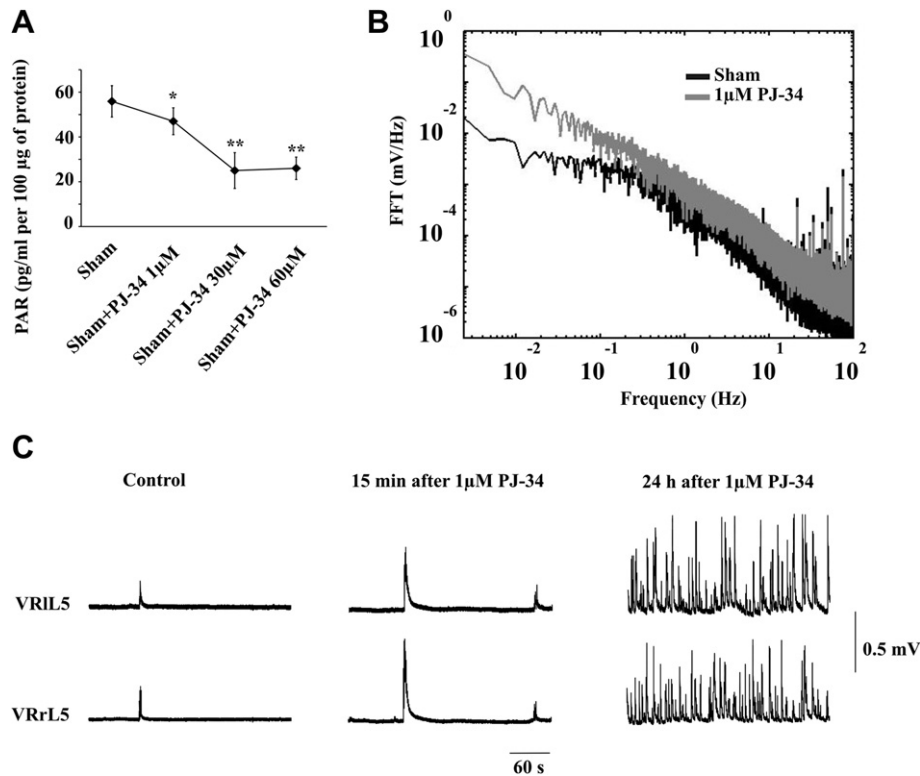
Fig. 3. Concentration-dependent effects of PJ-34 on PAR and network activity. (A) Plot quantifies PAR levels produced by PARP-1 activity of tissue lysates from sham or PJ-34 (1–60 µM) treated spinal cords. The values are significantly smaller than sham in all three groups (*$P = 0.05$ for 1 µM PJ-34, **$P = 0.001$ for 30 and 60 µM PJ-34) ($n = 3$ for each group). (B) FFT plot indicates the higher values of discharges 24 h after application of PJ-34 1 µM ($P < 0.001$, $n = 4$). (C) Example of sporadic spontaneous VR discharges recorded in control (before 1 µM PJ-34 application, left), early after PJ-34 (middle) and 24 h later (right); traces are all from the same preparation.
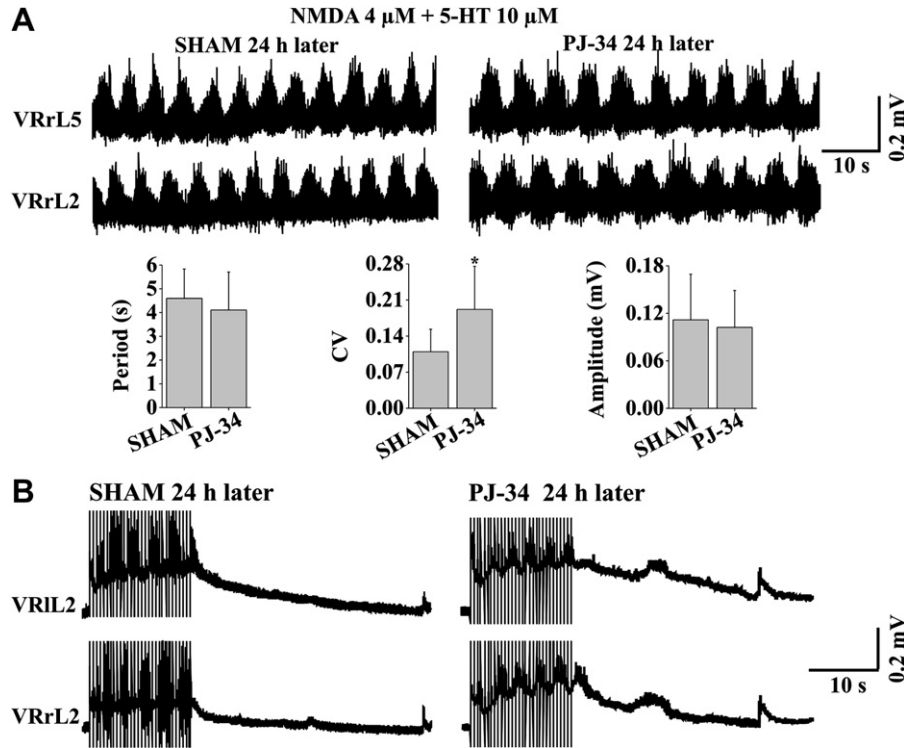
Fig. 4. Chemically or electrically induced fictive locomotion in sham preparations or after 24 h application of PJ-34 60 μM. (A) Examples of fictive locomotion (top traces) induced by NMDA (4 μM) plus 5-HT (10 μM) on sham (left) or PJ-34 treated spinal cord (right). The bottom histograms show similar characteristics of fictive locomotion (except for period CV value, $P = 0.01$, middle) of sham or PJ-34 treated spinal cords ($n = 9$). (B) Examples of alternating oscillatory cycles induced by trains of DR stimuli on sham or PJ-34 treated spinal cords. Number of oscillations and cumulative depolarization amplitude were similar in the two groups.

Fig. 4B shows, for the second day in vitro, examples of cumulative depolarization generated by sham or PJ-34 treated preparations with similar number of superimposed oscillations. Table 2 quantifies such data and also indicates that there was no change in mono and polysynaptic reflexes recorded after 24 h application of 1 or 60 μM PJ-34. Likewise, disinhibited bursting elicited by blocking synaptic inhibition with strychnine and bicuculline was unchanged by 24 h application of PJ-34 since the period was 42 ± 24 s (vs 45 ± 14 sham data; $n = 10$), and burst duration was 15 ± 9 s (vs. 15 ± 7 sham data). Hence, locomotor network activity tested with either neurochemicals or DR stimuli as well as basic circuit rhythmicity were not disrupted by long-lasting PJ-34 application.

3.4. Pharmacological block of PJ-34 evoked discharges

Since glutamate is the main excitatory transmitter of locomotor networks (Cazalets et al., 1992) acting on NMDA and non-NMDA receptors (Beato et al., 1997), we investigated whether block of ionotropic glutamate receptors by CNQX (10 μM) and D-APV (50 μM) could eliminate spontaneous as well as PJ-34 induced events. Fig. 5A (left) shows VR records from a preparation exhibiting strong ongoing discharges in Krebs solution (24 h after application of PJ-34 and washout). When CNQX and APV were applied for 15 min, spontaneous events disappeared (Fig. 4, middle), and returned after 10 min of washout of these antagonists, a result consistent with the dependence of spontaneous events on glutamatergic drive.

We also explored the potential contribution of GABA and glycine receptors to the PJ-34 elicited spontaneous events. This was difficult because the disinhibited bursting arising from block of synaptic inhibition is associated with strong depression of spontaneous excitatory events during the interburst interval (Bracci et al., 1996a), making it unfeasible to test glutamatergic events in isolation. Thus, we took advantage of a previous protocol whereby disinhibited bursts can be entrained on a 1:1 basis by low frequency DR stimulation (0.05 Hz; Bracci et al., 1997) as exemplified in Fig. 5B. Hence, after 24 h application of PJ-34 and washout, spontaneous disinhibited bursting was produced by strychnine and bicuculline, followed by a long (6.5 min) DR stimulus train that regularly entrained bursts. During the electrical stimulation, and unlike the interburst depression typical of control experiments (Bracci et al., 1997), spontaneous synchronous bursts emerged as exemplified, on a faster timebase, in Fig. 5 C. We next calculated whether appearance of such spontaneous events could influence the subsequent electrically-driven one: plotting the evoked burst amplitude (Fig. 5D, top) vs. the time interval from the preceding spontaneous burst showed a linear relation ($r = 0.716$), showing

Table 2

Characteristics of VR responses of sham or PJ-34 treated spinal cord to single (or trains of) DR stimuli on the second day in vitro.

	Monosynaptic reflex peak amplitude (mV)	Polysynaptic reflex peak amplitude (mV)	Cumulative depolarization amplitude (mV)	Number of oscillations induced by train of stimuli
Sham	0.25 ± 0.07 ($n = 7$)	0.73 ± 0.39 ($n = 7$)	0.54 ± 0.27 ($n = 6$)	5.17 ± 0.88 ($n = 6$)
After application of PJ-34 (60 μM)	0.31 ± 0.08 ($n = 6$)	0.82 ± 0.36 ($n = 7$)	0.35 ± 0.1 ($n = 6$)	5.97 ± 1.67 ($n = 7$)
P-value*	0.196	0.664	0.158	0.317
After application of PJ-34 (1 μM)	0.31 ± 0.15 ($n = 4$)	0.80 ± 0.27 ($n = 4$)	0.38 ± 0.05 ($n = 4$)	5.88 ± 1.95 ($n = 4$)
P-value†	0.367	0.770	0.352	0.762

* and † indicate the P-value of the comparison between Sham and 60 μM PJ-34 or 1 μM PJ-34 application respectively.
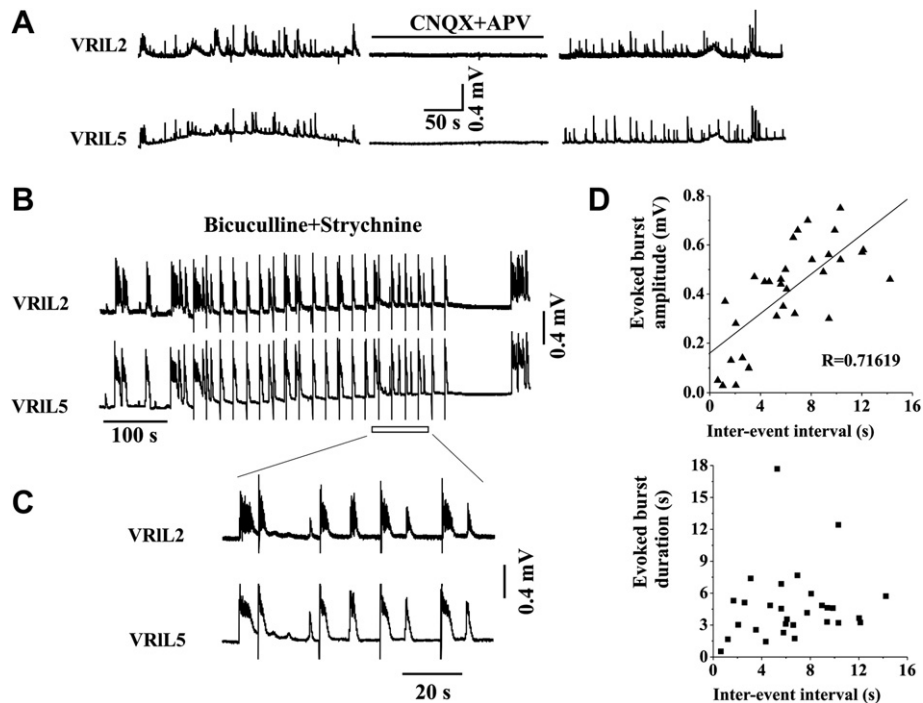
Fig. 5. Ionotropic receptor blockers influence discharges evoked by PJ-34. (A) Examples of spontaneous VR events recorded 24 h after application of PJ-34 and washout which are completely suppressed by co-application of CNQX (10 μM) and APV (50 μM) (middle). The spontaneous events return after 10 min washout with Krebs solution (right). (B) Disinhibited bursting is elicited by application of strychnine and bicuculline one day after PJ-34 application and wash. Although bursts are entrained (1:1) by a DR train of twenty stimuli (2× threshold, 0.05 Hz; see artefacts shown as downward deflections), spontaneous bursts emerge in the intervals between stimuli. (C) Faster timebase example of disinhibited bursting with electrically-driven and spontaneous events taken from (B). (D) A spontaneous burst affects the subsequent electrically-driven one. Top plot indicates that evoked burst amplitude is linearly related to the time interval between a spontaneous burst and the following electrically-evoked one ($P < 0.001$; $n = 5$). Nonetheless, no linear relation (bottom plot) between evoked burst duration and time interval from the previous spontaneous burst is apparent ($P = 0.39$).

that large bursts were preceded by a long quiescent period. Conversely, there was no apparent relation between evoked burst duration and time interval from previous spontaneous burst (Fig. 5D, bottom). Globally, these data were compatible with sustained increase in glutamatergic network activity as the main process responsible for continuous synchronous discharges, and that, when network discharges were fully engaged as bursts, there was a subsequent, transient downregulation of circuit excitability.

3.5. Histochemistry of PJ-34 treated spinal cords

In analogy with our previous studies (Taccola et al., 2008; Nasrabady et al., 2011a), we analyzed four ROIs of spinal cord sections from the same preparations used for our electrophysiological tests. First, we assessed whether pyknosis (condensed chromatin appearance) was more common 24 h after PJ-24 application: Fig. 6A, B indicates that pyknosis was a comparatively rare occurrence (<10%) in all ROIs from sham or treated preparations. Using immunostaining for S100, the main biomarker for grey matter astrocyte precursors in the neonatal rat spinal cord (Kuzhandaivel et al., 2010b; Cifra et al., in press), we also found no difference between sham and treated preparations (Fig. 6E, F). Fig. 6C, D shows no loss of NeuN-stained neurons across spinal cord sections after 24 h application of PJ-34, with good preservation of motoneuron numbers (Fig. 6G, H) evaluated with SMI 32 immunoreactivity (Taccola et al., 2008; Mazzone et al., 2010).

3.6. Effect of the glutamate uptake inhibitor TBOA

The strong increase in network excitability with spontaneous discharges evoked by PJ-34 without concomitant loss of neurons raised the possibility that this drug was partially inhibiting the uptake of glutamate without reaching toxic consequences for network structure and function. To examine this issue, we applied a low concentration of the selective uptake blocker TBOA at a dose close to its IC_{50} value (circa 7 μM) for inhibiting the glutamate glial transporters EAAT2 and 3 (Shigeri et al., 2004). Fig. 7A shows an example of the gradual increase in spontaneous event occurrence developing after the application of TBOA with strong electrical discharges emerging synchronously on L2 and L5 VRs (average CCF value after 40 min = 0.72 ± 0.17, and after 24 h = 0.71 ± 0.25; $n = 5$). By performing a FFT analysis of such events from 5 spinal cords and comparing them with the average data from PJ-34 treated preparations (24 h later), the power spectrum appeared overall similar (Fig. 7B) though a small significant ($P < 0.001$) difference was detected as the plot related to the TBOA treated preparations was shifted downwards.

We next investigated the long-term consequences of 24 h TBOA application (5 μM) on fictive locomotion. This pattern was present in 4 out of 5 preparations (see example in Fig. 7C) with characteristics similar to the activity observed in parallel sham preparations (period = 4.16 ± 0.59 s, CV = 0.09 ± 0.03, amplitude = 0.06 ± 0.02 mV after TBOA vs 4.59 ± 1.23 s, 0.10 ± 0.04, 0.11 ± 0.05 mV in sham conditions). The basic network rhythmicity expressed as disinhibited bursting was also present after 24 h application of TBOA. Although the bursts appeared at faster rate (bursts period = 28.6 ± 17.9 s vs 45.8 ± 14.0 s in sham, $P = 0.03$), the other characteristics of network bursting such as CV (0.61 ± 0.22 vs 0.44 ± 0.15 in sham), amplitude (0.75 ± 0.32 mV vs 0.79 ± 0.24 mV in sham), and burst duration (8.51 ± 5.08 s vs 15.78 ± 7.66 s in sham) remained similar. No deleterious action by TBOA (24 h application) on neurons, glia and motoneurons was found on histologically-processed spinal cords (Fig. 6B, D, F, H, open bars).
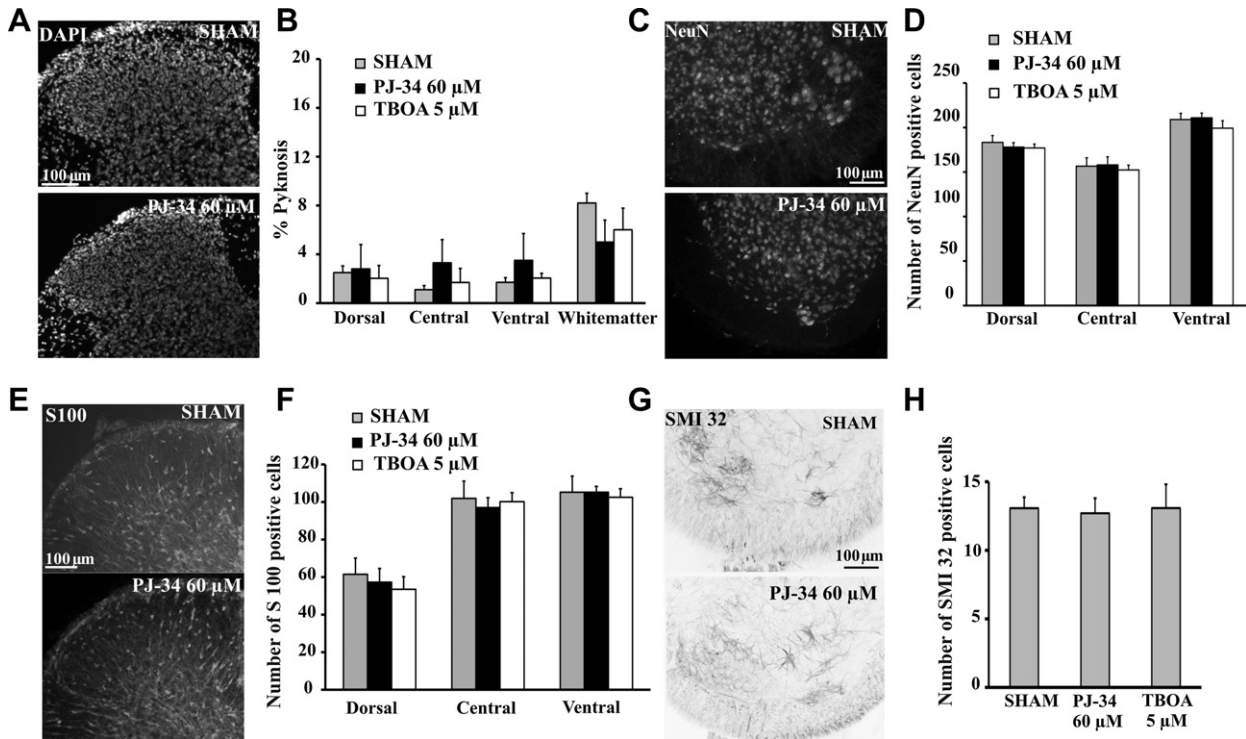
Fig. 6. PJ-34 or TBOA does not induce spinal cord histological damage one day later. (A) Representative images showing DAPI stained dorsal horn of sham or PJ-34 treated spinal cord 24 h later. (B) Histograms plot the low occurrence (<10%) of pyknosis detected in different ROIs of sham, PJ-34 or TBOA treated spinal cords. Pyknosis is normalized with respect to the total number of DAPI sensitive cells. (C) Representative images showing NeuN-stained ventral horn of sham or PJ-34 treated spinal cord. (D) Histogram plots the number of NeuN positive neurons in ROIs from sham, PJ-34 and TBOA treated spinal cords. (E) Representative images showing S100 stained dorsal horn of sham or PJ-34 treated spinal cord. (F) Histogram plots the number of S100 positive protoplasmic astrocytes in ROIs of sham, PJ-34 or TBOA treated spinal cords. (G) Representative images showing SMI 32 stained motoneurons in the ventral horn of sham or PJ-34 treated spinal cord. (H) Histogram plots the number of SMI 32 positive motoneurons in the ventral horn region of sham, PJ-34 or TBOA treated spinal cords. For all the experiments the number of spinal cords was 4, 9, 5 for sham, PJ-34 and TBOA, respectively.

3.7. Neurochemical measurement of glutamate uptake

The uptake of [3H]D-aspartate or [3H]GABA and its inhibition by PJ-34 were evaluated in synaptosomes purified from the spinal cord of 0–2 day old rats. The control uptake of [3H]D-aspartate and of [3H]GABA in synaptosomes exposed to 3 µM of the radioactive tracers amounted to 1355 ± 136 pmol/mg protein/2 min ($n = 12$) and 3225 ± 191 pmol/mg protein/2 min ($n = 5$), respectively. Fig. 8 shows the concentration-dependent decrease by PJ-34 (0.1–100 µM) of the uptake of [3H]D-aspartate: the maximal effect amounted to 30% inhibition with IC_{50} value, estimated from the fitted curve, equal to 0.33 µM. [3H]D-aspartate uptake was inhibited also by TBOA (0.1–100 µM) in a concentration-dependent manner (maximal inhibition about 90%: $IC_{50} = 2.18$ µM. Fig. 8). Synaptosomal [3H]GABA uptake was unaffected by 100 µM PJ-34 (3225 ± 191 nmol/mg protein/2 min in control vs 3089 ± 175 nmol/mg protein/2 min in the presence of PJ-34; $n = 5$). Conversely, [3H]GABA uptake was decreased from 3225 ± 191 pmol/mg protein/2 min to 225 ± 37 pmol/mg protein/2 min by 10 µM SKF 89976A, a canonical GABA uptake inhibitor (Milanese et al., 2010; $n = 5$; $P < 0.001$).

4. Discussion

The principal findings of the present report are that: 1. the PARP-1 inhibitor PJ-34 was a partial blocker of glutamate uptake, 2. this action was associated with a strong increase in network discharges persisting even after washout, and 3. it had no neurotoxic consequence, for at least 24 h, on neurons and glia in the neonatal rat spinal cord. These data demonstrate that prolonged electrical discharges per se did not damage complex network activities like the locomotor program.

4.1. PJ-34 as an inhibitor of glutamate uptake: functional consequences

Neurochemical data showed this agent to be a significant blocker of glutamate uptake with no action on GABA transport. It was interesting to detect this effect at micromolar concentrations of PJ-34, implying that this phenomenon might occur with pharmacological rather than toxic doses of this drug. The action of PJ-34 was translated into an early enhancement of glutamate-mediated monosynaptic reflexes, indicating that glutamate uptake was an important process to regulate excitatory transmission. This response was observed together with the smaller amplitude of cumulative depolarization probably due to steadily-depolarized neurons, still capable of generating a standard series of alternating oscillations. Polysynaptic reflexes were unchanged perhaps because of their heterogeneous presynaptic origin.

While the effect of PJ-34 on glutamate uptake and synaptic reflexes was relatively rapid, there was a gradual intensification of spontaneous network discharges: one day later, despite sustained washout of PJ-34, these strong discharges continued, suggesting that spinal circuits had become hyper-excitable.

4.2. Characteristics of spontaneous discharges induced by PJ-34

VR recordings were ill-suited to identify the electrophysiological nature of the PJ-34 evoked events which likely included the activity of several classes of premotoneuron impinging upon motoneurons. Experiments with pharmacological antagonists showed, however, that these discharges were fully dependent on ionotropic glutamate receptor activation, and that, when GABA and glycine receptors were blocked, spontaneous bursts could emerge in the interval between
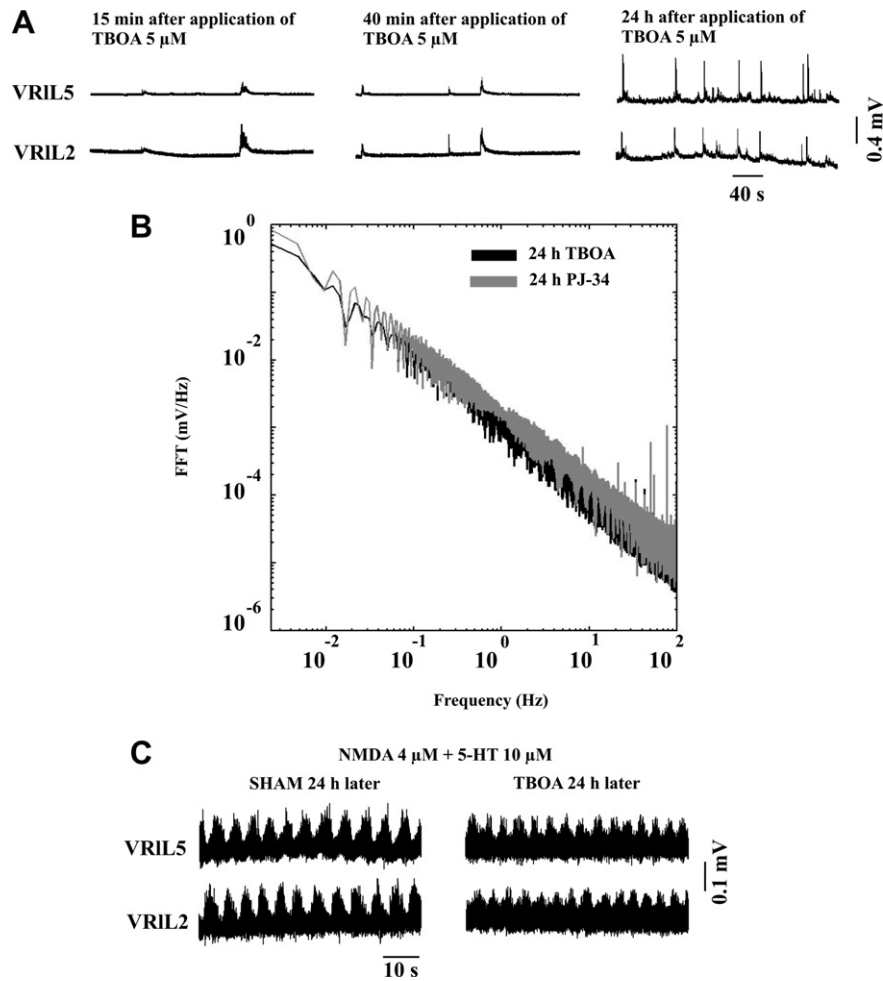
Fig. 7. Effect of TBOA (5 μM) on VR discharges of the spinal network. (A) Traces are examples of early (15 min and 40 min, left and middle, respectively) application of TBOA compared to long-lasting (24 h) application of this drug (right). (B) Comparison of FFT values between 24 h application of TBOA or PJ-34 shows that the TBOA plot is shifted downwards ($P < 0.001$; Mann–Whitney) with a power spectrum slightly different from PJ-34 ($n = 5$). (C) Examples of fictive locomotion induced by NMDA plus 5-HT on a sham and one preparation treated with TBOA for 24 h (and washout). The values of locomotor-like activity in the group treated with TBOA were similar to the sham.
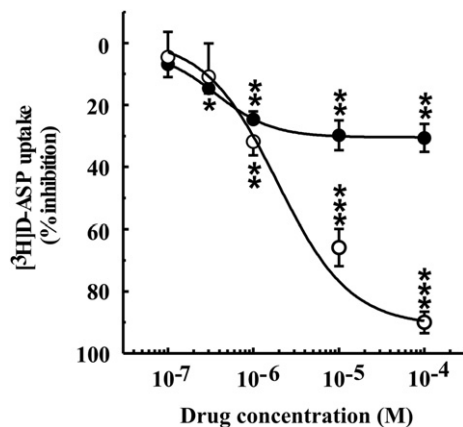
Fig. 8. Effect of PJ-34 (filled circles) or TBOA (open circles) on the uptake of [³H] D-aspartate by synaptosomes from the spinal cord of 0–2 old rats. Data are expressed as percent inhibition of [³H]D-aspartate uptake and represent the mean ± s.e.m of 6 independent experiments run in triplicate. *$P < 0.05$, **$P < 0.001$, ***$P < 0.0001$ vs. the respective controls (ANOVA plus Newman–Keuls test).

electrically-stimulated bursts. The presence of synchronous events across segments is compatible with the possibility of recurrent excitation recruiting a widespread neuronal assembly into collective discharge mode (Streit et al., 2001). In fact, our analysis indicated that these discharges were in general rather slow in accordance with the view that they originated from an ample neuronal population. As previously shown for the rat spinal dorsal horn (Nie and Weng, 2009), impaired glutamate uptake probably induced spill-over of extracellular glutamate outside the active synapses to extensively raise neuronal excitability. The present data cannot distinguish the relative contribution by uptake block and/or facilitated release of this excitatory transmitter to the strong enhancement in spontaneous discharges. In view of the difficulty to probe, in the spinal cord, endogenous glutamate release originating from multiple spinal sites, future experiments based on analysis of synaptic events with patch clamp recording might help to clarify this issue.

The PJ-34 evoked state of spinal cord hyperexcitability did not exert a deleterious action on locomotor-like patterns, nor was it translated into spontaneous bouts of fictive locomotion. Likewise, former studies with the glutamate uptake blocker dihydrokainate have shown that it could only facilitate fictive locomotion induced by bath-applied glutamate to the lamprey spinal cord in vitro (Brodin and Grillner, 1985) or by mesencephalic stimulation of the cat in vivo (Douglas et al., 1993), but rarely could it produce this pattern directly.

4.3. Relative contribution by glutamate uptake inhibition or PARP-1 depression to spontaneous network discharges

A relatively low concentration of PJ-34 (1 μM) produced a partial inhibition of PARP-1 activity amounting to circa 13% reduction in the production of PAR, the compound that (in high concentrations) underlies excitotoxic death (Kuzhandaivel et al., 2011). This rather modest decrease in PARP-1 function was probably unable to explain the strong rise in network excitability: indeed, application of PHE, a different PARP-1 inhibitor (Nasrabady et al., 2011b), did not generate an analogous rise in network discharges. The lowest PJ-34 concentration (1 μM) could, however, induce a significant depression of glutamate uptake (about 25%) which was not very different from the depression (30%) detected with the highest PJ-34 concentrations, and could also evoke delayed onset of strong network discharges. These data, therefore, suggest that partial inhibition of PARP-1 activity was not per se a crucial factor to increase network excitability, an effect more likely attributable to the partial depression of glutamate uptake. Hence, it seems probable that the induction of persistent network discharges was an unexpected property of PJ-34 because of its additional action on the glutamate transport system.

It is difficult to relate the present in vitro findings to the in vivo administration of PJ-34 since, to the best of our knowledge, the actual plasma concentration of this drug and its final redistribution to the brain tissue remain unclear. Since the dose of PJ-34 injected into experimental animal is 3-30 mg/kg (Abdelkarim et al., 2001; Virág and Szabó, 2002; Kauppinen et al., 2009; Crawford et al., 2010), assuming uniform drug distribution throughout body compartments of an adult rat (and ignoring any bound fraction that might lower the free drug concentration), one might estimate a plasma concentration of approximately 37 μM after 10 mg/kg, that is in the range of the concentrations tested in vitro in the present report. Even if the actual concentration of free PJ-34 at neuronal membrane level is likely to be lower, it seems feasible that it would still be compatible with those tested in the present study.

4.4. Downregulation of glutamate transport translated into network plasticity

Following perturbation of neurotransmitter systems, activity-dependent synaptic plasticity regulates brain network excitability (Marder, 1998; Abbott and Nelson, 2000; Neves et al., 2008). This process is known to develop in the spinal cord as well (Parker and Grillner, 2000). We propose that application of PJ-34 biased spinal network activity towards excitation over inhibition as shown by increased random discharges dependent on glutamatergic transmission. It is likely, however, that a degree of homeostatic plasticity had occurred whereby the enhanced level of extracellular glutamate must have led to a compensatory downregulation of glutamatergic transmission as demonstrated by the unchanged size of monosynaptic reflexes (and cumulative depolarization) one day later. Hence, in spinal networks, homeostatic plasticity (Galante et al., 2001; Rosato-Siri et al., 2002) and efficient synaptic inhibition (which enabled locomotor network function; Kiehn, 2006) possibly contributed to prevent any runaway excitation caused by the partial block of glutamate transport. When GABA and glycine receptors were blocked by bicuculline and strychnine, disinhibited bursting following PJ-34 exposure was similar to control. Nonetheless, spontaneous bursts emerged in the interval between electrically-driven bursts and exerted a rapid downregulation of subsequent bursts indicating state-dependent, short term plasticity (Bracci et al., 1997).

4.5. Persistent electrical discharges had no structural consequences on spinal networks

Although excitotoxic damage elicited by impaired glutamate uptake is thought to be a major process to lesion neurons (Kim et al., 2011), and, in particular, motoneurons (Foran and Trotti, 2009), the present study shows that persistently raised network discharges had not caused early loss of neurons or glia in the spinal cord. To account for the structural and functional resilience of spinal networks, it is proposed that build-up of extracellular glutamate might have also activated compensatory processes that have prevented neurotoxicity. In particular, it is likely that wider-scale activation of metabotropic glutamate receptors might have counteracted network hyperexcitability as proposed for brain circuits (Huang et al., 2004; Hartmann et al., 2008; Potier et al., 2010). All main subtypes of metabotropic glutamate receptor are largely expressed by the rat spinal cord (reviewed by Nistri et al., 2006) to regulate synaptic transmission and reflexes (Marchetti et al., 2003). Indeed, a recent study of the rat dorsal horn has shown that inhibition of glutamate transporters enhances group I mGluR-dependent oscillatory activity (Galik et al., 2008). Furthermore, in the rat hippocampus, raised glutamatergic signalling is reported to induce release of endocannabinoids from postsynaptic cells to depress, in a retrograde fashion, further neurotransmitter release (Hofmann et al., 2008; Nahir et al., 2010). Future studies are necessary to explore if a similar process occurs also in the spinal cord as it would represent a powerful system to dampen network excitability. Thus, the most parsimonious explanation is that, as far as locomotor networks were concerned, moderate block of glutamate transport did not trigger neurodegeneration because compensatory mechanisms were likely to contrast the potential risk of excitotoxicity. In support of our suggestion is the report that prolonged elevation of extracellular glutamate due to its transport blockade in vivo is innocuous for spinal motoneurons, while direct activation of glutamate receptors is highly neurotoxic (Tovar-Y-Romo et al., 2009).

4.6. Implications for neurodegeneration in the spinal cord

Previous models of spinal excitotoxicity and allied neurodegeneration had relied on the application of various concentrations of kainate (Mazzone et al., 2010), a glutamate analogue widely employed also for evoking experimental brain lesions with behavioural effects like generalized convulsions (Vincent and Mulle, 2009). Indeed, it is thought that repeated seizures are the cause for chronic epilepsy (Ben-Ari, 2001) since about 1 h of electrically-induced seizures is sufficient to obtain substantial neurodegeneration in the rat hippocampus (Norwood et al., 2011). The present results suggest that, in the rat spinal cord in vitro, intense synchronous discharges were not per se able to produce cell or functional damage. This observation differs from the neurotoxicity data following application of kainate that depolarizes neurons directly by binding to its receptors and it also triggers release of endogenous glutamate from depolarized neurons (Mazzone and Nistri, 2011) to perpetrate a vicious circuit of excitation-neurotoxicity.

In conclusion, strongly and persistently enhanced glutamatergic activity at spinal network level did not trigger neurodegeneration and allowed preservation of locomotor-like function. Thus, these results are consistent with the notion that delayed administration of PJ-34 could protect spinal neurons from excitotoxicity as long as the insult was relatively small (Mazzone and Nistri, 2011; Nasrabady et al., 2011a). It seems probable that, for spinal networks, summating the excitation evoked by PJ-34 to a strong excitotoxic stimulus becomes a tall order to cope with.

Acknowledgements

References

Abbott, L.F., Nelson, S.B., 2000. Synaptic plasticity: taming the beast. Nat. Neurosci. 3, 1178–1183.

Abdelkarim, G.E., Gertz, K., Harms, C., Katchanov, J., Dirnagl, U., Szabo, C., Endres, M., 2001. Protective effects of PJ-34, a novel, potent inhibitor of poly(ADP-ribose) polymerase (PARP) in in vitro and in vivo models of stroke. Int. J. Mol. Med. 7, 255–260.

Andrabi, S.A., Dawson, T.M., Dawson, V.L., 2008. Mitochondrial and nuclear cross talk in cell death: parthanatos. Ann. N. Y. Acad. Sci. 1147, 233–241.

Beato, M., Nistri, A., 1999. Interaction between disinhibited bursting and fictive locomotor patterns in the rat isolated spinal cord. J. Neurophysiol. 82, 2029–2038.

Beato, M., Bracci, E., Nistri, A., 1997. Contribution of NMDA and non-NMDA glutamate receptors to locomotor pattern generation in the neonatal rat spinal cord. Proc. Roy. Soc. B 264, 877–884.

Ben-Ari, Y., 2001. Cell death and synaptic reorganizations produced by seizures. Epilepsia 42 (Suppl. 3), 5–7.

Besson, V.C., 2009. Drug targets for traumatic brain injury from poly(ADP-ribose) polymerase pathway modulation. Br. J. Pharmacol. 157, 695–704.

Bracci, E., Ballerini, L., Nistri, A., 1996a. Spontaneous rhythmic bursts induced by pharmacological block of inhibition in lumbar motoneurons of the neonatal rat spinal cord. J. Neurophysiol. 75, 640–647.

Bracci, E., Ballerini, L., Nistri, A., 1996b. Localization of rhythmogenic networks responsible for spontaneous bursts induced by strychnine and bicuculline in the rat isolated spinal cord. J. Neurosci. 16, 7063–7076.

Bracci, E., Beato, M., Nistri, A., 1997. Afferent inputs modulate the activity of a rhythmic burst generator in the rat disinhibited spinal cord in vitro. J. Neurophysiol. 77, 3157–3167.

Bradford, M.M., 1976. A rapid and sensitive method for the quantitation of microgram quantities of protein utilizing the principle of protein dye binding. Anal. Biochem. 72, 248–254.

Brodin, L., Grillner, S., 1985. The role of putative excitatory amino acid neurotransmitters in the initiation of locomotion in the lamprey spinal cord. II. The effects of amino acid uptake inhibitors. Brain Res. 360, 149–158.

Butt, S.J., Lebret, J.M., Kiehn, O., 2002. Organization of left–right coordination in the mammalian locomotor network. Brain Res. Rev. 40, 107–117.

Casey, P.J., Black, J.H., Szabo, C., Frosch, M., Albadawi, H., Chen, M., Cambria, R.P., Watkins, M.T., 2005. Poly(adenosine diphosphate ribose) polymerase inhibition modulates spinal cord dysfunction after thoracoabdominal aortic ischemia-reperfusion. J. Vasc. Surg. 41, 99–107.

Cazalets, J.R., Sqalli-Houssaini, Y., Clarac, F., 1992. Activation of the central pattern generators for locomotion by serotonin and excitatory amino acids in neonatal rat. J. Physiol. 455, 187–204.

Cifra, A., Mazzone, G.L., Nani, F., Nistri, A., Mladinic, M., Postnatal developmental profile of neurons and glia in motor nuclei of the brainstem and spinal cord, and its comparison with organotypic slice cultures. Devel. Neurobiol., in press.

Crawford, R.S., Albadawi, H., Atkins, M.D., Jones, J.E., Yoo, H.J., Conrad, M.F., Austen Jr., W.G., Watkins, M.T., 2010. Postischemic poly (ADP-ribose) polymerase (PARP) inhibition reduces ischemia reperfusion injury in a hind-limb ischemia model. Surgery 148, 110–118.

Douglas, J.R., Noga, B.R., Dai, X., Jordan, L.M., 1993. The effects of intrathecal administration of excitatory amino acid agonists and antagonists on the initiation of locomotion in the adult cat. J. Neurosci. 13, 990–1000.

Evans, R.H., 1989. The pharmacology of segmental transmission in the spinal cord. Prog. Neurobiol. 33, 255–279.

Foran, E., Trotti, D., 2009. Glutamate transporters and the excitotoxic path to motor neuron degeneration in amyotrophic lateral sclerosis. Antioxid. Redox Signal. 11, 1587–1602.

Fulton, B.P., Walton, K., 1986. Electrophysiological properties of neonatal rat motoneurones studied in vitro. J. Physiol. 370, 651–678.

Galante, M., Avossa, D., Rosato-Siri, M., Ballerini, L., 2001. Homeostatic plasticità induced by chronic block of AMPA/kainate receptors modulates the generation of rhythmic bursting in rat spinal cord organotypic cultures. Eur. J. Neurosci. 14, 903–917.

Galik, J., Youn, D.H., Kolaj, M., Randić, M., 2008. Involvement of group I metabotropic glutamate receptors and glutamate transporters in the slow excitatory synaptic transmission in the spinal cord dorsal horn. Neuroscience 154, 1372–1387.

Genovese, T., Mazzon, E., Muia, C., Patel, N.S., Threadgill, M.D., Bramanti, P., De Sarro, A., Thiemermann, C., Cuzzocrea, S., 2005. Inhibitors of poly(ADP-ribose) polymerase modulate signal transduction pathways and secondary damage in experimental spinal cord trauma. J. Pharmacol. Exp. Ther. 312, 449–457.

Hartmann, K., Bruehl, C., Golovko, T., Draguhn, A., 2008. Fast homeostatic plasticity of inhibition via activity-dependent vesicular filling. PLoS One 3, e2979.

Hofmann, M.E., Nahir, B., Frazier, C.J., 2008. Excitatory afferents to CA3 pyramidal cells display differential sensitivity to CB1 dependent inhibition of synaptic transmission. Neuropharmacology 55, 1140–1146.

Huang, Y.H., Sinha, S.R., Tanaka, K., Rothstein, J.D., Bergles, D.E., 2004. Astrocyte glutamate transporters regulate metabotropic glutamate receptor-mediated excitation of hippocampal interneurons. J. Neurosci. 24, 4551–4559.

Kass, R.E., Ventura, V., Cai, C., 2003. Statistical smoothing of neuronal data. Netw. Comput. Neural Syst. 14, 5–15.

Kauppinen, T.M., Suh, S.W., Berman, A.E., Hamby, A.M., Swanson, R.A., 2009. Inhibition of poly(ADP-ribose) polymerase suppresses inflammation and promotes recovery after ischemic injury. J. Cereb. Blood Flow. Metab. 29, 820–829.

Kerkut, G.A., Bagust, J., 1995. The isolated mammalian spinal cord. Prog. Neurobiol. 46, 1–48.

Kiehn, O., Kjaerulff, O., 1998. Distribution of central pattern generators for rhythmic motor outputs in the spinal cord of limbed vertebrates. Ann. N. Y. Acad. Sci. 860, 110–129.

Kiehn, O., 2006. Locomotor circuits in the mammalian spinal cord. Annu. Rev. Neurosci. 29, 279–306.

Kim, K., Lee, S.G., Kegelman, T.P., Su, Z.Z., Das, S.K., Dash, R., Dasgupta, S., Barral, P.M., Hedvat, M., Diaz, P., Reed, J.C., Stebbins, J.L., Pellecchia, M., Sarkar, D., Fisher, P.B., 2011. Role of excitatory amino acid transporter-2 (EAAT2) and glutamate in neurodegeneration: opportunities for developing novel therapeutics. J. Cell. Physiol. 226, 2484–2493.

Kuzhandaivel, A., Nistri, A., Mladinic, M., 2010a. Kainate-mediated excitotoxicity induces neuronal death in the rat spinal cord in vitro via a PARP-1 dependent cell death pathway (Parthanatos). Cell. Mol. Neurobiol. 30, 1001–1012.

Kuzhandaivel, A., Margaryan, G., Nistri, A., Mladinic, M., 2010b. Extensive glial apoptosis develops early after hypoxic-dysmetabolic insult to the neonatal rat spinal cord in vitro. Neuroscience 169, 325–338.

Kuzhandaivel, A., Nistri, A., Mazzone, G., Mladinic, M., 2011. Molecular mechanisms underlying cell death in spinal networks in relation to locomotor activity after acute injury in vitro. Front. Cell. Neurosci. 5, 9.

Marchetti, C., Beato, M., Nistri, A., 2001. Alternating rhythmic activity induced by dorsal root stimulation in the neonatal rat spinal cord in vitro. J. Physiol. 530, 105–112.

Marchetti, C., Taccola, G., Nistri, A., 2003. Distinct subtypes of group I metabotropic glutamate receptors on rat spinal neurons mediate complex facilitatory and inhibitory effects. Eur. J. Neurosci. 18, 1873–1883.

Marder, E., 1998. From biophysics to models of network function. Annu. Rev. Neurosci. 21, 25–45.

Margaryan, G., Mladinic, M., Mattioli, C., Nistri, A., 2009. Extracellular magnesium enhances the damage to locomotor networks produced by metabolic perturbation mimicking spinal injury in the neonatal rat spinal cord in vitro. Neuroscience 163, 669–682.

Mazzone, G.L., Nistri, A., 2011. Effect of the PARP-1 inhibitor PJ-34 on excitotoxic damage evoked by kainate on rat spinal cord organotypic slices. Cell. Mol. Neurobiol. 31, 469–478.

Mazzone, G.L., Margaryan, G., Kuzhandaivel, A., Nasrabady, S.E., Mladinic, M., Nistri, A., 2010. Kainate-induced delayed onset of excitotoxicity with functional loss unrelated to the extent of neuronal damage in the in vitro spinal cord. Neuroscience 168, 451–462.

Milanese, M., Zappettini, S., Jacchetti, E., Bonifacino, T., Cervetto, C., Usai, C., Bonanno, G., 2010. In vitro activation of GAT1 transporters expressed in spinal cord gliosomes stimulates glutamate release that is abnormally elevated in the SOD1/G93A(+) mouse model of amyotrophic lateral sclerosis. J. Neurochem. 113, 489–501.

Moroni, F., Chiarugi, A., 2009. Post-ischemic brain damage: targeting PARP-1 within the ischemic neurovascular units as a realistic avenue to stroke treatment. FEBS J. 276, 36–45.

Moroni, F., 2008. Poly(ADP-ribose)polymerase 1 (PARP-1) and postischemic brain damage. Curr. Opin. Pharmacol. 8, 96–103.

Nahir, B., Lindsly, C., Frazier, C.J., 2010. mGluR-mediated and endocannabinoid-dependent long-term depression in the hilar region of the rat dentate gyrus. Neuropharmacology 58, 712–721.

Nasrabady, S.E., Kuzhandaivel, A., Nistri, A., 2011a. Studies of locomotor network neuroprotection by the selective poly(ADP-ribose) polymerase-1 inhibitor PJ-34 against excitotoxic injury to the rat spinal cord in vitro. Eur. J. Neurosci. 33, 2216–2227.

Nasrabady, S.E., Kuzhandaivel, A., Mladinic, M., Nistri, A., 2011b. Effects of 6(5H)-phenanthridinone, an inhibitor of poly(ADP-ribose)polymerase-1 activity (PARP-1), on locomotor networks of the rat isolated spinal cord. Cell. Mol. Neurobiol. 31, 503–508.

Neves, G., Cooke, S.F., Bliss, T.V., 2008. Synaptic plasticity, memory and the hippocampus: a neural network approach to causality. Nat. Rev. Neurosci. 9, 65–75.

Nie, H., Weng, H.R., 2009. Glutamate transporters prevent excessive activation of NMDA receptors and extrasynaptic glutamate spillover in the spinal dorsal horn. J. Neurophysiol. 101, 2041–2051.

Nistri, A., Ostroumov, K., Sharifullina, E., Taccola, G., 2006. Tuning and playing a motor rhythm: how metabotropic glutamate receptors orchestrate generation of motor patterns in the mammalian central nervous system. J. Physiol. 15, 323–334.

Norwood, B.A., Bauer, S., Wegner, S., Hamer, H.M., Oertel, W.H., Sloviter, R.S., Rosenow, F., 2011. Electrical stimulation-induced seizures in rats: a "dose–response" study on resultant neurodegeneration. Epilepsia 52, e109–112.

Parker, D., Grillner, S., 2000. Neuronal mechanisms of synaptic and network plasticity in the lamprey spinal cord. Prog. Brain Res. 125, 381—398.

Potier, B., Billard, J.M., Rivière, S., Sinet, P.M., Denis, I., Champeil-Potokar, G., Grintal, B., Jouvenceau, A., Kollen, M., Dutar, P., 2010. Reduction in glutamate uptake is associated with extrasynaptic NMDA and metabotropic glutamate receptor activation at the hippocampal CA1 synapse of aged rats. Aging Cell. 9, 722—735.

Rosato-Siri, M., Grandolfo, M., Ballerini, L., 2002. Activity-dependent modulation of GABAergic synapses in developing rat spinal networks in vitro. Eur. J. Neurosci. 16, 2123—2135.

Scott, G.S., Jakeman, L.B., Stokes, B.T., Szabó, C., 1999. Peroxynitrite production and activation of poly (adenosine diphosphate-ribose) synthetase in spinal cord injury. Ann. Neurol. 45, 120—124.

Shigeri, Y., Seal, R.P., Shimamoto, K., 2004. Molecular pharmacology of glutamate transporters, EAATs and VGLUTs. Brain Res. Rev. 45, 250—265.

Stigliani, S., Zappettini, S., Raiteri, L., Passalacqua, M., Melloni, E., Venturi, C., Tacchetti, C., Diaspro, A., Usai, C., Bonanno, G., 2006. Glia re-sealed particles freshly prepared from adult rat brain are competent for exocytotic release of glutamate. J. Neurochem. 96, 656—668.

Streit, J., Tscherter, A., Heuschkel, M.O., Renaud, P., 2001. The generation of rhythmic activity in dissociated cultures of rat spinal cord. Eur. J. Neurosci. 14, 191—202.

Taccola, G., Nistri, A., 2006a. Fictive locomotor patterns generated by tetraethylammonium application to the neonatal rat spinal cord in vitro. Neuroscience 137, 659—670.

Taccola, G., Nistri, A., 2006b. Oscillatory circuits underlying locomotor networks in the rat spinal cord. Crit. Rev. Neurobiol. 18, 25—36.

Taccola, G., Marchetti, C., Nistri, A., 2004. Modulation of rhythmic patterns and cumulative depolarization by group I metabotropic glutamate receptors in the neonatal rat spinal cord in vitro. Eur. J. Neurosci. 19, 533—541.

Taccola, G., Margaryan, G., Mladinic, M., Nistri, A., 2008. Kainate and metabolic perturbation mimicking spinal injury differentially contribute to early damage of locomotor networks in the in vitro neonatal rat spinal cord. Neuroscience 155, 538—555.

Thomson, D.J., Chave, A.D., 1991. Jackknife error estimates for spectra, coherences, and transfer functions. In: Haykin, S. (Ed.), Advances in Spectral Analysis and Array Processing. Prentice-Hall, Englewood Cliffs, NJ, pp. 58—113.

Tovar-Y-Romo, L.B., Santa-Cruz, L.D., Zepeda, A., Tapia, R., 2009. Chronic elevation of extracellular glutamate due to transport blockade is innocuous for spinal motoneurons in vivo. Neurochem. Int. 54, 186—191.

Vincent, P., Mulle, C., 2009. Kainate receptors in epilepsy and excitotoxicity. Neuroscience 158, 309—323.

Virág, L., Szabó, C., 2002. The therapeutic potential of poly(ADP-ribose) polymerase inhibitors. Pharmacol. Rev. 54, 375—429.

Wu, K.L., Hsu, C., Chan, J.Y., 2009. Nitric oxide and superoxide anion differentially activate poly(ADP-ribose) polymerase-1 and bax to induce nuclear translocation of apoptosis-inducing factor and mitochondrial release of cytochrome c after spinal cord injury. J. Neurotrauma 26, 965—977.

Yunger, L.M., Fowler, P.J., Zarevics, P., Setler, P.E., 1984. Novel inhibitors of gamma-aminobutyric acid (GABA) uptake: anticonvulsant actions in rats and mice. J. Pharmacol. Exp. Ther. 228, 109—115.

Methods, materials and results

Section 5

Samano C, Nasrabady SE, Nistri A (2012) A study of the potential neuroprotective effect of riluzole on locomotor networks of the neonatal rat spinal cord in vitro damaged by excitotoxicity. Neuroscience 222:356-365.

A STUDY OF THE POTENTIAL NEUROPROTECTIVE EFFECT OF RILUZOLE ON LOCOMOTOR NETWORKS OF THE NEONATAL RAT SPINAL CORD *IN VITRO* DAMAGED BY EXCITOTOXICITY

C. SÁMANO, [a] S. E. NASRABADY [a] AND A. NISTRI [a,b]*

[a] *Neuroscience Department, International School for Advanced Studies (SISSA), Trieste, Italy*

[b] *SPINAL (Spinal Person Injury Neurorehabilitation Applied Laboratory), Istituto di Medicina Fisica e Riabilitazione, Udine, Italy*

Abstract—Excitotoxicity triggered by over-stimulation of glutamatergic receptors is considered to be a major component of damage following acute spinal cord injury (SCI). Using an *in vitro* model of neonatal rat SCI caused by transient application (1 h) of the glutamate agonist kainate (0.05–0.1 mM) to produce limited excitotoxicity, the present study investigated whether riluzole, a drug inhibiting glutamate release and neuronal excitability, could prevent neuronal loss and protect locomotor patterns 24 h later. Immunohistochemical analysis of neuronal and motoneuronal populations was associated with recording of fictive locomotion induced by neurochemicals or dorsal root stimuli. Riluzole (5 μM; 24 h application) per se exerted strong and persistent neurodepressant effects on network synaptic transmission from which recovery was very slow. When continuously applied after kainate, riluzole partially reduced the number of pyknotic cells in the gray matter, although motoneurons remained vulnerable and no fictive locomotion was present. In further experiments, riluzole per se was applied for 3 h (expected to coincide with kainate peak excitotoxicity) and washed out for 24 h with full return of fictive locomotion. When this protocol was implemented after kainate, no efficient histological or functional recovery was observed. No additional benefit was detected even when riluzole was co-applied with kainate and continued for the following 3 h. These results show that modest neuronal losses evoked by excitotoxicity have a severe impact on locomotor network function, and that they cannot be satisfactorily blocked by strong neurodepression with riluzole, suggesting the need for more effective pharmacological approaches. © 2012 IRBO. Published by Elsevier Ltd. All rights reserved.

Key words: motoneuron, fictive locomotion, glutamate, neuroprotection, kainate.

INTRODUCTION

Spinal cord injury (SCI) is a major cause of chronic disability which affects millions worldwide (Hall and Springer, 2004; van den Berg et al., 2010; Cadotte and Fehlings, 2011). The pathophysiology of SCI is a biphasic process, consisting of a primary injury at the time of trauma and a secondary lesion that leads to loss of supraspinal control of sensory, autonomic and motor functions at the sublesional level. One important component of the post-traumatic degeneration following SCI is caused by glutamate-mediated excitotoxicity elicited by massive release of this transmitter with a subsequent overexcitation (Park et al., 2004; Norenberg et al., 2004; Ufuk et al., 2005; Schwab et al., 2006; Rowland et al., 2008; Kuzhandaivel et al., 2011). A multi-factorial process comprising an elevated intracellular Ca^{2+} concentration, superoxide dismutase 1 (SOD-1) deregulation, reactive oxygen species, free radicals and metabolic dysfunction likely contributes to neuron losses (Doble, 1999; Ufuk et al., 2005; Rowland et al., 2008; Lau and Tymianski, 2010). As full functional motor recovery after SCI is still unattainable for most individuals, it would be very important to target neuroprotective agents to those neurons affected by excitotoxicity and responsible for the control locomotion (Doble, 1999; Taccola and Nistri, 2006b; Taccola et al., 2008; Mazzone et al., 2010).

Among glutamate release inhibitors, riluzole has been reported to promote a positive behavioral outcome after experimental brain injury and SCI (Wahl et al., 1997; Schwartz and Fehlings, 2001, 2002; Lau and Tymianski, 2010). The mechanism of action of riluzole is complex (Bellingham, 2011; Cifra et al., 2012b) and involves several effects such as: (i) attenuation of presynaptic glutamate release, (ii) reduction of the persistent Na^+ current. Favorable experimental results have been described for riluzole in protecting injured adult spinal motoneurons after ventral root (VR) avulsion (Nógrádi et al., 2007) or hypoglossal motoneurons exposed to excitotoxic stress (Cifra et al., 2011). In clinical studies, while riluzole is the only current treatment for motoneuron

*Correspondence to: A. Nistri, SISSA, Via Bonomea 265, 34136 Trieste, Italy. Tel: +39-040-3787718; fax: +39-040-3787702.
E-mail address: nistri@sissa.it (A. Nistri).
Abbreviations: ALS, amyotrophic lateral sclerosis; ANOVA, analysis of variance; BSA, bovine serum albumin; CTR, control; CV, coefficient of period variation; DAKO, fluorescence mounting medium; DAPI, 4′,6-diamidino-2-phenylindole; DR, dorsal root; IR, immunoreactive; KA, kainate; l, left; L, lumbar; NeuN, neuronal specific nuclear protein; NMDA, N-methyl-D-aspartate; NeuN, Neuronal nuclei monoclonal antibody; NGS, normal goat serum; NIH, National Institute of Health; PBS, phosphate buffer saline; PJ-34, [N-6-Oxo-5,6-dihydrophenanthridin-2-yl)N,N-dimethylacetamide.HCl]; r, right; SCI, spinal cord injury; SMI 32, neurofilament H non-phosphorylated antibody; Rlz, riluzole; ROI, region of interest; SEM, standard error of the mean; SD, standard deviation; SOD-1, superoxide dismutase; VR, ventral root; 5-HT, 5-hydroxytryptamine.

disease, its effect consists in delaying disease progression for a few months only (Wokke, 1996; Cheah et al., 2010). The reason for the modest neuroprotection by riluzole and other agents reported in many studies remains elusive as explanations for the negative results of therapeutic trials include a likely heterogeneity, both in disease susceptibility and pathogenic mechanisms, and faulty methodology of clinical trials (Beghi et al., 2011). While this realization prompts further studies to widen the range of neuroprotective agents with potential activity to combat amyotrophic lateral sclerosis (ALS; Traynor et al., 2006), it seems also of interest to explore the effect of riluzole administration timing with respect to the pathology onset.

While administration of riluzole immediately after an excitotoxic stress has been recently reported to decrease the number of dead neurons in organotypic spinal cord cultures (Mazzone and Nistri, 2011), that study could not test whether locomotor networks had been protected efficiently because fictive locomotor patterns cannot be produced in culture. To address this issue, we investigated the effect of riluzole on kainate-evoked excitotoxicity in the isolated spinal cord *in vitro* (Taccola et al., 2008), taking as outcome the presence or absence of fictive locomotion (reviewed by Grillner, 2003; Clarac et al., 2004) one day after a transient excitotoxic stimulus, and its relation to histological preservation. This protocol assumes that, in clinical settings, any neuroprotective treatment would be very unlikely to begin precisely at the time of the lesion, and that it should show any potential benefit at least 24 h later (the maximum period of time the spinal cord can survive *in vitro* with intact network activity; Taccola et al., 2008). Since the majority of new SCI cases have an incomplete lesion (National Spinal Cord Injury Statistical Center, University of Alabama at Birmingham, 2010 Annual Statistical Report; https://www.nscisc.uab.edu/reports.aspx) as recently confirmed (DeVivo, 2012), the present study employed relatively low concentrations of kainate (0.05–0.1 mM) near or just above threshold to produce moderate neuronal loss in the spinal gray matter when applied for 1 h (Mazzone et al., 2010). Such a neurotoxic action develops within the first 2–4 h after kainate washout and reaches apparent steady state 24 h later (Mazzone et al., 2010; Kuzhandaivel et al., 2011), thus providing a model system to test the neuroprotective effect of riluzole.

EXPERIMENTAL PROCEDURES

Rat spinal cord preparation

The experiments were carried out on neonatal Wistar rats (1–2 days old). Under urethane anesthesia (0.2 ml i.p. of a 10% w/v solution), the spinal cords were carefully dissected and superfused (7.5 ml/min) with Krebs solution which contained (in mM): 113 NaCl, 4.5 KCl, 1 $MgCl_2 7H_2O$, 2 $CaCl_2$, 1 NaH_2PO_4, 25 $NaHCO_3$ and glucose 11; gassed with O_2 95%, CO_2 5%, pH 7.4 at room temperature (22 °C) (Taccola and Nistri, 2006a; Taccola et al., 2008; Margaryan et al., 2009). In accordance with the three Rs objective, all efforts were made to minimize the number of animals used for the experiments and their suffering. The experiments were performed in accordance with the ethical guidelines for the care and use of laboratory animals of National Institutes

of Health (NIH) guidelines and the Italian act D. L. 27/1/92 n. 116 (implementing the European Community directives n.86/609 and 93/88).

Electrophysiological recordings

DC-coupled electrophysiological recording with tight-fitting suction electrodes was from lumbar (L) VRs. Signals were recorded from right (r) and left (l) L2 and L5 VRs which convey electrical motor discharges mainly to flexor and extensor hind limb muscles, respectively (Kiehn and Kjaerulff, 1998; Kiehn, 2006; Taccola and Nistri, 2006b). Signals were captured, digitized and analyzed with pClamp software (version 9.2; Molecular Devices, Sunnyvale, CA, USA). Afferent fibers of a single dorsal root (DR) were stimulated via a bipolar suction electrode with electrical stimuli applied every 60 s. The minimum intensity of the stimulus to induce a reflex response in the ipsilateral homosegmental VR was considered as the stimulation threshold (Taccola et al., 2004). Trains of DR stimuli (0.1-ms duration, 30 pulse trains at 2 Hz) were used to elicit cumulative depolarization with superimposed alternating oscillatory activity typical of fictive locomotion by ⩾2x threshold pulses. The mean amplitude of these responses was calculated by averaging five events. Fictive locomotion was induced by application of N-methyl-D-aspartate (NMDA) (4 or 5 μM) and 5-hydroxytryptamine (5-HT; 10 μM) and observed as alternating cycles of VR discharges (Cazalets et al., 1992; Kjaerulff and Kiehn, 1996; Butt et al., 2002). The period (the interval between one cycle and the following cycle) and the coefficient of variation (CV; indicating the regularity of cycles) were calculated by averaging at least 20 cycles. Disinhibited bursting (Bracci et al., 1996a,b, 1997) was elicited by application of strychnine (1 μM) and bicuculline (20 μM), and burst parameters were calculated as reported by Bracci et al. (1996a,b).

Protocols for excitotoxicity and neuroprotection by riluzole

Four experimental groups were employed in parallel: sham preparations, preparations treated with riluzole alone, preparations treated with kainate (0.05–0.1 mM) alone, and preparations treated with kainate and riluzole (usually 5 μM). Sham spinal cords were kept for 24 h in Krebs solution (Taccola et al., 2008). The control groups treated with riluzole alone were kept for 3 or 24 h *in vitro*. Treatment with kainate always lasted for 1 h and was followed by riluzole applied for 3 or 24 h after washout of kainate. In a few experiments, kainate and riluzole were co-applied. At the end of the experiments, spinal cords were fixed with 4% paraformaldehyde and cryoprotected in sucrose solution (30% w/v) for subsequent immunohistochemistry (Taccola et al., 2008). The concentration of kainate was chosen according to Mazzone et al. (2010) who showed that 0.05 mM (threshold) kainate abolished the locomotor network function for at least 24 h with a moderate degree of cell damage, while stronger damage was produced by 0.1 mM. The majority of experiments were done with 5 μM concentration of riluzole because it is similar to the plasma therapeutic concentration used in clinical trials in patients with ALS (Bellingham, 2011), and can provide neuroprotection together with inhibition of glutamate release from organotypic spinal slices in culture (Cifra et al., 2011; Mazzone and Nistri, 2011). In a few experiments, we also tested 15 μM riluzole, which is the largest dose previously used in neonatal rat spinal cord studies (Tazerart et al., 2007; Kwon et al., 2011).

Immunohistochemistry procedure

Transverse sections (30 μm thick) of the spinal cord were cut with a sliding microtome at −20 °C and stored in phosphate-buffered saline (PBS) until use. Single or double immunohistochemical stainings were performed on the free-floating tissue

sections or on the sections immobilized on Superfrost plus slides (Thermo Fisher Scientific GmbH, Germany) and processed in a humid atmosphere. The sections were preincubated for 2 h at room temperature in 5% normal goat serum (NGS)/5% bovine serum albumin (BSA) and 0.3% Triton X-100, followed by overnight incubation at 4 °C in 1% NGS/1% BSA/0.1% Triton X-100 solution containing primary antibodies directed against the following antigens: anti-neuronal specific nuclear protein (NeuN) or anti-neurofilament H non-phosphorylated (SMI 32) (Table 1). Tissue sections were rinsed thrice for 10 min each in PBS-Triton X-100 (0.1 M PBS, 0.3% Triton X-100), and then incubated for 2 h with the appropriate secondary antibody, anti-mouse Alexa Fluor 488 or 594 antibodies. Finally, to identify pyknotic nuclei, sections were stained with 1 μg/ml solution of 4′,6-diamidino-2-phenylindole (DAPI) for 20 or 30 min at room temperature and processed with a fluorescence mounting medium (DAKO, fluorescence mounting medium; Milan, Italy, or Vectashield, Vector, Burlingame, CA, USA) for analysis with an epifluorescence microscope (Zeiss Axioskope 2, Carl Zeiss). Selected spinal cord serial sections with double or triple labeling staining were further analyzed with confocal Leica (DMRI2) equipped with argon/krypton laser and Metavue software (Molecular Devices).

Cell quantification and statistical analysis

Pyknotic nuclei were identified and quantified with the cell counter software "eCELLence" (Glance Vision Tech, Trieste, Italy). For each experimental condition, 2–4 spinal cords were analyzed and for each spinal cord 3–6 transversal sections from T12 to L2 segments were examined. The choice of these segments was based on the fact that they are the most rhythmogenic areas of the spinal cord and are believed to contain the essential elements of the central pattern generator for locomotion (Kjaerulff and Kiehn, 1996; Kiehn, 2006). Furthermore, our previous investigations have demonstrated that various lumbar segments show comparable sensitivity to excitotoxic damage (Taccola et al., 2008).

We quantified the percentage of pyknosis stained by DAPI, the number of NeuN-expressing cells and SMI 32 motoneurons-immunoreactive (IR) in each section of the spinal cord according to four regions of interest (ROIs): (i) dorsal gray matter (Rexed laminae I–IV), (ii) central gray matter (Rexed laminae V–VIII and X), (iii) ventral gray matter (Rexed laminae VIII–IX) and (iv) ventrolateral white matter. For each region, 5–7 fields of 350×350 μm (dorsal and central regions in the gray matter), 520×520 μm (ventral horn), or 100×500 μm (white matter) were analyzed. Further details have been previously reported (Taccola et al., 2008).

Statistical analysis was performed with SigmaStat (SigmaStat 3.1, Systat Software, Chicago, IL, USA) and Origin (Origin Pro 8, Northampton, MA, USA). Data are expressed as mean ± SD (or SEM for histology data). Parametric or non-parametric data distribution was established with a normality test and the significance of differences between the means was evaluated either with independent Student's t-test or Mann–Whitney test, respectively. ANOVA was used for analyzing multiple comparisons followed by a post hoc Mann–Whitney test. The accepted level of significance was set as $P < 0.05$.

Drugs

NMDA and riluzole were purchased from Tocris (Bristol, UK). 5-HT and strychnine hydrochloride were from Sigma (Milan, Italy). Bicuculline methiodide was obtained from Fluka (Milan, Italy). Kainate was purchased from Ascent (Abcam Biochemicals. Cambridge, UK).

RESULTS

Effects of riluzole on kainate-mediated excitotoxicity

Our previous studies have shown that kainate-evoked excitotoxicity is primarily directed against neurons rather than glia and is morphologically expressed as pyknosis with chromatin condensation (Taccola et al., 2008; Margaryan et al., 2009; Kuzhandaivel et al., 2010). Fig. 1A, B exemplifies and quantifies the excitotoxic damage evoked by 0.05 or 0.1 mM kainate (1 h application) in ROIs comprising the dorsal, central, and ventral gray and ventrolateral white matter regions of the spinal cord *in vitro* 24 h later. The region most sensitive was the dorsal horn one, where pyknosis reached the maximum value of 28 ± 4 % ($n = 6$) after 0.1 mM kainate, whereas the white matter ROI showed the smallest damage. A lower concentration (0.05 mM) of kainate induced comparatively less neurotoxicity (Fig. 1B). Riluzole (5 μM; 24 h) per se had no toxic effect on spinal cord cells (Fig. 1B). Nonetheless, when riluzole (5 μM) was applied immediately after kainate (0.1 mM) washout for the subsequent 24 h, it could significantly attenuate the pyknosis in the dorsal, central and ventral horn ROIs (Fig. 1A, C) when compared with the effect of kainate alone (Fig. 1B). Trebling the concentration of riluzole did not, however, improve the outcome after 0.1 mM kainate (Fig. 1C).

Effect of riluzole on electrophysiological network properties

Spinal cords treated with 0.1 mM kainate followed by 24 h riluzole (5 μM) and 2 h wash with standard solution, never showed fictive locomotion and generated only small VR reflexes (0.31 ± 0.17-mV amplitude) after DR stimulation ($n = 3$) vs. sham preparations (see Table 2). This depression of spinal network excitability led us to reconsider the drug application protocol. In fact, since riluzole depresses

Table 1. Antibodies used for immunofluorescence labeling

| Antibodies	Type	Coupled to	Dilution	Origin
Primary				
NeuN (mouse)	Mouse monoclonal	–	1:50; 1:100	Millipore; Chemicon. Milan, Italy
NeuN-RBFOX (rabbit)	Rabbit polyclonal	–	1:100	Novus Biologicals. Milan, Italy
SMI 32 (mouse)	Mouse monoclonal	–	1:200	Covance. Emeryville, CA, USA
Secondary				
α Mouse IgG	Goat	Alexa Fluor 488	1:250	Invitrogen. Milan, Italy
α Mouse IgG	Goat	Alexa Fluor 594	1:200	Invitrogen. Milan, Italy
α Rabbit IgG	Goat	Alexa Fluor 488	1:250; 1:500	Invitrogen. Milan, Italy
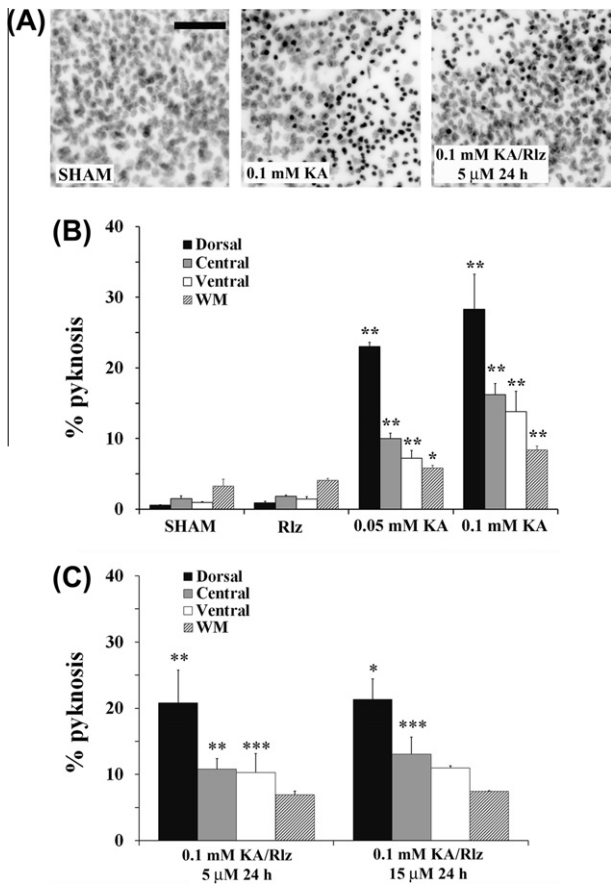
Fig. 1. Characterization of riluzole effects on kainate-evoked damage 24 h later. (A) Upper panels show representative micrographs of cell nuclei stained with DAPI in the dorsal horn of sham (left), 0.1 mM kainate (KA; middle) or kainate followed by riluzole (Rlz; 5 µM; right). Scale bar = 50 µm. (B) Graph of the percent occurrence of pyknotic nuclei detected in each ROI (dorsal, central, ventral and white matter) of the spinal cord, for sham, Rlz alone, or KA alone (0.05 or 0.1 mM). For each condition, pyknosis was normalized with respect to the total number of DAPI-sensitive cells ($n = 6$ spinal cords, 0.05 or 0.1 mM KA vs. sham: $*P < 0.01$ and $**P < 0.001$). (C) Graph showing the average percent occurrence of pyknosis 24 h after washout of 0.1 mM KA followed by Rlz (5 or 15 µM). Average data from 3 to 6 spinal cords; comparisons were vs. 0.1 mM KA ($*P < 0.01$, $**P < 0.001$, $***P < 0.05$).

presynaptic glutamate release (and facilitates Na^+-dependent glutamate uptake) together with block of voltage-dependent Na^+ channels (Taylor and Meldrum, 1995; Song et al., 1997; Fumagalli et al., 2008; Tazerart et al., 2007; Cifra et al., 2012b), we wondered if such a long-lasting riluzole application might have persistently depressed synaptic reflexes regardless of kainate-evoked toxicity. Thus, to separate the direct depressant action of riluzole on spinal networks from its potential to contrast neurotoxicity, we examined the effect of riluzole per se on fictive locomotion induced by neurochemicals or DR electrical stimulation. Fictive locomotion induced by NMDA (4–5 µM) plus 5-HT (10 µM) or by a train of DR stimuli was abolished 1–2 h after starting riluzole (5 µM) application (not shown), a result in accordance with the study by Tazerart et al. (2007) who have reported the slowly developing disruption in fictive locomotion evoked

by 10 µM riluzole. When riluzole application lasted 24 h, 2 h washout (with Krebs solution) was insufficient to restore fictive locomotion induced by either NMDA plus 5-HT as shown in Fig. 2A that depicts VR traces obtained from the same spinal cord prior to riluzole and then 24 h later. Similar observations were obtained with a train of DR stimuli (Fig. 2B). In analogy with previous studies (Taccola et al., 2008; Margaryan et al., 2009, 2010; Nasrabady et al., 2011a,b, 2012), fictive locomotion could consistently be detected in sham (untreated) preparations kept for 24 h in vitro (see example in the left panel of Fig. 2C). We, therefore, concluded that this protocol of prolonged riluzole application did not allow us investigating the functional neuroprotection by this drug.

Since kainate-evoked damage chiefly occurs within the first 2–3 h after its washout (Kuzhandaivel et al., 2010; Nasrabady et al., 2011a), we thought that neuroprotection by riluzole might be targeted to this crucial time period as long as the action of riluzole could be washed out by 24 h and fictive locomotion observed again. Hence, we first explored if 3-h riluzole application per se could allow us to observe functional activity 24 h later. The peak amplitude of the polysynaptic responses to DR stimulation of sham ($n = 6$) or 3-h riluzole-treated ($n = 3$) preparations was not significantly different ($P = 0.17$) as shown in Fig. 2D. Likewise, 24 h later, the reflex area was unchanged after 3-h riluzole administration (2169.35 ± 800.94 mV.ms vs. 2072.71 ± 815.59 mV.ms, respectively; $P = 0.38$). Period (4.45 ± 1.10 vs. 4.59 ± 1.23 s), CV (0.12 ± 0.06 vs. 0.10 ± 0.04), and amplitude of fictive locomotor cycles (0.08 ± 0.06 vs. 0.11 ± 0.05 mV; $n = 4$) were also unchanged (see example in Fig. 2C). As shown in Fig. 2E, cumulative depolarization amplitude and area elicited by a train of DR stimuli ($\geqslant 2$ th, 30, 2 Hz) were similar in sham and after 3-h riluzole (0.54 ± 0.27 mV sham vs. 0.57 ± 0.26 mV riluzole; $14,677 \pm 4,165$ mV.ms sham vs. $14,262 \pm 4857$ mV.ms riluzole, $n = 3$), although the number of oscillations elicited by the train was smaller than for sham preparations (3.6 ± 0.5 vs. 5.1 ± 0.8). These data, therefore, indicated that the strong depressant effect of 3 h application of riluzole was reversible 24 h later.

Effect of riluzole on network activity after kainate application

To explore any functional neuroprotection by riluzole, we tested if, using the time protocol described above, this agent could contrast the block of locomotor network function by 0.05 mM kainate, namely a concentration at threshold for irreversible loss of this pattern (Mazzone et al., 2010; Nasrabady et al., 2011b).

Table 2 shows that application of riluzole (5 µM; $n = 6$) for 3 h after kainate washout, did not significantly improve, 24 h later, the peak amplitude and area of the DR reflex in comparison with the group treated with kainate alone (0.05 mM). Fictive locomotion (induced chemically or electrically) was never present in any preparation treated with riluzole after kainate. Nonetheless, as indicated in Table 2, spinal networks did retain their intrinsic rhythmicity since disinhibited bursting after kainate alone was similar to the value after kainate and riluzole

Table 2. Effect of riluzole applied together with (or following) kainate on electrophysiological network activity

	Peak amplitude of the DR reflex (mV)	Area of the DR reflex (mV.ms)	Period of disinhibited bursting (s)	CV of disinhibited bursting
Sham ($n = 6$)	0.73 ± 0.39	2169 ± 800	45 ± 14	0.44 ± 0.15
Kainate 0.05 mM ($n = 5$)	0.40 ± 0.17	320 ± 255	93 ± 79	0.44 ± 1.92
Kainate 0.05 mM/Rlz 5 µM ($n = 6$)	0.55 ± 0.37	332 ± 267	90 ± 41	0.19 ± 0.05[*]
Kainate 0.05 mM + Rlz 5 µM co-applied ($n = 3$)	0.46 ± 0.36	120 ± 55	76 ± 37	0.41 ± 0.29

[*] Indicates the significant difference (P = 0.004) between CV of the group treated with Rlz after kainate and group treated with kainate. All comparisons are made between kainate alone and the groups treated with riluzole (Rlz).
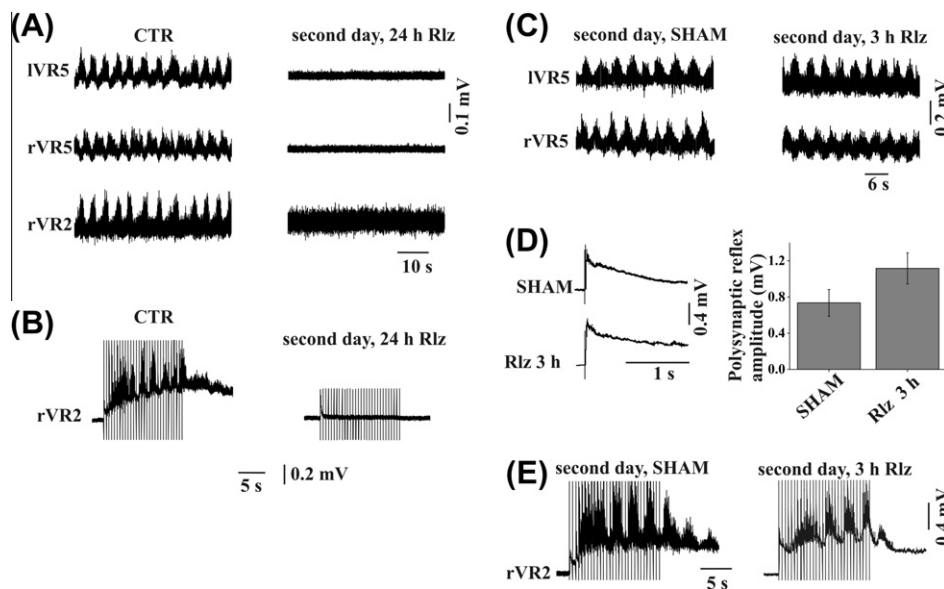

Fig. 2. Effect of riluzole per se on electrophysiological properties of spinal cords. (A) Example of fictive locomotion induced by application of NMDA (4 µM) plus 5-HT (10 µM) in control (CTR, left) and after 24-h riluzole application (right). Twenty-four-hour riluzole application and washout with Krebs solution for 1–2 h did not allow recovery of fictive locomotion. (B) Example of cumulative depolarization and oscillatory activity evoked by train of DR stimuli in control (left) and after 24-h riluzole application (right). (C) Example of fictive locomotion (induced by application of NMDA plus 5-HT) observed after 24 h *in vitro* in a sham preparation (left) or in preparation treated with riluzole for 3 h the day before (right). Fictive locomotion was present with similar characteristics. (D) Example of polysynaptic responses from sham (top-left) or riluzole-treated spinal cord for 3 h (bottom-left). Histograms show similar peak amplitudes of these two groups ($n = 6$ or 3, respectively). (E) Example of cumulative depolarization and oscillatory activity evoked by train of DR stimuli in sham (left) or 3-h riluzole-treated spinal cord and recorded on the second day *in vitro*.

although, in the latter case, the rhythm had become more regular.

As previous studies had shown the positive effect of pre or co-application of riluzole on chemically evoked neuronal damage (Chang et al., 2010; Verhave et al., 2012), we tested, on a further group of spinal cords ($n = 3$), co-application of kainate (0.05 mM) and riluzole (5 µM) followed by 3 h application of riluzole alone. Despite this protocol, fictive locomotion was never observed 24 h later. In addition, no significant improvement in reflex responses was observed (Table 2).

Cell survival after distinct riluzole administration protocols

Despite the disappointing electrophysiological outcome at 24 h, we checked whether the two application protocols, namely 3 h riluzole after kainate or kainate together with riluzole (the latter continued for 3 more h), could spare a different number of cells, perhaps yielding a number of surviving cells not far from the minimum membership of the locomotor network (Kuzhandaivel et al., 2011). In Fig. 3A, the left hand set of histograms shows that, in each ROI, application of riluzole for 3 h did not provide neuroprotection after kainate treatment (0.05 mM) when data are compared with those in Fig. 1B. Even when the two drugs were co-applied, there was no significant fall in pyknosis (Fig. 3A). Similar results were obtained with 0.1 mM kainate and delayed or concurrent application of riluzole (Fig. 3B). Only in the ventral horn ROI, a small decrement in the number of pyknotic nuclei was detected (Fig. 3B) with respect to 0.1 mM kainate alone (Fig. 1B).

To quantify neuronal numbers, we stained neurons with an antibody against the nuclear marker NeuN as exemplified for the dorsal horn (Fig. 3C). As previously reported by Mazzone et al. (2010) and in accordance with the current pyknosis data, kainate (0.05 or 0.1 mM) was primarily toxic to dorsal horn neurons, while riluzole per se had no neurotoxic action (Fig. 3D). Fig. 3E, F shows that riluzole could not significantly protect neurons even
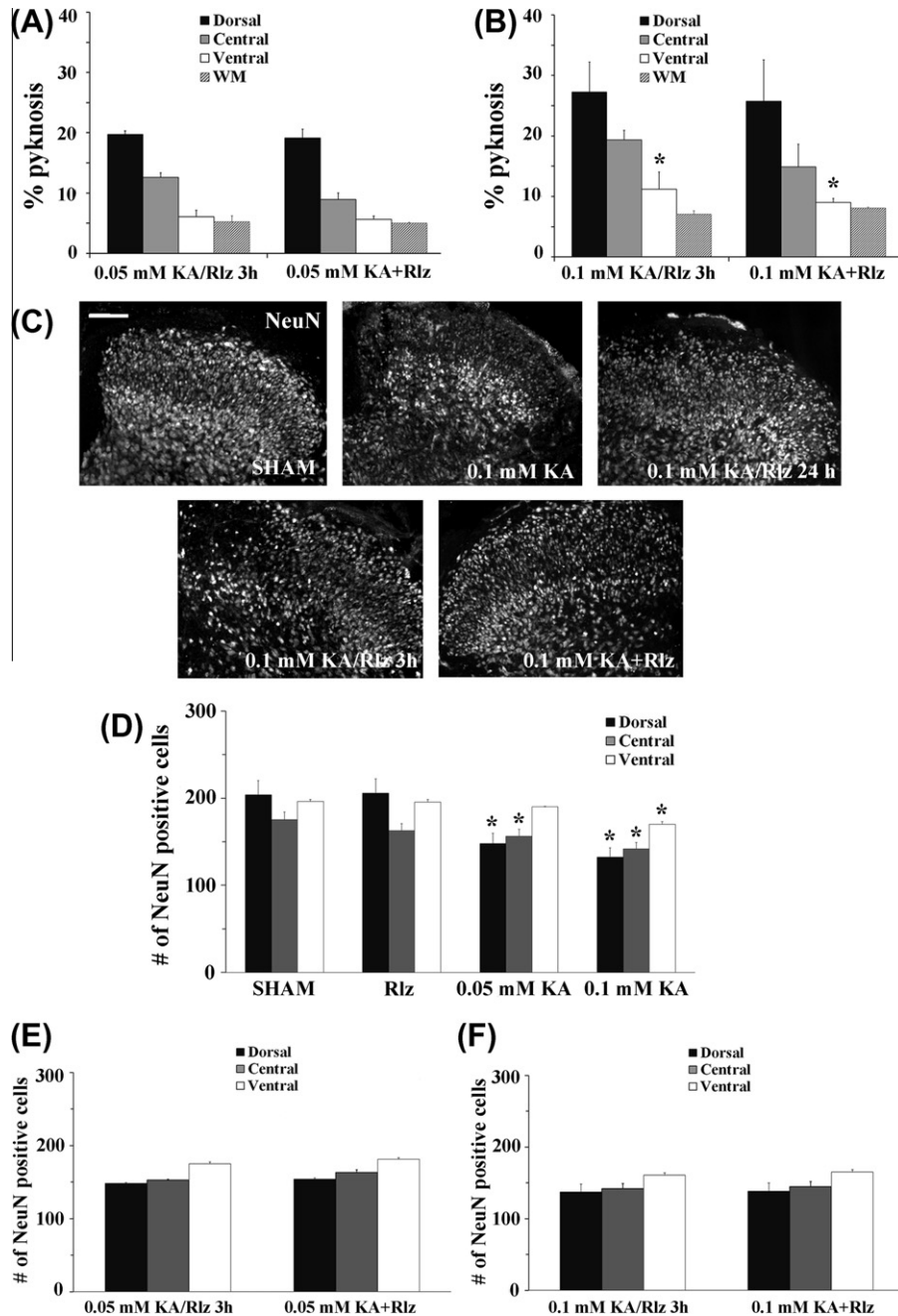
Fig. 3. Pyknotic nuclei and neuronal survival after distinct riluzole administration protocols. (A) Histograms showing average percent of pyknotic cells in four ROIs after 0.05 mM KA (1-h application) followed by Rlz (5 µM) for 3 h (KA/Rlz) or with Rlz applied together with KA (KA + Rlz). (B) Similar protocols as detailed in A with larger (0.1 mM) KA application. Comparisons of data vs. 0.1 mM KA alone (Fig. 1B) yielded $^*P < 0.05$ for the ventral ROI ($n = 3$ spinal cords). (C) Representative images (dorsal horn) showing NeuN-stained positive cells of sham, 0.1 mM KA alone, or with different Rlz protocols (0.1 mM KA/Rlz for 24 h, 0.1 mM KA/Rlz for 3 h, or 0.1 mM KA + Rlz co-applied). In each case, kainate was applied for 1 h only. Scale bar = 100 µm. (D) Plots showing average number of NeuN-positive neurons in the gray matter (three ROIs analyzed) in control conditions (sham or Rlz alone) or after washout of KA (0.05 or 0.1 mM; 1 h application). $^*P < 0.001$ for 0.05 ($n = 3$) or 0.1 mM KA ($n = 6$) vs. sham. (E, F) summarize quantitative data for neuronal numbers 24 h after 0.05 or 0.1 mM KA (1 application) followed by Rlz 5 µM (for 3 h; KA/Rlz) or applied together with riluzole (KA + Rlz).

when it was co-applied with 0.05 mM kainate (in comparison with data shown in Fig. 3D).

Globally, these results indicated that a relatively short application (or co-application) of riluzole could not adequately protect spinal neurons, in full accordance with the electrophysiological data. We, therefore, enquired whether a long-lasting (24-h) continuous application of

riluzole might prove to be more histologically protective even if it was observed to strongly inhibit network activity. After all, functionally depressed neurons might be able to recover later, beyond the experimental survival in vitro.

When riluzole was continuously applied for 24 h after kainate (0.1 mM), there was a significant, albeit slightly higher number of dorsal (168 ± 3) and central (149 ± 2)
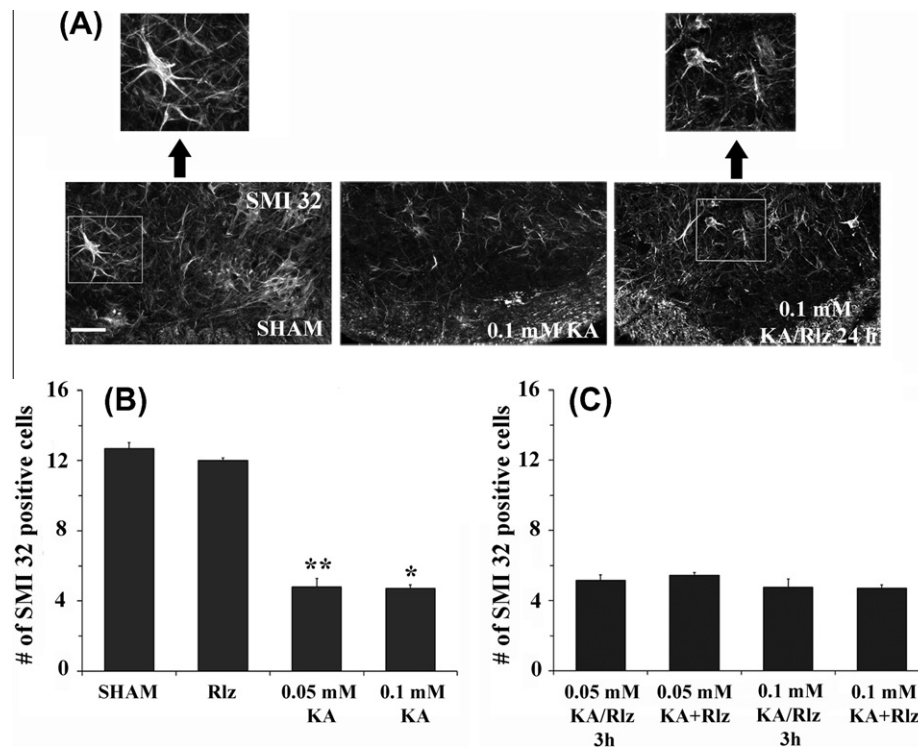
Fig. 4. Riluzole application did not protect motoneurons after excitotoxic insult. (A) Micrographs show examples of motoneurons (stained with SMI 32 antibody) in the ventral ROI in sham (left), after KA (0.1 mM; middle) or KA followed by Rlz applied for 24 h (right). The arrows (top) show two insets at a higher magnification of SMI 32 positive cells. Scale bar = 100 µm. (B) Histograms showing total number of SMI 32-immunoreactive cells in ventral ROI 24 h after in sham, Rlz alone or KA (0.05 or 0.1 mM for 1 h) protocols. $^{**}P < 0.05$ for 0.05 ($n = 3$) or $^{*}P < 0.01$ for 0.1 mM KA ($n = 6$). (C) Number of SMI 32 positive cells after KA (0.05 or 0.1 mM) followed by Rlz application for 3 h (KA/Rlz) or after the co-application treatment (KA + Rlz). Data are not different from results with kainate alone in panel B.

neurons vs. those after kainate alone (133 ± 2 and 142 ± 4, respectively), although no difference was observed for the ventral ROI data (172 ± 2 and 170 ± 5, respectively; $n = 6$ spinal cords).

In keeping with these data, motoneurons were highly vulnerable to kainate as surviving SMI 32 IR cells amounted to about 1/3rd of their population following 0.05 or 0.1 mM kainate (Fig. 4A, B) without any significant improvement after riluzole administration regardless of the protocol used (Fig. 4A, C).

DISCUSSION

The principal findings of the present report are that, despite the small sample of spinal cord preparations tested, riluzole could not adequately contrast the excitotoxicity evoked by moderate concentrations of kainate and that no functional recovery of locomotor network activity was obtained 24 h later. The poor histological and functional outcome was similar when riluzole was applied for 3 or 24 h after the excitotoxic stimulation. Furthermore, the present data indicated that the long-lasting neurodepressant effect of riluzole could cloud the interpretation of any functional protection by this drug.

Riluzole effects on network histology

Riluzole is a rare example of a drug clinically licensed to treat ALS motoneuron degeneration, even if clinical benefits are rather small and time-limited. A large number of studies that have been performed to clarify if riluzole could combat various types of neurodegeneration, have produced mixed results depending on the models used *in vivo* (Verhave et al., 2012) or *in vitro* (Rammes et al., 2008; Chang et al., 2010; Mazzone and Nistri, 2011).

Using a standard protocol for inducing excitotoxicity with transient application of kainate (Taccola et al., 2008) followed by 24 h riluzole administration, we observed a very limited fall in pyknosis and modest neuronal preservation. Numbers of surviving neurons did not closely match the number of pyknotic cells in the gray matter because there is a region-specific disparity in the ratio of neurons to the global cell number (Cifra et al., 2011a). Nonetheless, any beneficial action by riluzole taken as either lessened pyknosis or larger neuronal numbers was clearly modest. It is noteworthy that, in terms of cell protection, there was little difference between the outcome following either 24 or 3 h riluzole application (see Figs. 1C and 3B). This observation suggests that the administration timeframe of the present study was not critical to determine the extent of cell survival and could be exploited for functional studies as explained below.

With this continuous drug administration schedule it was impossible to observe fictive locomotion, which was persistently inhibited by riluzole per se, and whose action could not be washed out within the time frame of the present experiments. We cannot exclude that the small

neuroprotection by riluzole might bring some functional benefit at much later times after riluzole washout: this possibility will require the use of an experimental preparation with more prolonged survival *in vitro*, a goal currently not available. Nonetheless, it seems unlikely that this slight histological improvement produced by riluzole might subsequently restore locomotor network output because the number of surviving neurons (including motoneurons) remained significantly lower than the one constituting the minimal network membership to express locomotor cycles (Kuzhandaivel et al., 2011).

The histological protection by riluzole was comparatively less than the result obtained with organotypic spinal slices (Mazzone and Nistri, 2011); we suspect that the drug penetration through the thicker tissue of the isolated spinal cord might have been relatively slower and, thus, less effective to contrast kainate toxicity. In support of this notion, we observed a delayed depression of fictive locomotion by riluzole whose effect on spinal synaptic transmission is typically slow (Tazerart et al., 2007). Indeed, slightly better histological neuroprotection was detected when riluzole was co-applied with kainate. This protocol is, of course, a very unsuitable model of human SCI treatment which, even under the most favorable conditions, starts with some delay following injury. Nonetheless, this observation suggests the desirability of implementing a neuroprotective strategy to combat excitotoxicity soon after the primary insult.

Electrophysiology of locomotor networks in the presence of riluzole

As the peak plasma concentration of riluzole in man is in the low micromolar range (Groeneveld et al., 2001; Abbara et al., 2011; Bellingham, 2011), our experiments mainly used 5 μM of this agent (trebling its concentration actually produced no further benefit). When this concentration was applied for 3 h, good recovery of fictive locomotion and spinal reflexes was observed 24 h later. Since riluzole is a liposoluble compound, its pharmacokinetic properties probably determined its ability to permeate through cell membranes and its slow elimination. Nevertheless, as the excitotoxic action by kainate strongly develops during the first 2–3 h after its wash, we tested whether 3 h application of riluzole could be sufficient (via inhibition of glutamate release and of the persistent sodium current; see reviews by Bellingham, 2011; Cifra et al., 2012b) to contrast the deleterious effect of kainate. This protocol failed to restore fictive locomotion and did not improve synaptic reflexes, or disinhibited bursting. The only significant functional gain was the improved regularity of these bursts, a result suggesting a modest enhancement in network spread of excitation, far away from a functional recovery. This observation accords with the reported improvement in disinhibited bursting by riluzole application to organotypic slice cultures (Yvon et al., 2007; Czarnecki et al., 2008), and suggests that the riluzole ability to block the persistent sodium current (Theiss et al., 2007) and, therefore, the kainate-mediated neuronal excitation spreading through the spinal networks, was presumably inadequate to prevent excitotoxic damage. Indeed, we have recently observed that 24 h intense electrical discharges have no negative impact on locomotor network function (Nasrabady et al., 2012), implying that neuronal damage was not closely related to abnormal firing activity. It seems likely that, in the rat spinal cord *in vitro*, excitotoxic death was caused by the direct action of kainate on neurons.

CONCLUSIONS

Even a moderate excitotoxic challenge evoked by kainate had a profound negative impact on network histology and locomotor-like patterns of the rat spinal cord *in vitro*. These phenomena could not be adequately contrasted by riluzole, despite various drug regimen protocols. A clear outcome of the present studies is the demonstration that even small neuronal losses have very deleterious consequences on locomotor network function. Our current results differ from a previous report on brainstem motoneurons that could be well protected by riluzole (Cifra et al., 2011) and raise the possibility of cell-specific vulnerability to an excitotoxic challenge. In support of this notion are the clinical observations that, although riluzole improves ALS survival by a short period of time only, bulbar-onset patients appear to particularly benefit from riluzole (Traynor et al., 2003; Zoccolella et al., 2007). This differential therapeutic effect of riluzole on ALS could not be attributed to disease stage and might be related to intrinsic diversity in the glutamate handling process between brainstem and spinal regions (Zoccolella et al., 2007).

From recent data on potential neuroprotection of spinal networks *in vitro*, it is apparent that excitotoxicity is rather resistant to various drugs with distinct modes of action. Even block of ionotropic glutamate receptors may be insufficient to contrast kainate-evoked excitotoxicity (Margaryan et al., 2010). Partial histological and functional protection is obtainable with PJ-34, a drug which inhibits lethal intracellular signaling associated with cell death (Nasrabady et al., 2011b) and that also, paradoxically, inhibits glutamate uptake (Nasrabady et al., 2012). One hypothesis is that excitotoxic damage develops so rapidly that contrasting it is a hard task, especially when dealing with drugs that have slow pharmacokinetic properties or are administered with a certain delay. Perhaps a more attractive possibility would be to pharmacologically boost intrinsic autoregulatory mechanisms that may constrain excitotoxicity via metabotropic glutamate receptor activation (Niswender and Conn, 2010) or release of endocannabinoids (Alger and Kim, 2011).

REFERENCES

Abbara C, Estournet B, Lacomblez L, Lelièvre B, Ouslimani A, Lehmann B, Viollet L, Barois A, Diquet B (2011) Riluzole pharmacokinetics in young patients with spinal muscular atrophy. Br J Clin Pharmacol 71:403–410.

Alger BE, Kim J (2011) Supply and demand for endocannabinoids. Trends Neurosci 34:304–315.

Beghi E, Chiò A, Couratier P, Esteban J, Hardiman O, Logroscino G, Millul A, Mitchell D, Preux PM, Pupillo E, Stevic Z, Swingler R, Traynor BJ, Van den Berg LH, Veldink JH, Zoccolella S, Eurals Consortium (2011) The epidemiology and treatment of ALS: focus on the heterogeneity of the disease and critical appraisal of therapeutic trials. Amyotroph Lateral Scler 12:1–10.

Bellingham MC (2011) A review of the neural mechanisms of action and clinical efficiency of riluzole in treating amyotrophic lateral sclerosis: what have we learned in the last decade? CNS Neurosci Ther 17:4–31.

Bracci E, Ballerini L, Nistri A (1996a) Spontaneous rhythmic bursts induced by pharmacological block of inhibition in lumbar motoneurons of the neonatal rat spinal cord. J Neurophysiol 75:640–647.

Bracci E, Ballerini L, Nistri A (1996b) Localization of rhythmogenic networks responsible for spontaneous bursts induced by strychnine and bicuculline in the rat isolated spinal cord. J Neurosci 16:7063–7076.

Bracci E, Beato M, Nistri A (1997) Afferent inputs modulate the activity of a rhythmic burst generator in the rat disinhibited spinal cord in vitro. J Neurophysiol 77:3157–3167.

Butt SJ, Lebret JM, Kiehn O (2002) Organization of left–right coordination in the mammalian locomotor network. Brain Res Rev 40:107–117.

Cadotte DW, Fehlings MG (2011) Spinal cord injury: a systematic review of current treatment options. Clin Orthop Relat Res 469:732–741.

Cazalets JR, Sqalli-Houssaini Y, Clarac F (1992) Activation of the central pattern generators for locomotion by serotonin and excitatory amino acids in neonatal rat. J Physiol 455:187–204.

Chang G, Guo Y, Jia Y, Duan W, Li B, Yu J, Li C (2010) Protective effect of combination of sulforaphane and riluzole on glutamate-mediated excitotoxicity. Biol Pharm Bull 33:1477–1483.

Cheah BC, Vucic S, Krishnan AV, Kiernan MC (2010) Riluzole, neuroprotection and amyotrophic lateral sclerosis. Curr Med Chem 17:1942–1959.

Cifra A, Nani F, Nistri A (2011) Respiratory motoneurons and pathological conditions: lessons from hypoglossal motoneurons challenged by excitotoxic or oxidative stress. Respir Physiol Neurobiol 179:89–96.

Cifra A, Mazzone GL, Nani F, Nistri A, Mladinic M (2012a) Postnatal developmental profile of neurons and glia in motor nuclei of the brainstem and spinal cord, and its comparison with organotypic slice cultures. Dev Neurobiol 72:1140–1160.

Cifra A, Mazzone GL, Nistri A (2012b) Riluzole: what it does to spinal and brainstem neurons and how it does it. Neuroscientist. http://dx.doi.org/10.1177/1073858412444932.

Clarac F, Brocard F, Vinay L (2004) The maturation of locomotor networks. Prog Brain Res 143:57–66.

Czarnecki A, Magloire V, Streit J (2008) Local oscillations of spiking activity in organotypic spinal cord slice cultures. Eur J Neurosci 27:2076–2088.

DeVivo MJ (2012) Epidemiology of traumatic spinal cord injury: trends and future implications. Spinal cord 50:365–372.

Doble A (1999) The role of excitotoxicity in neurodegenerative disease: implications for therapy. Pharmacol Ther 81:163–221.

Fumagalli E, Funicello M, Rauen T, Gobbi M, Mennini T (2008) Riluzole enhances the activity of glutamate transporters GLAST, GLT1 and EAAC1. Eur J Pharmacol 578:171–176.

Grillner S (2003) The motor infrastructure: from ion channels to neuronal networks. Nat Rev Neurosci 4:573–586.

Groeneveld GJ, van Kan HJ, Toraño JS, Veldink JH, Guchelaar HJ, Wokke JH, van den Berg LH (2001) Inter- and intraindividual variability of riluzole serum concentrations in patients with ALS. J Neurol Sci 191:121–125.

Hall ED, Springer JE (2004) Neuroprotection and acute spinal cord injury: a reappraisal. NeuroRx 1:80–100.

Kiehn O (2006) Locomotor circuits in the mammalian spinal cord. Annu Rev Neurosci 29:279–306.

Kiehn O, Kjaerulff O (1998) Distribution of central pattern generators for rhythmic motor outputs in the spinal cord of limbed vertebrates. Ann N Y Acad Sci 860:110–129.

Kjaerulff O, Kiehn O (1996) Distribution of networks generating and coordinating locomotor activity in the neonatal rat spinal cord in vitro: a lesion study. J Neurosci 16:5777–5794.

Kuzhandaivel A, Nistri A, Mladinic M (2010) Kainate-mediated excitotoxicity induces neuronal death in the rat spinal cord in vitro via a PARP-1 dependent cell death pathway (Parthanatos). Cell Mol Neurobiol 30:1001–1012.

Kuzhandaivel A, Nistri A, Mazzone GL, Mladinic M (2011) Molecular mechanisms underlying cell death in spinal networks in relation to locomotor Activity After Acute Injury in vitro. Front Cell Neurosci 5:9.

Kwon BK, Okon E, Hillyer J, Mann C, Baptiste D, Weaver LC, Fehlings MG, Tetzlaff W (2011) A systematic review of non-invasive pharmacologic neuroprotective treatments for acute spinal cord injury. J Neurotrauma 28:1545–1588.

Lau A, Tymianski M (2010) Glutamate receptors, neurotoxicity and neurodegeneration. Pflugers Arch 460:525–542.

Margaryan G, Mladinic M, Mattioli C, Nistri A (2009) Extracellular magnesium enhances the damage to locomotor networks produced by metabolic perturbation mimicking spinal injury in the neonatal rat spinal cord in vitro. Neuroscience 163:669–682.

Margaryan G, Mattioli C, Mladinic M, Nistri A (2010) Neuroprotection of locomotor networks after experimental injury to the neonatal rat spinal cord in vitro. Neuroscience 165:996–1010.

Mazzone GL, Margaryan G, Kuzhandaivel A, Nasrabady SE, Mladinic M, Nistri A (2010) Kainate-induced delayed onset of excitotoxicity with functional loss unrelated to the extent of neuronal damage in the in vitro spinal cord. Neuroscience 168:451–462.

Mazzone GL, Nistri A (2011) Delayed neuroprotection by riluzole against excitotoxic damage evoked by kainate on rat organotypic spinal cord cultures. Neuroscience 190:318–327.

Nasrabady SE, Kuzhandaivel A, Mladinic M, Nistri A (2011a) Effects of 6(5H)-phenanthridinone, an inhibitor of poly(ADP-ribose)polymerase-1 activity (PARP-1), on locomotor networks of the rat isolated spinal cord. Cell Mol Neurobiol 31:503–508.

Nasrabady SE, Kuzhandaivel A, Nistri A (2011b) Studies of locomotor network neuroprotection by the selective poly(ADP-ribose) polymerase-1 inhibitor PJ-34 against excitotoxic injury to the rat spinal cord in vitro. Eur J Neurosci 33:2216–2227.

Nasrabady SE, Kuzhandaivel A, Nistri A (2012) Unusual increase in lumbar network excitability of the rat spinal cord evoked by the PARP-1 inhibitor PJ-34 through inhibition of glutamate uptake. Neuropharmacology 63:41–426.

Niswender CM, Conn PJ (2010) Metabotropic glutamate receptors: physiology, pharmacology, and disease. Annu Rev Pharmacol Toxicol 50:295–322.

Nógrádi A, Szabó A, Pintér S, Vrbová G (2007) Delayed riluzole treatment is able to rescue injured rat spinal motoneurons. Neuroscience 144:431–438.

Norenberg MD, Smith J, Marcillo A (2004) The pathology of human spinal cord injury: defining the problems. J Neurotrauma 21:429–440.

Park E, Velumian AA, Fehlings MG (2004) The role of excitotoxicity in secondary mechanisms of spinal cord injury: a review with an emphasis on the implications for white matter degeneration. J Neurotrauma 21:754–774.

Rammes G, Zieglgänsberger W, Parsons CG (2008) The fraction of activated N-methyl-D-aspartate receptors during synaptic transmission remains constant in the presence of the glutamate release inhibitor riluzole. J Neural Transm 115:1119–1126.

Rowland JW, Hawryluk GW, Kwon B, Fehlings MG (2008) Current status of acute spinal cord injury pathophysiology and emerging therapies: promise on the horizon. Neurosurg Focus 25:E2:1–17.

Schwab JM, Brechtel K, Mueller CA, Failli V, Kaps HP, Tuli SK, Schluesener HJ (2006) Experimental strategies to promote spinal cord regeneration–an integrative perspective. Prog Neurobiol 78:91–116.

Schwartz G, Fehlings MG (2001) Evaluation of the neuroprotective effects of sodium channel blockers after spinal cord injury: improved behavioral and neuroanatomical recovery with riluzole. J Neurosurg 94(2 Suppl):245–256.

Schwartz G, Fehlings MG (2002) Secondary injury mechanisms of spinal cord trauma: a novel therapeutic approach for the management of secondary pathophysiology with the sodium channel blocker riluzole. Prog Brain Res 137:177–190.

Song JH, Huang CS, Nagata K, Yeh JZ, Narahashi T (1997) Differential action of riluzole on tetrodotoxin-sensitive and tetrodotoxin-resistant sodium channels. J Pharmacol Exp Ther 282:707–714.

Taccola G, Marchetti C, Nistri A (2004) Modulation of rhythmic patterns and cumulative depolarization by group I metabotropic glutamate receptors in the neonatal rat spinal cord in vitro. Eur J Neurosci 19:533–541.

Taccola G, Nistri A (2006a) Fictive locomotor patterns generated by tetraethylammonium application to the neonatal rat spinal cord in vitro. Neuroscience 137:659–670.

Taccola G, Nistri A (2006b) Oscillatory circuits underlying locomotor networks in the rat spinal cord. Crit Rev Neurobiol 18:25–36.

Taccola G, Margaryan G, Mladinic M, Nistri A (2008) Kainate and metabolic perturbation mimicking spinal injury differentially contribute to early damage of locomotor networks in the in vitro neonatal rat spinal cord. Neuroscience 155:538–555.

Taylor CP, Meldrum BS (1995) Na^+ channels as targets for neuroprotective drugs. Trends Pharmacol Sci 16:309–316.

Tazerart S, Viemari JC, Darbon P, Vinay L, Brocard F (2007) Contribution of persistent sodium current to locomotor pattern generation in neonatal rats. J Neurophysiol 98:613–628.

Theiss RD, Kuo JJ, Heckman CJ (2007) Persistent inward currents in rat ventral horn neurones. J Physiol 580:507–522.

Traynor BJ, Alexander M, Corr B, Frost E, Hardiman O (2003) An outcome study of riluzole in amyotrophic lateral sclerosis–a population-based study in Ireland, 1996–2000. J Neurol 250:473–479.

Traynor BJ, Bruijn L, Conwit R, Beal F, O'Neill G, Fagan SC, Cudkowicz ME (2006) Neuroprotective agents for clinical trials in ALS: a systematic assessment. Neurology 67:20–27.

Ufuk T, Ganesh S, Sigurd B (2005) Spine cord injury: an update. Semin Spine Surg 17:73–83.

van den Berg ME, Castellote JM, Mahillo-Fernandez I, de Pedro-Cuesta J (2010) Incidence of spinal cord injury worldwide: a systematic review. Neuroepidemiology 34:184–192.

Verhave PS, Jongsma MJ, Van Den Berg RM, Vanwersch RA, Smit AB, Philippens IH (2012) Neuroprotective effects of riluzole in early phase Parkinson's disease on clinically relevant parameters in the marmoset MPTP model. Neuropharmacology 62:1700–1707.

Wahl F, Renou E, Mary V, Stutzmann JM (1997) Riluzole reduces brain lesions and improves neurological function in rats after a traumatic brain injury. Brain Res 756:247–255.

Wokke J (1996) Riluzole. Lancet 348:795–799.

Yvon C, Czarnecki A, Streit J (2007) Riluzole-induced oscillations in spinal networks. J Neurophysiol 97:3607–3620.

Zoccolella S, Beghi E, Palagano G, Fraddosio A, Guerra V, Samarelli V, Lepore V, Simone IL, Lamberti P, Serlenga L, Logroscino G, SLAP registry (2007) Riluzole and amyotrophic lateral sclerosis survival: a population-based study in Southern Italy. Eur J Neurol 1:262–268.

Discussion

   The principal findings of this PhD project provide new information about the downstream pathways activated by excitotoxic injury in the neonatal rat isolated spinal cord. The in vitro model of excitotoxic spinal cord injury led us to test the potential neuroprotective effect of PARP-1 inhibitors and different pharmacological agents which are supposed to control the hyper-excitation state. Although, the in vitro spinal cord model has some limitations because of tissue immaturity (Cifra et al., 2012) and lack of vascular circulation supply, it is a useful model to study the basic mechanisms controlling CPG rhythmogenesis and looking at the network membership involved in locomotor program generation.

The details of our novel results are discussed in the attached papers; however, the following session summarizes the main findings of the present research project and tries to address the similarities and differences with the findings of other studies.

1. Functional deficits due to excitotoxicity

Kainate is a potent non-degradable analog of glutamate which has strong excitatory effect on spinal neurons (Constanti and Nistri, 1976, Farooqui et al., 2001, Wang et al., 2005). Electrophysiological recordings suggested that there was a critical threshold for excitotoxicity mediated by kainate which could fully suppress fictive locomotion. Using 10 µM kainate resulted in typical fictive locomotion (induced by NMDA plus 5-HT) 24 h after the insult although with smaller amplitude and slower periodicity than sham preparations. Higher concentrations (≥50 µM) of kainate produced consistent disappearance of fictive locomotion. These data show the dose-related excitotoxic effect of kainate and are in accordance with previous studies which have shown that neonatal rat spinal cord can tolerate concentration of kainate below 10 µM in terms of locomotor cycle activity (Cazalets et al., 1992). Kainate application induced a dose-dependent ventral root depolarization in all cases. When fictive locomotion had irreversibly disappeared (50 µM), VR depolarization was almost half of the maximum depolarization induced by 1 mM kainate. However, the basic functional activity of spinal cord was still present on the second day when induced by application of strychnine and bicuculline. Burst amplitude was the only factor which differed after different kainate concentrations (the lowest with the highest kainate concentration). However, disinhibited bursting had slower, irregular periodicity even by using 10 µM kainate in comparison with the one normally observed in control (Taccola et al., 2008, Margaryan et al., 2010).

Excitotoxicity also affected the ability of spinal cord to integrate the afferent inputs. Application of 1 mM kainate extensively decreased the peak amplitude of mono and polysynaptic reflex response to DR electrical stimulation. Increasing the intensity of the stimulus failed to increase the amplitude values to the values closer to sham preparations after 24 h. Similar to previous studies, induction of fictive locomotion with trains of electrical pulses also failed (Taccola et al., 2008). Even with decreasing kainate concentration to 50 µM, the reflex response amplitude was much smaller than sham preparations. Fictive locomotion could not be elicited by trains of DR pulses.

2. Structural deficits due to excitotoxicity

As previous studies have described, in the model of in vitro spinal cord, excitotoxic insult appears with pyknotic nuclei which is a term used for cells undergoing nuclei chromatin condensation (Tacclola et al., 2008, Margaryan et al, 2009, Kuzhandaivel et al., 2010). In present project (in collaboration with Dr. Kuzhandaivel), we observed a dose-dependent increase in pyknosis appearance in the dorsal region of grey matter. It was less intense in the central and ventral grey matter. The same was detected for ventrolateral white matter. These data were similar to the data obtained with this model previously reported by our group (Tacclola et al., 2008, Margaryan et al, 2009, Kuzhandaivel et al., 2010). Glial cells in grey and white matter did not develop pyknosis in first 24 h (Kuzhandaivel et al., 2010), although they have been reported to be sensitive to excitotoxicity (McDonald et al., 1998, Deng et al., 2004).

The total number of neurons stained by NeuN (neuronal nucleus marker) was counted in three regions of grey matter. Twenty four hours after kainate application (≥ 50 µM; 1 h) NeuN positive cells were significantly decreased in dorsal and central grey matter in comparison with sham. In accordance with the data obtained from DAPI staining (pyknosis), global number of neurons was less severely decreased by kainate in ventral horn. The values of surviving neurons grew as the kainate concentration was smaller and with 50µM kainate, the neuronal counts in the ventral horn were similar to sham preparations. Our data confirm the result of previous studies indicating the presence of the highest density of kainate receptors in the dorsal grey matter (Tolle et al., 1993).

Motoneurons which make up a relatively small number of cells and are located in the ventral horn of the spinal cord are highly sensitive to excitotoxic damage (Taccola et al., 2010). They lack certain calcium binding proteins and remain vulnerable to the consequences of calcium overload (Dekkers et al., 2004). Their labeling with an antibody against nonphosphorylated form of motoneuronal cytoplasmic neurofilament (SMI 32) showed drastical decrease in motoneuron number after 24 h by using different concentrations of kainate. Our data were in analogy with those previously obtained with 1 mM kainate (Taccola et al., 2008).

Using spinal organotypic cultures (experiments performed by my colleague Dr. Mazzone) not only confirmed the destructive effect of excitotoxicity on motoneurons and neuronal survival, but also provided the demonstration of the time-related rise in the pyknosis. The result indicated a delayed onset of excitotoxicity with spinal cell loss dependent on kainate concentration.

3. Hyperactivity of PARP-1 due to excitotoxicity

The newly discovered cell death pathway "Parthanatos" (Eliasson et al., 1997, Endres et al., 1997, Andrabi et al., 2006) is thought to be related to hyperactivation of PARP-1 (Kuzhandaivel et al., 2010). PARP-1 is mentioned as a major cause of neuronal damage after spinal cord injury (Scott et al., 2004, Genovese et al., 2005, Wu et al., 2009). Measuring PARP-1 product (PAR) led us to estimate the enzyme activity after excitotoxic insult. Four hours after 1 mM kainate washout a large increment in PAR level was detected which was approximately three times higher than in sham preparations. The lower concentration of kainate (50 µM) evoked smaller level of PAR. Apoptosis inducing factor (AIF) was also measured as the PARP-1 translocation effector. As it is translocated from stressed mitochondria to the cell nucleus (Li et al., 2010), we observed that the mature form of AIF translocated to nucleus in accordance with previous studies following PARP-1 activation (Wang et al., 2009). We demonstrated that kainate could make PARP-1 hyper-activated which was indicated by the strong tissue PAR production and this phenomenon was significantly blocked by PARP-1 inhibitor PJ-34.

4. Poor outcome after PHE application

Irreversible loss of fictive locomotion (by application of 1 mM kainate) was not contrasted in preparations treated with PHE which was started after kainate washout or 30 min after kainate application. The mono and polysynaptic response values were also the same as in the group injured with kainate. The period and amplitude of disinhibited bursting remained

unchanged in the group treated with PHE. However, the neuronal loss (stained by DAPI) in the most sensitive region to excitotoxicity (dorsal horn) induced by kainate seemed to be decreased and the total number of neurons (NeuN staining positive cells) was improved after PHE application. In general, we observed that, although there was a significant neuroprotection in terms of histology, it could not block the functional insult to CPG and could not contrast the excitotoxic damage. We assume that the poor functional outcome of PHE was due to the early hyperactivity of PARP-1 which is likely to start even before the earliest application of the drug. In addition, PHE is a relatively non-selective blocker of PARP-1 (Banasik et al., 1992, Li et al., 2001). Therefore, we moved forward to use a more selective inhibitor of PARP-1, namely PJ-34.

5. Neuroprotective effects of PJ-34

5.1. PJ-34 effectiveness

Our experiments (performed by Dr. Kuzhandaivel) showed that kainate evoked PARP-1 hyperactivation was best inhibited by 60 µM PJ-34 application. Reduced PAR levels were the evidence for the effectiveness of PJ-34 against excitotoxic effect of kainate (50 µM or 1mM). Enhanced AIF translocation induced by 1 mM kainate was also significantly reduced by PJ-34. When excitotoxicity was moderate (50 µM kainate), AIF translocation was completely suppressed by PJ-34. Thus, our results confirmed the previous studies data on cultures indicating that PAR can be fully suppressed by application of PJ-34 (Mazzone and Nistri, 2011b).

5.2. Functional effect of PJ-34

Synaptic transmission, cumulative depolarization, fictive locomotion and disinhibited bursting were checked in order to investigate the functional effectiveness of PJ-34. The very dramatic decrease of polysynaptic response 24 h after strong excitotoxic injury (1 mM

kainate) was partly counteracted by PJ-34 in terms of amplitude and area. Much less successful was the protection of cumulative depolarization induced by train of stimuli. Despite the fact that integration of afferent inputs was not retained, disinhibited bursting was expressed with larger amplitude in comparison with 1 mM kainate alone. However, the burst periodicity remained unchanged.

The weaker excitotoxic insult (50 µM kainate) produced less spinal cord damage than the strong one and the electrophysiological deficit was smaller than the one produced by 1 mM kainate. Therefore, it was more efficaciously counteracted by PJ-34. The response amplitude and area of polysynaptic response were both significantly enhanced by PJ-34 when compared with those of kainate treated preparations. Despite the sparse superimposed alternating oscillations emerging in preparations treated with 24 h PJ-34, the cumulative depolarization value was not improved. It could be due to the damage of dorsal horn cells where polysynaptic sensory inputs are integrated into locomotor activity (Baranauskas and Nistri, 1998). Thus, the locomotor-like patterns produced by sensory afferent stimulation were very sensitive to excitotoxic damage (Taccola et al., 2008), even by a small dose of kainate, and could not be fully restored by PJ-34.

Interestingly, the combination of NMDA and 5-HT was able to generate fictive locomotion in more than half of the preparations 24 h after PJ-34 application. The neuroprotection towards chemically-induced fictive locomotion was observed in 6 out of 11 preparations. However, in such preparations the cycle period was significantly slower than sham values.

5.3. Histological effect of PJ-34

In five preparations which did not show fictive locomotion, higher values of pyknosis (DAPI staining) were observed in dorsal and central regions in comparison with those (6 preparations) retaining fictive locomotion. NeuN staining demonstrated that neuronal population of the dorsal horn was better preserved in preparations retaining fictive locomotion. PJ-34 systematically protected motoneuron numbers from kainate neurotoxicity. It was notable that the application of PJ-34 after 100 or 50 µM kainate yielded similar motoneuron numbers, regardless of ability to express fictive locomotion. These data implied

that protecting motoneurons was important, but, when histological evidence for excitotoxic damage was quite small, the functional outcome in terms of fictive locomotion should have depended on the preservation of other cell types other than motoneurons.

5.4. Effect of PJ-34 on network excitability

In the course of our experiments, the observation of strong increase in network discharges during PJ-34 application led us to study the pharmacological effect of PJ-34 per se. It was also important to understand whether this drug could have some unexpected effects on neurons and glia.

Neurochemical data (performed by Dr. Milanese, University of Genoa) demonstrated that PJ-34 is a significant blocker of glutamate uptake with no action on GABA transport. Using different concentration of PJ-34 showed that, since this effect was also detected at micromolar PJ-34 concentrations, this phenomenon might occur with pharmacological doses rather than toxic doses of the drug.

The earliest effect of PJ-34 appeared with enhancement of glutamate-mediated monosynaptic reflexes. It demonstrated that glutamate uptake was an important process to regulate excitatory transmission. Weng et al. (2006) also reported that glutamate transporters regulate baseline excitability and responses of dorsal horn neurons to peripheral stimulation, and suggested that dysfunction of glutamate transporters may contribute to certain types of pathological pain (Weng et al., 2006).

Polysynaptic reflexes remained unchanged perhaps because of their heterogeneous presynaptic origin. On the other hand, the smaller amplitude of cumulative depolarization was probably due to steadily-depolarized neurons which were still capable of generating a standard series of alternating oscillations. Glutamate uptake block by PJ-34 was relatively rapid; however, the intensification of spontaneous activity recorded from VRs was gradual. After 24 h, despite sustained washout of PJ-34, the strong discharges continued suggesting that spinal circuits had become hyper-excitable.

While spontaneous events could still emerge in the interval between electrically stimulated bursts in the presence of GABA and glycine, blocking the discharges by APV and CNQX

demonstrated that they were fully dependent on ionotropic glutamate receptor activation. This is in accordance with the neuronal excitability induced by spillover of extracellular glutamate due to impaired glutamate uptake in the rat spinal dorsal horn (Nie and Weng, 2009). We propose that application of PJ-34 biased spinal network activity into excitation over inhibition as shown by increased random discharges dependent on glutamatergic transmission. However, evoked hyperexcitability of spinal cord did not exert a deleterious action on fictive locomotion nor any loss of neurons or glia in the spinal cord. Although excitotoxic damage elicited by impaired glutamate uptake is thought to be a major process to damage neurons (Kim et al., 2011) and in particular motoneurons (Foran and Trotti, 2009), the structural resistance to build-up of extracellular glutamate in our model can be explained by activation of compensatory process preventing from toxicity such as activation of metabotropic glutamate receptors (proposed for brain network; Huang et al., 2004, Hartmann et al., 2008, Potier et al., 2010). Metabotropic glutamate receptors are widely expressed in the rat spinal cord where they can regulate synaptic transmission and reflexes (Marchetti et al., 2003, Nistri et al., 2006). In addition, it is shown that higher glutamatergic signaling in the rat hippocampus induces release of endocannabinoids from postsynaptic cells to retrogradely depress excess neurotransmitter release (El Manira et al., 2008, Hofmann et al., 2008, Nahir et al., 2010) which can be another explanation for non-toxic effect of moderate block of glutamate transport in our experiments. Result of another study (Tovar et al., 2009) supports our result by reporting that prolonged elevation of extracellular glutamate due to its transport blockade in vivo is safe for, motoneurons, while direct activation of glutamate receptors is neurotoxic.

6. Poor functional outcome of riluzole

Since our goal was to protect the locomotor network against excitotoxicity, we chose riluzole which can attenuate the presynaptic glutamate release and can also reduce persistent sodium current (Bellingham, 2011). The positive results obtain form using hypoglossal motoneurons (Cifra et al., 2011) and injured motoneurons after ventral root avulsion (Nogradi et al., 2007) led us to try this agent with our experimental model.

Twenty four hours application of riluzole (5 μM) after kainate washout did not help locomotor activity restoration. Fictive locomotion never returned and VR reflex response amplitude remained very small. Since riluzole depresses presynaptic glutamate release (beside the block of voltage-dependent sodium channels), we assumed that the long-lasting riluzole application had depressed synaptic reflexes regardless of kainate evoked toxicity. Thus, we tested the effect of riluzole per se on network activity. Fictive locomotion was disrupted after riluzole application 24 h which confirmed the result of another study using 10 μM riluzole (Tazerart et al., 2007). However, when the time course of riluzole application per se was decreased to 3 h, after 24 h washout, fictive locomotion was observed with the same characteristics as sham.

Inducing moderate excitotoxic insult (50 μM kainate) followed by 3 h riluzole application showed that, except improvement in the regularity of disinhibited busrting (in accordance with other studies; (Yvon et al., 2007, Czarnecki et al., 2008), other network activities remained unchanged in comparison with the group injured by kainate and there was just a small difference between the histological outcome following 24 or 3 h riluzole application (histological experiment performed by Dr. Samano).

Therefore, in the neonatal isolated spinal cord, riluzole could not protect neuronal networks from excitotoxicity evoked by moderate concentrations of kainate, even if there are several studies indicating the positive effect of riluzole in combating various types of neurodegeneration (Rammes et al., 2008, Chang et al., 2010, Mazzone and Nistri, 2011a, Verhave et al., 2012). Furthermore, the long-lasting neurodepressant effect of riluzole could obscure any functional neuroprotection of this drug in our model. One of the possible reasons for the different histological result in our model and the good result in organotypic culture of the spinal cord (Mazzone and Nistri, 2011a) is that the drug penetration into the entire tissues is slower than in culture and results in less effectiveness of riluzole. In fact in our model, the functional depression due to riluzole was delayed in comparison with previous studies (Tazerart et al., 2007).

Conclusions

Even a moderate excitotoxic insult can affect strongly the spinal locomotor network in terms of function and histology. The preservation of locomotor function after excitotoxic challenge should be directed toward identified biochemical targets which play the important role in the cell death mechanisms. On the other hand, the timing of neuroprotective agent application also plays a very important role in controlling the damage. Survival of central and dorsal grey matter is essential as much as motoneuron protection in order to achieve the goal of locomotor function preservation. The prolonged electrical discharges induced by changes in synaptic glutamate reuptake can result in a very strong network discharges which surprisingly did not have any neurotoxic consequence at least for 24 h on neurons and glia in neonatal rat isolated spinal cord. Thus, circuit damage in the spinal cord is probably caused by deranged intracellular signaling rather than simple over-excitation for a long time.

References

Abdelkarim GE, Gertz K, Harms C, Katchanov J, Dirnagl U, Szabo C, Endres M (2001) Protective effects of PJ34, a novel, potent inhibitor of poly(ADP-ribose) polymerase (PARP) in in vitro and in vivo models of stroke. Int J Mol Med 7:255-260.

Acton PA, Farley T, Freni LW, Ilegbodu VA, Sniezek JE, Wohlleb JC (1993) Traumatic spinal cord injury in Arkansas, 1980 to 1989. Archives of physical medicine and rehabilitation 74:1035-1040.

Anderson DK, Hall ED (1993) Pathophysiology of spinal cord trauma. Annals of emergency medicine 22:987-992.

Anderson DK, Means ED, Waters TR, Green ES (1982) Microvascular perfusion and metabolism in injured spinal cord after methylprednisolone treatment. Journal of neurosurgery 56:106-113.

Andrabi SA, Kim NS, Yu SW, Wang H, Koh DW, Sasaki M, Klaus JA, Otsuka T, Zhang Z, Koehler RC, Hurn PD, Poirier GG, Dawson VL, Dawson TM (2006) Poly(ADP-ribose) (PAR) polymer is a death signal. Proceedings of the National Academy of Sciences of the United States of America 103:18308-18313.

Bach-y-Rita P, Illis LS (1993) Spinal shock: possible role of receptor plasticity and non synaptic transmission. Paraplegia 31:82-87.

Banasik M, Komura H, Shimoyama M, Ueda K (1992) Specific inhibitors of poly(ADP-ribose) synthetase and mono(ADP-ribosyl)transferase. The Journal of biological chemistry 267:1569-1575.

Baptiste DC, Fehlings MG (2007) Update on the treatment of spinal cord injury. Prog Brain Res 161:217-233.

Baranauskas G, Nistri A (1995) Membrane potential oscillations of neonatal rat spinal motoneurons evoked by electrical stimulation of dorsal root fibres. The European journal of neuroscience 7:2403-2408.

Baranauskas G, Nistri A (1998) Sensitization of pain pathways in the spinal cord: cellular mechanisms. Progress in neurobiology 54:349-365.

Beato M, Nistri A (1999) Interaction between disinhibited bursting and fictive locomotor patterns in the rat isolated spinal cord. Journal of neurophysiology 82:2029-2038.

Behrmann DL, Bresnahan JC, Beattie MS (1994) Modeling of acute spinal cord injury in the rat: neuroprotection and enhanced recovery with methylprednisolone, U-74006F and YM-14673. Experimental neurology 126:61-75.

Bellingham MC (2011) A review of the neural mechanisms of action and clinical efficiency of riluzole in treating amyotrophic lateral sclerosis: what have we learned in the last decade? CNS neuroscience & therapeutics 17:4-31.

Berger NA (1985) Poly(ADP-ribose) in the cellular response to DNA damage. Radiat Res 101:4-15.

Berkowitz A (2004) Propriospinal projections to the ventral horn of the rostral and caudal hindlimb enlargement in turtles. Brain research 1014:164-176.

Bonnot A, Morin D (1998) Hemisegmental localisation of rhythmic networks in the lumbosacral spinal cord of neonate mouse. Brain research 793:136-148.

Bonnot A, Whelan PJ, Mentis GZ, O'Donovan MJ (2002a) Locomotor-like activity generated by the neonatal mouse spinal cord. Brain research Brain research reviews 40:141-151.

Bonnot A, Whelan PJ, Mentis GZ, O'Donovan MJ (2002b) Spatiotemporal pattern of motoneuron activation in the rostral lumbar and the sacral segments during locomotor-like activity in the neonatal mouse spinal cord. J Neurosci 22:RC203.

Bracci E, Ballerini L, Nistri A (1996) Localization of rhythmogenic networks responsible for spontaneous bursts induced by strychnine and bicuculline in the rat isolated spinal cord. J Neurosci 16:7063-7076.

Bracci E, Beato M, Nistri A (1997) Afferent inputs modulate the activity of a rhythmic burst generator in the rat disinhibited spinal cord in vitro. Journal of neurophysiology 77:3157-3167.

Bracken MB, Holford TR (1993) Effects of timing of methylprednisolone or naloxone administration on recovery of segmental and long-tract neurological function in NASCIS 2. Journal of neurosurgery 79:500-507.

Braughler JM, Hall ED (1982) Correlation of methylprednisolone levels in cat spinal cord with its effects on (Na+ + K+)-ATPase, lipid peroxidation, and alpha motor neuron function. Journal of neurosurgery 56:838-844.

Braughler JM, Hall ED (1983a) Lactate and pyruvate metabolism in injured cat spinal cord before and after a single large intravenous dose of methylprednisolone. Journal of neurosurgery 59:256-261.

Braughler JM, Hall ED (1983b) Uptake and elimination of methylprednisolone from contused cat spinal cord following intravenous injection of the sodium succinate ester. Journal of neurosurgery 58:538-542.

Braughler JM, Hall ED (1984) Effects of multi-dose methylprednisolone sodium succinate administration on injured cat spinal cord neurofilament degradation and energy metabolism. Journal of neurosurgery 61:290-295.

Burke D (1988) Spasticity as an adaptation to pyramidal tract injury. In: Waxman SG (ed.) Functional Recovery in Neurological Disease. Raven Press: New York, pp 401–423.

Burke RE, Degtyarenko AM, Simon ES (2001) Patterns of locomotor drive to motoneurons and last-order interneurons: clues to the structure of the CPG. Journal of neurophysiology 86:447-462.

Burkle A (2001) Poly(APD-ribosyl)ation, a DNA damage-driven protein modification and regulator of genomic instability. Cancer letters 163:1-5.

Buschges A, Scholz H, El Manira A (2011) New moves in motor control. Current biology : CB 21:R513-524.

Butt SJ, Harris-Warrick RM, Kiehn O (2002) Firing properties of identified interneuron populations in the mammalian hindlimb central pattern generator. J Neurosci 22:9961-9971.

Carroll RT, Galatsis P, Borosky S, Kopec KK, Kumar V, Althaus JS, Hall ED (2000) 4-Hydroxy-2,2,6,6-tetramethylpiperidine-1-oxyl (Tempol) inhibits peroxynitrite-mediated phenol nitration. Chem Res Toxicol 13:294-300.

Cazalets JR, Sqalli-Houssaini Y, Clarac F (1992) Activation of the central pattern generators for locomotion by serotonin and excitatory amino acids in neonatal rat. The Journal of physiology 455:187-204.

Chabrier PE, Auguet M, Spinnewyn B, Auvin S, Cornet S, Demerle-Pallardy C, Guilmard-Favre C, Marin JG, Pignol B, Gillard-Roubert V, Roussillot-Charnet C, Schulz J, Viossat I, Bigg D, Moncada S (1999) BN 80933, a dual inhibitor of neuronal nitric oxide synthase and lipid peroxidation: a promising neuroprotective strategy. Proceedings of the National Academy of Sciences of the United States of America 96:10824-10829.

Chang G, Guo Y, Jia Y, Duan W, Li B, Yu J, Li C (2010) Protective effect of combination of sulforaphane and riluzole on glutamate-mediated excitotoxicity. Biological & pharmaceutical bulletin 33:1477-1483.

Christensen MD, Everhart AW, Pickelman JT, Hulsebosch CE (1996) Mechanical and thermal allodynia in chronic central pain following spinal cord injury. Pain 68:97-107.

Christensen MD, Hulsebosch CE (1997) Chronic central pain after spinal cord injury. Journal of neurotrauma 14:517-537.

Christie KJ, Whelan PJ (2005) Monoaminergic establishment of rostrocaudal gradients of rhythmicity in the neonatal mouse spinal cord. Journal of neurophysiology 94:1554-1564.

Cifra A, Mazzone GL, Nani F, Nistri A, Mladinic M (2012) Postnatal developmental profile of neurons and glia in motor nuclei of the brainstem and spinal cord, and its comparison with organotypic slice cultures. Developmental neurobiology 72:1140-1160.

Cifra A, Nani F, Nistri A (2011) Riluzole is a potent drug to protect neonatal rat hypoglossal motoneurons in vitro from excitotoxicity due to glutamate uptake block. The European journal of neuroscience 33:899-913.

Cina C, Hochman S (2000) Diffuse distribution of sulforhodamine-labeled neurons during serotonin-evoked locomotion in the neonatal rat thoracolumbar spinal cord. J Comp Neurol 423:590-602.

Constanti A, Nistri A (1976) A comparative study of the effects of glutamate and kainate on the lobster muscle fibre and the frog spinal cord. British journal of pharmacology 57:359-368.

Cosi C, Suzuki H, Milani D, Facci L, Menegazzi M, Vantini G, Kanai Y, Skaper SD (1994) Poly(ADP-ribose) polymerase: early involvement in glutamate-induced neurotoxicity in cultured cerebellar granule cells. J Neurosci Res 39:38-46.

Cowley KC, Schmidt BJ (1997) Regional distribution of the locomotor pattern-generating network in the neonatal rat spinal cord. Journal of neurophysiology 77:247-259.

Crowe MJ, Bresnahan JC, Shuman SL, Masters JN, Beattie MS (1997) Apoptosis and delayed degeneration after spinal cord injury in rats and monkeys. Nature medicine 3:73-76.

Czarnecki A, Magloire V, Streit J (2008) Local oscillations of spiking activity in organotypic spinal cord slice cultures. The European journal of neuroscience 27:2076-2088.

D'Amours D, Desnoyers S, D'Silva I, Poirier GG (1999) Poly(ADP-ribosyl)ation reactions in the regulation of nuclear functions. The Biochemical journal 342 (Pt 2):249-268.

Dai X, Noga BR, Douglas JR, Jordan LM (2005) Localization of spinal neurons activated during locomotion using the c-fos immunohistochemical method. Journal of neurophysiology 93:3442-3452.

David KK, Andrabi SA, Dawson TM, Dawson VL (2009) Parthanatos, a messenger of death. Frontiers in bioscience : a journal and virtual library 14:1116-1128.

Dekkers J, Bayley P, Dick JR, Schwaller B, Berchtold MW, Greensmith L (2004) Over-expression of parvalbumin in transgenic mice rescues motoneurons from injury-induced cell death. Neuroscience 123:459-466.

Deng W, Wang H, Rosenberg PA, Volpe JJ, Jensen FE (2004) Role of metabotropic glutamate receptors in oligodendrocyte excitotoxicity and oxidative stress. Proceedings of the National Academy of Sciences of the United States of America 101:7751-7756.

Dimitrijevic MR, Gerasimenko Y, Pinter MM (1998) Evidence for a spinal central pattern generator in humans. Annals of the New York Academy of Sciences 860:360-376.

Dirnagl U, Iadecola C, Moskowitz MA (1999) Pathobiology of ischaemic stroke: an integrated view. Trends in neurosciences 22:391-397.

Ditunno JF, Little JW, Tessler A, Burns AS (2004) Spinal shock revisited: a four-phase model. Spinal cord 42:383-395.

Donnelly DJ, Popovich PG (2008) Inflammation and its role in neuroprotection, axonal regeneration and functional recovery after spinal cord injury. Experimental neurology 209:378-388.

El Manira A, Kyriakatos A, Nanou E, Mahmood R (2008) Endocannabinoid signaling in the spinal locomotor circuitry. Brain research reviews 57:29-36.

Eliasson MJ, Sampei K, Mandir AS, Hurn PD, Traystman RJ, Bao J, Pieper A, Wang ZQ, Dawson TM, Snyder SH, Dawson VL (1997) Poly(ADP-ribose) polymerase gene disruption renders mice resistant to cerebral ischemia. Nature medicine 3:1089-1095.

Eltorai IM (2003) Spinal Cord Medicine: Principles and practice. Lin VW, Cardenas DD, Cutter NC, et al., editors. Demos Medical Publishing. New York. pp 3-14.

Endres M, Wang ZQ, Namura S, Waeber C, Moskowitz MA (1997) Ischemic brain injury is mediated by the activation of poly(ADP-ribose)polymerase. Journal of cerebral blood flow and metabolism : official journal of the International Society of Cerebral Blood Flow and Metabolism 17:1143-1151.

Evans RH, Francis AA, Jones AW, Smith DA, Watkins JC (1982) The effects of a series of omega-phosphonic alpha-carboxylic amino acids on electrically evoked and excitant

amino acid-induced responses in isolated spinal cord preparations. British journal of pharmacology 75:65-75.

Faden AI (1997) Therapeutic approaches to spinal cord injury. Advances in neurology 72:377-386.

Faden AI, Salzman S (1992) Pharmacological strategies in CNS trauma. Trends in pharmacological sciences 13:29-35.

Faden AI, Stoica B (2007) Neuroprotection: challenges and opportunities. Archives of neurology 64:794-800.

Farooque M, Hillered L, Holtz A, Olsson Y (1996a) Changes of extracellular levels of amino acids after graded compression trauma to the spinal cord: an experimental study in the rat using microdialysis. Journal of neurotrauma 13:537-548.

Farooque M, Hillered L, Holtz A, Olsson Y (1996b) Effects of methylprednisolone on extracellular lactic acidosis and amino acids after severe compression injury of rat spinal cord. Journal of neurochemistry 66:1125-1130.

Farooqui AA, Yi Ong W, Lu XR, Halliwell B, Horrocks LA (2001) Neurochemical consequences of kainate-induced toxicity in brain: involvement of arachidonic acid release and prevention of toxicity by phospholipase A(2) inhibitors. Brain research Brain research reviews 38:61-78.

Fehlings MG, Tator CH, Linden RD (1989) The effect of nimodipine and dextran on axonal function and blood flow following experimental spinal cord injury. Journal of neurosurgery 71:403-416.

Foran E, Trotti D (2009) Glutamate transporters and the excitotoxic path to motor neuron degeneration in amyotrophic lateral sclerosis. Antioxidants & redox signaling 11:1587-1602.

Fuortes MG, Nelson PG (1963) Strychnine: its action on spinal motoneurons of cats. Science 140:806-808.

Gabbay H, Delvolve I, Lev-Tov A (2002) Pattern generation in caudal-lumbar and sacrococcygeal segments of the neonatal rat spinal cord. Journal of neurophysiology 88:732-739.

Genovese T, Mazzon E, Muia C, Patel NS, Threadgill MD, Bramanti P, De Sarro A, Thiemermann C, Cuzzocrea S (2005) Inhibitors of poly(ADP-ribose) polymerase modulate signal transduction pathways and secondary damage in experimental spinal cord trauma. The Journal of pharmacology and experimental therapeutics 312:449-457.

Gordon IT, Whelan PJ (2006) Deciphering the organization and modulation of spinal locomotor central pattern generators. J Exp Biol 209:2007-2014.

Graham-Brown T (1911) The intrinsic factors in the act of progression in the mammal. Proc R Soc Lond 84:308-319.

Graziani G, Szabo C (2005) Clinical perspectives of PARP inhibitors. Pharmacol Res 52:109-118.

Grillner S (1985) Neurobiological bases of rhythmic motor acts in vertebrates. Science 228:143-149.

Grillner S (2003) The motor infrastructure: from ion channels to neuronal networks. Nat Rev Neurosci 4:573-586.

Grillner S, Ekeberg, El Manira A, Lansner A, Parker D, Tegner J, Wallen P (1998) Intrinsic function of a neuronal network - a vertebrate central pattern generator. Brain research Brain research reviews 26:184-197.

Grillner S, Rossignol S, Wallen P (1977) The adaptation of a reflex response to the ongoing phase of locomotion in fish. Experimental brain research Experimentelle Hirnforschung Experimentation cerebrale 30:1-11.

Grillner S, Wallen P, Hill R, Cangiano L, El Manira A (2001) Ion channels of importance for the locomotor pattern generation in the lamprey brainstem-spinal cord. The Journal of physiology 533:23-30.

Grillner S, Zangger P (1979) On the central generation of locomotion in the low spinal cat. Experimental brain research Experimentelle Hirnforschung Experimentation cerebrale 34:241-261.

Hains BC, Yucra JA, Hulsebosch CE (2001) Reduction of pathological and behavioral deficits following spinal cord contusion injury with the selective cyclooxygenase-2 inhibitor NS-398. Journal of neurotrauma 18:409-423.

Hall ED (1992) The neuroprotective pharmacology of methylprednisolone. Journal of neurosurgery 76:13-22.

Hall ED (1993) Neuroprotective actions of glucocorticoid and nonglucocorticoid steroids in acute neuronal injury. Cellular and molecular neurobiology 13:415-432.

Hall ED (1996) Free radicals and lipid peroxidation. In: Narayan RK, Wilberger JE, Povlishock JT (Eds.). Neurotrauma, 1st ed, New York, pp. 1405-1419.

Hall ED, Braughler JM (1981) Acute effects of intravenous glucocorticoid pretreatment on the in vitro peroxidation of cat spinal cord tissue. Experimental neurology 73:321-324.

Hall ED, Braughler JM (1989) Central nervous system trauma and stroke. II. Physiological and pharmacological evidence for involvement of oxygen radicals and lipid peroxidation. Free radical biology & medicine 6:303-313.

Hall ED, Kupina NC, Althaus JS (1999) Peroxynitrite scavengers for the acute treatment of traumatic brain injury. Annals of the New York Academy of Sciences 890:462-468.

Hall ED, Springer JE (2004) Neuroprotection and acute spinal cord injury: a reappraisal. NeuroRx 1:80-100.

Hartmann K, Bruehl C, Golovko T, Draguhn A (2008) Fast homeostatic plasticity of inhibition via activity-dependent vesicular filling. PloS one 3:e2979.

Heyer EJ, Nowak LM, Macdonald RL (1981) Bicuculline: a convulsant with synaptic and nonsynaptic actions. Neurology 31:1381-1390.

Hill CE, Beattie MS, Bresnahan JC (2001) Degeneration and sprouting of identified descending supraspinal axons after contusive spinal cord injury in the rat. Experimental neurology 171:153-169.

Hirbec H, Gaviria M, Vignon J (2001) Gacyclidine: a new neuroprotective agent acting at the N-methyl-D-aspartate receptor. CNS drug reviews 7:172-198.

Hoffmann C (2000) COX-2 in brain and spinal cord implications for therapeutic use. Curr Med Chem 7:1113-1120.

Hofmann ME, Nahir B, Frazier CJ (2008) Excitatory afferents to CA3 pyramidal cells display differential sensitivity to CB1 dependent inhibition of synaptic transmission. Neuropharmacology 55:1140-1146.

Holaday JW, Faden AI (1981a) Naloxone reverses the pathophysiology of shock through an antagonism of endorphin systems. Advances in biochemical psychopharmacology 28:421-434.

Holaday JW, Faden AI (1981b) Naloxone treatment in shock. Lancet 2:201.

Holtz A, Nystrom B, Gerdin B (1990) Effect of methylprednisolone on motor function and spinal cord blood flow after spinal cord compression in rats. Acta neurologica Scandinavica 82:68-73.

Huang YH, Sinha SR, Tanaka K, Rothstein JD, Bergles DE (2004) Astrocyte glutamate transporters regulate metabotropic glutamate receptor-mediated excitation of hippocampal interneurons. J Neurosci 24:4551-4559.

Hulsebosch CE (2002) Recent advances in pathophysiology and treatment of spinal cord injury. Advances in physiology education 26:238-255.

Iwahara T, Atsuta Y, Garcia-Rill E, Skinner RD (1992) Spinal cord stimulation-induced locomotion in the adult cat. Brain Res Bull 28:99-105.

Iwasaki Y, Ikeda K, Shiojima T, Kinoshita M (1995) CNQX prevents spinal motor neuron death following sciatic nerve transection in newborn rats. Journal of the neurological sciences 134:21-25.

Jiang Z, Carlin KP, Brownstone RM (1999) An in vitro functionally mature mouse spinal cord preparation for the study of spinal motor networks. Brain research 816:493-499.

Johnson RL, Gabella BA, Gerhart KA, McCray J, Menconi JC, Whiteneck GG (1997) Evaluating sources of traumatic spinal cord injury surveillance data in Colorado. American journal of epidemiology 146:266-272.

Katoh K, Ikata T, Katoh S, Hamada Y, Nakauchi K, Sano T, Niwa M (1996) Induction and its spread of apoptosis in rat spinal cord after mechanical trauma. Neuroscience letters 216:9-12.

Kauppinen TM, Suh SW, Berman AE, Hamby AM, Swanson RA (2009) Inhibition of poly(ADP-ribose) polymerase suppresses inflammation and promotes recovery after ischemic injury. Journal of cerebral blood flow and metabolism : official journal of the International Society of Cerebral Blood Flow and Metabolism 29:820-829.

Kiehn O, Hounsgaard J, Sillar KT (1997) Basic buildings blocks of vertebrate central pattern generators. In Neurons, Networks and Motor Behavior, ed. PSG Stein, S Grillner, A Selverston, DG Stuart, Cambridge, MA: MIT Press pp. 47–59.

Kiehn J, Thomas D, Karle CA, Schols W, Kubler W (1999a) Inhibitory effects of the class III antiarrhythmic drug amiodarone on cloned HERG potassium channels. Naunyn Schmiedebergs Arch Pharmacol 359:212-219.

Kiehn O (2006) Locomotor circuits in the mammalian spinal cord. Annual review of neuroscience 29:279-306.

Kiehn O, Kjaerulff O (1996) Spatiotemporal characteristics of 5-HT and dopamine-induced rhythmic hindlimb activity in the in vitro neonatal rat. Journal of neurophysiology 75:1472-1482.

Kiehn O, Sillar KT, Kjaerulff O, McDearmid JR (1999b) Effects of noradrenaline on locomotor rhythm-generating networks in the isolated neonatal rat spinal cord. Journal of neurophysiology 82:741-746.

Kim K, Lee SG, Kegelman TP, Su ZZ, Das SK, Dash R, Dasgupta S, Barral PM, Hedvat M, Diaz P, Reed JC, Stebbins JL, Pellecchia M, Sarkar D, Fisher PB (2011) Role of excitatory amino acid transporter-2 (EAAT2) and glutamate in neurodegeneration: opportunities for developing novel therapeutics. Journal of cellular physiology 226:2484-2493.

Kim MY, Mauro S, Gevry N, Lis JT, Kraus WL (2004) NAD+-dependent modulation of chromatin structure and transcription by nucleosome binding properties of PARP-1. Cell 119:803-814.

Kjaerulff O, Barajon I, Kiehn O (1994) Sulphorhodamine-labelled cells in the neonatal rat spinal cord following chemically induced locomotor activity in vitro. The Journal of physiology 478 (Pt 2):265-273.

Kjaerulff O, Kiehn O (1996) Distribution of networks generating and coordinating locomotor activity in the neonatal rat spinal cord in vitro: a lesion study. J Neurosci 16:5777-5794.

Klussmann S, Martin-Villalba A (2005) Molecular targets in spinal cord injury. Journal of molecular medicine 83:657-671.

Ko HY, Ditunno JF, Jr., Graziani V, Little JW (1999) The pattern of reflex recovery during spinal shock. Spinal cord 37:402-409.

Koyanagi I, Tator CH (1997) Effect of a single huge dose of methylprednisolone on blood flow, evoked potentials, and histology after acute spinal cord injury in the rat. Neurological research 19:289-299.

Kremer E, Lev-Tov A (1997) Localization of the spinal network associated with generation of hindlimb locomotion in the neonatal rat and organization of its transverse coupling system. Journal of neurophysiology 77:1155-1170.

Kriellaars DJ, Brownstone RM, Noga BR, Jordan LM (1994) Mechanical entrainment of fictive locomotion in the decerebrate cat. Journal of neurophysiology 71:2074-2086.

Kroemer G, Galluzzi L, Vandenabeele P, Abrams J, Alnemri ES, Baehrecke EH, Blagosklonny MV, El-Deiry WS, Golstein P, Green DR, Hengartner M, Knight RA, Kumar S, Lipton SA, Malorni W, Nunez G, Peter ME, Tschopp J, Yuan J, Piacentini M, Zhivotovsky B, Melino G, Nomenclature Committee on Cell D (2009) Classification of cell death: recommendations of the Nomenclature Committee on Cell Death 2009. Cell death and differentiation 16:3-11.

Kudo N, Yamada T (1987) N-methyl-D,L-aspartate-induced locomotor activity in a spinal cord-hindlimb muscles preparation of the newborn rat studied in vitro. Neuroscience letters 75:43-48.

Kun E, Kirsten E, Ordahl CP (2002) Coenzymatic activity of randomly broken or intact double-stranded DNAs in auto and histone H1 trans-poly(ADP-ribosylation), catalyzed by poly(ADP-ribose) polymerase (PARP I). The Journal of biological chemistry 277:39066-39069.

Kuzhandaivel A, Nistri A, Mladinic M (2010) Kainate-mediated excitotoxicity induces neuronal death in the rat spinal cord in vitro via a PARP-1 dependent cell death pathway (Parthanatos). Cellular and molecular neurobiology 30:1001-1012.

Kyriakatos A, Mahmood R, Ausborn J, Porres CP, Buschges A, El Manira A (2011) Initiation of locomotion in adult zebrafish. J Neurosci 31:8422-8431.

Lafreniere-Roula M, McCrea DA (2005) Deletions of rhythmic motoneuron activity during fictive locomotion and scratch provide clues to the organization of the mammalian central pattern generator. Journal of neurophysiology 94:1120-1132.

Lau A, Tymianski M (2010) Glutamate receptors, neurotoxicity and neurodegeneration. Pflugers Archiv : European journal of physiology 460:525-542.

Li JH, Serdyuk L, Ferraris DV, Xiao G, Tays KL, Kletzly PW, Li W, Lautar S, Zhang J, Kalish VJ (2001) Synthesis of substituted 5[H]phenanthridin-6-ones as potent poly(ADP-ribose)polymerase-1 (PARP1) inhibitors. Bioorganic & medicinal chemistry letters 11:1687-1690.

Li X, Klaus JA, Zhang J, Xu Z, Kibler KK, Andrabi SA, Rao K, Yang ZJ, Dawson TM, Dawson VL, Koehler RC (2010) Contributions of poly(ADP-ribose) polymerase-1 and -2 to nuclear translocation of apoptosis-inducing factor and injury from focal cerebral ischemia. Journal of neurochemistry 113:1012-1022.

Liu D, Thangnipon W, McAdoo DJ (1991) Excitatory amino acids rise to toxic levels upon impact injury to the rat spinal cord. Brain research 547:344-348.

Liu D, Xu GY, Pan E, McAdoo DJ (1999) Neurotoxicity of glutamate at the concentration released upon spinal cord injury. Neuroscience 93:1383-1389.

Liu J, Jordan LM (2005) Stimulation of the parapyramidal region of the neonatal rat brain stem produces locomotor-like activity involving spinal 5-HT7 and 5-HT2A receptors. Journal of neurophysiology 94:1392-1404.

Liu XZ, Xu XM, Hu R, Du C, Zhang SX, McDonald JW, Dong HX, Wu YJ, Fan GS, Jacquin MF, Hsu CY, Choi DW (1997) Neuronal and glial apoptosis after traumatic spinal cord injury. J Neurosci 17:5395-5406.

Lo EH, Bosque-Hamilton P, Meng W (1998) Inhibition of poly(ADP-ribose) polymerase: reduction of ischemic injury and attenuation of N-methyl-D-aspartate-induced neurotransmitter dysregulation. Stroke; a journal of cerebral circulation 29:830-836.

Long SK, Smith DA, Siarey RJ, Evans RH (1990) Effect of 6-cyano-2,3-dihydroxy-7-nitro-quinoxaline (CNQX) on dorsal root-, NMDA-, kainate- and quisqualate-mediated depolarization of rat motoneurones in vitro. British journal of pharmacology 100:850-854.

Lorenzo HK, Susin SA (2007) Therapeutic potential of AIF-mediated caspase-independent programmed cell death. Drug resistance updates : reviews and commentaries in antimicrobial and anticancer chemotherapy 10:235-255.

Madriaga MA, McPhee LC, Chersa T, Christie KJ, Whelan PJ (2004) Modulation of locomotor activity by multiple 5-HT and dopaminergic receptor subtypes in the neonatal mouse spinal cord. Journal of neurophysiology 92:1566-1576.

Mandir AS, Poitras MF, Berliner AR, Herring WJ, Guastella DB, Feldman A, Poirier GG, Wang ZQ, Dawson TM, Dawson VL (2000) NMDA but not non-NMDA excitotoxicity is mediated by Poly(ADP-ribose) polymerase. J Neurosci 20:8005-8011.

Mandir AS, Przedborski S, Jackson-Lewis V, Wang ZQ, Simbulan-Rosenthal CM, Smulson ME, Hoffman BE, Guastella DB, Dawson VL, Dawson TM (1999) Poly(ADP-ribose) polymerase activation mediates 1-methyl-4-phenyl-1, 2,3,6-tetrahydropyridine (MPTP)-induced parkinsonism. Proceedings of the National Academy of Sciences of the United States of America 96:5774-5779.

Marchetti C, Beato M, Nistri A (2001) Alternating rhythmic activity induced by dorsal root stimulation in the neonatal rat spinal cord in vitro. The Journal of physiology 530:105-112.

Marchetti C, Taccola G, Nistri A (2003) Distinct subtypes of group I metabotropic glutamate receptors on rat spinal neurons mediate complex facilitatory and inhibitory effects. The European journal of neuroscience 18:1873-1883.

Margaryan G, Mattioli C, Mladinic M, Nistri A (2010) Neuroprotection of locomotor networks after experimental injury to the neonatal rat spinal cord in vitro. Neuroscience 165:996-1010.

Masson M, Niedergang C, Schreiber V, Muller S, Menissier-de Murcia J, de Murcia G (1998) XRCC1 is specifically associated with poly(ADP-ribose) polymerase and negatively regulates its activity following DNA damage. Mol Cell Biol 18:3563-3571.

Mazzone GL, Nistri A (2011a) Delayed neuroprotection by riluzole against excitotoxic damage evoked by kainate on rat organotypic spinal cord cultures. Neuroscience 190:318-327.

Mazzone GL, Nistri A (2011b) Effect of the PARP-1 inhibitor PJ 34 on excitotoxic damage evoked by kainate on rat spinal cord organotypic slices. Cellular and molecular neurobiology 31:469-478.

McAdoo DJ, Xu GY, Robak G, Hughes MG (1999) Changes in amino acid concentrations over time and space around an impact injury and their diffusion through the rat spinal cord. Experimental neurology 159:538-544.

McDonald JW, Levine JM, Qu Y (1998) Multiple classes of the oligodendrocyte lineage are highly vulnerable to excitotoxicity. Neuroreport 9:2757-2762.

Nagata S (1997) Apoptosis by death factor. Cell 88:355-365.

Nahir B, Lindsly C, Frazier CJ (2010) mGluR-mediated and endocannabinoid-dependent long-term depression in the hilar region of the rat dentate gyrus. Neuropharmacology 58:712-721.

Nie H, Weng HR (2009) Glutamate transporters prevent excessive activation of NMDA receptors and extrasynaptic glutamate spillover in the spinal dorsal horn. Journal of neurophysiology 101:2041-2051.

Nistri A, Ostroumov K, Sharifullina E, Taccola G (2006) Tuning and playing a motor rhythm: how metabotropic glutamate receptors orchestrate generation of motor patterns in the mammalian central nervous system. The Journal of physiology 572:323-334.

Nogradi A, Szabo A, Pinter S, Vrbova G (2007) Delayed riluzole treatment is able to rescue injured rat spinal motoneurons. Neuroscience 144:431-438.

Oei SL, Shi Y (2001) Poly(ADP-ribosyl)ation of transcription factor Yin Yang 1 under conditions of DNA damage. Biochemical and biophysical research communications 285:27-31.

Park E, Velumian AA, Fehlings MG (2004) The role of excitotoxicity in secondary mechanisms of spinal cord injury: a review with an emphasis on the implications for white matter degeneration. Journal of neurotrauma 21:754-774.

Pearson KG, Acharya H, Fouad K (2005) A new electrode configuration for recording electromyographic activity in behaving mice. J Neurosci Methods 148:36-42.

Pearson SA, Mouihate A, Pittman QJ, Whelan PJ (2003) Peptidergic activation of locomotor pattern generators in the neonatal spinal cord. J Neurosci 23:10154-10163.

Pena F, Parkis MA, Tryba AK, Ramirez JM (2004) Differential contribution of pacemaker properties to the generation of respiratory rhythms during normoxia and hypoxia. Neuron 43:105-117.

Pineau I, Lacroix S (2007) Proinflammatory cytokine synthesis in the injured mouse spinal cord: multiphasic expression pattern and identification of the cell types involved. J Comp Neurol 500:267-285.

Potier B, Billard JM, Riviere S, Sinet PM, Denis I, Champeil-Potokar G, Grintal B, Jouvenceau A, Kollen M, Dutar P (2010) Reduction in glutamate uptake is associated with extrasynaptic NMDA and metabotropic glutamate receptor activation at the hippocampal CA1 synapse of aged rats. Aging cell 9:722-735.

Price C, Makintubee S, Herndon W, Istre GR (1994) Epidemiology of traumatic spinal cord injury and acute hospitalization and rehabilitation charges for spinal cord injuries in Oklahoma, 1988-1990. American journal of epidemiology 139:37-47.

Rabchevsky AG, Fugaccia I, Sullivan PG, Blades DA, Scheff SW (2002) Efficacy of methylprednisolone therapy for the injured rat spinal cord. J Neurosci Res 68:7-18.

Rammes G, Zieglgansberger W, Parsons CG (2008) The fraction of activated N-methyl-D-aspartate receptors during synaptic transmission remains constant in the presence of the glutamate release inhibitor riluzole. Journal of neural transmission 115:1119-1126.

Resnick DK, Graham SH, Dixon CE, Marion DW (1998) Role of cyclooxygenase 2 in acute spinal cord injury. Journal of neurotrauma 15:1005-1013.

Roberts A, Soffe SR, Wolf ES, Yoshida M, Zhao FY (1998) Central circuits controlling locomotion in young frog tadpoles. Annals of the New York Academy of Sciences 860:19-34.

Ronsyn MW, Berneman ZN, Van Tendeloo VF, Jorens PG, Ponsaerts P (2008) Can cell therapy heal a spinal cord injury? Spinal cord 46:532-539.

Rossignol S, Schwab M, Schwartz M, Fehlings MG (2007) Spinal cord injury: time to move? J Neurosci 27:11782-11792.

Ruscetti T, Lehnert BE, Halbrook J, Le Trong H, Hoekstra MF, Chen DJ, Peterson SR (1998) Stimulation of the DNA-dependent protein kinase by poly(ADP-ribose) polymerase. The Journal of biological chemistry 273:14461-14467.

Schindler-Ivens S, Shields RK (2000) Low frequency depression of H-reflexes in humans with acute and chronic spinal-cord injury. Experimental brain research Experimentelle Hirnforschung Experimentation cerebrale 133:233-241.

Schwab JM, Brechtel K, Nguyen TD, Schluesener HJ (2000) Persistent accumulation of cyclooxygenase-1 (COX-1) expressing microglia/macrophages and upregulation by endothelium following spinal cord injury. J Neuroimmunol 111:122-130.

Schwartz G, Fehlings MG (2001) Evaluation of the neuroprotective effects of sodium channel blockers after spinal cord injury: improved behavioral and neuroanatomical recovery with riluzole. Journal of neurosurgery 94:245-256.

Schwindt PC, Crill WE (1981) Voltage clamp study of cat spinal motoneurons during strychnine-induced seizures. Brain research 204:226-230.

Scott GS, Jakeman LB, Stokes BT, Szabo C (1999) Peroxynitrite production and activation of poly (adenosine diphosphate-ribose) synthetase in spinal cord injury. Annals of neurology 45:120-124.

Scott GS, Szabo C, Hooper DC (2004) Poly(ADP-ribose) polymerase activity contributes to peroxynitrite-induced spinal cord neuronal cell death in vitro. Journal of neurotrauma 21:1255-1263.

Sherrington CS (1897) On the Question whether any Fibres of the Mammalian Dorsal (Afferent) Spinal Root are of Intraspinal Origin. The Journal of physiology 21:209-212.

Smith JC, Butera RJ, Koshiya N, Del Negro C, Wilson CG, Johnson SM (2000) Respiratory rhythm generation in neonatal and adult mammals: the hybrid pacemaker-network model. Respiration physiology 122:131-147.

Streit J (1993) Regular oscillations of synaptic activity in spinal networks in vitro. Journal of neurophysiology 70:871-878.

Surkin J, Smith M, Penman A, Currier M, Harkey HL, 3rd, Chang YF (1998) Spinal cord injury incidence in Mississippi: a capture-recapture approach. The Journal of trauma 45:502-504.

Szabo C, Dawson VL (1998) Role of poly(ADP-ribose) synthetase in inflammation and ischaemia-reperfusion. Trends in pharmacological sciences 19:287-298.

Taccola G, Marchetti C, Nistri A (2004) Modulation of rhythmic patterns and cumulative depolarization by group I metabotropic glutamate receptors in the neonatal rat spinal cord in vitro. The European journal of neuroscience 19:533-541.

Taccola G, Margaryan G, Mladinic M, Nistri A (2008) Kainate and metabolic perturbation mimicking spinal injury differentially contribute to early damage of locomotor networks in the in vitro neonatal rat spinal cord. Neuroscience 155:538-555.

Taccola G, Nistri A (2006) Oscillatory circuits underlying locomotor networks in the rat spinal cord. Crit Rev Neurobiol 18:25-36.

Taoka Y, Okajima K, Uchiba M, Johno M (2001) Methylprednisolone reduces spinal cord injury in rats without affecting tumor necrosis factor-alpha production. Journal of neurotrauma 18:533-543.

Tator CH (1995) Update on the pathophysiology and pathology of acute spinal cord injury. Brain pathology 5:407-413.

Tator CH (1996) Experimental and clinical studies of the pathophysiology and management of acute spinal cord injury. The journal of spinal cord medicine 19:206-214.

Tator CH (1998) Biology of neurological recovery and functional restoration after spinal cord injury. Neurosurgery 42:696-707; discussion 707-698.

Tator CH, Fehlings MG (1991) Review of the secondary injury theory of acute spinal cord trauma with emphasis on vascular mechanisms. Journal of neurosurgery 75:15-26.

Tazerart S, Viemari JC, Darbon P, Vinay L, Brocard F (2007) Contribution of persistent sodium current to locomotor pattern generation in neonatal rats. Journal of neurophysiology 98:613-628.

Thurman DJ, Burnett CL, Jeppson L, Beaudoin DE, Sniezek JE (1994) Surveillance of spinal cord injuries in Utah, USA. Paraplegia 32:665-669.

Tolle TR, Berthele A, Zieglgansberger W, Seeburg PH, Wisden W (1993) The differential expression of 16 NMDA and non-NMDA receptor subunits in the rat spinal cord and in periaqueductal gray. J Neurosci 13:5009-5028.

Tonai T, Taketani Y, Ohmoto Y, Ueda N, Nishisho T, Yamamoto S (2002) Cyclooxygenase-2 induction in rat spinal cord injury mediated by proinflammatory tumor necrosis factor-alpha and interleukin-1. Adv Exp Med Biol 507:397-401.

Tovar YRLB, Santa-Cruz LD, Zepeda A, Tapia R (2009) Chronic elevation of extracellular glutamate due to transport blockade is innocuous for spinal motoneurons in vivo. Neurochemistry international 54:186-191.

Tresch MC, Kiehn O (1999) Coding of locomotor phase in populations of neurons in rostral and caudal segments of the neonatal rat lumbar spinal cord. Journal of neurophysiology 82:3563-3574.

van den Berg ME, Castellote JM, Mahillo-Fernandez I, de Pedro-Cuesta J (2010) Incidence of spinal cord injury worldwide: a systematic review. Neuroepidemiology 34:184-192; discussion 192.

Verhave PS, Jongsma MJ, Van Den Berg RM, Vanwersch RA, Smit AB, Philippens IH (2012) Neuroprotective effects of riluzole in early phase Parkinson's disease on clinically relevant parameters in the marmoset MPTP model. Neuropharmacology 62:1700-1707.

Wahl F, Renou E, Mary V, Stutzmann JM (1997) Riluzole reduces brain lesions and improves neurological function in rats after a traumatic brain injury. Brain research 756:247-255.

Wang Q, Yu S, Simonyi A, Sun GY, Sun AY (2005) Kainic acid-mediated excitotoxicity as a model for neurodegeneration. Molecular neurobiology 31:3-16.

Wang Y, Kim NS, Li X, Greer PA, Koehler RC, Dawson VL, Dawson TM (2009) Calpain activation is not required for AIF translocation in PARP-1-dependent cell death (parthanatos). Journal of neurochemistry 110:687-696.

Weng HR, Chen JH, Cata JP (2006) Inhibition of glutamate uptake in the spinal cord induces hyperalgesia and increased responses of spinal dorsal horn neurons to peripheral afferent stimulation. Neuroscience 138:1351-1360.

Westgren N, Levi R (1998) Quality of life and traumatic spinal cord injury. Archives of physical medicine and rehabilitation 79:1433-1439.

Whelan P, Bonnot A, O'Donovan MJ (2000) Properties of rhythmic activity generated by the isolated spinal cord of the neonatal mouse. Journal of neurophysiology 84:2821-2833.

Whelan PJ (2003) Developmental aspects of spinal locomotor function: insights from using the in vitro mouse spinal cord preparation. The Journal of physiology 553:695-706.

Wrathall JR, Teng YD, Choiniere D (1996) Amelioration of functional deficits from spinal cord trauma with systemically administered NBQX, an antagonist of non-N-methyl-D-aspartate receptors. Experimental neurology 137:119-126.

Wu KL, Hsu C, Chan JY (2009) Nitric oxide and superoxide anion differentially activate poly(ADP-ribose) polymerase-1 and Bax to induce nuclear translocation of apoptosis-inducing factor and mitochondrial release of cytochrome c after spinal cord injury. Journal of neurotrauma 26:965-977.

Xu GY, Hughes MG, Ye Z, Hulsebosch CE, McAdoo DJ (2004) Concentrations of glutamate released following spinal cord injury kill oligodendrocytes in the spinal cord. Experimental neurology 187:329-336.

Xu GY, McAdoo DJ, Hughes MG, Robak G, de Castro R, Jr. (1998) Considerations in the determination by microdialysis of resting extracellular amino acid concentrations and release upon spinal cord injury. Neuroscience 86:1011-1021.

Yuan J, Lipinski M, Degterev A (2003) Diversity in the mechanisms of neuronal cell death. Neuron 40:401-413.

Yvon C, Czarnecki A, Streit J (2007) Riluzole-induced oscillations in spinal networks. Journal of neurophysiology 97:3607-3620.

Ziegler M, Oei SL (2001) A cellular survival switch: poly(ADP-ribosyl)ation stimulates DNA repair and silences transcription. BioEssays : news and reviews in molecular, cellular and developmental biology 23:543-548.

https://www.nscisc.uab.edu/PublicDocuments/reports/pdf/2011%20NSCISC%20Annual%20Statistical%20Report%20-%20Complete%20Public%20Version.pdf

Acknowledgement

I wish to express my deepest gratitude to Prof. Andrea Nistri for all his support and encouragement during these four years. I would like to thank him again for being a wonderful supervisor and for his admirable guidance and blessing. I am indebted to him for being a real teacher who guided me in all the aspects of the project and gave me the chance of experiencing new works, new places and new life.

I am very grateful to Prof. Enrico Cherubini and Prof. Anna Menini for their kind support.

I thank sincerely Gayane and Alexey who were beside me from the starting point and taught me how to work in electrophysiology laboratory. I am also grateful to them for gifting me their true friendship.

I wish to thank Giuliano and Miranda for their enormous helps and support.

I thank all the members of our lab, especially spinal cord group, for being always helpful and kind to me.

I thank Ayisha and Elena who were always more than colleagues to me and helped me a lot.

I thank all SISSA staff and technicians sincerely for their support and I would like to give my special thanks to Mr. Riccardo Iancer, Tullio, Renato, Jessica, Gabriella and Sandra.

Finally, I thank my lovely family whose omnipresent memories blessed every moment of my life.